

The Contribution of Viral and Host Cell Factors to Replication of the Hepatitis C Virus RNA Genome

Daniel M. Jones

A thesis presented for the degree of Doctor of Philosophy
Faculty of Biomedical and Life Sciences
University of Glasgow

MRC Virology Unit

Church Street

Glasgow

G11 5JR

April 2009

Table of Contents

List of Figures, Tables, Appendices and Accompanying Material	VI
Acknowledgements	X
Abbreviations	XI
Abstract	XVI
One and Three Letter Amino Acid Abbreviations	XIX
Author's Declaration.....	XX
1 Introduction.....	1
1.1 Background.....	1
1.1.1 Discovery of Hepatitis C Virus	1
1.1.2 Classification and Genotypes of HCV	2
1.1.3 HCV Epidemiology and Transmission	3
1.1.4 Clinical Features of HCV Infection.....	4
1.1.5 Immunological Response to HCV Infection	6
1.1.6 Diagnosis of HCV Infection	7
1.1.7 Treatment of HCV Infection	8
1.2 Molecular Features of HCV	11
1.2.1 Virion Morphology	11
1.2.2 The Viral Genome	12
1.3 Systems used to Study the HCV Life Cycle	25
1.3.1 Binding and Entry Analysis.....	25
1.3.2 RNA Replication Analysis.....	27
1.3.3 Virus Assembly and Release.....	28
1.4 The HCV Life Cycle.....	29
1.4.1 Binding and Entry	29
1.4.2 Translation and Polyprotein Processing	32
1.4.3 RNA Replication	33
1.4.4 Virus Assembly and Release.....	35
1.5 <i>Trans</i> -Complementation of Virus Functions	38
1.5.1 <i>Trans</i> -Complementation of HCV RNA Replication	38
1.5.2 <i>Trans</i> -Complementation of HCV Virion Assembly.....	39
1.5.3 <i>Trans</i> -Complementation of Other Positive-Strand RNA Viruses	40
1.6 Modulation of HCV Infection by RNA Interference (RNAi)	41
1.6.1 Targeting the HCV Genome Directly	41
1.6.2 Targeting Host Cell Genes Involved in HCV RNA Synthesis.	42
1.6.3 Discovery and Mechanism of RNAi	43
1.7 Fluorescent Proteins and their Applications	44
1.7.1 GFP	44
1.7.2 Photoactivatable-GFP (PAGFP).....	45
1.7.3 Fluorescence Recovery After Photobleaching (FRAP).....	46
1.8 Aims of the Study.....	46

2	Materials and Methods	48
2.1	Materials	48
2.1.1	Vectors	48
2.1.2	Kits and Enzymes.....	48
2.1.3	Cells	49
2.1.4	Transfection/Transformation reagents.....	49
2.1.5	Cell Culture Growth Medium	49
2.1.6	Antibodies.....	50
2.1.7	Commonly Used Chemicals	51
2.1.8	Clones	52
2.1.9	Solutions	52
2.1.10	Oligonucleotide Synthesis and DNA Sequence Analysis	54
2.1.11	siRNA Library	54
2.2	Methods	54
2.2.1	Tissue Culture Maintenance.....	54
2.2.2	DNA Manipulation	55
2.2.3	Isolation and Purification of DNA.....	58
2.2.4	RNA Manipulation	60
2.2.5	Introduction of DNA/RNA into Eukaryotic cells	61
2.2.6	Assessment of HCV RNA Replication	62
2.2.7	Preparation of Mammalian Cell Extracts for SDS-PAGE Analysis.....	63
2.2.8	SDS-PAGE Analysis	63
2.2.9	Western Blot Analysis	64
2.2.10	Microscopy Techniques and Analysis.....	64
2.2.11	Assessment of HCV Infectious Virus Production	66
2.2.12	siRNA Library Screen	67
3	Live Cell Analysis of the HCV-Encoded NS5A Protein	69
3.1	Introduction	69
3.2	Creation and Characterisation of the luc-JFH1 _{GFP} SGR.....	70
3.2.1	Insertion of GFP into the luc-JFH1 SGR	70
3.2.2	Characterisation of luc-JFH1 _{GFP}	72
3.3	The NS Proteins Influence Localisation and Mobility of NS5A.....	75
3.3.1	Analysis of NS5A-Photoactivatable GFP (PAGFP)	76
3.4	NS5A Localisation and Mobility is Influenced by NS4B.....	77
3.4.1	Construction of Plasmids Expressing the HCV NS3-NS5B Coding Region from Strain JFH1.....	78
3.4.2	NS4B Distributes NS5A to Foci.....	80
3.4.3	NS4B Reduces the Mobility of NS5A	80
3.5	Discussion.....	81
4	Mutational Analysis of the NS4B C-terminus	85
4.1	Introduction	85
4.2	The NS4B C-terminus is well conserved and is predicted to contain two α -helices.....	85
4.3	Mutation of the NS4B C-terminus	86
4.4	Characterisation of HCV NS4B Mutants	87
4.4.1	The C-terminus of NS4B is Involved in HCV RNA Replication.....	87

4.4.2	Foci-Forming Abilities of Non-Replicating NS4B Mutants	.88
4.4.3	The NS4B-C-terminus Influences NS5A Mobility91
4.4.4	The NS4B C-terminus Influences Hyperphosphorylation of NS5A92
4.5	Discussion92
5	Trans-Complementation Studies Utilising NS4B and NS5A Mutant SGRs97
5.1	Introduction97
5.2	Non-Replicating NS4B Mutant SGRs can be Complemented <i>in trans</i>98
5.3	A Non-Replicating NS5A Mutant SGR can be Complemented <i>in trans</i>100
5.4	Reconstitution of Replication from Non-Replicating NS4B and NS5A Mutant SGRs101
5.4.1	Detection of NS4B Mutant SGR Replication101
5.4.2	Detection of NS5A Mutant SGR Replication102
5.4.3	Creation of a Cell Line from Non-Replicating NS4B and NS5A Mutant SGRs103
5.5	Discussion104
6	NS4B Influences the Production of Infectious Virus Particles109
6.1	Introduction109
6.2	TCID ₅₀ Analysis of JFH1 Mutants Harboring Mutations Within the C-terminus of NS4B109
6.3	Characterisation of JFH1 _{M6}111
6.3.1	JFH1 _{M6} Enhances the Production of Infectious Virus Particles111
6.3.2	Replication of JFH1 _{M6} RNA is not Enhanced in Electroporated Cells112
6.3.3	JFH1 _{M6} does not Alter the Localisation of NS5A, Core or dsRNA in Infected Cells112
6.4	Introduction of mutation M6 into J6-JFH1113
6.4.1	Characterisation of J6-JFH1113
6.4.2	Introduction of M6 into J6-JFH1 Represses Infectious Particle Production113
6.5	Discussion114
7	Identification of Cellular Genes that Influence HCV RNA Replication117
7.1	Introduction117
7.2	Production of a System Suitable for Screening a siRNA Library117
7.2.1	Selection and Characterisation of a Positive Control siRNA117
7.2.2	Creation and Characterisation of a Tri-cistronic JFH1 Replicon119
7.2.3	Characterisation of Cell Lines Supporting Autonomous Replication of Tri-JFH1121
7.2.4	siHCV Reduces Tri-JFH1 Replication in Tri-Huh-7 and Tri-U2OS Cells122

7.2.5	Knockdown of CKI- α Reduces Tri-JFH1 Replication in Tri-Huh-7 and Tri-U2OS Cells.....	123
7.3	Screening of the siRNA Library in Tri-Huh-7 and Tri-U2OS Cells.....	124
7.3.1	Genes That Increased Luciferase Activity In Both Cell Lines	129
7.3.2	Genes That Decreased Luciferase Activity In Both Cell Lines.....	130
7.3.3	Genes that had Opposing Effects on Luciferase Activity	130
7.4	Knockdown of ISG15 and XRN1 can Increase HCV RNA Replication in Transient Assays	130
7.5	Discussion.....	131
8	Conclusions and Further Perspectives	138
8.1	Summary.....	138
8.2	Applications of Technology to Examine HCV RNA Replication.....	139
8.2.1	GFP and FRAP	139
8.2.2	Alternative Fluorescent Technologies	141
8.2.3	siRNA and Alternative Approaches	143
8.3	HCV and <i>trans</i> -Complementation	144
8.3.1	Implications for Quasispecies Maintenance	145
	Appendices.....	147
	References.....	162

List of Figures, Tables, Appendices and Accompanying Material

Chapter 1

Figures

- Figure 1.1 Worldwide distribution of the six HCV genotypes
- Figure 1.2 The HCV virion
- Figure 1.3 The HCV genome and encoded viral proteins
- Figure 1.4 Subgenomic and genomic HCV replicons
- Figure 1.5 Model for HCV binding and entry
- Figure 1.6 HCV genome replication and virus assembly
- Figure 1.7 Cellular proteins that influence HCV RNA replication
- Figure 1.8 *Trans*-complementation of viral functions
- Figure 1.9 The RNA interference (RNAi) pathway
- Figure 1.10 GFP, PAGFP and FRAP

Chapter 3

Figures

- Figure 3.1 Primers used to create 5A1 and 5A2
- Figure 3.2 Creation of pGEM-5A1-GFP-5A2
- Figure 3.3 Creation of luc-JFH1_{GFP}
- Figure 3.4 luc-JFH1_{GFP} replicates efficiently in Huh-7 cells
- Figure 3.5 Onset of replication by luc-JFH1_{GFP} is delayed compared to luc-JFH1
- Figure 3.6 Visualisation of NS5A, NS5A-GFP and dsRNA in cells actively replicating luc-JFH1 and luc-JFH1_{GFP} RNA
- Figure 3.7 NS5A-GFP and NS5A staining coincide, and NS5A-GFP can be directly visualised in live cells actively replicating luc-JFH1_{GFP} RNA
- Figure 3.8 The NS proteins influence the localisation and mobility of NS5A
- Figure 3.9 luc-JFH1_{PAGFP} replicates efficiently in Huh-7 cells and NS5A-PAGFP displays a low level of mobility in cells

- Figure 3.10 Construction of JFH1_{Poly}
 Figure 3.11 Construction of JFH1_{Poly}Δ4B
 Figure 3.12 NS4B influences the localisation and distribution of NS5A

Chapter 4 Figures

- Figure 4.1 Conservation and predicted secondary structure of the JFH1 NS4B C-terminus
 Figure 4.2 Topology of the NS4B protein and mutational analysis of the C-terminal domain
 Figure 4.3 Construction of NS4B C-terminal mutants by site directed mutagenesis
 Figure 4.4 Construction of luc-GFP_{M1-M15} and Poly_{M1-M15} NS4B mutants
 Figure 4.5 Replication competence of NS4B mutants
 Figure 4.6 Creation of pNS4B-GFP and pCMV-NS4B
 Figure 4.7 NS4B mutants expressed in isolation form foci
 Figure 4.8 The NS4B C-terminus contains determinants for foci formation
 Figure 4.9 The NS4B C-terminus influences NS5A-GFP localisation to foci and the number of foci in cells
 Figure 4.10 The NS4B C-terminus influences NS5A-GFP mobility
 Figure 4.11 The NS4B C-terminus influences NS5A-GFP phosphorylation
 Figure 4.12 Summary of the characteristics of the mutants at the C-terminus of NS4B

Chapter 5 Figures

- Figure 5.1 Transient *trans*-complementation of non-replicating NS4B mutant SGRs
 Figure 5.2 Non-replicating NS4B mutant SGRs can be *trans*-complemented
 Figure 5.3 A Ser to Ile change at amino acid 232 abolishes luc-JFH1 replication
 Figure 5.4 luc-JFH1_{S232I} RNA replication can be *trans*-complemented

- Figure 5.5 Reconstitution of replication from non-replicating NS4B and NS5A mutants SGRs
- Figure 5.6 *Trans*-complementation of a defective SGR with a NS5A mutation by non-replicating SGRs expressing mutant NS4B
- Figure 5.7 Generation of cell lines from non-replicating NS4B and NS5A mutant SGRs
- Figure 5.8 Summary of the *trans*-complementation data for non-replicating NS4B mutant SGRs
- Figure 5.9 Proposed model for NS4B *trans*-complementation and reconstitution of active RNA replication

Chapter 6

Figures

- Figure 6.1 Insertion of NS4B C-terminal mutations into the genomic JFH1 cDNA
- Figure 6.2 TCID₅₀ analysis of JFH1 harbouring mutations within the C-terminus of NS4B
- Figure 6.3 JFH1_{M6} enhances the production of infectious virus particles
- Figure 6.4 JFH1_{M6} does not alter the localisation of NS5A, core or dsRNA
- Figure 6.5 Characterisation of J6-JFH1
- Figure 6.6 Introduction of M6 into J6-JFH1 reduces production of infectious virus particles

Chapter 7

Figures

- Figure 7.1 siHCV targets the HCV IRES
- Figure 7.2 siHCV reduces transient HCV RNA replication in Huh-7 cells
- Figure 7.3 Creation of Tri-JFH1
- Figure 7.4 Tri-JFH1 replicates transiently in both Huh-7 and U2OS cells
- Figure 7.5 Generation of two cell lines; Tri-Huh-7 and Tri-U2OS
- Figure 7.6 siHCV reduces viral RNA replication in Tri-Huh-7 cells
- Figure 7.7 siHCV reduces viral RNA replication in Tri-U2OS cells

- Figure 7.8 Knockdown of CKI- α in Tri-Huh-7 and Tri-U2OS cells
Figure 7.9 Effect of silencing ISG15 and XRN1 on transient HCV RNA replication

Tables

- Table 1 Ribosomal proteins (large)
Table 2 Ribosomal proteins (small)
Table 3 Translation factors
Table 4 RNA-binding proteins
Table 5 Proteins involved in IFN induction
Table 6 Degredation pathway proteins
Table 7 Cell cycle control proteins
Table 8 Non-assigned proteins

Appendices

- Appendix 1 Primers for NS4B C-terminal Mutagenesis
Appendix 2 siRNA Library Screen – Names and Data for all 299 Genes

Accompanying material

Jones, D.M., Patel, A.H., Targett-Adams, P. and McLauchlan, J. (2009). The hepatitis C virus NS4B protein can *trans*-complement viral RNA replication and modulates production of infectious virus. *J Virol* **83**, 2163-2177.

Jones, D.M., Gretton, S.N., McLauchlan, J. and Targett-Adams, P. (2007). Mobility analysis of an NS5A-GFP fusion protein in cells actively replicating hepatitis C virus subgenomic RNA. *J Gen Virol* **88**, 470-475.

Acknowledgements

Firstly I would like to thank Professor McGeoch for the opportunity to undertake my PhD studies at the unit.

My unending gratitude goes to my supervisor, John, for his excellent supervision, friendship, thorough proofreading of this thesis and many a dram of whisky over my 3-and-a-bit years in Glasgow. I promise to never take you River Bugging again. I would also like to thank Paul for his supervision and banter during his time in the MRC.

Many thanks also go to the members of labs 301 and 304, particularly Graham, for his capacity to answer my stupid questions and, more importantly, those fun times with 'Car park Catchphrase'. Thank you also to Patricia and Brenna for providing useful information and data.

I would like to say thank you to all my friends here in Glasgow, including Sarah (for revealing the wonders of Microsoft Word), Morag (for help proofreading this thesis), Vera, Chris and my fellow writing-room detainees Ash and Maureen. Gratitude also goes to Gallus, for supplying me with many nights out and hangovers. Here, I would also like to say a big thank you to Megan, for quizzing me on all matters HCV-related prior to my viva!

Last but by no means least, I would like to thank my mum and Ian, dad and Maria and my grandparents for their love, encouragement and support (both emotional and financial!) over the years. I would not have gotten this far without you!

Abbreviations

°C	degrees celcius
%	percentage
μ	micro (10 ⁻⁶)
A	amp(s)
ADRP	adipocyte differentiation-related protein
ALT	alanine aminotransferase
AGO	argonaute
Amp	ampicillin
Apo	apolipoprotein
APS	ammonium persulphate
ATP	adenosine-5'-triphosphate
bDNA	branched DNA
bp	base pair(s)
BPB	bromophenol blue
BrUTP	5-bromouridine 5'-triphosphate
BSA	bovine serum albumin
BVDV	bovine viral diarrhoea virus
C-	carboxy-terminus
CCAM	cell culture adaptive mutation
cDNA	complementary DNA
CHO	Chinese hamster ovary (cells)
CLDN	claudin
CTP	cytidine-5'-triphosphate
CV-N	cyanovirin-N
DAB	diaminobenzidine
DAPI	4',6-diamidino-2-phenylindole
dH ₂ O	deionised molecular biology grade water
DMEM	Dulbecco's modified Eagles media
DMSO	dimethyl sulphoxide
DNA	deoxyribonucleic acid
ds	double-stranded
DV	dengue virus
<i>E.coli</i>	<i>Escherichia coli</i>

EDTA	ethylenediaminetetra-acetic acid
EGF	epidermal growth factor
EIA	enzyme immunoassay
EIF/eIF	eukaryotic translation initiation factor
EM	electron microscopy
EMCV	encephalomyocarditis virus
ER	endoplasmic reticulum
F	Farad(s)
FCS	foetal calf serum
FFU	focus-forming unit(s)
FITC	fluorescein isothiocyanate
FRAP	fluorescence recovery after photobleaching
g	gram(s)
G	gravitational force
GAG	glycosaminoglycan
GFP	green fluorescent protein
GTP	guanosine-5'-triphosphate
h	hour(s)
HAV	hepatitis A virus
HBV	hepatitis B virus
HCC	hepatocellular carcinoma
HCl	hydrochloric acid
HCV	hepatitis C virus
HCV _{cc} (virus)	HCV cell culture-derived virus
HCV-LP	HCV-like particle
HCV _{pp}	HCV pseudoparticles
HCV _{TCP}	<i>trans</i> -complemented HCV particles
HDL	high-density lipoprotein
HIV	human immunodeficiency virus
HL	hydrophobic loop
HRP	horseradish peroxidase
HVR	hypervariable region
IF	indirect immunofluorescence
IFN	interferon
Ig	immunoglobulin

IRES	internal ribosome entry site
IRF3	IFN regulatory factor 3
ISG	IFN-stimulated gene
ITAF	IRES-specific cellular transacting factor
JFH	Japanese fulminant hepatitis
Kan	kanamycin
kb	kilobase pair(s)
kDa	kilodalton(s)
KV	Kunjin virus
l	litre(s)
LCS	low-complexity sequence
LD	lipid droplet
LDL	low-density lipoprotein
LEL	large extracellular loop
LVP	lipoviroparticle
m	milli (10^{-3})
m	metre(s)
M	molar
MAF	membrane-associated foci
MBN	mung bean nuclease
ME	mercaptoethanol
miRNA	micro RNA
mRNA	messenger RNA
MTOC	microtubule organising centre
MTP	microsomal triglyceride transfer protein
n	nano (10^{-9})
N-	amino terminus
NANBH	non-A, non-B hepatitis
NBM	nucleotide-binding motif
Neo/G418	neomycin phosphotransferase
NMD	nonsense mediated decay
NS	non-structural
NTP	nucleoside triphosphate
OCLN	occludin
ORF	open reading frame

PAGE	polyacrylamide gel electrophoresis
PAGFP	photoactivatable GFP
PAMP	pathogen-associated molecular pattern
PAP	protein-A peroxidase
PAT	parenteral antischistosomal therapy
PBS	phosphate-buffered saline
PCR	polymerase chain reaction
PFA	paraformaldehyde
pH	potential of hydrogen
PI	protease inhibitor
PKR	protein kinase R
PSTCD	<i>Propionibacterium shermanii</i> transcarboxylase
PTGS	post-transcriptional gene silencing
PV	poliovirus
QD	quantum dot
qRT-PCR	quantitative real time PCR
RC	replication complex
RdRp	RNA-dependent RNA polymerase
RGB	running gel buffer
RIG-I	retinoic-acid-inducible gene I
RISC	RNA-induced silencing complex
RLU	relative light unit(s)
RNA	ribonucleic acid
RNAi	RNA interference
rpm	revolutions per minute
RSV	respiratory syncytial virus
RTP	ribavirin triphosphate
RT-PCR	reverse transcriptase PCR
s	second(s)
SDS	sodium dodecyl sulphate
SEL	small extracellular loop
SFV	Semliki Forest virus
SGB	stacking gel buffer
SGR	subgenomic replicon
shRNA	short hairpin RNA

siRNA	small inhibitory RNA
SP	signal peptidase
SPP	signal peptide peptidase
SR-BI	scavenger receptor class B member I
ss	single-stranded
STAT-C	specifically targeted antiviral therapy for hepatitis C
SV40	simian virus 40
TCID ₅₀	median tissue culture infective dose
TEMED	N'N'N'N'-tetramethylethylene-diamine
TMA	transcription-mediated amplification
TMD	transmembrane domain
TRBP	TAR RNA-binding protein
TRIS	2-Amino-2-(hydroxymethyl)-1,3-propanediol
TRITC	tetramethyl rhodamine isothiocyanate
TTP	thymidine-5'-triphosphate
UTP	uridine-5'-triphosphate
UTR	untranslated region
UV	ultraviolet
VLDL	very-low density lipoprotein
v/v	volume/volume ratio
wt	wild-type
w/v	weight/volume ratio
YFV	yellow fever virus
YT	yeast tryptose

Abstract

Studies on the hepatitis C virus (HCV) life cycle have been aided by the development of *in vitro* systems that permit replication of the viral RNA genome and virus particle production. However, the exact functions of the viral proteins, particularly those engaged in RNA synthesis, are poorly understood. It is thought that NS4B, one of the replicase components, induces the formation of replication complexes (RCs) derived from host cell membranes. These RCs appear as punctate foci at the endoplasmic reticulum (ER) membrane and incorporate the viral and cellular proteins necessary for HCV RNA synthesis.

To gain insight into the nature of RCs, green fluorescent protein (GFP) was inserted into the coding region of NS5A, one of the HCV-encoded replicase components. The impact of the GFP insertion was examined in the context of a subgenomic replicon (SGR) based on JFH1, a genotype 2a HCV strain that exhibits efficient RNA replication in cell culture. The resulting construct was capable of robust replication and allowed characterisation of NS5A in live cells that synthesised viral RNA. NS5A displayed a diffuse, ER-like distribution and was also observed in foci. These foci are presumed to represent RCs and NS5A was relatively immobile at these sites. This result was confirmed using SGRs harbouring a photoactivatable derivative of GFP (PAGFP). Utilising plasmid-encoded HCV polyproteins, it was apparent that the targeting of NS5A to these structures was dependent on NS4B. Removal of the NS4B coding region resulted in a diffuse, ER-like distribution of NS5A, with little evidence of the protein within RCs. NS5A was mobile under these conditions, suggesting that the dynamics of NS5A are linked to focus formation by NS4B.

To further investigate these findings, a panel of 15 alanine substitutions was constructed in the C-terminal region of NS4B. Transient replication assays revealed that five mutants were incapable of replication, two displayed an attenuated phenotype, and eight exhibited replication levels comparable to the wild-type (wt) genome. Of the five non-replicating mutants, two were defective in their ability to produce foci, while one failed to generate any foci. Thus, the C-terminus of NS4B is important for RC formation. Loss of NS4B foci

correlated with decreased NS5A located in these structures. Furthermore, NS5A hyperphosphorylation was reduced for mutants compromised in foci production. This suggests that the membranous changes induced by NS4B provide a favourable environment for post-translational modifications of NS5A. Interestingly, the remaining two non-replicating mutants displayed no impairment in foci production and the characteristics of NS5A were also unaltered. Therefore, in addition to producing the cellular environment for HCV genome synthesis, NS4B is likely to play a more direct role in RNA replication.

HCV RCs are believed to be relatively enclosed structures that permit limited exchange of materials with the cytoplasm. In support of this hypothesis, previous reports have shown that NS5A is the only replicase component capable of restoring replication to defective genomes when supplied *in trans*. In those studies, SGRs harbouring replication-lethal NS4B mutations could not be rescued by *trans*-complementation. Utilising the five novel non-replicating genomes described above, the potential to *trans*-complement NS4B in transient replication assays was re-examined. Wt protein produced from a functional HCV replicon could *trans*-complement defective NS4B expressed from two of the five mutants. Moreover, active replication could be reconstituted from two defective viral RNAs harbouring mutations within NS4B and NS5A. These findings have important implications for our understanding of RC formation.

Genome-length JFH1 RNA produces infectious virus particles in Huh-7 cells. Using this system, it has become increasingly apparent that some HCV-encoded replication components are also involved in virus assembly and release. To determine whether NS4B had any influence on these latter stages of the virus life cycle, the NS4B mutations that did not block RNA replication were introduced into the full-length JFH1 genome. While the majority of mutants had no effect on virus production, one mutant consistently enhanced infectious virus titres by up to five-fold compared to wt JFH1. Interestingly, introduction of the same mutation into a chimeric J6-JFH1 genome resulted in repressed virion production. Together, these results suggest that NS4B contributes to virus assembly and release in a genotype-specific manner.

In an attempt to identify novel cellular proteins involved in HCV genome replication, a siRNA library targeting 299 nucleotide-binding proteins was screened. For the screen, a robust system was established using two cell lines (derived from Huh-7 and U2OS cells) that replicated tri-cistronic SGRs. While the U2OS cell line supported HCV RNA replication less efficiently compared to Huh-7 cells, this cell type was efficiently transfected with siRNA. Consequently, increased gene-silencing and greater effects on HCV replication were observed in the U2OS cell line. Thus, U2OS cells may be a suitable alternative to Huh-7 cells for HCV-related siRNA studies. For the library screen, all siRNAs were tested in both cell lines, and cell viability measurements allowed specific effects on viral RNA synthesis to be characterised. The screen identified several cellular proteins that enhanced and suppressed HCV RNA replication. This study provides an important framework for more detailed analyses of these proteins in the future.

One and Three Letter Amino Acid Abbreviations

Amino acid	Three letter code	One letter code
Alanine	Ala	A
Arginine	Arg	R
Asparagine	Asn	N
Aspartic acid	Asp	D
Cysteine	Cys	C
Glutamine	Gln	Q
Glutamic acid	Glu	E
Glycine	Gly	G
Histidine	His	H
Isoleucine	Ile	I
Leucine	Leu	L
Lysine	Lys	K
Methionine	Met	M
Phenylalanine	Phe	F
Proline	Pro	P
Serine	Ser	S
Threonine	Thr	T
Tryptophan	Trp	W
Tyrosine	Tyr	Y
Valine	Val	V

Author's Declaration

All work presented in this thesis was obtained by the author's own efforts, unless otherwise stated.

1 Introduction

1.1 Background

1.1.1 Discovery of Hepatitis C Virus

By the early 1970s, specific viral and antigenic markers of hepatitis A virus (HAV) and hepatitis B virus (HBV) had been identified. This led to the development of sensitive serologic tests that allowed the diagnosis of these viruses in patients suffering viral hepatitis. However, a significant number of hepatitis cases in individuals receiving blood transfusion could not be attributed to either HAV or HBV (Feinstone et al., 1975, Prince et al., 1974), and the agent responsible was termed non-A, non-B hepatitis (NANBH).

Inoculation of chimpanzees with plasma or serum from human patients with NANBH resulted in persistent elevated serum alanine aminotransferase (ALT) levels, indicating that the NANBH agent was infectious and capable of establishing a chronic state (Alter et al., 1978, Hollinger et al., 1978). Further work, in which known-infectious human plasma treated with chloroform was inoculated into chimpanzees, showed that the NANBH agent was susceptible to this lipid solvent (Feinstone et al., 1983). In a separate study, human plasma retained its infectivity in chimpanzees following passage through 80nm filters (Bradley et al., 1985). Collectively, these data suggested that the cause of NANBH was a small, enveloped virus. However, further efforts to identify the NANBH agent were hampered by the lack of cell culture models, and the inability to infect animals other than chimpanzees.

The development of sensitive molecular biological techniques in the 1980s eventually led to the discovery of the causative agent of NANBH. Prior to this point in time, conventional immunological methods had failed to identify specific viral antibodies and antigens, which was attributed to a low concentration of viral antigen in NANBH infections (Choo et al., 1989). In an attempt to overcome this limitation, nucleic acids were extracted from infectious material, and a complementary DNA (cDNA) library was generated in bacteriophage (strain λ gt11) to express polypeptides encoded by the cDNA (Choo et al., 1989). Sera derived from patients with documented NANBH were then used to screen the library. A single bacteriophage clone (termed 5-1-1) was identified that expressed a

polypeptide recognised by serum from donors with NANBH, but not by serum derived from control individuals (Choo et al., 1989).

Further experimentation showed that RNA extracted from infected chimpanzee liver hybridised with the cloned cDNA, but to only one of the strands. Furthermore, this signal was not retained upon treatment with ribonuclease (Choo et al., 1989). These data indicated that the infectious agent was a single-stranded RNA (ssRNA) molecule, and nucleotide sequence analysis demonstrated the cDNA strand within 5-1-1 possessed one continuous open reading frame (ORF). The authors concluded that a new virus, named hepatitis C virus (HCV), was the causative agent of NANBH.

1.1.2 Classification and Genotypes of HCV

Analysis of the HCV genome indicated that it was organised in a similar manner to both flaviviruses and pestiviruses, which are members of the *flaviviridae* family (Choo et al., 1991, Miller & Purcell, 1990). However, there was little sequence homology between HCV and these viruses, resulting in classification of HCV to a novel *hepacivirus* genus. Thus, the viruses within the *flaviviridae* family are related by their genome organisation of monopartite, ssRNA genomes of positive polarity, which encode a single polyprotein.

HCV exhibits extraordinary genetic diversity. Comparison of HCV nucleotide sequences recovered from infected individuals across the globe has revealed the existence of six major genetic groups or clades, which differ by 30-35% at the nucleotide level (Simmonds, 2004). This variability is not evenly spread throughout the genome. For example, the viral glycoproteins E1 and E2 display the greatest diversity, whereas the 5' untranslated region (5' UTR) is much less variable (see Section 1.2.2 for more details). The six HCV genotypes can be further subdivided into more closely related subtypes, which differ in nucleotide sequence by 20-25% (Simmonds, 2004). Although it was suggested that more than six HCV genotypes might exist, the current consensus states that the genotypic division should be limited to six (Simmonds et al., 2005). Assignment of strains into a new clade would require the demonstration of consistent phylogenetic grouping that is distinct from any of the currently existing HCV genotypes.

Like all positive-strand RNA viruses, the HCV-encoded RNA polymerase possesses no proofreading or 5'-3' exonuclease activity, and therefore introduces

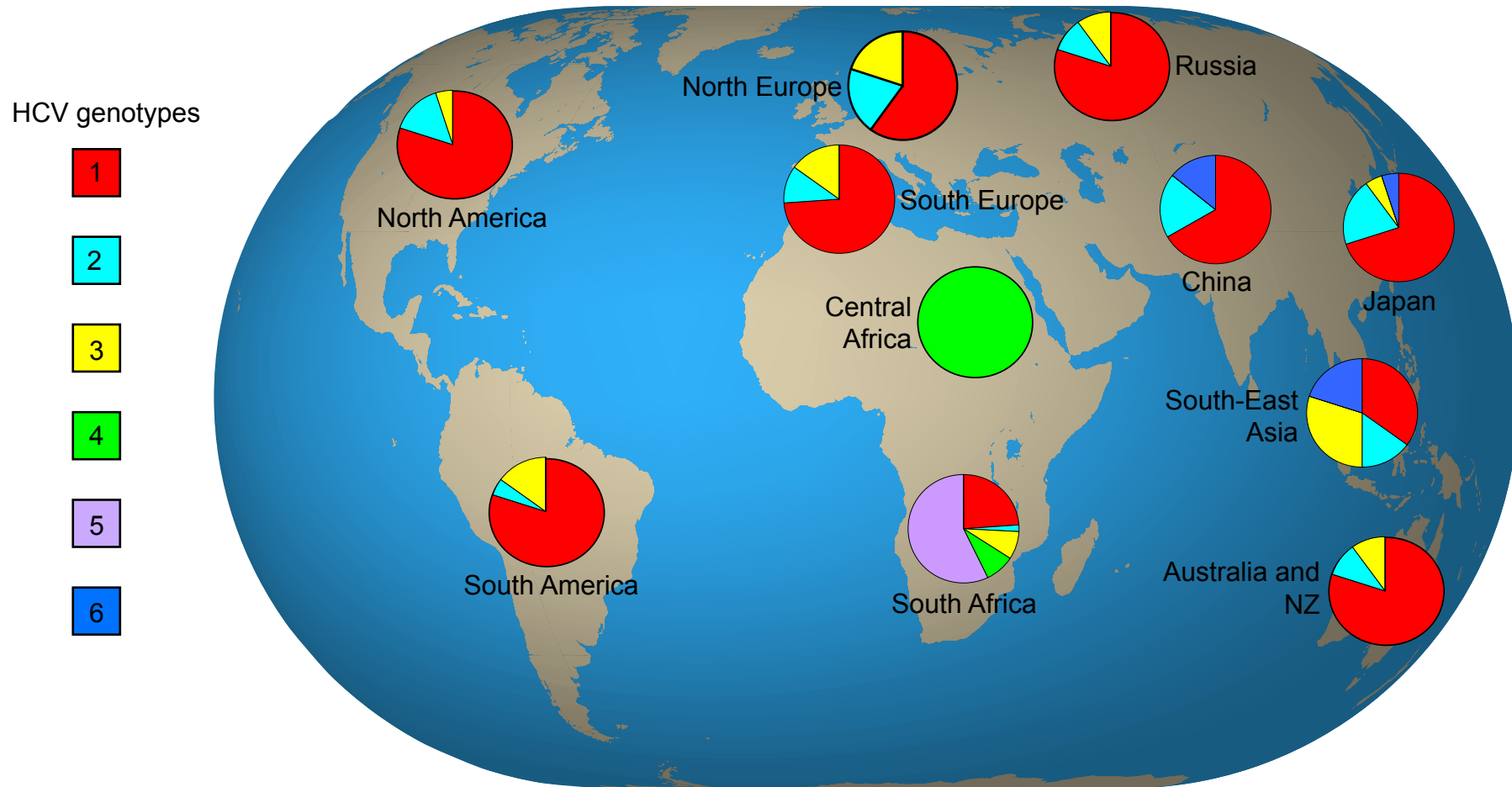


Figure 1.1 Worldwide distribution of the six HCV genotypes

A world map highlighting the distribution of the six HCV genotypes across the globe. Pie charts for each genotype are shown for those regions where information is available.

mutations into the viral genome during replication. Based on comparisons of complete genomes obtained after eight (in chimpanzee) and 13 (in human) years of evolution, it is estimated that the mean frequency of mutation is $\sim 1.4 \times 10^{-3}$ - 1.9×10^{-3} substitutions per nucleotide per year (Ogata et al., 1991, Okamoto et al., 1992). Consequently, not only is there substantial genetic variation between viruses infecting different people, but also between those HCV viruses within individual infected patients. In the infected individual, this heterogeneous spectrum of circulating mutant viruses is referred to as quasispecies (Martell et al., 1992).

1.1.3 HCV Epidemiology and Transmission

The current estimate for the prevalence of HCV infection is $\sim 3\%$ of the world population, equivalent to 170 million people (Thomson, 2009). Precise figures are difficult to determine, since most countries do not routinely screen for HCV infection. Furthermore, most HCV infections are asymptomatic for decades and therefore remain undetected. Although HCV is endemic in most parts of the world, there is a substantial degree of geographic variability in its prevalence. HCV is estimated to infect 0.6% of the population in the UK, but almost 2% of the population in the USA (Thomson, 2009). Fewer data are available for developing countries, where it is considered that HCV prevalence is generally higher. For example, HCV antibodies have been detected in 15-20% of the general population in Egypt (Frank et al., 2000), mainly as a result of parenteral antischistosomal therapy (PAT, see below). Interestingly, the distribution of each HCV genotype can also be mapped geographically (Nguyen & Keeffe, 2005). For instance, the prevalent genotype found in Europe, the USA and China (genotype 1) differs from that predominantly found in countries such as Egypt and Africa (genotype 4), and South Africa (genotype 5). This distribution is represented in Figure 1.1.

Age-specific analysis of prevalence has identified three patterns of HCV transmission (Wasley & Alter, 2000). In countries with the first pattern (such as Australia and USA), the majority of infections are found in individuals between 30 and 49 years of age, indicating that the risk of infection occurred relatively recently (~ 40 years ago) and primarily affected young adults (Armstrong et al., 2006). In countries with the second pattern (such as Japan, China and parts of Europe including Italy and Spain), most infections are found in older individuals, suggesting that the risk of HCV infection in these countries was greatest in the past, ~ 40 -60 years ago (Campello et al., 2002, Dominguez et al., 2001, Zhang et

al., 2005). In countries with the third pattern (such as Egypt), the prevalence of HCV infection increases with age, and high rates of infection are found in all age groups (Frank et al., 2000). This pattern of infection suggests an increased risk in the past in addition to an ongoing risk of infection (Wasley & Alter, 2000). Much of this regional variability can be attributed to the frequency and extent to which different risk factors have contributed to HCV transmission.

HCV infection occurs by direct percutaneous exposure to blood, mainly in the form of transfusion of blood products from infected donors, unsafe therapeutic injections, and injecting drug use (Shepard et al., 2005). Since the introduction of donated blood screening by antibody and nucleic acid testing, new cases of transfusion-associated HCV infection have been virtually eliminated (Lemon et al., 2007). However, transmission via this route remains a problem in countries where screening practices are not common. Indeed, unsafe medical practice in general still accounts for a large degree of HCV infections. One study estimated that in 2000, 2 million cases of HCV infection were caused worldwide via contaminated medical injections (Hauri et al., 2004). Similarly, the high prevalence of HCV in Egypt can be mostly attributed to poor medical practice, including the PAT campaign, where many people became infected with HCV due to reuse of glass syringes (Frank et al., 2000). Needle-stick injuries, as well as improper cleaning and disinfection of medical equipment can also contribute to HCV transmission. In developed countries, including the UK, USA and Australia, injecting drug use accounts for most newly acquired HCV infections (Thomson, 2009). For example, 90% of those diagnosed with HCV in Scotland in 2003 had injected drugs (Hutchinson et al., 2005). HCV infection has also been attributed to perinatal transmission and sexual activity, although studies on both of these routes of transmission have provided inconsistent results.

1.1.4 Clinical Features of HCV Infection

The predominant site for HCV infection and replication is the liver. The virus is a major cause of end-stage liver disease and hepatocellular carcinoma (HCC), and is now the most common indication for liver transplantation (Sharma & Lok, 2006). HCV frequently establishes a chronic infection following an acute infection. Both conditions are described in the following sections.

1.1.4.1 Acute HCV Infection

Following exposure to HCV, the majority of individuals exhibit mild or no symptoms, meaning that acute infections are rarely recognised and diagnosed (Thomson, 2009). However, some patients may display malaise, fatigue, nausea and sometimes jaundice, although without the use of specific testing, such symptoms could also be attributed to hepatitis A or B infections. While fulminant hepatitis (characterised by a severe acute phase, potentially causing liver failure) can occur during acute infection, this condition is rare. Despite the asymptomatic profile of HCV infection, elevated ALT levels can be detected in the majority of cases (Lemon et al., 2007). Acute HCV infection will resolve spontaneously in ~15-30% of infected individuals, although the exact mechanisms underlying viral clearance are currently uncertain. Major contributing factors are likely to include host and environmental factors (such as age, sex and alcohol intake), viral load and, particularly, the vigour of the infected individual's immune response (Lemon et al., 2007). Patients with acute resolving hepatitis typically mount an early, multi-specific T-cell response, whereas patients displaying weak and inefficient immune responses tend to develop persistent HCV infection (see Section 1.1.5).

1.1.4.2 Chronic HCV Infection

The majority (~70-85%) of individuals infected with HCV will develop a chronic infection, typically characterised by a long period in which symptoms are absent. During this stage, there is usually a continuing and constant viremia, although not as high as that found during the acute phase of infection. Nonetheless, it is estimated that $\sim 10^{12}$ virions are produced daily in a chronically infected person (Neumann et al., 1998). Chronically infected patients may remain symptomless for 35 years or more, but can eventually develop serious liver disease including steatosis (fat accumulation in the liver), hepatic fibrosis (resulting from sustained inflammation) and compensated and decompensated cirrhosis (Lemon et al., 2007). ~20% of chronically infected patients will develop liver cirrhosis over a 20-year period, although this estimate is highly variable (Ishii & Koziel, 2008). While the liver is able to function in compensated cirrhosis, this is not the case for decompensated cirrhosis. Such pathologies can lead to complications including portal hypertension (a block of blood flow into the liver, causing bleeding) and hepatic encephalopathy (where toxin-filtration is compromised, possibly leading to attention deficiency and confusion, Thomson & Finch, 2005). HCC is a late

consequence of HCV infection, and develops in ~0-3% of cirrhotic patients per year (Ishii & Koziel, 2008). Decompensated cirrhosis and HCC are life threatening, although progression to such serious disease states is difficult to predict in the individual patient.

Whereas some DNA viruses are able to integrate their genomes into the host cell genome resulting in tumour formation, HCV is a RNA virus and therefore confined to the cytoplasm of cells. Therefore, it is generally thought that HCC arises from HCV-induced cirrhosis and long-term inflammatory responses that cause oxidative stress, potentially damaging cellular DNA (Okuda et al., 2002). Other evidence suggests that HCV-encoded proteins, such as core, may be directly oncogenic (Moriya et al., 1998). Interestingly, distinct HCV genotypes exhibit differences in their ability to establish long-term infections that lead to liver disease (Zein, 2000). For example, genotype 3 HCV strains are associated with prominent hepatic steatosis, and have lower tendency to cause chronic infections compared to genotype 1 strains (Lehmann et al., 2004, Rubbia-Brandt et al., 2000).

1.1.5 Immunological Response to HCV Infection

The immune response to virus infection can be broadly divided into two categories, the humoral immune response (governed by B-lymphocytes) and the cell-mediated immune response (governed by T-lymphocytes).

B-lymphocytes are responsible for producing antibodies involved in the humoral immune response. Following HCV infection, viral RNA can typically be detected 1-2 weeks after infection, and HCV-specific antibodies can be detected by ~7-8 weeks (Pawlotsky, 1999). Antibodies against NS3, core and the envelope glycoproteins are usually first to appear, and the hypervariable region 1 (HVR1) of E2 (see Section 1.2.2.3) is thought to be a major target for antibodies (Orland et al., 2001). Antibodies are capable of neutralising HCV infection since infectivity in chimpanzees can be neutralised by *in vitro* antibody treatment (Farci et al., 1994). In this study, HCV (obtained from a patient with acute infection) was mixed with seropositive plasma from a chronically infected patient *in vitro*. Upon inoculation of this mixture into chimpanzees, no infectivity was observed (Farci et al., 1994). By comparison, chimpanzees inoculated with HCV mixed with seronegative plasma did develop an infection. These results suggest that antibodies are capable of preventing HCV infection. Experiments using HCV pseudoparticles (see Section 1.3.1.2) have shown that HCV-specific neutralising antibodies possess cross-

reactivity, meaning they can prevent infection with pseudoparticles harbouring homologous and heterologous HCV glycoproteins (Bartosch et al., 2003a, Meunier et al., 2005, Meunier et al., 2008). However, anti-HCV antibodies do not prevent reinfection of chimpanzees or humans (Bowen & Walker, 2005). Furthermore, HCV clearance has been associated with a lack of antibody production in chimpanzees (Cooper et al., 1999) and an absence of seroconversion in humans (Post et al., 2004). Hence, it appears that antibodies do play a role in the neutralisation of HCV but it is probable that other immune mechanisms contribute to viral clearance.

T-lymphocytes such as helper T-cells ($CD4^+$) and cytotoxic T-cells ($CD8^+$) act in concert to regulate the cell-mediated immune response. A pattern of poorly controlled viremia can predict persistence in HCV-infected patients and this can be attributed (at least in part) to ineffective $CD4^+$ and $CD8^+$ T-lymphocyte responses (Missale et al., 1996, Thimme et al., 2001). This poor response can result from insufficient production of these cells, or a response that is maintained for too short a duration (Bowen & Walker, 2005). In contrast, vigorous, sustained and broadly directed $CD4^+$ and $CD8^+$ responses have been associated with a self-limiting course of infection (Missale et al., 1996, Thimme et al., 2001). It is thought that the $CD4^+$ response is particularly important, since HCV-specific antibodies and $CD8^+$ T-lymphocytes are able to develop in the absence of $CD4^+$, yet cannot control viremia (Kaplan et al., 2007). $CD8^+$ T-lymphocytes are capable of targeting infected cells displaying viral epitopes, but also modulate infection by producing cytokines such as interferon (IFN)- γ and tumour necrosis factor (TNF). These cytokines are important for the clearance of several viruses (Guidotti & Chisari, 2001), although little insight into $CD8^+$ -mediated clearance of HCV currently exists. There is evidence that $CD8^+$ T-lymphocytes can be impaired for IFN - γ production during acute and chronic HCV infection, possibly representing a mechanism by which the virus establishes persistence (Ishii & Koziel, 2008).

1.1.6 Diagnosis of HCV Infection

HCV infection can be diagnosed utilising both serological and virological assays, which are described in the following sections.

1.1.6.1 Serological Assays

Serological assays are performed using an enzyme immunoassay (EIA) to detect antibodies targeting various HCV epitopes. The presence of anti-HCV antibodies is then revealed by anti-antibodies labelled with an enzyme, which catalyses the conversion of a substrate into a coloured compound that can be measured. The degree of colour change is proportional to the level of antibody present in the plasma/serum sample (Pawlotsky, 2002). This method can be used for genotype determination, via the detection of antibodies targeting genotype-specific HCV epitopes.

1.1.6.2 Virological Assays

Virological assays for the detection of HCV RNA permit both qualitative and quantitative analysis of viral load. These tests are more beneficial than serological assays since they can detect virus before antibodies are produced. Following extraction from plasma/serum, RNA is reverse-transcribed into cDNA, which is amplified by the polymerase chain reaction (PCR) to generate double-stranded DNA (dsDNA) copies, or by transcription-mediated amplification (TMA) to produce ssRNA copies (Chevaliez & Pawlotsky, 2007). These methods give a qualitative measure of HCV RNA. Quantitative analysis of RNA load can be determined using RT-PCR or signal amplification methods such as the branched DNA (bDNA) assay. bDNA assays use ssDNA oligonucleotides harbouring enzymes that catalyse colour change, which bind to HCV RNA molecules by hybridisation. Unlike RT-PCR, this technique requires no reverse transcription step. Similar to serological assays, virological assays can determine HCV genotype using PCR primers that bind well-characterised polymorphisms in the 5' UTR (Lemon et al., 2007).

1.1.7 Treatment of HCV Infection

Currently there is no vaccine for HCV and this topic remains highly challenging due to the heterogeneity of the virus, the tendency of HCV to promote chronic infection, and the uncertainty concerning protection from re-infection upon further exposure to the virus (Houghton & Abrignani, 2005). For those patients who develop decompensated cirrhosis and HCC, liver transplantation is the only available treatment. However, reinfection of the graft typically occurs due to

circulating HCV in the blood (Terrault & Berenguer, 2006), and is associated with a more rapid progression of cirrhosis within 5-10 years of transplantation (Berenguer et al., 2000).

1.1.7.1 Treatment of Infection by IFN- α and Ribavirin Combination Therapy

At present, the standard treatment for HCV infection is a combination of pegylated IFN- α and ribavirin. Originally, monotherapy with IFN was administered to patients but 12-18 month treatment periods (3 million units of IFN administered three times a week) eliminated the virus in only 20-30% of individuals (Poynard et al., 1996). However, the conjugation of polyethylene glycol to IFN improves the half-life of the molecule, allowing treatment administration to be reduced to once per week (Heathcote et al., 2000, Zeuzem et al., 2000). It was originally found that ribavirin monotherapy had little activity against HCV infection (Di Bisceglie et al., 1992). Surprisingly, by combining ribavirin treatment with pegylated IFN- α administration, sustained viral responses can be achieved in ~40-50% of patients with genotype 1 infections, and in 70-80% of patients with genotype 2 or 3 infections (Soriano et al., 2009). To date, combination therapy provides the most effective HCV treatment. Unfortunately, as well as the limited response rate in treated patients, therapy is costly, and can cause severe side effects including myalgia, fever, headaches, haemolytic anaemia and severe depression (Fried et al., 2002). Consequently, more effective and better-tolerated therapies to treat HCV infection are urgently required.

The mechanism by which IFN administration exerts a therapeutic effect against HCV infection is unknown. The type-1 IFNs (IFN- α , β , ω , and λ) are host cell-synthesised proteins that play crucial roles in the innate antiviral immune response, and have antiviral, antiproliferative, and immunomodulatory activities (Sen, 2001). IFN- α does not target HCV in a virus-specific manner but acts by inducing the expression of IFN-stimulated genes (ISGs), which establish an antiviral state within cells (Feld & Hoofnagle, 2005). However, the IFN pathway is complex and it is not known which of the many ISGs induced by IFN is/are responsible for inhibiting HCV.

Like IFN treatment, the anti-HCV mechanism of ribavirin is also not understood. Ribavirin is a guanosine analogue, and is processed within the cell to form phosphorylated forms of ribavirin. It is hypothesised that the viral polymerase may

misincorporate ribavirin triphosphate (RTP) during RNA synthesis, leading to premature chain termination (Feld & Hoofnagle, 2005). However, ribavirin has also been suggested to act as a viral mutagen, since treatment appears to increase the rate at which errors are introduced into the viral genome during replication in cell culture (Contreras et al., 2002, Tanabe et al., 2004). It has been hypothesised that such a mechanism (termed 'error catastrophe') may be able to abolish a population of HCV quasispecies within the infected host (Crotty et al., 2001), although this proposal is controversial.

1.1.7.2 Potential Future Therapies

Major research efforts are focused on the production of STAT-C (specifically targeted antiviral therapy for hepatitis C) compounds that can specifically and directly target the HCV life cycle. Optimally, novel HCV therapies should be less toxic and more effective, yet permit a shorter duration of therapy compared to the current standard of treatment. However, drug resistance still presents the major hurdle for all newly developed treatments due to the vast number of quasispecies generated during the course of infection, which allow rapid viral adaptation to the selective pressure of the antiviral drug. Therefore, therapies should preferably target all viral variants, in addition to preventing the emergence of resistant viruses (De Francesco & Migliaccio, 2005). The most popular targets for small-molecule inhibitors are the NS3/4A serine protease and the NS5B RNA polymerase (see Section 1.2.2 for more details).

Viral replication requires cleavage of the viral polyprotein, a function performed (although not exclusively) by the NS3/4A serine protease. Protease inhibitors (PIs) that target this activity are currently under development, one of the most promising of which is the compound telaprevir (VX-950). Telaprevir is a reversible inhibitor of the NS3/4A protease, and treatment of cell lines harbouring HCV genomes could eliminate viral RNA (Lin et al., 2006). In phase II clinical trials, triple therapy (pegylated IFN- α , ribavirin and telaprevir) achieved sustained virological responses of 62% in treated individuals and, interestingly, the presence of ribavirin in the therapy reduced the risk of emerging telaprevir-resistant HCV strains (Soriano et al., 2009). Skin rashes, nausea and anaemia are the main side effects of telaprevir. This compound is currently undergoing phase III clinical trials.

The HCV polymerase is essential for replication of viral RNA and has therefore been a major target for drug development. The types of polymerase inhibitors

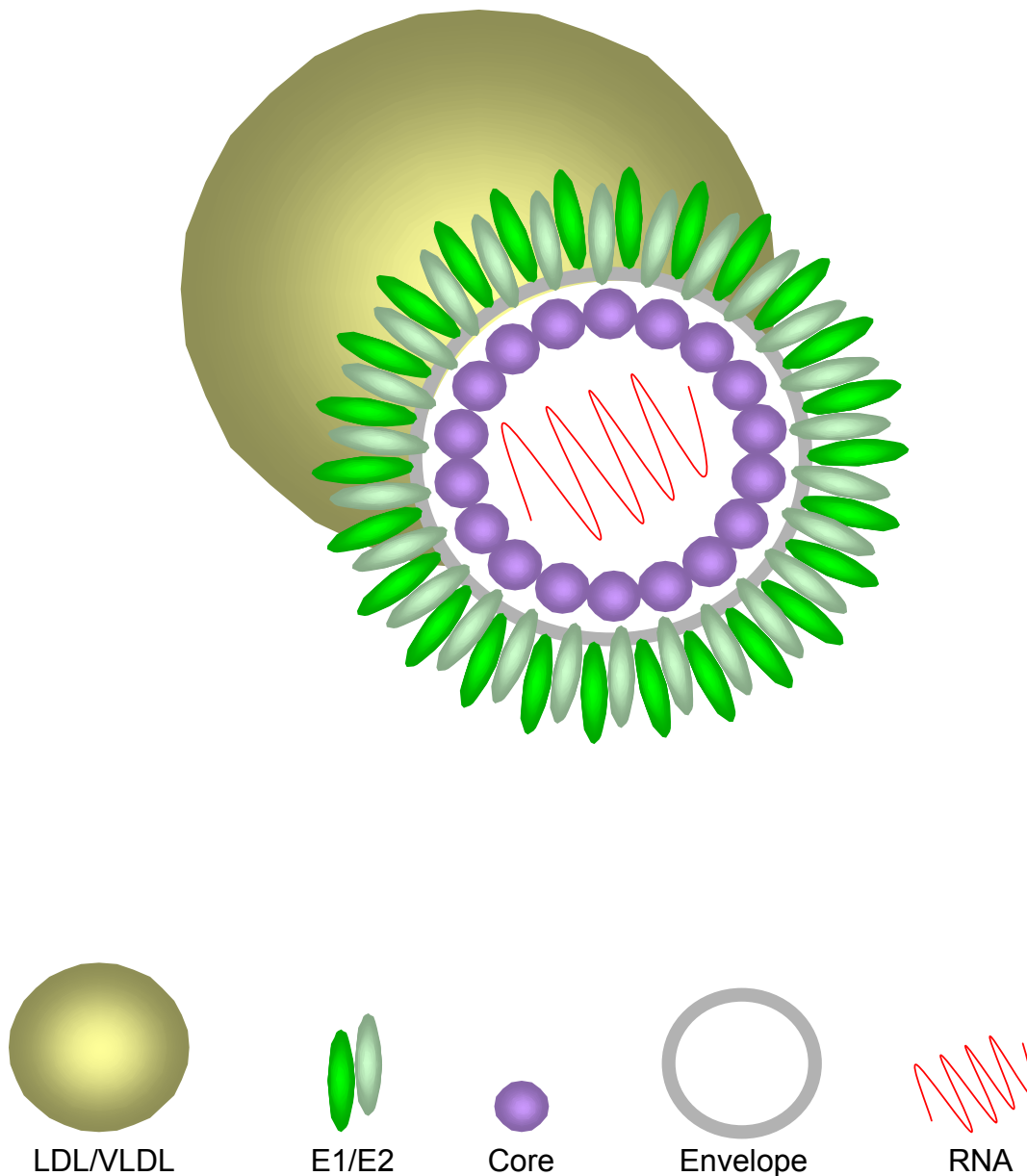


Figure 1.2 The HCV virion

A representation of a HCV particle (top) and its components (bottom). The single-stranded RNA genome is enclosed within the capsid, presumed to be composed of core protein. An envelope derived from host cell membranes surrounds the viral capsid and the HCV glycoprotein E1/E2 heterodimers are embedded within it. The virion is approximated to be 50-65nm in diameter and is proposed to complex with LDL/VLDL, resulting in the generation of a lipoviroparticle (LVP). □

currently being developed include nucleoside analogues (chain terminators) and non-nucleoside analogues (allosteric inhibitors). R-1626 is a nucleoside analogue, which is converted into R-1479 within the intestinal mucosa. Due to the high conservation of the NS5B nucleotide-binding site, R-1479 possesses potent antiviral activity against all HCV genotypes *in vitro* (Soriano et al., 2009). During phase II trials however, R-1626 caused severe neutropenia (a low white blood cell count), and a high rate of HCV infection relapse occurred after completion of therapy (Pockros et al., 2008). Consequently, development of R-1626 was halted at the end of 2008. Currently, no non-nucleoside analogue polymerase inhibitors have reached advanced stages of clinical development.

1.2 Molecular Features of HCV

1.2.1 Virion Morphology

Due to the difficulties involved in isolating pure HCV particles, physicochemical data for HCV virions is lacking. HCV RNA-containing particles from infected individuals circulate complexed with very low- and/or low-density lipoproteins (VLDLs and LDLs), which are particles that export cholesterol and triglyceride from hepatocytes in the liver (Andre et al., 2002, Nielsen et al., 2006). Recent data suggest that the processes of HCV assembly and release are tightly coupled to VLDL production (see Section 1.4.4.2). The entities resulting from combination of HCV with LDL/VLDLs have been referred to as lipoviroparticles (LVPs).

Beside lipoprotein, the HCV virion is thought to contain three virus-encoded components (Figure 1.2). These are a RNA genome, a capsid and envelope glycoproteins. The viral core protein comprises the capsid (see Section 1.2.2.2) and this structure harbours the HCV genome. The envelope (a lipid layer derived from host cell membranes) surrounds the capsid and contains the viral glycoproteins E1 and E2 (see Section 1.2.2.3). It has been proposed that following assembly at lipid droplets (LDs), HCV nucleocapsids bud through endoplasmic reticulum (ER) membranes, acquiring an envelope and surface glycoproteins in the process (Roingard et al., 2008). However, the exact mechanism by which nascent virus particles traffick from LDs and acquire lipoprotein components en route to the cell surface is currently unknown.

Electron microscopy (EM) analysis of virus particles produced in cell culture indicate that HCV has an inner ring of 30-35nm (thought to be the capsid) and an

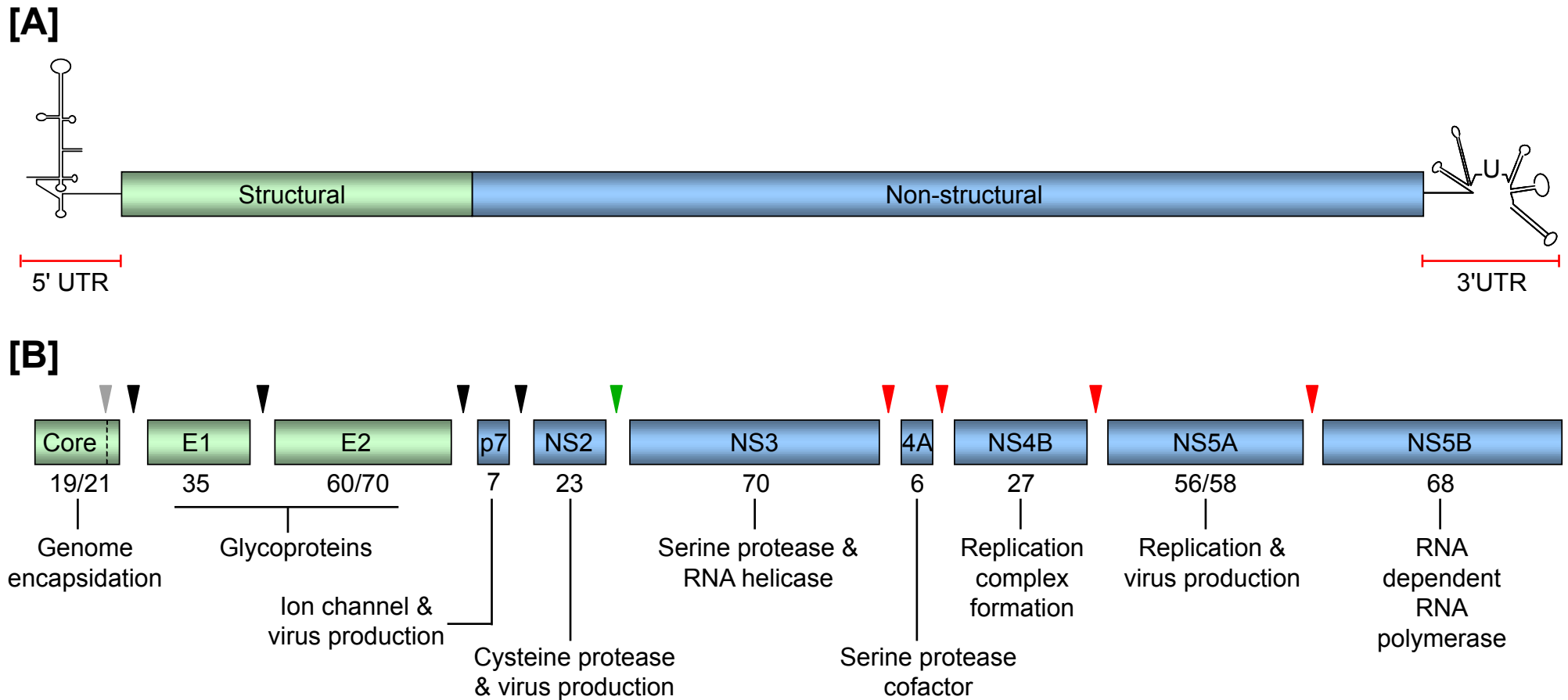


Figure 1.3 The HCV genome and encoded viral proteins

[A] Schematic representation of the HCV genome. The single open reading frame (ORF) is shown and the structural and non-structural (NS) protein coding regions are depicted. The RNA is flanked by two untranslated regions (UTRs) at the 5' and 3' ends. The viral RNA is translated to generate a single polyprotein. **[B]** Following and during translation, the polyprotein is processed by host and viral proteases to generate the individual HCV proteins. Two host proteases, signal peptidase (SP, black arrowheads) and signal peptide peptidase (SPP, grey arrowhead), generate the structural proteins and p7. The NS2/NS3 protease (green arrowhead) and NS3 serine protease (red arrowheads) cleave the indicated protein interfaces. The role and size (kDa) of each protein is indicated.

overall diameter of 50-65nm (Wakita et al., 2005). These particles are similar in size to those observed *in vivo*, in both infected chimpanzees (Shimizu et al., 1996) and human serum (Kaito et al., 1994). Interestingly, intracellular virus particles exhibit a buoyant density (1.15-1.20 g/ml) that is higher than that observed for secreted virions (1.03-1.16 g/ml) (Gastaminza et al., 2006). Thus, the biochemical composition of HCV particles appears to be modified during viral egress, a likely consequence of the aforementioned association with lipoprotein components (Andre et al., 2002, Nielsen et al., 2006).

1.2.2 The Viral Genome

The HCV genome is a 9.6kb ssRNA molecule of positive polarity, and encodes a single ORF flanked by 5' and 3' UTRs. Translation of the RNA genome produces a polyprotein of 3010 amino acids (for the genotype 1a consensus strain H77, although this figure can vary between strains). Host and viral proteases process the polyprotein precursor to yield the structural (core, E1 and E2) and non-structural (NS) proteins (NS2, NS3, NS4A, NS4B, NS5A and NS5B, see Figure 1.3). Cleavage also produces p7, a protein that is currently unassigned to either category, although recent work suggests that p7 may be a virion component (Griffin et al., 2008).

1.2.2.1 The 5' UTR

The 5' UTR is a highly conserved sequence consisting of 341 nucleotides that contributes towards replication and translation of the viral genome (Friebe et al., 2001, Honda et al., 1999). The 5' UTR harbours an internal ribosome entry site (IRES), a RNA structure that is responsible for initiating cap-independent translation of viral RNA. Here, the only eukaryotic translation initiation factors required are eIF2 and eIF3 (Ji et al., 2004). Structural analyses of the IRES suggest that it contains four distinct domains (termed I-IV, Honda et al., 1996a). Domain I forms a small, stem-loop structure that is dispensable for overall IRES activity but may have a regulatory role in translation efficiency (Honda et al., 1996b). Domains II and III are essential for genome translation, since they directly contact and position the small (40S) ribosomal subunit at the AUG codon for core protein (Honda et al., 1996a and 1996b). The 3' end of the 5' UTR and the 5' end of the core coding region form domain IV of the IRES (Honda et al., 1996a and

1996b). While domain IV is not required for ribosome binding, the structural stability of this region is inversely proportional to translation efficiency (Honda et al., 1996a). Thus, all regions of the IRES are essential for, or at least contribute to HCV translation. Additionally, the 5' UTR is essential for replication. For example, domains I and II are sufficient for viral RNA synthesis, although the efficiency of this process is enhanced by the presence of the complete 5' UTR (Friebe et al., 2001, Kim et al., 2002).

A variety of host-encoded factors associate with the HCV 5' UTR and regulate both replication and translation of the viral genome. For example, polypyrimidine tract binding protein (PTB), La autoantigen and poly (rC)-binding protein (PCBP2) all bind to regions within the 5' UTR (Ali & Siddiqui, 1995, Ali & Siddiqui, 1997, Fukushi et al., 2001). Each of these factors is capable of influencing viral RNA replication, while PTB and La autoantigen are also necessary for translation (Domitrovich et al., 2005, Fukushi et al., 2001). Recently, the liver-specific microRNA-122 (miR-122) was shown to bind two locations within the unstructured region between domains I and II of the 5' UTR sequence and this binding is essential for both viral RNA replication (Jopling et al., 2008, Jopling et al., 2005) and translation (Henke et al., 2008).

1.2.2.2 Core

The core coding region is found at the very N-terminus of the HCV polyprotein and is presumed to form the viral capsid into which the viral genome is packaged (McLauchlan, 2009). Upon translation, core (and the nascent polypeptide chain) is targeted to the ER membrane by a signal peptide located between core and E1, which is cleaved by the cellular enzyme signal peptidase (SP) to liberate E1 and generate the immature (21kDa) form of core (Santolini et al., 1994). Subsequently, core undergoes a second cleavage event mediated by cellular signal peptide peptidase (SPP), giving rise to the mature (19kDa) species of core (Hussy et al., 1996, McLauchlan et al., 2002). This SPP-mediated cleavage event is essential for trafficking of core to LDs, the presumed site for initiation of virus assembly (McLauchlan et al., 2002, Miyanari et al., 2007).

The mature form of core is a dimeric α -helical protein that consists of two domains termed D1 and D2. D1 harbours positively-charged residues and is involved in RNA binding (Boulant et al., 2005). D2 is essential for the trafficking of core to LDs and deletions within this region can block the association of core with LDs (Hope &

McLauchlan, 2000). Structural analysis of D2 has revealed the presence of two amphipathic α -helices (termed HI and HII), separated by an unstructured region referred to as the hydrophobic loop (HL, Boulant et al., 2006). The hydrophobic residues within each helix are likely to interact with the phospholipid layer surrounding LDs, since mutation of these residues can abolish core-LD association (Boulant et al., 2006).

Core protein is essential for virus production, as demonstrated by a recent mutagenic analysis (Murray et al., 2007). Furthermore, the D2-mediated association of core with LDs is necessary for this process (Boulant et al., 2007, Miyanari et al., 2007) and the loading of core onto LDs over time coincides with increased virus production (Boulant et al., 2007). Interestingly, mobility studies using GFP-D2 fusion proteins revealed that the D2 domain of two HCV genotypes differed in their mobility (Shavinskaya et al., 2007). Lower GFP-D2 mobility is presumed to indicate tighter binding of the GFP fusion protein with LDs. Since the HCV genotype that possessed lower D2 mobility released more virus, it was proposed that enhanced virus production is associated with a tighter core-LD interaction (Shavinskaya et al., 2007). The essential nature of core-LD association has also been demonstrated by studies on SPP cleavage. Here, mutation of the signal peptide at the C-terminal end of immature core, or reduction of enzymatically active SPP by inhibitor or small inhibitory RNA (siRNA) treatment prevented the trafficking of core to LDs, consequently reducing viral titres (Okamoto et al., 2008, Targett-Adams et al., 2008b). Thus, fully mature core is required for efficient viral particle assembly.

1.2.2.3 E1 and E2

E1 (35kDa) and E2 (60/70kDa) are glycoproteins that are thought to reside on the envelope of viral particles, forming non-covalent heterodimers that are essential for virus entry (Dubuisson, 2007). Both proteins harbour a single C-terminal transmembrane domain (TMD) that anchors the proteins to the ER membrane (Cocquerel et al., 1999, Cocquerel et al., 1998), resulting in the N-termini being orientated in the ER lumen. The TMDs are composed of two hydrophobic regions that are separated by at least one invariant charged residue (Cocquerel et al., 2000). During translation, E1 is directed to the ER membrane by the signal peptide residing within the C-terminus of core, where SP-mediated cleavage subsequently produces the N-terminus of E1 (Dubuisson et al., 2002). Similarly, the TMD of E1

acts as a signal sequence that targets E2 to the ER membrane and further SP-mediated cleavage at the E1/E2 and E2/p7 boundaries releases both glycoproteins from the adjacent polyprotein (Dubuisson et al., 2002). Importantly, the TMDs of E1 and E2 also facilitate E1/E2 heterodimer formation (Op De Beeck et al., 2000), as well as the fusion properties of both proteins (Ciczora et al., 2007). E1 and E2 contain up to five (E1) and eleven (E2) conserved glycosylation motifs that undergo N-linked glycosylation upon retention of both proteins within the ER (Goffard & Dubuisson, 2003). This modification is believed to aid glycoprotein folding and facilitate HCV entry (Goffard et al., 2005).

Analysis of several HCV isolates revealed two hypervariable regions within E2, termed HVR1 and HVR2 (Weiner et al., 1991). HVR1 is located at the N-terminus of E2 and the variability of this region can be attributed to (i) the ability of this region to tolerate amino acid substitutions and (ii) the strong selective pressures exerted on HVR1 by the host immune response (Penin et al., 2001). Indeed, antibodies targeting HVR1 epitopes change during the course of chronic infection, indicating selective immune pressure upon this region (Forns et al., 1999). Despite this variability, sequence analysis has demonstrated that the overall conformation and physicochemical properties of HVR1 are conserved, revealing a basic stretch of residues that may be involved in binding other proteins, lipids or glycosaminoglycans (GAGs, Penin et al., 2001). Furthermore, mutation of the basic residues within HVR1 reduces virus entry, although this has no apparent effect on glycoprotein-receptor binding (Callens et al., 2005). Therefore, HVR1 may facilitate viral entry.

The E1/E2 heterodimer is essential for virus entry and E2 binds to three cellular receptor proteins; scavenger receptor class B member I (SR-BI), occludin (OCLN) and CD81 (Liu et al., 2009, Pileri et al., 1998, Scarselli et al., 2002). An interaction between HCV glycoproteins and the entry co-receptor claudin-1 (CLDN1) has yet to be demonstrated, although this is likely since knockdown of CLDN1 inhibits HCV entry (Evans et al., 2007). Utilising antibodies or compounds that target E1/E2 have confirmed the role of these glycoproteins in virus entry. For example, cyanovirin-N (CV-N) can inhibit HCV entry by interacting with the N-linked glycans present on both glycoproteins, thereby inhibiting the E2-CD81 interaction (Helle et al., 2006).

1.2.2.4 p7

p7 is a hydrophobic 7kDa protein located between the E2 and NS2 proteins of the HCV polyprotein. During translation, p7 is directed to the ER membrane where SP cleaves the protein from E2 and NS2 (Lin et al., 1994a). However, cleavage events at the E2-p7 and p7-NS2 junctions are delayed (and in the case of the latter, incomplete), leading to the production of E2-p7-NS2 and E2-p7 precursor proteins (Dubuisson et al., 1994, Lin et al., 1994a). These precursors have no apparent role in virus production, although their significance cannot be dismissed (Jones et al., 2007). p7 harbours two TMDs (TM1 and TM2) connected by a cytoplasmic loop, and exhibits a double-spanning topology whereby the N- and C-termini are orientated towards the ER lumen and the loop is located within the cytoplasm (Carrere-Kremer et al., 2002, Patargias et al., 2006).

p7 has no obvious function in viral RNA replication (Lohmann et al., 1999), but injection of viral RNAs harbouring p7 deletions into chimpanzees has shown that the protein is essential for HCV infectivity *in vivo* (Sakai et al., 2003). It has since been demonstrated that viral RNA genomes lacking p7 are incapable of producing infectious virus in cell culture and furthermore, that this block occurs prior to the assembly of HCV virions (Jones et al., 2007, Steinmann et al., 2007). Adaptive mutations in p7 can enhance virus production (Russell et al., 2008) and studies utilising chimeric viruses have also implicated p7 as being a virulence factor that may influence viral fitness (Steinmann et al., 2007).

p7 has been classified as a member of the viroporin protein family, since it can form hexameric structures that exhibit cation channel activity in artificial membranes (Griffin et al., 2003, StGelais et al., 2007). The ion channel activity of p7 is essential for HCV infectivity in chimpanzees (Sakai et al., 2003) and relies on the cytoplasmic loop of the protein (Griffin et al., 2004). p7 function can be inhibited by amantadine, a compound that blocks ion channels and has previously been used to reduce influenza A-encoded M2 ion channel activity (Fleming, 2001). The sensitivity of p7 to amantadine and other ion channel inhibitors is genotype-dependent (Griffin et al., 2008), therefore more potent compounds that can inhibit multiple p7 sequences would be required if this protein were to be a target for anti-HCV therapy.

1.2.2.5 NS2

NS2 is a 23kDa protein harbouring multiple membrane-spanning domains that localise the protein to the ER membrane (Santolini et al., 1995, Yamaga & Ou, 2002). Crystallography of the NS2 C-terminal region, which contains a protease domain, revealed a globular structure that is thought to reside on the cytosolic side of the ER membrane, whereas the N-terminus of NS2 is predicted to contain three TMDs (Lorenz et al., 2006). Of these TMDs, only the first has been structurally characterised and consists of a flexible helical element connected to a stable α -helix (Jirasko et al., 2008). Further studies are required to define the exact topology of NS2 at the ER membrane.

The NS2 protein is responsible for autoproteolytic cleavage at the NS2/NS3 junction (Grakoui et al., 1993b, Hijikata et al., 1993), while the N-terminus of NS2 is liberated by SP-mediated cleavage of the signal peptide at the C-terminus of p7 (Lin et al., 1994a). Mutagenic analyses have demonstrated that cleavage of the NS2/NS3 junction requires the NS3 serine protease domain but not its enzyme activity (Grakoui et al., 1993b, Hijikata et al., 1993). The structural integrity of the NS3 serine protease domain relies on its ability to bind a zinc atom (De Francesco et al., 1996) and NS2/NS3 protease activity is enhanced by zinc but inhibited by metal chelating agents such as EDTA (Pieroni et al., 1997). It is therefore likely that NS3 contributes structurally towards NS2/NS3 protease activity.

Although NS2 is dispensable for viral RNA replication (Lohmann et al., 1999), recent studies have revealed a key role for NS2 in the production of infectious virus particles. The use of chimeric viral genomes containing the NS3-NS5B region from HCV strain JFH1, coupled with the structural genes from other genotypes, have shown that the position of the intra/inter-genotypic junction within NS2 affects infectious particle production (Pietschmann et al., 2006). For most chimeras, a junction between the first and second TMDs is optimal, indicating that interactions between the N-terminus of NS2 and p7 or the structural proteins is important for virus production (Pietschmann et al., 2006). Additionally, cell culture adaptive mutations (CCAMs) that enhance virus production have been found within the NS2 coding region (Russell et al., 2008, Yi et al., 2007). Finally, full-length NS2 is important for the production of virus particles, although the proteolytic function of the protein is dispensable in the virus assembly pathway (Jirasko et al., 2008, Jones et al., 2007). Like p7, NS2 apparently functions at a step prior to the assembly of infectious HCV particles (Jones et al., 2007).

1.2.2.6 NS3

NS3 is a multifunctional 70kDa protein that features a N-terminal serine-type protease, while the C-terminal two-thirds of the protein encode a RNA helicase/NTPase domain. NS3 forms a non-covalent interaction with the central region of its protein co-factor, NS4A (Bartenschlager et al., 1995, Lin et al., 1995). This interaction allows NS3 to localise to the ER membrane, where it is retained via the N-terminal TMD of NS4A (Wolk et al., 2000).

Upon association with the ER membrane, the serine-type protease domain of NS3 associates with NS2 to cleave the NS2/NS3 junction (see previous section). Subsequently, NS3 cleaves between the NS3/NS4A, NS4A/NS4B, NS4B/NS5A and NS5A/NS5B junctions (Bartenschlager et al., 1993, Grakoui et al., 1993a). With the exception of the NS3/NS4A junction, all boundaries are processed *in trans* (Bartenschlager et al., 1994). NS3-mediated cleavage occurs in a shallow binding pocket containing a catalytic triad composed of His, Asp and Ser residues, and mutation of any of these amino acids abolishes NS3-mediated cleavage (Bartenschlager et al., 1993, Grakoui et al., 1993a). NS3 also binds a zinc atom by coordinating with three Cys residues plus a His residue (De Francesco et al., 1996) and these amino acids are critical for efficient NS3 activity (Hijikata et al., 1993). Importantly, association of NS3 with its co-factor NS4A is crucial for the NS3/NS4A and NS4B/NS5A cleavage events and also aids processing at the NS4A/NS4B and NS5A/NS5B junctions (Failla et al., 1994, Gallinari et al., 1998, Lin et al., 1994b). This is presumably due to a contribution from NS4A to facilitate NS3 folding (Kim et al., 1996, Love et al., 1996).

The C-terminal two-thirds of NS3 encode a Y-shaped molecule that harbours both RNA helicase and NTPase activities (Kim et al., 1998, Yao et al., 1997). Although monomeric NS3 can bind to RNA substrates, a NS3 dimer is required in order to unwind RNA (Serebrov & Pyle, 2004). This process is proposed to occur in a series of coordinated but discontinuous movements of the helicase, which pauses every 18bp of unwound RNA substrate when the helicase adjusts its conformation in an ATP-dependent fashion (Serebrov & Pyle, 2004). In isolation, NS3 is a relatively poor RNA helicase and is dependent upon the presence of both its protease domain and its NS4A cofactor for efficient RNA unwinding activity (Beran et al., 2009, Frick et al., 2004, Pang et al., 2002). Interestingly, NS3 is also capable of unwinding DNA duplexes, suggesting that the protein may influence

cellular DNA (Pang et al., 2002, Tai et al., 1996). The exact function of the NS3 helicase is unknown but it has been hypothesised to be involved in unwinding RNA secondary structures at the termini of viral RNA or dsRNA replicative intermediates (Dubuisson, 2007).

NS3 is essential for HCV RNA replication (Lam & Frick, 2006, Lohmann et al., 1999) and this process also requires the RNA binding and helicase activity of the protein (Beran et al., 2009). CCAMs that enhance RNA replication efficiency have been identified in both the protease and helicase domains of NS3 (Lohmann et al., 2003). Recently, the NS3 helicase domain has been implicated in virus assembly, since mutations within its coding region can rescue virus production from inter-genotypic chimeras that are otherwise defective for virion production (Ma et al., 2008, Yi et al., 2007).

1.2.2.7 NS4A

NS4A is the smallest HCV-encoded protein at only 6kDa, and consists of a N-terminal hydrophobic sequence, a central domain that interacts with and stabilises NS3 (see above) and a C-terminal acidic region. The N-terminus of NS4A is responsible for targeting the NS3-NS4A complex to ER membranes (Wolk et al., 2000), while the C-terminal acidic region influences both NS5A phosphorylation and RNA replication efficiency (Lindenbach et al., 2007). NS4A acts as a cofactor for both the serine protease (Bartenschlager et al., 1994, Failla et al., 1994, Lin et al., 1995) and helicase activities of NS3 (Frick et al., 2004, Pang et al., 2002). Recent data demonstrate that the active, ATP-bound state of NS3 binds RNA tightly only when NS4A is present, allowing the NS3-4A complex to reach maximal ATP-hydrolysis activity at lower RNA concentrations compared to NS3 expressed alone (Beran et al., 2009). Thus, the RNA binding strength and ATPase activity of NS3 are coupled and both processes are enhanced by NS4A.

1.2.2.8 NS4B

NS4B is 27kDa in size and is a highly hydrophobic protein. Consequently, investigation into NS4B structure has been restricted and identifying structured regions within the protein typically relies on predictive methodology. The central portion of NS4B is predicted to contain 4 TMDs that bind the protein tightly to ER membranes, while the remaining regions of the protein are thought to reside on

either the cytosolic or luminal sides of the ER membrane (Hugle et al., 2001, Lundin et al., 2003). NS4B is co-translationally targeted to the ER by a N-terminal amphipathic helix (Elazar et al., 2004). However, the precise orientation of the N-terminal region is uncertain since glycosylation studies have revealed that, at least in some NS4B molecules, this region may translocate to the luminal side of the ER membrane post-cleavage, creating a fifth TMD termed TMX (Lundin et al., 2006, Lundin et al., 2003). The TMDs of NS4B are linked via three transmembrane loops, and the loop connecting TM2 and TM3 is believed to reside on the cytosolic side of the ER membrane (Lundin et al., 2003). Analysis of this loop has revealed the presence of a nucleotide-binding motif (NBM) involved in the binding and hydrolysis of GTP (Einav et al., 2004), which may influence cell transformation (Einav et al., 2008b). Additionally, *in vitro* purified preparations of NS4B possess adenylate kinase activity, indicating that NS4B may be involved in ATP production (Thompson et al., 2009). The C-terminus of NS4B is predicted to reside in the cytoplasm (Hugle et al., 2001, Lundin et al., 2003) and is highly conserved (Welsch et al., 2007). Two cysteine residues at the end of the C-terminus (amino acids 257 and 261) apparently undergo palmitoylation, a lipid modification that may be important for the formation of protein-protein interactions within viral replication complexes (RCs, Yu et al., 2006).

Expression of NS4B induces rearrangements of cellular ER membranes, producing punctate structures that have been termed the 'membranous web' and membrane-associated foci (MAFs, Egger et al., 2002, Gosert et al., 2003, Gretton et al., 2005). Two important observations indicate that these structures are the complexes in which viral RNA replication takes place. Firstly, other NS proteins involved in replication localise to these punctate sites (Elazar et al., 2004, Hugle et al., 2001) and disrupting the ability of NS4B to bind to ER membranes leads to a loss of proteins at these foci (Elazar et al., 2004). Secondly, studies utilising FISH (Gosert et al., 2003, Targett-Adams et al., 2008a), BrUTP labelling (El-Hage & Luo, 2003, Moradpour et al., 2004b) and an antibody that binds to dsRNA intermediates (Targett-Adams et al., 2008a) have all demonstrated that viral RNA colocalises with NS proteins at punctate structures on the membrane. Therefore, the membrane rearrangements induced by NS4B are likely to be essential for viral RNA replication.

Aside from generating an environment suitable for HCV RNA synthesis, NS4B apparently contributes directly to viral replication. Studies have shown that CCAMs within NS4B are able to enhance RNA replication by up to 30-fold compared to

genomes containing wild-type (wt) NS4B (Lohmann et al., 2003, Lohmann et al., 2001). A mutagenic analysis of NS4B revealed amino acids that influenced HCV genome synthesis and these had a variety of effects, from enhancing to abolishing RNA replication (Lindstrom et al., 2006). Insertion of the Con1 (genotype 1b) NS4B coding region into the H77 (genotype 1a) genome enhanced RNA synthesis by 10-fold (Blight, 2007) and similarly, Con1 genomes harbouring H77 NS4B sequences were defective for replication (Paredes & Blight, 2008). Furthermore, the replication efficiency of these defective chimeric genomes could be recovered by mutations within NS3 (Paredes & Blight, 2008). These data suggest that NS4B interacts with the replication machinery in a genotype-specific manner, where compatibility between NS3 and NS4B is required for efficient RNA replication (Paredes & Blight, 2008). NS4B can bind specifically to negative-stranded viral RNA and disruption of this process inhibits HCV replication (Einav et al., 2008a). Hence, the role of NS4B appears to be twofold; firstly, to create an environment that permits RC assembly and secondly, to modulate viral RNA synthesis within RCs.

1.2.2.9 NS5A

NS5A is a phosphoprotein that exists as two species, termed the hypo- (56kDa) and hyperphosphorylated (58kDa) forms. NS5A can be divided into three domains (I-III), which are separated by two low complexity sequences (LCS I and LCS II, Tellinghuisen et al., 2004). Domain I is the best characterised region of NS5A and binds a single zinc atom per protein molecule, which is essential for HCV RNA replication (Tellinghuisen et al., 2004). Based on the crystallographic structure of domain I, this region may dimerise to form a basic groove that could accommodate a single or double strand of RNA (Tellinghuisen et al., 2005). Indeed, NS5A is capable of binding to both positive- and negative-strand viral RNA (Huang et al., 2005). Domain I also harbours an amphipathic α -helix that mediates the association of NS5A with ER membranes and disruption of this structure results in a loss of membrane binding and viral RNA replication (Brass et al., 2002, Elazar et al., 2003). Domains II and III are poorly characterised compared to domain I, although recent studies have suggested that domain II is flexible and disordered in nature (Liang et al., 2006), while domain III is mostly unstructured (Hanouille et al., 2009).

Hypophosphorylated NS5A represents the basally phosphorylated form of the protein and phosphorylation occurs primarily on serine residues that reside in LCS I, domain II and domain III (Huang et al., 2007b). Although not mapped directly, three serine residues located within LCS I (referred to as S2197, S2201 and S2204 in Tanji et al., 1995) are important for hyperphosphorylation of NS5A, since reduced levels of the hyperphosphorylated protein are detected upon mutation of these residues (Blight et al., 2000). For hyperphosphorylation, NS5A must be expressed from a polyprotein that also encodes NS3, NS4A and NS4B, indicating that these proteins are likely to interact with the cellular machinery to promote NS5A phosphorylation (Koch & Bartenschlager, 1999, Neddermann et al., 1999).

NS5A is essential for HCV RNA replication and while domains I and II are required for this process, domain III is dispensable (Appel et al., 2008, Tellinghuisen et al., 2008b). As a result, domain III can tolerate the insertion of molecules including green fluorescent protein (GFP) and dsRed without abrogating RNA replication (Appel et al., 2005b, Liu et al., 2006, McCormick et al., 2006, Moradpour et al., 2004b), thus allowing characterisation of NS5A in live cells. For example, studies with NS5A-GFP fusion protein have shown that NS5A is frequently localised with HCV RNA in cells actively replicating viral genomes (Targett-Adams et al., 2008a). In genotype 1 subgenomic replicons (SGRs), CCAMs typically cluster within domain II and LCS I, which are implicated in NS5A hyperphosphorylation (Blight et al., 2000, Tanji et al., 1995). Furthermore, the phosphorylation status of NS5A influences replication and several studies have shown that reducing hyperphosphorylation results in enhanced RNA synthesis (Appel et al., 2005b, Evans et al., 2004b, Neddermann et al., 2004). Interaction between NS5A and human vesicle-associated-membrane protein A (hVAP-A), a protein involved in intracellular vesicle trafficking, is required for HCV RNA synthesis (Gao et al., 2004, Zhang et al., 2004b) and hyperphosphorylated NS5A binds hVAP-A less efficiently compared to the basally phosphorylated protein (Evans et al., 2004b). Thus, phosphorylation may provide a mechanism for switching between viral replication and other stages of the HCV life cycle, via the modulation of protein-protein interactions within the viral RC. Indeed, NS5A interacts with an expansive list of cellular proteins that are essential for, or at least facilitate HCV replication (see Section 1.4.3.3).

It has recently been established that domain III of NS5A is essential for virus particle production in cells harbouring genome-length HCV RNA (Appel et al., 2008, Tellinghuisen et al., 2008a). One study also demonstrated that mutations

within domain I of NS5A can prevent the protein associating with LDs, thought to be the sites of virus assembly (Miyanari et al., 2007). These mutations also prevented trafficking of other NS proteins and viral RNA to LDs, reducing infectious virus production as a result (Miyanari et al., 2007). In a separate study, mutation of a single serine residue within domain III prevented virus production without abolishing the association between NS5A and LDs (Tellinghuisen et al., 2008a). Indeed, NS5A harbouring deletions within domain III retains the ability to interact with LDs but the protein is unable to associate with core at these sites (Appel et al., 2008). Thus, domains I and III may contribute to virus assembly by distinct mechanisms. While the work by Miyanari et al., and Appel et al., demonstrate that recruitment of viral NS proteins and RNA is essential for virus formation, the study conducted by Tellinghuisen et al., suggests that NS5A hyperphosphorylation is also important, since a reduction in this modification reduced infectious virus production. Overall, these results demonstrate the importance of NS5A to virus assembly, although its precise role has yet to be identified.

Beside roles in viral replication and assembly, NS5A also interacts with a range of cellular signalling pathways (Macdonald & Harris, 2004). For example, protein kinase R (PKR) is an IFN-induced protein that phosphorylates eIF-2 α upon detection of dsRNA exceeding 30bp, shutting down protein translation as a result (Samuel, 1993). NS5A is able to bind to PKR, preventing shutdown of protein synthesis, presumably allowing HCV translation to continue unhindered (Gale et al., 1997). In addition to interfering with the host cell IFN-response, NS5A is able to interact with signal cascades that mediate cell growth, such as the Ras-Erk pathway. NS5A can perturb epidermal growth factor (EGF)-stimulated activation of the Ras-Erk signalling pathway (Macdonald et al., 2003, Macdonald et al., 2005), at least in part by directing EGF-EGFR complexes from late endosomes where activation of Ras usually takes place (Mankouri et al., 2008). These studies, as well as others, suggest that NS5A may be able to optimise the cellular environment to facilitate the HCV life cycle.

1.2.2.10 NS5B

NS5B is a 68kDa protein located at the very C-terminus of the HCV polyprotein. NS5B is a tail-anchored protein, meaning it attaches to the ER membrane via a highly conserved C-terminal TMD (Ivashkina et al., 2002, Schmidt-Mende et al.,

2001) and this association is critical for HCV RNA replication (Moradpour et al., 2004a). NS5B is the RdRp and can copy HCV genomes in the absence of other viral or cellular factors (Behrens et al., 1996, Lohmann et al., 1997). NS5B is therefore responsible for generating both positive- and negative-strand RNAs during viral replication. NS5B is described as a typical 'right-hand' polymerase, where the thumb and finger domains create a channel for binding the RNA template and surround the palm domain that harbours the catalytic GDD motif (Penin et al., 2004). This active site chelates magnesium cations to drive polymerase function.

The interactions of NS5B with other proteins, both viral and cellular, are important for modulating polymerase activity. For example, NS5A interacts with NS5B (Shirota et al., 2002) and disrupting this association inhibits HCV RNA replication (Shimakami et al., 2004). NS3 and NS4B also regulate NS5B activity (Piccininni et al., 2002). Similarly, cellular proteins cyclophilin B (CyPB) and nucleolin interact with NS5B, enhancing RNA synthesis (Shimakami et al., 2006, Watashi et al., 2005). CyPB stimulates the RNA binding activity of NS5B and cyclosporin A (CsA, a CyPB inhibitor) can prevent this enhancement (Watashi et al., 2003).

1.2.2.11 The 3' UTR

The 3' UTR has a tripartite structure consisting of a variable region, a poly (U/UC) tract and a highly conserved 98-nucleotide sequence designated the 3' X-tail, which together are involved in both viral RNA replication and translation (Blight & Rice, 1997, Tanaka et al., 1996, Yamada et al., 1996). The variable region is proposed to contain two stem-loops (termed VSL1 and VSL2), although these regions are dispensable for RNA replication in cell culture (Friebe & Bartenschlager, 2002) and for HCV infectivity in chimpanzees (Yanagi et al., 1999). The poly (U/UC) region is variable in length and composition, consisting of uridine residues that are interspersed with occasional cytidine residues. This segment must be at least 26 nucleotides in length to permit viral RNA replication (Friebe & Bartenschlager, 2002). The 3' X-tail is a highly conserved RNA sequence that is proposed to harbour three stable stem-loop structures (termed SL1-SL3). Deletion of any one of these elements prevents replication in cell culture (Friebe & Bartenschlager, 2002, Yi & Lemon, 2003) as well as infectivity in chimpanzees (Yanagi et al., 1999).

Aside from roles in replication, the 3' UTR also stimulates IRES-mediated translation of viral RNA (Song et al., 2006). Interestingly, cellular factors PTB and La autoantigen, which interact with the 5' UTR (see Section 1.2.2.1), also recognise the 3' UTR (Ito & Lai, 1997, Spangberg et al., 1999). It has been proposed that the 3' UTR enhances IRES-dependent translation by increasing the efficiency of termination (Bradrick et al., 2006).

1.3 Systems used to Study the HCV Life Cycle

The HCV life cycle consists of three main phases (i) binding and entry of the virus to target cells (ii) translation and replication of the viral genome and (iii) assembly and release of new virus particles. In 2005, three separate groups demonstrated that JFH1, a genotype 2a HCV strain (see Section 1.3.1.3), was capable of producing virus particles that could establish productive infection in naïve cells (Lindenbach et al., 2005, Wakita et al., 2005, Zhong et al., 2005). Thus, JFH1 provides a robust tool for the study of the entire HCV life cycle. Prior to the discovery of JFH1, much investigation into HCV was conducted utilising surrogate models such as pseudoparticles (for analysing virus entry) and SGRs (to study RNA replication). The characteristics and application of these and other systems are described below.

1.3.1 Binding and Entry Analysis

To infect target cells, viruses typically bind to specific receptors on the cell surface to initiate entry. Although the precise composition of infectious HCV particles is currently unknown, the envelope glycoproteins E1 and E2 are obvious candidates for the binding of HCV particles to cells. Before the discovery of JFH1, a number of systems were used to study HCV binding and entry.

1.3.1.1 Solubilised Glycoproteins

The expression of E1 and E2 *in vitro* has demonstrated that a substantial proportion of these proteins exist as high molecular weight aggregates that likely represent misfolded complexes (Deleersnyder et al., 1997, Dubuisson et al., 1994). To overcome this problem, several groups have utilised soluble versions of the E1/E2 glycoproteins that are generated via removal of the hydrophobic C-

terminal TMDs (Flint et al., 1999, Scarselli et al., 2002). The truncated glycoproteins (sE1 and sE2) exhibit a lower tendency to form non-productive aggregates (Michalak et al., 1997). Solubilised glycoproteins can be utilised to investigate the binding of HCV envelope proteins to cellular receptors but are unsuitable for examining any subsequent stages in the entry process.

1.3.1.2 HCV Pseudoparticles (HCVpp)

The development of the HCVpp system allowed study of the complete HCV entry process. HCVpp are produced by transfecting 293T cells with plasmids expressing (i) a HCV E1/E2 polyprotein (ii) retroviral core proteins and (iii) a packaging-competent, retrovirus-derived genome harbouring a reporter gene (Bartosch et al., 2003b). Thus, secreted HCVpp consist of retroviral core particles containing DNA that encodes a reporter gene, with HCV E1/E2 heterodimers anchored in the surrounding lipid envelope. Several groups have utilised the HCVpp system, demonstrating that the particles exhibit a tropism for liver cells and can be neutralised by anti-E2 antibodies or sera from HCV-infected individuals (Bartosch et al., 2003b, Hsu et al., 2003, Op De Beeck et al., 2004).

1.3.1.3 HCV Cell Culture System (HCVcc)

Three groups simultaneously reported the development of a cell culture system capable of producing infectious HCV particles (HCVcc) in 2005 (Lindenbach et al., 2005, Wakita et al., 2005, Zhong et al., 2005). This system involves introducing genome-length HCV RNA into human hepatoma Huh-7 cells. The RNA is derived from a cloned viral genome of the HCV isolate JFH1, a genotype 2a strain obtained from a Japanese individual with fulminant hepatitis (Kato et al., 2001). The UTRs and NS3-NS5B region of JFH1 permit SGRs derived from this HCV strain to replicate their RNA genomes efficiently in cell culture (see Section 1.3.2). Furthermore, HCVcc-derived virus particles are infectious in inoculated chimpanzees (Wakita et al., 2005), although the animals do not progress to chronicity after acute infection. To date, the HCVcc system represents the most authentic system for analysing viral entry.

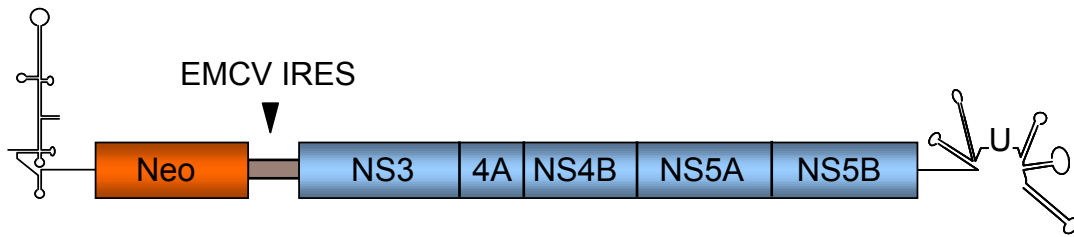
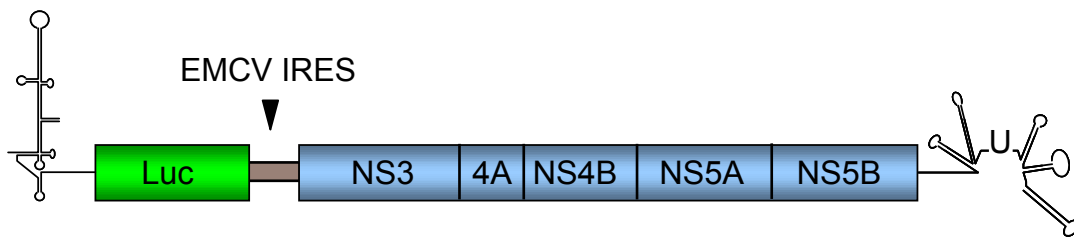
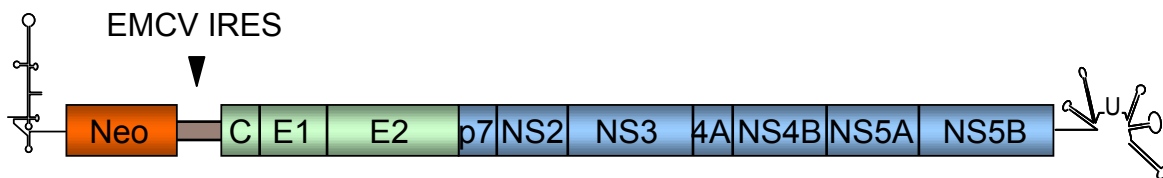
[A]**[B]****[C]**

Figure 1.4 Subgenomic and genomic HCV replicons

[A] Schematic representation of the first described subgenomic replicon (SGR). The construct is a bi-cistronic RNA molecule composed of the HCV 5' UTR linked to the neomycin resistance gene (Neo), an EMCV IRES, the NS coding region (NS3-NS5B) and finally the 3' UTR. Derivatives of this construct have subsequently been developed, including **[B]** SGRs where Neo is replaced with the luciferase reporter gene (Luc) and **[C]** full-length genomes that also harbour the Neo gene. These SGRs often contain adaptive mutations within the NS proteins to increase replication efficiency.

1.3.2 RNA Replication Analysis

Despite the construction of the first HCV cDNA clone in 1989, examining viral replication has only become possible since the late 1990s. The first functional, full-length cDNA clones were reported in 1997 (Kolykhalov et al., 1997). Inoculation of these RNAs into chimpanzees caused the animals to become HCV seropositive and exhibit elevated ALT levels, but replication of the transcripts in cell culture could not be demonstrated (Kolykhalov et al., 1997). It was not until 1999 that the SGR system was developed, permitting autonomous replication of modified HCV genomes in Huh-7 cells (Lohmann et al., 1999). The SGR system has evolved to become the benchmark for studying HCV RNA replication and remains an important tool despite the advances made with the HCVcc system.

SGRs were initially derived from Con1, a genotype 1b HCV strain. The coding region from core-p7 or core-NS2 was replaced with a gene encoding neomycin phosphotransferase (neo) and the HCV IRES directed translation of this gene. The NS coding region (NS3-NS5B) was placed under the control of a second IRES, derived from encephalomyocarditis virus (EMCV). Hence, the first SGRs were bicistronic constructs (Figure 1.4, A). Transfection of *in vitro* transcribed SGR RNA into Huh-7 cells followed by G418 selection resulted in a small number of resistant colonies that supported stable replication of HCV RNAs, which could be maintained persistently under continuous drug selection (Lohmann et al., 1999). Unfortunately, replication of these RNA species was relatively inefficient.

Advances with the SGR system were quickly made with the discovery that persistent selection of cells harbouring HCV RNAs promoted the generation of CCAMs, which enhanced viral replication (Blight et al., 2000). These mutations tended to cluster in NS5A (Blight et al., 2000). Other studies also reported the existence of CCAMs within this protein, as well as within NS3, NS4B and NS5B (Krieger et al., 2001, Lohmann et al., 2001). The mutations enhanced replication sufficiently to permit the construction of SGRs in which the neo gene was replaced by the luciferase coding region (Figure 1.4, B). This modification allowed assessment of RNA replication transiently, removing the need for time-consuming selection processes (Krieger et al., 2001). Furthermore, CCAMs were used to generate full-length selectable HCV genomes (Figure 1.4, C), which supported RNA synthesis and expressed all of the viral proteins (Blight et al., 2003, Blight et al., 2002, Pietschmann et al., 2002). Unfortunately, both subgenomic and genome-length RNAs had limited properties. Firstly, adapted full-length HCV genomes

failed to produce infectious virus despite robust replication in tissue culture cells (Blight et al., 2003, Pietschmann et al., 2002). Secondly, adapted SGRs did not replicate in chimpanzees, suggesting that CCAMs were highly attenuating *in vivo* (Bukh et al., 2002). In support of this notion, adaptive mutations selected in tissue culture cells have never been found in virus isolated from HCV-infected individuals.

Following studies with Con1, SGRs derived from other HCV strains (such as H77, genotype 1a) were developed (Yi & Lemon, 2004). Like Con1, these SGRs were reliant upon adaptive mutations within the NS protein coding region in order to produce detectable levels of RNA replication (Yi & Lemon, 2004). Employing an approach identical to that adopted with Con1 and H77 HCV strains, a JFH1-based SGR was also developed (Kato et al., 2003). Importantly, RNA transcribed from this construct replicated with far greater efficiency compared to previously described SGRs and furthermore, did not require G418 selection or CCAMs (Kato et al., 2003). Replacement of the neo gene in JFH1 SGRs with the luciferase coding region created a much-improved system for quantitative measurement of viral RNA replication compared to genotype 1 SGR systems (Targett-Adams & McLauchlan, 2005).

1.3.3 Virus Assembly and Release

The development of the HCVcc system in 2005 has permitted investigation into the latter stages of the HCV life cycle for the first time. Genome-length JFH1 produces virus particles with a specific infectivity of 1.4×10^2 RNA copies per focus-forming unit (FFU), as derived from comparing the abundance of virus particle RNA to the infectious titre (Yi et al., 2006). Infectious titres are measured by TCID₅₀ (median tissue culture infective dose) analysis, an assay determining the amount of pathogenic agent required to produce pathological change in 50% of cell cultures. The isolation of JFH1 has also permitted the development of chimeric viruses, which contain the core-NS2 region from various HCV genotype fused to the NS3-NS5B coding sequence of JFH1. The most efficient of these is a chimera termed Jc1, which consists of strain HC-J6- and JFH1-derived sequences and is capable of yielding infectious titres up to 1000-fold higher than JFH1 (Pietschmann et al., 2006). Such increased production of infectious progeny may result partly from the LD binding efficiency of HCV-encoded core protein (see Section 1.2.2.2). While the generation of such viruses and chimeras has facilitated

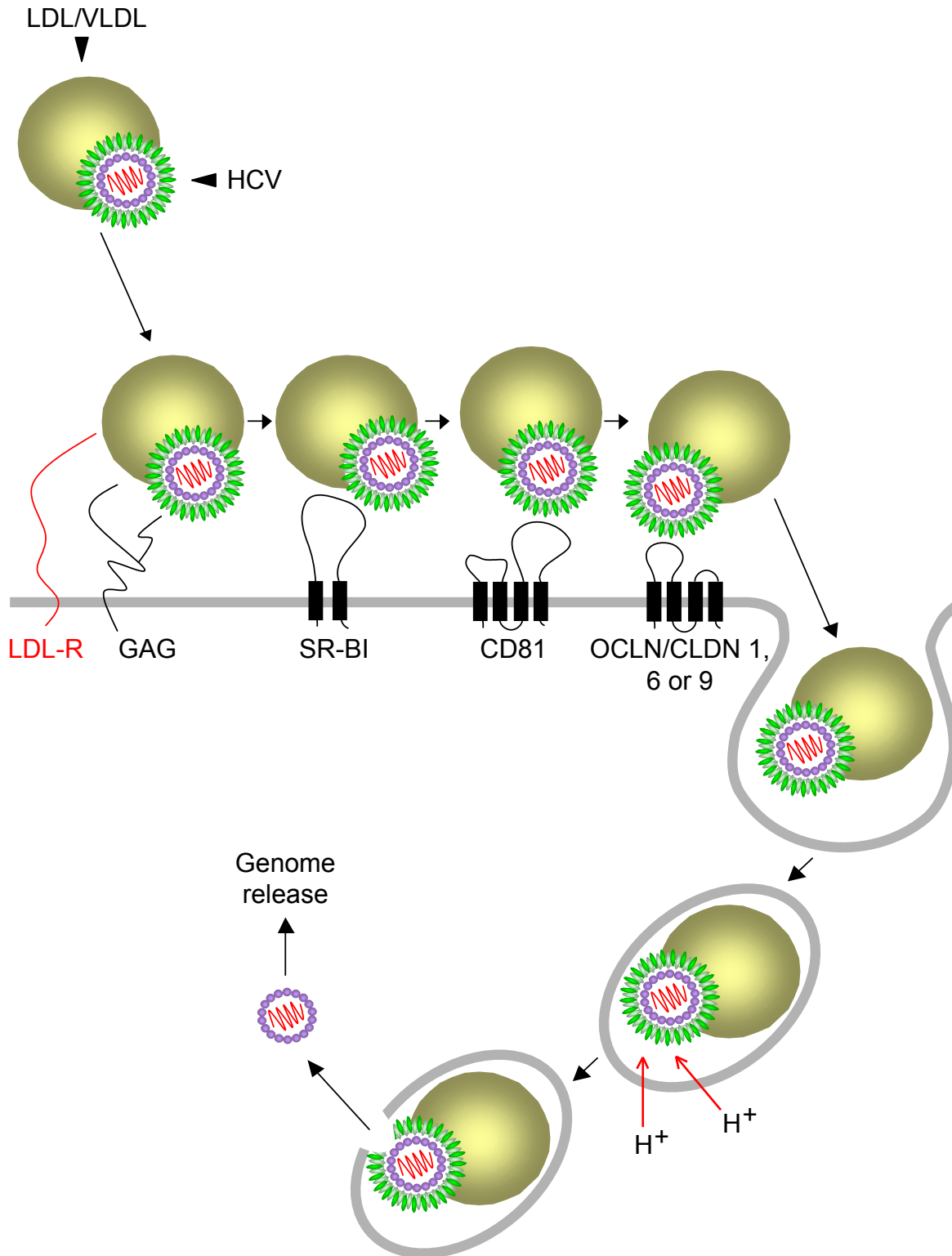


Figure 1.5 Model for HCV binding and entry

HCV particles are brought into contact with cell surfaces via the complexed LDL/VLDL interacting with the LDL receptor (LDL-R). Glycosaminoglycans (GAGs) may also be important for initial attachment. Subsequently, the HCV virion is proposed to interact with SR-BI, CD81 and the tight junction proteins CLDN-1/6/9 and OCLN. Many of these interactions are mediated by the E2 protein present on the virion surface. HCV entry is thought to occur by clathrin-mediated endocytosis, followed by acidification of the endosome. This leads to a fusion event between the viral envelope and the endosome membrane, releasing the HCV genome into the cell cytosol for translation and replication.

the study of virus assembly and release, the relatively recent discovery of JFH1 means that these stages of the HCV life cycle remain poorly understood.

1.4 The HCV Life Cycle

1.4.1 Binding and Entry

Typically, virus entry is initiated when virions bind to attachment factors on the cell surface. Binding can be relatively non-specific and serves to concentrate virus on the cell surface before it attaches to one or more specific receptors, leading to release of the genome into the cell interior (Dubuisson et al., 2008). The attachment factors and specific viral receptors necessary for HCV binding and entry into cells are discussed in the relative order they are believed to be utilised by the virus. This stage of the life cycle is also depicted in Figure 1.5.

1.4.1.1 Attachment factors

As mentioned previously (see Section 1.2.1), HCV particles are thought to circulate as LVPs, complexed with LDLs and/or VLDLs (Andre et al., 2002, Nielsen et al., 2006) and these components may aid the attachment of HCV to target cells. Supporting this hypothesis, antibodies directed against the LDL receptor (LDL-R) can inhibit the accumulation of viral RNA in cells (Agnello et al., 1999, Germe et al., 2002, Molina et al., 2007). This finding was accompanied by the observation that increased LDL-R expression and LDL entry correlated with increased viral RNA accumulation in cells (Molina et al., 2007). Additionally, antibodies targeting apolipoproteins B and E (apoB and apoE, major protein components of VLDLs) neutralised HCV infectivity in a dose-dependent manner (Agnello et al., 1999, Chang et al., 2007). These data collectively suggest that LDL and/or VLDL are important for the HCV entry process and that the LDL-R might serve as an initial attachment factor for the virus.

In addition to the LDL-R, GAGs may also represent an initial docking site for HCV particles. The composition and quantity of GAGs varies substantially from cell to cell and may therefore be an important determinant for viral tropism. It has been proposed that the positively-charged residues within the N-terminus of E2 may be able to interact with negatively-charged structures such as GAGs (Penin et al., 2001). Although GAGs such as heparin and heparan sulfate bind recombinant E2 proteins (Barth et al., 2003), no such binding has been observed using the HCVpp

system (Helle & Dubuisson, 2008). However, an indirect interaction between HCV and GAGs via virus-associated lipoproteins such as VLDL cannot be dismissed. While the mechanism of interaction between GAGs and HCV remains uncertain, evidence suggests that these factors are indeed important for virus entry. For example, treatment of cells, or the virus directly, with increasing concentrations of heparin decreased the amount of HCVcc infection, presumably due to competition (Germi et al., 2002, Koutsoudakis et al., 2006). Similarly, treating cells with heparinase, enzymes that cleave heparan sulphate molecules, reduced recombinant E2 binding and furthermore, HCVcc entry into cells (Barth et al., 2003, Koutsoudakis et al., 2006).

1.4.1.2 Specific Viral Receptors

Following attachment of HCV virions to the exterior of cells, the virus interacts with specific receptors to initiate entry. To date, four receptors have been identified. The first, SR-BI, is a multi-ligand receptor that contains two TMDs and a highly glycosylated extracellular loop that directly interacts with sE2 via HVR1 (Bartosch et al., 2003c, Scarselli et al., 2002). In addition to this direct association between HCV and SR-BI, it is proposed that the lipoproteins attached to the virion also interact with the receptor. For example, interaction between HCV and SR-BI is not inhibited by antibodies targeting E2 and HVR1, yet exogenous VLDL or antibodies targeting apoB both decrease HCV entry into cells (Maillard et al., 2006). An interaction between SR-BI and HCV-associated lipoproteins is plausible, since SR-BI was initially identified as the major receptor for high-density lipoprotein (HDL) in the liver and is involved in selective lipid uptake (Dubuisson et al., 2008). The importance of SR-BI in HCV entry has been confirmed using both the HCVpp (Bartosch et al., 2003c, Voisset et al., 2005) and HCVcc systems (Catanese et al., 2007, Grove et al., 2007, Kapadia et al., 2007). Importantly, HCVcc is able to bind to Chinese hamster ovary (CHO) cells expressing SR-BI, but not to those expressing CD81 (Evans et al., 2007), suggesting that HCV binds to SR-BI before interaction with other specific receptors involved in virus entry.

The first identified and best defined HCV receptor is CD81, a tetraspanin that was initially demonstrated to interact with sE2 (Pileri et al., 1998). Furthermore, E1/E2 heterodimers exhibit stronger interactions with CD81 compared to sE2, implying that E1 may modulate the binding process (Cocquerel et al., 2003). CD81 contains four TMDs, a small extracellular loop (SEL) and a large extracellular loop

(LEL), the latter of which interacts with E2 (Helle & Dubuisson, 2008). CD81 has been confirmed as an essential receptor for HCV entry utilising HCVpp (Bartosch et al., 2003c, Cormier et al., 2004, Zhang et al., 2004a) and HCVcc (Kapadia et al., 2007, Lindenbach et al., 2005, Wakita et al., 2005). While antibodies targeting CD81 impair HCV entry, inhibition occurs after the virus has attached to cells (Cormier et al., 2004). Therefore, CD81 likely acts as a co-receptor that aids HCV entry after the virus has already bound to cells, possibly via SR-BI (see above).

In an attempt to discover genes that render non-permissive cell lines susceptible to HCV entry, CLDN1 was identified as another essential viral entry receptor (Evans et al., 2007). CLDN1 belongs to the family of tight junction proteins and, like CD81, possesses four TMDs with two extracellular loops. The first extracellular loop is required for HCV entry, although no interaction between the viral glycoproteins and CLDN1 has been demonstrated (Evans et al., 2007, Zheng et al., 2007). CLDN1 is thought to act at a post-binding step and kinetic studies suggest that the receptor is utilised downstream of HCV interaction with CD81 (Zheng et al., 2007). A limited number of other CLDN family members are also able to mediate HCVcc entry, including CLDN6 and CLDN9 (Meertens et al., 2008, Zheng et al., 2007).

Recently another tight junction protein, OCLN, has been implicated in the entry of HCVpp and HCVcc (Liu et al., 2009, Ploss et al., 2009). As for SR-BI and CD81, the interaction between HCV and OCLN is thought to be mediated via interaction with E2 and direct binding of the two factors has been observed (Liu et al., 2009). Silencing of OCLN in cell lines permissive for HCV entry reduces both HCVpp and HCVcc infection (Ploss et al., 2009). Similarly, expression of OCLN alongside SR-BI, CD81 and CLDN1 rendered non-permissive cell lines competent for HCV infection (Ploss et al., 2009). It was noted that viral infection led to a decrease in CLDN1 and OCLN expression levels, suggesting that regulation of cell surface receptors may provide a mechanism for superinfection exclusion (Liu et al., 2009). A similar downregulation of the other entry factors, SR-BI and CD81, has not been observed in HCVcc-infected cells (Schaller et al., 2007).

Importantly, the expression of SR-BI, CD81, CLDN1 and OCLN renders murine and hamster cells permissive for HCVpp infection, suggesting that these four host receptors are sufficient for HCV entry (Ploss et al., 2009). The identification of all necessary entry factors is a major step towards the construction of a small animal model for HCV infection.

1.4.1.3 Internalisation of HCV virions

Enveloped viruses typically enter cells by (i) fusion of their envelope with the cell plasma membrane, releasing the viral genome into the cytosol or (ii) by endocytosis. In the case of the latter, an activation step usually leads to fusion of the viral envelope with the endosome membrane and the acidic pH of endosomes is thought to play a key role in this process. Thus, pH sensitivity is a reasonable indicator for viral entry by endocytosis.

Both HCVpp and HCVcc entry is sensitive to agents that neutralise the acidic pH of cellular endosomes (Blanchard et al., 2006, Hsu et al., 2003, Meertens et al., 2006). Furthermore, treatment of cells with chlorpromazine (which disrupts the formation of clathrin-coated pits) or the use of siRNA targeting clathrin, reduces HCVpp and HCVcc entry (Blanchard et al., 2006, Meertens et al., 2006). Hence, clathrin-mediated endocytosis represents a likely mechanism for HCV entry. Once internalised, the virus envelope is proposed to fuse with the membranes of early endosomes in order to release the HCV genome into the cytosol (Meertens et al., 2006). Further work is required to fully define these early steps of the HCV life cycle.

1.4.2 Translation and Polyprotein Processing

1.4.2.1 Translation

Upon release into the cytoplasm, the host ribosomal machinery translates the viral genome after binding to the HCV IRES within the 5' UTR (see Section 1.2.2.1). Ribosomes consist of (i) a small (40S) subunit that mediates interactions between the anticodons of the tRNA and the codons of the mRNA and (ii) a large (60S) subunit, which catalyses peptide bond formation in the growing polypeptide chain (Steitz, 2008). Whereas translation of cellular mRNA involves the eukaryotic initiation factor (eIF) 4F protein complex (consisting of eIF4E, eIF4G and eIF4A), HCV translation requires only eIF2 and eIF3 (Pestova et al., 1998). eIF2 places the initiator tRNA (Met-tRNA) on the surface of the 40S ribosomal subunit, which is bound directly to the HCV IRES to form a pre-initiation 48S complex and this complex is stabilised by eIF3 (Ji et al., 2004). Subsequent association of the 60S ribosomal subunit results in a translationally active 80S complex that initiates protein synthesis to generate the HCV polyprotein precursor.

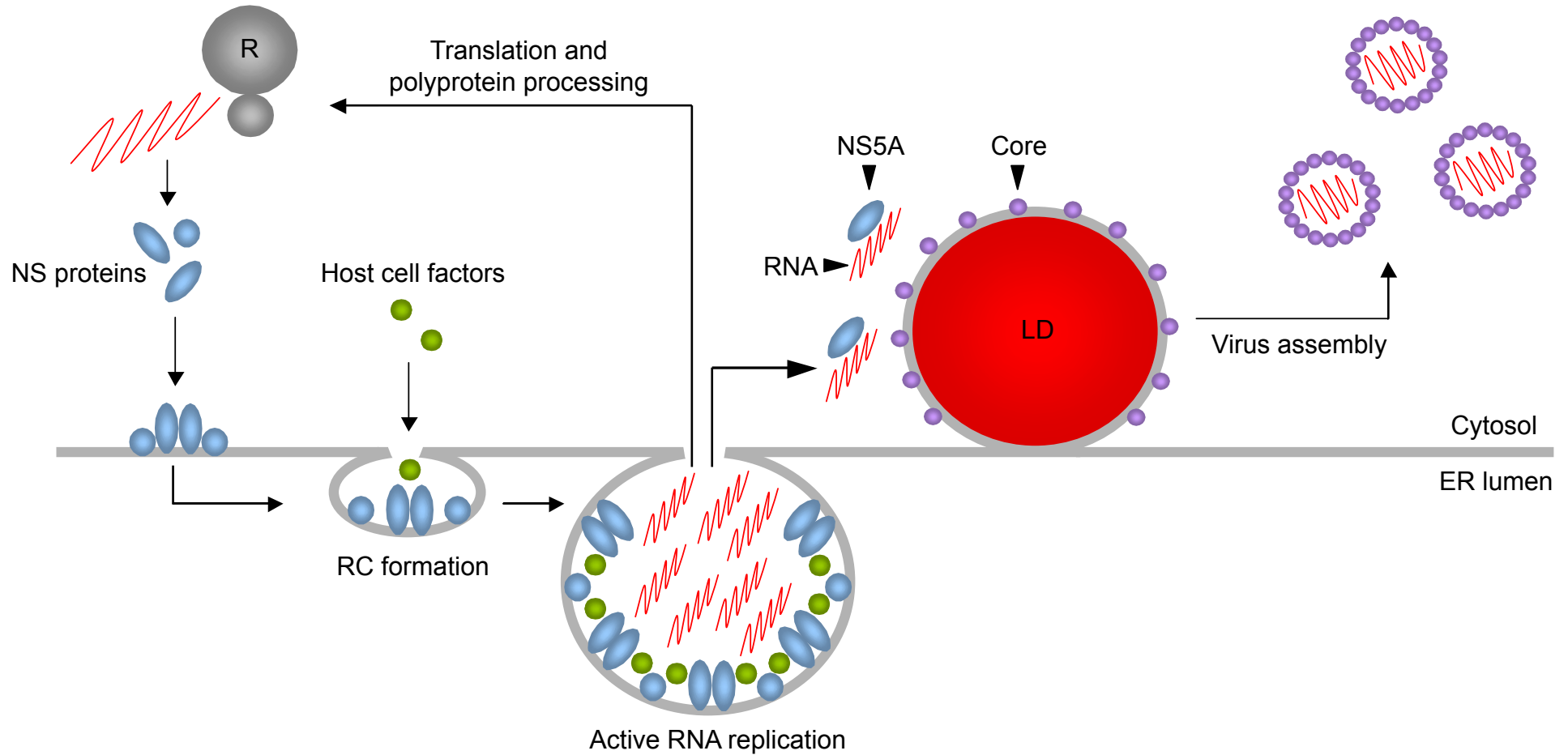


Figure 1.6 HCV genome replication and virus assembly

Replication of the viral genome is thought to occur within altered membranes derived from the ER. These replication complexes (RCs) are thought to protect viral RNA and proteins from cellular degradative processes. Replicated RNA can then associate with ribosomes (depicted by R above) for further production of viral proteins, or be transported to lipid droplets (depicted by LD above) for packaging into viral capsids. The trafficking of RNA to LDs has been proposed to occur in an NS5A-dependent manner.

1.4.2.2 Polyprotein Processing

Following translation, cellular and viral proteases process the HCV polyprotein to produce the mature structural and NS proteins. Core, E1, E2 and p7 are generated by SP and SPP-mediated events (see Sections 1.2.2.2-1.2.2.4). NS2 is liberated by the combined activity of the NS2/NS3 protease (see Section 1.2.2.5). The remaining NS proteins, NS3, NS4A, NS4B, NS5A and NS5B, are all generated by NS3/NS4A-mediated cleavage (see Section 1.2.2.6).

1.4.3 RNA Replication

1.4.3.1 Nature of the HCV RC

Replication of HCV RNA is thought to occur rapidly after virus entry, since both positive- and negative-strand RNAs have been detected using Northern blot hybridisation by 2-4 hours after introduction of RNA into cells (Binder et al., 2007). RNA synthesis takes place within RCs, structures derived from altered ER membranes (Figure 1.6). RCs contain all the necessary components for RNA synthesis, including NS proteins, viral RNA and cellular factors involved in genome replication (Egger et al., 2002, Gosert et al., 2003, Mottola et al., 2002, Waris et al., 2004). Interestingly, viral RNA and NS proteins are ribonuclease and protease resistant, unless cells are first treated with detergents. This indicates that RCs are possibly enclosed membranous structures that protect HCV genomes from the intracellular environment (El-Hage & Luo, 2003, Quinkert et al., 2005, Waris et al., 2004). In support of this notion, RCs are unable to replicate exogenously introduced RNA templates (Lai et al., 2003). Nonetheless, exit from RCs must be possible for the transport of replicated viral RNA to sites of viral assembly. It is estimated that RCs consist of minimally one negative-strand RNA template, up to ten positive-strand RNA copies and several hundred NS proteins (Quinkert et al., 2005). Clusters of RCs on the ER membrane are thought to represent the 'membranous web', a structure previously visualised by EM analysis (Egger et al., 2002, Gosert et al., 2003). Strong evidence suggests that the HCV-encoded NS4B protein is responsible for inducing the membranous changes that bring about RC formation; the contributions of each of the NS proteins to RNA replication have already been described (see Section 1.2.2).

1.4.3.2 Mechanism of RNA Replication

HCV genome replication involves the production of a negative-strand RNA template from the positive-strand genome by the NS5B polymerase, which is then used for the production of multiple positive-strand RNA molecules (Lohmann et al., 1999, Takehara et al., 1992). The negative- and positive-strand RNAs are thought to form a dsRNA replicative intermediate, from which nascent strands are synthesised by strand-displacement (Targett-Adams et al., 2008a). The generation of replicative intermediates is not specific to HCV and dsRNA has been visualised during viral replication of other positive-strand RNA viruses (Weber et al., 2006). Indeed, other members of the *flaviviridae*, including Kunjin virus (KV) and dengue virus (DV) replicate their genomes via dsRNA intermediates (Miller et al., 2007, Westaway et al., 1997). In cells actively replicating HCV, dsRNA is detected in close proximity to RCs, suggesting that the intermediates are protected within these complexes (Targett-Adams et al., 2008a). It is likely that such protection would be necessary in order to prevent cellular dsRNA-activated enzymes (such as PKR) from triggering the shutdown of the host translational machinery.

1.4.3.3 Contribution of Cellular Factors to HCV RNA Replication

In cell culture, Huh-7 cells are typically used for the propagation of HCV SGRs. Attempts to utilise other cells have revealed that HCV replication can be accomplished in human liver-derived cell lines such as HepG2s and IMY-N9s (Date et al., 2004), cervical carcinoma-derived cells (HeLa, Kato et al., 2005, Zhu et al., 2003), embryonic kidney cells (293, Ali et al., 2004, Kato et al., 2005) and cells from osteosarcoma (U2OS, Targett-Adams & McLauchlan, 2005). Moreover, subgenomic HCV RNAs replicate in the murine hepatoma cell line Hepa 1-6 (Zhu et al., 2003), suggesting that viral genome synthesis can occur in cells derived from hosts that are not naturally infected with HCV. However, HCV viral RNA synthesis is typically inefficient in all of these cell types compared to the Huh-7 cell line and replication has not been detected in many other cell-types that have been tested. Thus, HCV-encoded replicase components alone are insufficient to support viral genome synthesis, suggesting that specific factors derived from the host cell are essential for this process.

Data obtained using Huh-7 cells illustrate at least two lines of evidence that the host cell environment substantially affects viral RNA synthesis. Firstly, treatment of Huh-7 cell lines harbouring autonomously replicating HCV genomes with IFN or

Cellular protein	Interacting partner	Reference
PTB	5' UTR/3' UTR	Ali & Siddiqui, 1995
La autoantigen	5' UTR/3' UTR	Ali & Siddiqui, 1997
hnRNP A1	5' UTR/3' UTR	Kim et al., 2007
PCBP2	5' UTR	Fukushi et al., 2001
miR122	5' UTR	Jopling et al., 2005
FBP	3' UTR	Zhang et al., 2008
hVAP-A	NS5A	Evans et al., 2004b
FBL2	NS5A	Wang et al., 2005
FKBP8	NS5A	Okamoto et al., 2006
Hsp90	NS5A	Okamoto et al., 2006
hB-ind1	NS5A	Taguwa et al., 2008
Raf-1 kinase	NS5A	Burckstummer et al., 2006
TBC1D20	NS5A	Sklan et al., 2007
Rab5	NS4B	Stone et al., 2007
ATM	NS3/NS4A/NS5B	Ariumi et al., 2008
Chk2	NS5B	Ariumi et al., 2008

Figure 1.7 Cellular proteins that influence HCV RNA replication

A list of some of the documented cellular factors that promote viral RNA synthesis.

viral inhibitors generates cells in which the SGRs have been eliminated. Upon retransfection of these 'cured' cells with a second HCV SGR, enhanced RNA replication is observed compared to naïve cells (Blight et al., 2002, Murray et al., 2003). Several groups have utilised cured Huh-7 derivatives, such as Huh-7.5 and Huh-7.5.1 cells, to achieve higher levels of HCV RNA replication (Bartenschlager & Pietschmann, 2005). Secondly, transfection of increasing amounts of SGR transcripts results in decreased HCV RNA synthesis (Lohmann et al., 2003), implying that host factors necessary for viral replication are limiting in Huh-7 cells. This hypothesis is strengthened by studies examining competition between HCV SGRs, where decreased RNA synthesis is observed upon introduction of multiple genomes into cells (Evans et al., 2004a).

The studies described above indicate that HCV genome replication does not depend solely on hepatocyte- or primate-specific factors. Nevertheless, specific host factors are required for viral replication, which are only present or expressed to sufficient levels in certain cell types. Indeed, an extensive list of cellular proteins that modulate HCV genome synthesis has been generated. Some of these factors have been described previously in Section 1.2.2 and others are depicted in Figure 1.7. The proteins are involved in regulating a range of cellular processes. For example, ATM and Chk2 are DNA damage sensors (Ariumi et al., 2008), while Rab5 is a protein found in early endosomes (Stone et al., 2007). The mechanisms by which many of these cellular factors influence HCV RNA synthesis is not known and further investigation is required to fully understand their involvement in this process.

1.4.4 Virus Assembly and Release

Based on assembly and egress strategies for other viruses, it is presumed that replicated RNA is packaged into capsids, which acquire a host-derived lipid envelope before transport to the cell surface for release. Investigation into the assembly and release of HCV has only become possible since the development of the JFH1 HCVcc system, meaning that this area of research remains in its infancy. The current understanding of HCV assembly and release is described below.

1.4.4.1 HCV Assembly

The first stages of assembly require HCV core, which comprises the viral capsid. Core is targeted to LDs (Barba et al., 1997, Hope & McLauchlan, 2000, Moradpour et al., 1996), which are crucial for the production of infectious virus particles (Boulant et al., 2007, Miyanari et al., 2007). The attachment of core to LDs is mediated by D2, following maturation of the protein by SPP (see Section 1.2.2.2). EM analysis has revealed the presence of particles containing core and E2 around LDs coated with core (Miyanari et al., 2007), suggesting that virion formation may occur at LDs. Furthermore, core is responsible for co-localisation of LDs with RCs containing NS proteins and viral RNA (Miyanari et al., 2007). Thus, core may recruit the viral components necessary for virus assembly at LDs (Figure 1.6).

Apart from core, other HCV-encoded proteins are essential for the assembly of virions. For example, p7 has been suggested to be a virion component (Griffin et al., 2008) and is essential for a pre-assembly step in virion production (Jones et al., 2007, see Section 1.2.2.4). Similarly, NS2, the only NS protein not essential for RNA replication, is required for events that precede the assembly of infectious virus at LDs (Jones et al., 2007, see Section 1.2.2.5). It has been thought that the NS3-NS5B proteins function solely in viral genome synthesis, but recent reports demonstrate that these components also have roles in viral assembly. For example, although domains I and II of NS5A are involved in RNA replication, domain III participates in virus particle assembly and is necessary for the trafficking of RCs to core found on LDs (Miyanari et al., 2007, see Section 1.2.2.9). In support of this mechanism, increased interaction between NS5A and core correlates with enhanced virus production (Masaki et al., 2008). More recently, NS3 has been shown to influence the production of infectious progeny, since mutations within the protein are able to rescue virus production from otherwise defective chimeric viruses (Ma et al., 2008, Yi et al., 2007). In these studies, NS3 and NS5A expressed from non-productive chimeras were recruited to core on the surface of LDs but no intracellular virus was produced (Ma et al., 2008). Hence, NS3 possibly mediates virus assembly following the recruitment of RCs to LDs but preceding particle assembly.

As described above, the association of RCs with LDs occurs in a core- and NS5A-dependent manner. However, there is limited insight into the precise mechanisms by which these proteins bring together sites of RNA replication and sites of virion assembly. One hypothesis is that the coating of LDs by core induces their

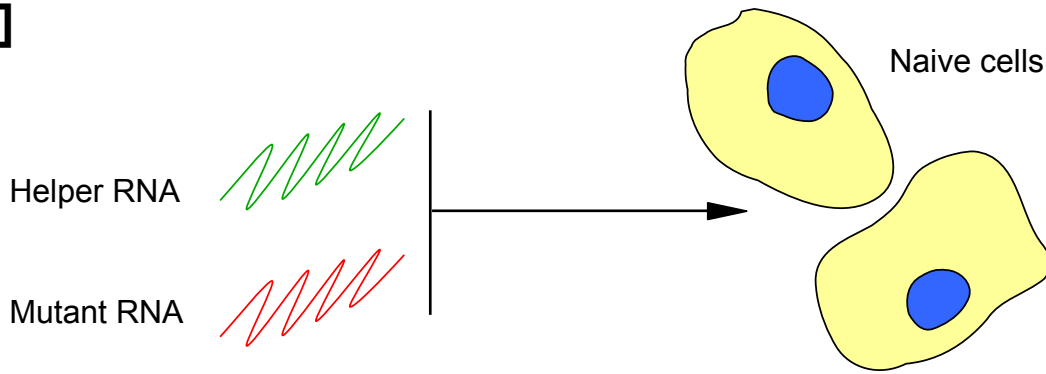
redistribution from the cytoplasm to the microtubule organising centre (MTOC) at the perinuclear region (Boulant et al., 2008). The trafficking of LDs is dependent on the microtubule network and disruption of this process leads to a reduction in infectious progeny (Boulant et al., 2008). Hence, LD redistribution may serve to concentrate core-coated LDs at sites where viral replication takes place. A similar but separate mechanism may involve interactions between NS3, NS5A and actin filaments, permitting the trafficking of RCs along the microtubule network (Lai et al., 2008). Therefore, HCV-encoded proteins such as core and NS5A may modulate the trafficking of RCs and LDs via the microtubule network in order to increase the probability of their interaction, possibly enhancing the likelihood of assembly events.

To date, visualisation of HCV particles within cells remains problematic. HCV-like particle (HCV-LP) budding has been observed when core is overproduced using a Semliki Forest virus (SFV) replicon vector, which expresses HCV structural proteins (Blanchard et al., 2003, Hourieux et al., 2007, Roingard et al., 2004). Furthermore, 3D electron microscopy has shown that HCV-LP budding initiates at membranes close to LDs, rather than membranes directly juxtaposed with LDs (Roingard et al., 2008). It would be useful to observe such events with authentic HCV particles, especially since HCV-LP budding is abortive in nature (Roingard et al., 2008). However, HCV particles produced using the HCVcc system have yet to be detected convincingly by EM. Prior attempts to do so have been unsuccessful (Rouille et al., 2006), although spherical virus-like structures have been identified in close proximity to LDs in cells producing HCVcc (Miyanari et al., 2007). These structures were recognised by core- and E2-specific antibodies, indicating that the particles possibly represent HCV virions (Miyanari et al., 2007).

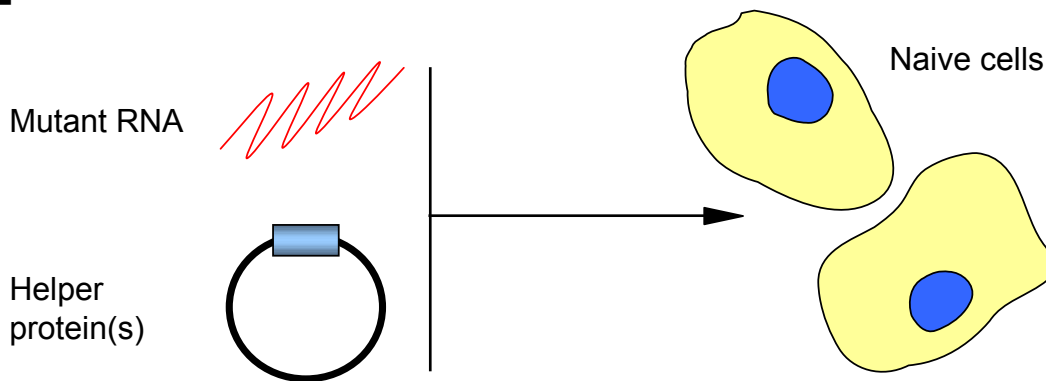
1.4.4.2 HCV Release

Following genome packaging, details regarding further maturation of the virion before egress are limited. An increasing body of evidence suggests that the LDL/VLDL assembly and secretion pathway may provide a means for transport of HCV virions from the cell. HCV particles can circulate complexed with VLDLs (Andre et al., 2002, Nielsen et al., 2006), which are produced in hepatocytes to export triglyceride and cholesterol into the extracellular environment (Gibbons et al., 2004). VLDL assembly is thought to occur in two different stages, (i) microsomal triglyceride transfer protein (MTP) transfers triglyceride from either

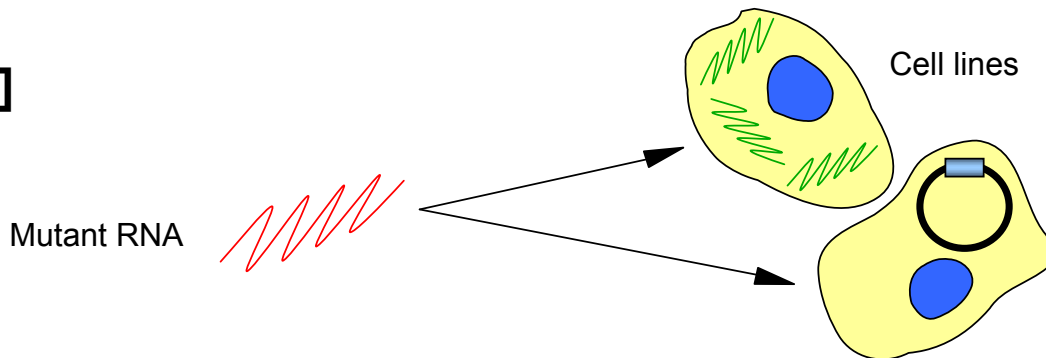
[A]



[B]



[C]



[D]

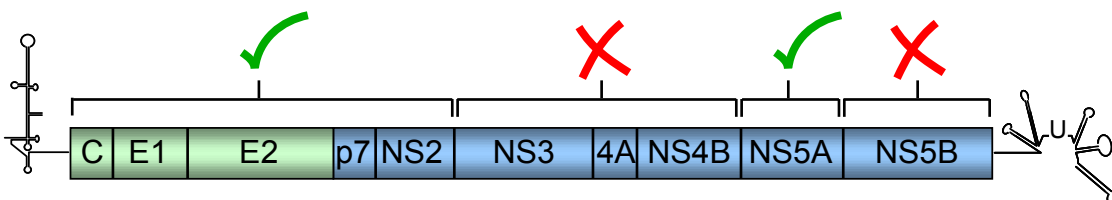


Figure 1.8 *Trans*-complementation of viral functions

Representation of the systems used to analyse *trans*-complementation of viral proteins, where mutant RNA is introduced [A] simultaneously into cells with helper RNAs [B] simultaneously into cells with plasmid-expressed proteins/polyproteins [C] into cell lines already containing helper RNA genomes or plasmid-expressed proteins. [D] Representation of the HCV polyprotein, indicating which proteins can (ticks) and cannot (crosses) be complemented *in trans*.

LDs or the ER lumen to apoB, allowing the growing apoB molecule to fold on a hydrophobic core and form a pre-VLDL (Olofsson & Boren, 2005) (ii) apoE, another VLDL component, aids the fusion of pre-VLDLs with triglyceride droplets derived from LDs in the ER/Golgi (Mensenkamp et al., 2001). Hence, LDs provide the bulk of lipid for VLDL formation in hepatocytes (McLauchlan, 2009). Importantly, an MTP inhibitor and siRNA targeting apoB are capable of reducing the release of virus particles (Huang et al., 2007a) and apoB is a rate-limiting factor for HCV assembly (Gastaminza et al., 2008). Moreover, silencing of apoE reduced infectious titres of intracellular HCV virions, indicating that the VLDL assembly pathway may be important for viral assembly as well as secretion (Chang et al., 2007). Comparison of intracellular and extracellular HCV virions suggest that the association of virus particles with lipoprotein particles lowers their buoyant density (Gastaminza et al., 2006), possibly having implications for the infectivity of the virus. For example, virus particles isolated from infected chimpanzees exhibit a lower buoyant density compared to those obtained in cell culture, and exhibit enhanced infectivity when used to infect naïve cells (Lindenbach et al., 2006).

1.5 *Trans*-Complementation of Virus Functions

Studies on HCV and other positive-strand RNA viruses have revealed that non-functional viral RNAs containing deleterious coding regions can have function restored to them by supplying wt components *in trans*. This process is referred to as *trans*-complementation and can provide insights into the functional organisation of viral RCs and the mechanisms that govern virus assembly. The ‘helper’ components that can restore function are usually supplied via (i) transient introduction of replicating or non-replicating RNA, (ii) introduction of plasmid-expressed proteins, or (iii) autonomous expression of proteins or replication of the helper RNA within a cell line. These approaches are represented in Figure 1.8, A-C.

1.5.1 *Trans*-Complementation of HCV RNA Replication

To date, investigation into *trans*-complementation of HCV RNA replication has utilised genotype 1b SGRs containing CCAMs and revealed that NS5A is the sole viral NS protein involved in RNA synthesis that can be supplied *in trans* (Appel et

al., 2005a, Tong & Malcolm, 2006). These analyses have yielded conflicting results regarding the context of NS5A expression in relation to its ability to *trans*-complement a defective genome. For example, one study showed that complementation by NS5A relied on its expression as part of a polyprotein (NS3-NS5A), since expression of NS5A alone failed to restore replication of an inactive SGR (Appel et al., 2005a). In a separate study however, NS5A produced stably within a cell line was able to complement a defective replicon without the need for expression as part of a polyprotein (Tong & Malcolm, 2006). The assays employed in these two reports differed slightly and it is therefore possible that distinct results may arise from the type of system used to study *trans*-complementation. However, both studies agreed that replication could not be restored to SGRs harbouring replication-lethal mutations in NS3, NS4B and NS5B by supplying these proteins *in trans* (Appel et al., 2005a, Tong & Malcolm, 2006). Therefore, it seems that the majority of the HCV replicase components can only function *in cis* for HCV RNA synthesis. The results presented by Appel et al. suggest that the NS components within a NS3-NS5A polyprotein are essential for the production of NS5A protein that is capable of restoring replication to defective genomes. Indeed, these proteins are required for post-translational modifications of NS5A, such as hyperphosphorylation (Koch & Bartenschlager, 1999, Neddermann et al., 1999). Alternatively, NS5A precursors may be important for replication, as found for other positive-strand RNA viruses (see Section 1.5.1.3). Interestingly, mutations affecting the N-terminal amphipathic α -helix of NS5A could not be rescued by *trans*-complementation (Appel et al., 2005a), suggesting that these mutants may fold incorrectly and interact with other replicase components in a manner incapable of rescue. The available data imply that NS5A is able to gain entry to RCs harbouring non-functional proteins, thereby restoring function by *trans*-complementation. Such a scenario fits with its perceived role in replication and assembly, since NS5A is proposed to be responsible for the trafficking of NS proteins and viral RNA to core situated on LDs (Miyanari et al., 2007).

1.5.2 *Trans*-Complementation of HCV Virion Assembly

The HCVcc system has allowed examination of the ability to *trans*-complement other stages of the HCV life cycle, besides genome synthesis. As described previously, NS5A is not only a replicase component but is also required for virus assembly and domain III of the protein is critical for this process (see Section

1.2.2.9). Using the HCVcc system, it was shown that virus production from HCV RNAs containing deletions in domain III could be rescued by supplying intact NS5A *in trans* (Appel et al., 2008). Another NS protein, NS2, is also involved in a pre-assembly step of HCV virion production (see Section 1.2.2.5) and the HCVcc system has revealed that assembly defects caused by mutations within NS2 can be complemented by functional NS2 supplied *in trans* (Jirasko et al., 2008). Regarding the structural proteins, HCV genomes containing lethal mutations within core can be rescued by ectopic expression of functional core protein (Miyanari et al., 2007). Furthermore, HCV RNA molecules lacking the entire core-NS2 coding region can be packaged in the presence of helper genomes supplying these proteins, or when introduced into 'packaging cell lines', in which the core-NS2 region is autonomously produced (Ishii et al., 2008, Steinmann et al., 2008). These *trans*-complemented HCV particles (HCV_{TCP}) exhibit characteristics identical to HCVcc. Thus, a *cis*-acting interaction between the core-NS2 proteins and the NS3-NS5B coding region is apparently unnecessary for virus assembly and release. This indicates that the mechanisms engaged in *trans*-complementation of HCV assembly are apparently less stringent compared to those involved in viral RNA synthesis. A summary of the HCV proteins, which can and cannot be *trans*-complemented, is shown in Figure 1.8, D.

1.5.3 *Trans*-Complementation of Other Positive-Strand RNA Viruses

Prior to analysis of HCV *trans*-complementation, studies using several other positive-strand RNA viruses highlighted differences in the ability to *trans*-complement proteins involved in their life cycles. Within the *flaviviridae* family, study of KV has shown that functional proteins expressed *in trans* can restore the replication of RNAs harbouring deletions within the NS1 (replication component), NS3 (helicase) and NS5 (RdRp) proteins (Khromykh et al., 1999b, Khromykh et al., 2000). *Trans*-complementation is also possible for RNAs harbouring mutations in all three of these proteins (Khromykh et al., 2000). Interestingly, while NS1 supplied alone *in trans* can rescue replication, the NS5 protein can only restore replication efficiently when expressed in the context of a NS1-NS5 polyprotein (Khromykh et al., 1999a). With bovine viral diarrhoea virus (BVDV), NS5 can function *in trans* (Grassmann et al., 2001), although it is unclear whether NS5 must be expressed from a polyprotein in order to restore replication to inactive RNAs. As with KV, yellow fever virus (YFV) RNAs harbouring a defective NS1

protein can be *trans*-complemented by NS1 supplied alone (Lindenbach & Rice, 1997). Taken as a whole, these data indicate two important points. Firstly, there is no apparent consistency between those proteins that can and cannot be *trans*-complemented for members of the *flaviviridae*, possibly suggesting differing mechanisms through which these viruses form functional RCs. Secondly, the results suggest that for some viruses (such as KV and HCV), the mature proteins comprising RCs may only be targeted to the appropriate location, or function correctly, when delivered from precursor polyproteins. The importance of precursors in *trans*-complementation is not restricted to members of the *flaviviridae*. For example, *trans*-complementation assays with poliovirus (PV, a member of the *picornaviridae*) have shown that viral RNA harbouring lethal mutations within the 3AB coding region can only be complemented by a 3AB-3D polyprotein and not by 3AB alone (Towner et al., 1998). Hence, protein precursors may be important for RNA replication in positive-strand viruses in general.

1.6 Modulation of HCV Infection by RNA Interference (RNAi)

RNAi is an intrinsic cellular system that allows regulation of gene expression. In this process, short-interfering (si) RNA molecules are able to silence genes by mediating cleavage of messenger RNA (mRNA) prior to translation. Hence, this technology can be used to silence RNA molecules of known sequence and has become a promising therapeutic strategy to target viral infections. siRNA-mediated interference as a means of targeting the HCV life cycle has been demonstrated by two approaches. Firstly, by direct targeting of the HCV RNA genome using virus-specific siRNAs and secondly, by modulating expression of host cell factors that have a role in the virus life cycle (see Section 1.4.3.3). Because siRNA technology was utilised for the studies presented in this thesis, these two approaches are described in the following sections and a third section outlines the mechanisms underlying siRNA-mediated cleavage of RNA.

1.6.1 Targeting the HCV Genome Directly

siRNAs bind to complementary ssRNA molecules in order to initiate the cleavage events that lead to silencing. Therefore, the ssRNA genome of HCV is an ideal target for RNAi. Several studies have shown that in cell culture, HCV gene expression can be reduced using siRNAs that are complementary to the viral

genome (Randall & Rice, 2004). While the majority of the HCV genome is apparently accessible to the RNAi machinery, the most successful approaches have been achieved by targeting highly conserved viral sequences, since siRNAs that differ from their target sequence by two or more bases are inefficient at silencing HCV replication (Randall et al., 2003). Therefore, siRNAs directed against the 5' UTR (Chevalier et al., 2007, Kanda et al., 2007, Kronke et al., 2004, Seo et al., 2003, Yokota et al., 2003), NS3 and NS5B (Kapadia et al., 2003, Prabhu et al., 2005) are the most efficient options for reducing HCV RNA replication, since these regions of the genome are well conserved. The HCV 5' UTR is particularly highly conserved across HCV genotypes and therefore siRNAs directed against this sequence are able to potently inhibit viral RNA synthesis for several HCV strains, including Con1, H77 and JFH1. For example, siRNA treatment of cells harbouring Con1 SGRs can decrease viral RNA levels by 80-fold and replicating viral genomes can be cleared from >98% of cells (Randall et al., 2003). Furthermore, siRNA treatment of naïve cells can reduce viral replication upon infection with HCVcc derived from strain JFH1 (Chevalier et al., 2007).

It is currently unclear whether HCV is targeted directly by the RNAi response pathway *in vivo*. Recently, the HCV-encoded proteins core and E2 have been shown to interact with components of the cellular machinery responsible for gene silencing (Ji et al., 2008, Wang et al., 2006). These results suggest that the RNAi pathway may target HCV RNA in cells and that the virus has evolved strategies to circumvent this host response. However, other groups have presented evidence to the contrary; for example, cells harbouring replicating HCV genomes show no detectable presence of viral siRNAs (Pfeffer et al., 2005). Hence, it remains to be confirmed whether RNAi represents an antiviral pathway that responds to HCV infection.

1.6.2 Targeting Host Cell Genes Involved in HCV RNA Synthesis

In addition to targeting the HCV genome directly, siRNAs have been used to demonstrate the importance of various host cell proteins for viral replication. For instance, siRNA has been used to confirm the contribution of cellular proteins hVAP-A (which interacts with NS5A, see Section 1.2.2.9), La autoantigen and PTB (which both interact with the 5' and 3' UTRs, see Sections 1.2.2.1 and 1.2.2.11) to viral replication (Xue et al., 2007). Several groups have screened libraries of siRNAs targeting host cell factors in an attempt to discover novel proteins involved

in HCV RNA replication. Such approaches have identified several human kinases (Supekova et al., 2008), transporter proteins and transcription factors (Ng et al., 2007), to name but a few. A study conducted by Randall et al. in 2007 screened 62 cellular genes previously reported to interact with HCV proteins or RNA and assessed the effect of their knockdown on JFH1 RNA production. From this screen, 26 genes that influenced HCV RNA replication were identified. Interestingly, in cells transfected with siRNAs targeting the RNAi component Dicer, HCV RNA synthesis was reduced by ~7-fold (Randall et al., 2007). This result is surprising, since it would be predicted that reducing Dicer should lead to a crippled anti-HCV RNAi response. Thus, the RNAi pathway may facilitate, rather than hinder, HCV replication. This screen also confirmed the importance of miR-122 in viral RNA synthesis, which has previously been reported to bind to the 5' UTR in genotype 1 SGRs (Jopling et al., 2005, Randall et al., 2007). Therefore, it is possible that miR-122 is important for the replication of all HCV genotypes.

Overall, siRNA technology represents an ideal system for identifying host cell genes that influence HCV genome synthesis. As mentioned previously, siRNAs could represent a promising candidate for HCV therapy. However, much work is needed to improve siRNA delivery to cells, limit off-target effects and minimise the development of viral resistance (Lopez-Fraga et al., 2008).

1.6.3 Discovery and Mechanism of RNAi

RNAi was first characterised after injection of dsRNA molecules into the nematode *C. elegans* resulted in potent and specific reductions in levels of complementary mRNA transcripts (Fire et al., 1998). RNAi was thereafter identified in mammalian cells through the introduction of double-stranded siRNAs of 21bp in length (Elbashir et al., 2001a). The fact that IFN production can be induced by the presence of dsRNA molecules of >30bp in length complicated the initial demonstration of RNAi in mammalian cells. siRNAs induce the cleavage of complementary mRNAs in a process called post-transcriptional gene silencing (PTGS). PTGS functions as an innate antiviral defence mechanism in nematodes, insects, plants and fungi but endogenously expressed siRNAs have yet to be identified in mammals (Kim & Rossi, 2007).

siRNA-mediated RNAi occurs when dsRNA molecules in the cytoplasm are processed by a complex comprising Dicer (a RNase enzyme), TAR RNA-binding protein (TRBP) and Argonaute 2 (AGO2). Upon binding to dsRNA, Dicer cleaves

the molecule into 19-23bp siRNAs characterised by 2-3bp overhangs at the 3' end and 5' phosphate groups (Dykxhoorn et al., 2003). Following cleavage, AGO2 cuts the sense 'passenger' RNA strand, leaving only the single antisense 'guide' strand associated with the Dicer complex (Matranga et al., 2005, Rand et al., 2005). A number of other Argonaute proteins associate at this stage, leading to the formation of an active RNA-induced silencing complex (RISC) that is targeted to mRNA molecules via the complementary pairing of the complexed guide strand. Once the guide strand binds the complementary sequence, RISC cleaves the mRNA strand in the centre of the duplex formed by annealing of the guide siRNA to the target mRNA (Elbashir et al., 2001b). Cleaved mRNA transcripts are subsequently degraded by cellular exonucleases, while the RISC complex is recycled for further cleavage events. The stages of siRNA mediated gene silencing are depicted in Figure 1.9.

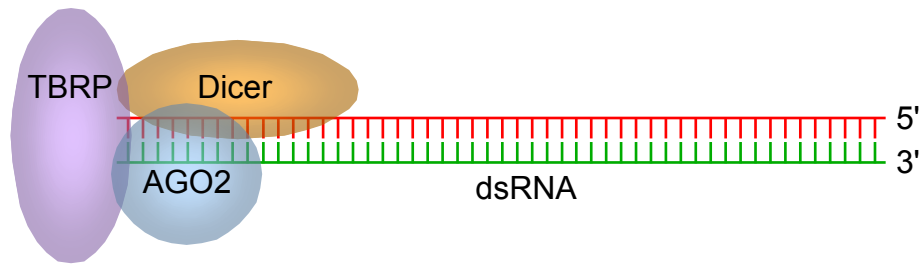
1.7 Fluorescent Proteins and their Applications

Fluorescent proteins such as GFP have been extensively used for the characterisation of viral proteins, including those encoded by HCV. This approach is particularly useful for live-cell studies, since fixation and antibody staining is not required to observe fluorescence. For example, reports utilising GFP-tagged NS4B have shown that the protein localises to punctate structures on the ER membrane in live cells (Gretton et al., 2005, Lundin et al., 2006, Lundin et al., 2003). Similarly, insertion of GFP into the NS5A coding region revealed that it localised with viral RNA at punctate sites (Moradpour et al., 2004b). Since GFP was utilised for many of the studies presented in this thesis, a brief description of the protein and its applications are presented below.

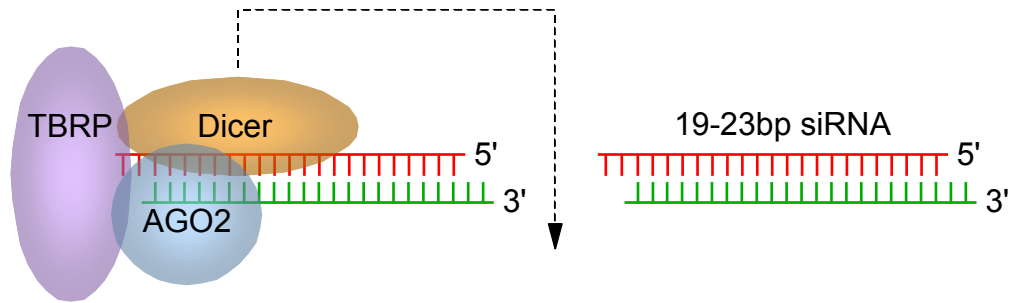
1.7.1 GFP

Fluorescent proteins belonging to the so-called GFP-like protein family have been identified in a variety of marine organisms. Due to their bright colours ranging from cyan to green to red, the proteins have been used extensively in cell and molecular biology (Wachter, 2006). GFP is a 27kDa protein first discovered in the Pacific Northwest jellyfish *Aequorea victoria* more than 45 years ago (Shimomura et al., 1962). X-ray crystallography has revealed the three-dimensional structure of GFP and the biochemical and physical properties of its chromophore have been

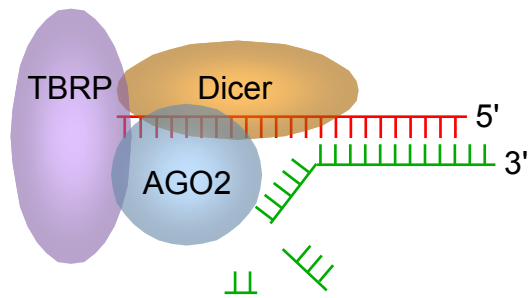
[A]



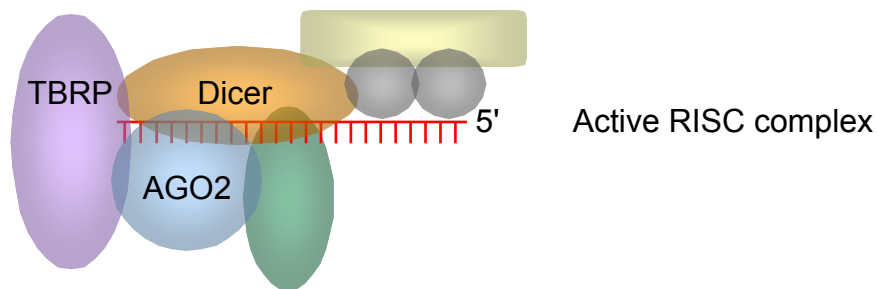
[B]



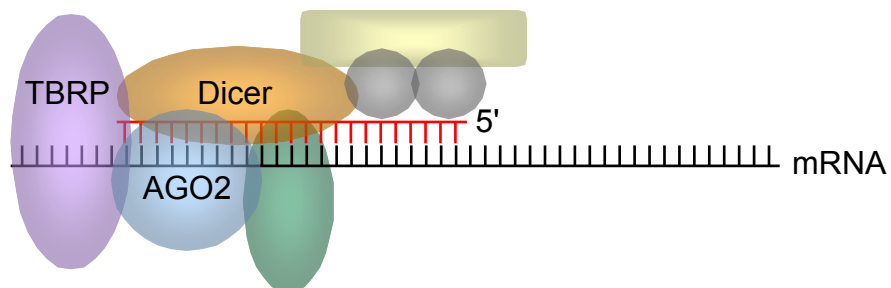
[C]



[D]



[E]



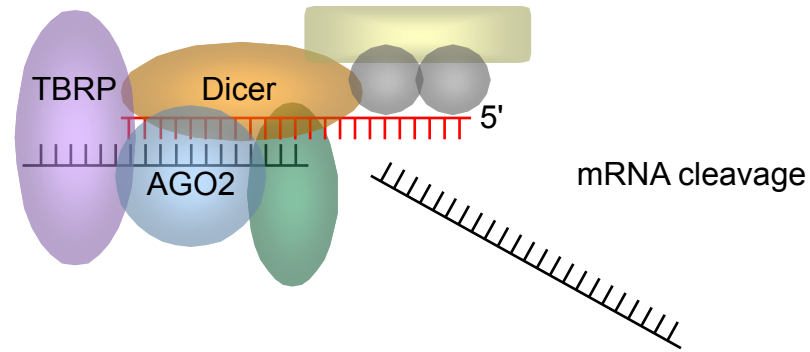
[F]

Figure 1.9 The RNA interference (RNAi) pathway

An overview of the mechanism by which RNAi mediates gene silencing. **[A]** A complex comprising Dicer, TAR RNA-binding protein (TRBP) and Argonaute 2 (AGO2) is recruited to dsRNA molecules in the cytoplasm. **[B]** Dicer cleaves the dsRNA into 19-23bp fragments. **[C]** AGO2 then cleaves the sense RNA strand (green), leaving behind the antisense RNA strand (red). **[D]** Argonautes and argonaute-associated proteins are recruited to the complex, forming the active RNA-induced silencing (RISC) complex. **[E]** The antisense RNA molecule specifically guides the RISC complex to target mRNA molecules by binding the complementary mRNA sequence. **[F]** mRNA is cleaved by AGO2 and subsequently degraded by cellular exonucleases.

defined (Tsien, 1998). GFP exists as a mixed population of neutral phenols and anionic phenolates, which produce major (397nm) and minor (475nm) absorbance peaks respectively (Patterson & Lippincott-Schwartz, 2002). Upon illumination of GFP with ultraviolet or ~400nm light, the chromophore population undergoes photoconversion, shifting predominantly to the anionic form and increasing the minor peak absorbance (Figure 1.10, A). It is this minor peak population that emits green fluorescence upon excitation with a 488nm laser. The GFP chromophore is derived from the amino acid triplet Ser-Tyr-Gly, which is located within the centre of the barrel-like structure of the protein (Yang et al., 1996).

GFP has proven to be a highly useful tool for studying the properties and behaviour of proteins in biological systems and possesses several key features that make it advantageous over other approaches. Firstly, the folding of GFP into a functional unit is autocatalytic and independent of external substrates or cofactors (except oxygen). Moreover, the fusion of GFP to cellular proteins rarely affects the native properties of the tagged-protein and is typically non-toxic in cells (Zimmer, 2002). The applications for GFP are wide and varied. GFP was first utilised as a reporter gene, where several promoters controlled the expression of the protein, allowing fluorescence intensity to indicate the level of gene expression in living cells (Chalfie et al., 1994). Probably the most common use for GFP is as a fusion tag, permitting the localisation and behaviour of heterologous proteins to be monitored. This fusion can be at the N- or C-terminus of the protein of interest, but GFP can also be inserted within protein-coding sequences, as demonstrated with HCV-encoded NS5A (see Section 1.2.2.9). Furthermore, the stability of GFP fluorescence means that insights into protein behaviour can be gained over extended time periods.

1.7.2 Photoactivatable-GFP (PAGFP)

As described above, GFP fluorescence is observed upon excitation of the minor absorbance peak chromophore population using a 488nm laser. Preceding excitation, chromophores undergo photoconversion from the major to minor absorbance peak upon exposure to ultraviolet or ~400nm light. For GFP, a population of chromophores produce a small minor absorption peak before photoconversion occurs (Figure 1.10, A). Hence, a ~3-fold increase is detected upon excitation at 488nm. PAGFP also exists as a dual population of chromophores, with the important difference that a barely detectable minor

absorbance peak is evident prior to photoconversion (Figure 1.10, B). Therefore, exposure to ultraviolet or ~400nm light followed by excitation at 488nm, produces fluorescence increases of >60-fold (Patterson & Lippincott-Schwartz, 2002). These properties rely upon a single T203H mutation within the GFP coding sequence.

PAGFP can be tagged to cellular proteins in the same way as GFP, with the advantage that distinct regions within cells can be activated. This approach allows protein movement to be monitored, especially since fluorescence activation is irreversible and therefore will not diminish over time. PAGFP has been used for mobility studies of lysosomes (Patterson & Lippincott-Schwartz, 2002), voltage-gated potassium channels (O'Connell & Tamkun, 2005) and mitochondria (Haigh et al., 2007).

1.7.3 Fluorescence Recovery After Photobleaching (FRAP)

GFP is a suitable molecule for photobleaching studies, since the fluorescence emitted from the protein can be irreversibly abolished upon bleaching with high intensity laser power. FRAP analysis involves the selective photobleaching of a defined area of the cell, followed by measurement of fluorescence recovery within the bleached region over a period of time (Figure 1.10, C). Fluorescence will only recover if mobile, non-bleached molecules are able to move into the bleached area. The different rates and extents to which fluorescence recovers can provide insights into protein dynamics, including interactions of proteins with other cellular components (Reits & Neefjes, 2001).

FRAP has previously been used to examine the mobility of HCV proteins harbouring GFP. For example, mobility analysis of GFP-tagged NS4B revealed that the protein was relatively mobile on the ER membrane compared to when it was localised to punctate membranous structures (Gretton et al., 2005). These structures are thought to be analogous to RCs. Similarly, GFP-tagged NS5A expressed from a replicating genome exhibited no appreciable mobility within these structures (Wolk et al., 2008). Therefore, FRAP is a useful tool that is able to define the dynamics of viral proteins expressed in cells.

1.8 Aims of the Study

Initially, the aim of the project was broadly divided into two lines of investigation. The first aim was to insert GFP and PAGFP into the C-terminal coding region of

NS5A in the context of a JFH1-based SGR. This strategy would enable characterisation of NS5A in a live-cell environment harbouring actively replicating HCV RNA (Chapter 3). Secondly, we sought to determine the role of NS4B in HCV RNA replication, specifically with respect to its ability to alter cellular membranes. This investigation would utilise mutagenesis of the NS4B coding region (Chapter 4).

The NS4B mutagenesis studies yielded several novel replicating and non-replicating mutant SGRs, leading to the establishment of two further projects. Firstly, the ability to complement defective NS4B protein in *trans* utilising non-replicating viral RNAs would be assessed (Chapter 5). Secondly, replicating HCV SGRs harbouring NS4B mutations would be used to determine whether NS4B had any influence on virus assembly and release (Chapter 6).

Finally, in an attempt to identify novel cellular proteins involved in HCV genome replication, a library of siRNAs targeting nucleotide-binding proteins was screened in two cell lines (Chapter 7). It was hoped that this study would also expand the scope of the project beyond investigation solely into viral components.

2 Materials and Methods

2.1 Materials

2.1.1 Vectors

Plasmid	Source
pGEM-T-Easy	Promega
pGFP-C1	Clontech
pPAGFP-C1	Jennifer Lippincott-Schwartz [National Institutes of Health, USA]
pZero 2.1	Invitrogen
pCMV10	Nigel Stow [MRC Virology Unit]

2.1.2 Kits and Enzymes

2.1.2.1 Kits

Kit	Source
PureLink HiPure plasmid midi-prep kit	Invitrogen
QIAQuick gel extraction kit	Qiagen
KOD Hot Start DNA Polymerase kit	Novagen
QuickChange Site-Directed Mutagenesis kit	Stratagene
QuickChange II XL Site-Directed Mutagenesis kit	Stratagene
T7 RiboMAX Express Large Scale RNA Production System	Promega
Luciferase Assay system	Promega
Enhanced Chemiluminescence Plus Western Blotting Detection System	Amersham Biosciences
NovaRED substrate kit for peroxidase	Vector
Aquabluer Cell-Viability assay	MultiTarget Pharmaceuticals
RNeasy mini kit	Qiagen
Taqman kit	Applied Biosciences

2.1.2.2 Enzymes

Enzyme	Source
Restriction enzymes	NEB/Roche
T4 DNA ligase	NEB
Calf intestinal phosphatase	NEB
Mung bean nuclease	NEB
Taq polymerase	NEB
KOD polymerase	Novagen
Multiscribe RT	Applied Biosciences

2.1.3 Cells

Cells	Description	Source
Huh-7 cells	Human hepatoma cell line	John McLauchlan [MRC Virology Unit]
2/1 cells	Huh-7 cells harbouring the JFH1 replicon	Paul Targett-Adams [MRC Virology Unit] (Targett-Adams and McLauchlan, 2005)
U2OS cells	Human osteosarcoma cell line	Chris Boutell [MRC Virology Unit]

2.1.4 Transfection/Transformation reagents

Reagent	Source
Lipofectamine 2000	Invitrogen
Lipofectamine RNAiMAX	Invitrogen
Opti-mem-1	Gibco

2.1.5 Cell Culture Growth Medium

All cell culture media were supplied by Gibco (Invitrogen Life Technologies). Huh-7 and U2OS cells were grown in DMEM_{Complete} (Dulbecco's Modified Eagle Medium [DMEM] supplemented with 10% foetal calf serum (FCS), 100 units/ml penicillin/streptomycin and 1x non-essential amino acids). 2/1 cells, Tri-Huh-7 cells and Tri-U2OS cells were maintained in DMEM_{Complete} supplemented with 100µg/ml

G418-sulphate (Melford). All cells were harvested using 1x Trypsin (10x stock supplied from Sigma).

PBS, versene, L-broth and yeast tryptose (YT) broth were prepared in-house by the media department.

2.1.6 Antibodies

2.1.6.1 Primary Antibodies

Antibody	Species	Source
Anti-NS5A	Sheep polyclonal	Mark Harris and Steve Griffin, [University of Leeds] (Macdonald et al., 2003)
Anti-NS4B	Rabbit polyclonal	Sarah Gretton [University of Leeds] and Graham Hope [MRC Virology Unit]
Anti-Core	Rabbit polyclonal	Graham Hope and John McLauchlan [MRC Virology Unit] (Hope and McLauchlan., 2000)
Anti-dsRNA	Mouse monoclonal	Scicons [Hungary] (Targett-Adams et al., 2008)
Anti-Actin	Mouse monoclonal	Sigma
Anti-CKI- α	Goat polyclonal	Santa Cruz Biotechnology

2.1.6.2 Secondary Antibodies

Antibody	Species	Source
Anti-mouse IgG-HRP	Goat polyclonal	Sigma
Anti-goat/sheep IgG-HRP	Mouse monoclonal	Sigma
Anti-rabbit IgG-PAP	Goat polyclonal	Sigma
Anti-mouse-Alexa-488 (FITC)	Donkey polyclonal	Invitrogen
Anti-mouse-Alexa-568 (TRITC)	Goat polyclonal	Invitrogen
Anti-rabbit-Alexa-488 (FITC)	Donkey polyclonal	Invitrogen
Anti-rabbit-Alexa-594 (TRITC)	Donkey polyclonal	Invitrogen
Anti-sheep-Alexa-488 (FITC)	Donkey polyclonal	Invitrogen
Anti-sheep-Alexa-594 (TRITC)	Donkey polyclonal	Invitrogen

2.1.7 Commonly Used Chemicals

Chemical	Abbreviation	Source
2-Amino-2-(hydroxymethyl)-1,3-propanediol	TRIS	BDH
2-Mercaptoethanol	β -ME	Sigma
37.5:1 acrylamide/bis solution	-	Bio-RAD
4',6-diamidino-2-phenylindole	DAPI	Promega
Agarose	-	Melford
Ammonium persulphate	APS	Bio-RAD
Ampicillin	Amp	Melford
Bromophenol Blue	BPB	BDH
Chloroform	-	Sigma
Ethanol	EtOH	Fischer Scientific
Ethidium Bromide	EtBr	Sigma
Kanamycin	Kan	Melford
Glucose	-	BDH
Glycine	-	BDH
Hydrogen peroxide	H ₂ O ₂	Sigma
Methanol	MeOH	BDH
N,N,N',N'-Tetramethylethylene-diamine	TEMED	Sigma
Neomycin phosphotransferase	G418	Melford
Paraformaldehyde	PFA	Sigma
Phenol	-	Sigma
Propan-2-ol	-	BDH
Sodium carbonate	Na ₂ CO ₃	BDH
Sodium chloride	NaCl	BDH
Sodium dodecyl sulphate	SDS	BDH
Sodium hydroxide	NaOH	BDH
Sucrose	-	BDH
Triton X-100	TX-100	Sigma
Triton X-114	TX-114	Sigma
Tween 20	-	Sigma

2.1.8 Clones

Clone	Source
pGFP-DNase X	Johannes Coy [MTM Laboratories AG, Germany]
pSGR-JFH1	Takaji Wakita [National Institute of Infectious Diseases, Japan]
pSGR-luc-JFH1	Paul Targett-Adams [MRC Virology Unit]
pJFH1	Takaji Wakita [National Institute of Infectious Diseases, Japan]
pJ6-JFH1	Arvind Patel [MRC Virology Unit]

2.1.9 Solutions

2.1.9.1 Bacterial Expression

Solution	Components
L-Broth	170mM NaCl, 10g/l Bactopectone, 5g/l yeast extract
L-Broth agar	L-broth plus 1.5% (w/v) agar
Yeast tryptose broth	85mM NaCl, 16g/l Bactopectone, 10g/l yeast extract

2.1.9.2 DNA Manipulation & Purification

Solution	Components
Equilibration buffer (EQ1)	0.1M sodium acetate (pH 5.0), 0.6M NaCl, 0.15% (v/v) Triton X-100
Cell resuspension buffer (R3)	50mM Tris-HCl (pH 8.0), 10mM EDTA, 100µg/ml RNase A
Lysis buffer (L7)	0.2M NaOH, 1% (w/v) SDS
Precipitation buffer (N3)	3.1M potassium acetate (pH 5.5)
Wash buffer (W8)	0.1M sodium acetate (pH 5.0), 825mM NaCl
Elution buffer (E4)	100mM Tris-HCl (pH 8.5), 1.25M NaCl
TE buffer (TE)	10mM Tris-HCl (pH 8.0), 0.1mM EDTA
Agarose gel loading buffer	5x TBE, 50% sucrose, 1µg/ml BPB
TBE (10x)	0.9M Tris-HCl, 0.9M boric acid, 0.02M EDTA

T4 DNA Ligase buffer (10x)	400mM Tris-HCl, 100mM MgCl ₂ , 100mM DTT, 5mM ATP (pH 7.8)
ThermoPol buffer (10x)	200mM Tris-HCl, 100mM (NH ₄) ₂ SO ₄ , 100mM KCl, 20mM MgSO ₄ , 1% Triton X-100, (pH 8.8)
Reaction buffer (10x)	200mM Tris-HCl, 100mM (NH ₄) ₂ SO ₄ , 100mM KCl, 20mM MgSO ₄ , 1% Triton X-100, (pH 8.8)

2.1.9.3 SDS-PAGE

Solution	Components
Running gel buffer (RGB, 4x)	1.5M Tris-HCl (pH 8.9), 0.4% (w/v) SDS
Stacking gel buffer (SGB, 4x)	0.5M Tris-HCl (pH 6.7), 0.4% (w/v) SDS
Boiling mix (3x)	29% (v/v) SGB, 6% (w/v) SDS, 2M β-ME, 29% (v/v) glycerol, 1μg/ml BPB
Tank buffer	25mM Tris-HCl, 200mM glycine, 0.1% (w/v) SDS
Phase separation lysis buffer	10μM Tris-HCl (pH 7.4), 150μM NaCl, 2% (v/v) Triton X-114
Phase separation solution	10μM Tris-HCl (pH 7.4), 150μM NaCl, 6% (w/v) sucrose, 0.06% (v/v) Triton X-114

2.1.9.4 Western Blot Analysis

Solution	Components
Towbin buffer	25mM Tris-HCl (pH 8.0), 192mM glycine, 20% (v/v) methanol
PBS (A)	170mM NaCl, 3.4mM KCl, 10mM Na ₂ HPO ₄ , 1.8mM KH ₂ PO ₄ , 25mM Tris-HCl (pH 7.2)
PBS (A)- Tween	PBS (A), plus 0.05% (v/v) Tween-20
Block buffer	PBS (A)-Tween, plus either 2% or 5% (w/v) dried milk (Marvel)

2.1.9.5 Tissue Culture

Solution	Components
Trypsin	0.25% (w/v) Difco trypsin dissolved in PBS (A), 0.0005% (w/v) phenol red
Versene	0.6mM EDTA in PBS-(A), 0.002% (w/v) phenol red

2.1.10 Oligonucleotide Synthesis and DNA Sequence Analysis

Oligonucleotides were synthesised and supplied by Sigma-Aldrich. All sequence analysis was performed by the sequencing service at the University of Dundee.

2.1.11 siRNA Library

Positive (siHCV) and negative (Con) control siRNAs and a library of 897 siRNAs directed against cellular nucleotide-binding proteins were supplied by Ambion. 1nM of each library siRNA was supplied by the manufacturer, and resuspended in dH₂O to yield a stock concentration of 100µM (siHCV and Con) or 50µM (library siRNAs). Each cellular gene in the library was targeted by 3 siRNAs directed against different regions of the mRNA sequence. Hence, the library comprised siRNAs targeted against 299 cellular genes.

2.2 Methods

2.2.1 Tissue Culture Maintenance

All cell lines were cultured in DMEM_{Complete} at 37°C in an atmosphere of 5% CO₂. Cells harbouring the neomycin resistance gene as part of the HCV SGR were cultured in the presence of G418 at a concentration of 100µg/ml. Cell lines were typically grown in 160cm² tissue culture flasks (Nunc). At confluency, cells were removed by trypsin treatment and resuspended in 10ml of DMEM_{Complete}, before use either for experiments or flask re-seeding.

2.2.2 DNA Manipulation

2.2.2.1 DNA Restriction Enzyme Digestion

Digests were performed at 37°C (unless otherwise specified by the supplier) typically in 50µl reactions, using 10 units of restriction enzyme per 0.5µg DNA per hour. All reactions were carried out using the supplier-specified buffer and BSA if necessary.

2.2.2.2 DNA Ligation

Purified DNA fragments were ligated in 10µl reactions containing 1x ligase buffer and 2 units of T4 DNA ligase. Reactions were incubated at 4°C for 16-18 hours. Resulting ligated DNA was diluted 1:20 in dH₂O, prior to electroporation into competent *E.coli* bacteria.

2.2.2.3 Transformation of Competent Bacteria

Transformation was carried out using electrocompetent GeneHogs (a DH10B-derived *E.coli* strain [Invitrogen]). 10µl of GeneHogs were thawed on ice before the addition of 2µl pre-diluted DNA (see above). The mixture was then transferred into a pre-chilled cuvette (1mm gap [Apollo]) for electroporation at 1.6kV, 25µF using a Bio-Rad Gene Pulser II. Electroporated bacteria were resuspended in 500µl YT broth and incubated at 37°C with shaking at 180rpm for 1 hour. This step allowed bacterial expression of the antibiotic resistance gene present in the electroporated plasmid DNA. 10-50µl of cultures were plated onto L-broth agar plates containing 100µg/ml of appropriate antibiotic and incubated at 30°C overnight.

2.2.2.4 Transformation of Competent Bacteria for Site-Directed Mutagenesis

DpnI-treated DNA from PCR reactions (Section 2.2.2.8) was used to transform either 50µl XL1-Blue Supercompetent cells or 45µl XL10-Gold Ultracompetent cells (Stratagene). All cells were thawed on ice (at this point for XL10-Gold cells only, 2µl β-ME was added and the cells were incubated on ice for 10 minutes). 2µl mutant DNA was added to the competent cells, which were incubated on ice for a further 30 minutes. DNA-bacteria mixtures were then heat-pulsed at 42°C for either 30 seconds (XL10-Gold cells) or 45 seconds (XL1-Blue cells) and then incubated on ice for a further 2 minutes. 0.5ml of YT broth pre-heated to 42°C was

added to each mixture, followed by incubation at 37°C for 1 hour with shaking at 180rpm. 2x 250µl aliquots of cultures were plated onto L-broth agar plates containing 100µg/ml of appropriate antibiotic and incubated at 37°C overnight.

2.2.2.5 Small-Scale DNA Purification (Minipreps)

Single colonies of transformed bacteria were used to inoculate 2ml of L-broth containing a selective antibiotic, followed by incubation overnight at 30°C with shaking at 180rpm. 200µl of cultures were added to an equal volume of lysis buffer, vortexed briefly and then incubated for 5 minutes at room temperature. 200µl precipitation buffer was added and samples were vortexed briefly. Cellular debris was pelleted by centrifugation at 15000x G for 2 minutes before the supernatant was removed and added to 600µl isopropanol to precipitate the plasmid DNA. Samples were centrifuged at 15000x G for 5 minutes to pellet the DNA. The supernatant was removed and the pellet was washed with 70% ethanol, and spun again at 15000x G for 5 minutes. The supernatant was removed and the pellet was allowed to air-dry. The pellet was then resuspended in an appropriate volume of dH₂O for analysis by restriction enzyme digestion.

2.2.2.6 Large-Scale DNA Purification (Midipreps)

Transformed bacteria were used to inoculate 150ml L-broth containing a selective antibiotic, followed by overnight incubation at 30°C with shaking at 180rpm. Bacterial cells were pelleted by centrifugation at 4000x G for 10 minutes at 4°C and the supernatant was removed. The following purification steps were performed using the PureLink HiPure plasmid midiprep kit (Invitrogen). The pellet was resuspended in 4ml of buffer R3 (cell resuspension buffer) by pipetting. 4ml of buffer L7 (lysis buffer) was added to the suspension and mixed gently by inversion. The solution was incubated at room temperature for 5 minutes before addition of buffer N3 (precipitation buffer) and further mixing by inversion, at which point the cellular debris was pelleted by centrifugation at 6500x G for 10 minutes at room temperature. The supernatant (containing plasmid DNA) was filtered through an equilibrated HiPure Midi column (Invitrogen) by gravity. Once the supernatant had filtered through and plasmid DNA had bound, the column was washed twice with 8ml of buffer W8 (wash buffer), each time allowed to filter by gravity. Plasmid DNA was then eluted by adding 5ml of buffer E4 (elution buffer)

and mixed gently with 3.5ml of isopropanol to precipitate plasmid DNA. DNA was pelleted by centrifugation of samples at 6500x G for 15 minutes at 4°C. The supernatant was removed from the pellets, which were then washed once with 70% ethanol and centrifuged at 6500x G for 5 minutes at 4°C. Finally, the supernatant was removed and, after being allowed to air-dry, plasmid DNA was resuspended in 200µl of TE buffer.

2.2.2.7 PCR Amplification and dA-Tailing of DNA

PCR reactions were performed using the KOD Hot Start DNA Polymerase kit (Novagen), typically in a final volume of 50µl. The reaction contained ~25ng DNA template, 10µM forward and reverse primers, 2mM dNTPs, 1x KOD buffer, 1nM MgSO₄ and 1 unit of KOD polymerase. Reactions were made up to 50µl with dH₂O. All PCR reactions were performed in a ThermoHybaid PX2 Thermal Cycler. Typically, reactions were heated to 94°C for 2 minutes to allow complete denaturation of dsDNA. PCR was then performed as follows: (i) DNA strand separation at 94°C for 15 seconds (ii) primer annealing at 55°C for 1 minute (iii) strand elongation at 72°C for 1 minute/Kb of DNA. Steps (i)-(iii) were repeated 35 times. KOD polymerase produces blunt-ended PCR products, which were dA-tailed before ligation into commercial vectors such as pGEM-T-Easy. dA-tailing was performed by adding 2µl dATP, 1x ThermoPol buffer and Taq polymerase (5 units) to 15µl of purified PCR product. The reaction was then incubated at 70°C for 20 minutes, followed by re-purification of the PCR product through a QIAquick spin column (Section 2.2.3.2). This resulted in PCR products with 3' dA-tailed overhangs that could be ligated into the dT-tailed pGEM-T-Easy vector.

2.2.2.8 Site-Directed Mutagenesis

Mutagenesis reactions were performed using either the QuickChange Site-Directed Mutagenesis kit (for DNA templates up to ~8kb) or QuickChange II XL Site-Directed Mutagenesis kit (for DNA templates >8kb, both from Stratagene). Forward and reverse primers for mutagenesis were designed to incorporate the desired mutation(s) in the middle of the primer sequence and were between 25 and 45 bases in length. PCR reactions were performed in a final volume of 50µl and consisted of ~25ng DNA template, 10µM forward and reverse mutagenic primers, dNTPs, 1x Reaction buffer and either *PfuTurbo* DNA polymerase (normal

kit) or *PfuUltra* HF DNA polymerase (XL kit). In the case of the XL kit, the manufacturer recommended addition of QuickSolution at this point to improve linear amplification. Reactions were made up to 50µl with dH₂O. PCR reactions were performed in a ThermoHybaid PX2 Thermal Cycler. Typically, reactions were heated to 95°C for 1 minute to allow complete denaturation of dsDNA. PCR was then performed as follows: (i) DNA strand separation at 95°C for 30 seconds (50 seconds for the XL kit) (ii) primer annealing at 55°C for 30 seconds (60°C for 50 seconds for the XL kit) (iii) strand elongation at 68°C for 1 minute/Kb of DNA (2.5 minutes/Kb for the XL kit). Steps (i)-(iii) were repeated 18 times. Finally, reactions were heated to 68°C for 1 minute/kb of DNA template length. Following PCR, *DpnI* (10 units) was added to each reaction to digest the non-mutated *dam*-methylated parental DNA. Reactions were mixed by pipetting, then centrifuged at 15000x G for 1 minute, followed by incubation at 37°C for 1 hour. *DpnI*-treated DNA was then used to transform either XL1-Blue Supercompetent cells, or XL10-Gold Ultracompetent cells.

2.2.2.9 Linearisation of HCV SGR and HCV Genomic Plasmid DNA

Plasmids were linearised with *XbaI* in a 50µl reaction. After linearisation, DNA was purified through a QIAquick spin column (Section 2.2.3.2) before addition of 2 units of Mung bean nuclease (MBN). The reaction was incubated at 30°C for 30 minutes, to allow complete removal of the sticky-ends generated by the *XbaI* digestion. Linearised DNA then underwent phenol/chloroform purification (Section 2.2.3.3), before resuspension in an appropriate volume of dH₂O.

2.2.3 Isolation and Purification of DNA

2.2.3.1 Agarose Gel Electrophoresis

This method was employed to resolve DNA fragments produced by PCR or restriction enzyme digestion. 1% agarose gels (120mm x 90mm) were used to separate fragments larger than 500bp. Shorter DNA fragments were resolved using 2% gels. Agarose gels were prepared using 0.5x TBE buffer and contained a final concentration of 1µg/ml ethidium bromide. Typically, gels were run at 150V in 0.5x TBE buffer. Where appropriate, DNA fragments were run alongside 1Kbp or 100bp ladders (NEB). DNA was visualised under long-wave UV light (if the DNA

was to be used for cloning) or short-wave UV light. Gel photography was performed on a BioRad gel documentation system.

2.2.3.2 Purification of DNA from Agarose Gels

Gel slices containing digested DNA fragments were excised with the aid of long-wave UV light and then purified using the QIAQuick gel extraction kit (Qiagen). This system was also used to purify PCR products prior to dA-tailing (Section 2.2.2.7) or to purify linearised DNA products (Section 2.2.2.9). Buffer QG (solubilisation buffer) was added to the DNA-containing gel slice at a ratio of 3:1 and then incubated at 50°C to dissolve the agarose. If the DNA to be purified was <500bp or >4kb in size, 1 gel volume of isopropanol was added at this stage to increase DNA yield. DNA in the gel solution was then bound to a QIAquick spin column by centrifugation at 15000x G for 1 minute. The column was washed once with 750µl buffer PE (wash buffer) and centrifugation was repeated at 15000x G for 1 minute. DNA was eluted from the column by addition of 30-50µl of buffer EB (elution buffer) followed by further centrifugation at 15000x G for 1 minute. Purified DNA was eluted into a fresh 1.5ml tube.

2.2.3.3 Phenol/Chloroform Extraction

Linearised DNA (Section 2.2.2.9) was purified by addition of an equal volume (typically 60µl) of a 1:1 solution of phenol/chloroform, followed by vigorous vortexing. The solution was then centrifuged at 15000x G for 1 minute to separate the organic layer (containing proteins) and aqueous layer (containing nucleic acids). The upper aqueous layer was transferred to a fresh tube and an equal volume of chloroform was added before vortexing. Centrifugation at 15000x G for 1 minute separated the aqueous and organic layers. The aqueous phase was transferred to a fresh tube and DNA was obtained via ethanol precipitation (see below).

2.2.3.4 Ethanol Precipitation

DNA was precipitated from solution by addition of 5M sodium chloride to a final concentration of 250µM, followed by addition of 2.5 volumes of 100% ethanol. The solution was vortexed briefly before storage at -20°C for at least 20 minutes. Following precipitation, DNA was pelleted by centrifugation at 15000x G for 5

minutes. The supernatant was removed and the pellet was washed with 70% ethanol before centrifugation was repeated at 15000x G for 5 minutes. Supernatant was removed and the pellet was allowed to air-dry before resuspension in an appropriate volume of dH₂O.

2.2.4 RNA Manipulation

2.2.4.1 *In Vitro* RNA Transcription

In vitro transcription reactions were performed using the T7 RiboMAX Express Large Scale RNA Production System (Promega). Reaction volumes varied depending on the experiment but consisted of 1x Express buffer (containing all NTPs), 2 μ l T7 enzyme mix and 1-2 μ l of linearised DNA template. Reactions were incubated at 37°C for 30-60 minutes. 1-2 μ l transcribed RNA was analysed on an agarose gel to ascertain RNA quality and yield, before electroporation into mammalian cells (Section 2.2.5.1).

2.2.4.2 RNA Extraction and Purification

The following steps were performed using the RNeasy Mini kit (Qiagen) to extract RNA from cells grown on a 24-well dish. Cells were washed once with PBS (A) before the addition of 600 μ l of RLT buffer (containing 10 μ l of β -ME/ml) per well, followed by incubation at room temperature for 2 minutes. Cell lysates were transferred to a microcentrifuge tube and vortexed, before being passed through a QIAshredder spin column to remove cell debris. Samples were centrifuged at 15000x G for 2 minutes and supernatant was recovered. 1 volume (typically 600 μ l) of 70% ethanol was added to the homogenised lysate and mixed thoroughly by pipetting. Samples were then transferred to an RNeasy spin column and centrifuged at 15000x G for 15 seconds and supernatant was discarded. 700 μ l buffer RW1 (wash buffer) was then added to the column and centrifugation was repeated at 15000x G for 15 seconds. Again, supernatant was discarded. 500 μ l buffer RPE (wash buffer with ethanol) was then added to the column and centrifugation at 15000x G for 2 minutes was performed. At this point the column was placed into a fresh collection tube and centrifuged at 15000x G for 1 minute. The column was again transferred to a fresh tube prior to the addition of 30-50 μ l of RNase-free water. RNA was eluted from the column by centrifugation at 15000x G

for 1 minute. Purified RNA was then stored at -70°C or used for quantification of specific RNAs by qRT-PCR (Section 2.2.6.2).

2.2.5 Introduction of DNA/RNA into Eukaryotic cells

2.2.5.1 RNA Electroporation of Eukaryotic cells

After resuspension following trypsin treatment, the appropriate number of cells was centrifuged at 200x G for 5 minutes at room temperature. Media was removed and pelleted cells were washed by resuspension in PBS (A), followed by further centrifugation at 200x G for 5 minutes at room temperature. Cells were resuspended in an appropriate volume of PBS (A) for electroporation to give a cell count of $\sim 4 \times 10^6/\text{ml}$. For each electroporation, 0.8ml of resuspended cells was transferred to a cuvette (4mm gap, [Apollo]) along with 10 μg of *in vitro* transcribed RNA (Section 2.2.4.1). Electroporation was performed at 0.36kV, 950 μF using a Bio-Rad Gene Pulser II. Electroporated cells were transferred into an appropriate volume of DMEM_{Complete}, mixed thoroughly by pipetting, then seeded into cell culture dishes as follows: (i) 24-well plates at 2×10^5 cells/well (ii) 35mm dishes at 8×10^5 cells/well (iii) 60mm dishes at 3×10^6 cells/well. Once seeded, cells were incubated at 37°C .

2.2.5.2 DNA Transfection of Eukaryotic Cells

After resuspension following trypsin treatment, cells were counted and cell culture dishes were seeded as follows: (i) 24-well plates at 7×10^4 cells/well in 500 μl DMEM_{Complete} (ii) 6-well plates at 2×10^5 cells/well in 2ml DMEM_{Complete}. Prior to DNA transfection, cells were allowed to settle for 24 hours at 37°C . Dependent on cell culture dish area, 0.5-2 μg DNA and 2-10 μl Lipofectamine 2000 (Invitrogen) were diluted separately into individual 50-250 μl volumes of Opti-mem-I (Gibco) and incubated at room temperature for 5 minutes. The diluted DNA and Lipofectamine 2000 were combined and incubated at room temperature for a further 20 minutes. The DNA-Lipofectamine 2000 mixture was added to the plated cells and incubated at 37°C for 16-20 hours.

2.2.6 Assessment of HCV RNA Replication

2.2.6.1 Luciferase Assays

To indirectly determine levels of HCV RNA replication, media was removed from cells previously electroporated with subgenomic viral RNA carrying a luciferase reporter enzyme. Cells were washed once with PBS (A) and then lysed by addition of 100µl of 1x cell lysis buffer (Promega). After 2 minutes, 50µl of lysed cells was added to 100µl of luciferase assay substrate (Promega) in a 1.5ml centrifuge tube. The mixture was immediately vortexed before being placed into a GLOMAX luminometer (Turner Biosystems) to determine luciferase activity. All assays were performed in duplicate.

2.2.6.2 qRT-PCR

RT-PCR reactions were performed as a two-step process. The first step involved generation of cDNA from purified cellular RNA (Section 2.2.4.2) and was performed using the Taqman kit (Applied Biosciences), typically in a final volume of 20µl. The reaction contained 1µl of cellular RNA, 2.5µM random hexamers, dNTPs, 1x RT buffer, 5.5µM MgCl₂, 8 units of RNase inhibitor and 25 units of Multiscribe RT. Reactions were made up to 20µl with dH₂O. Reverse transcription was performed in a ThermoHybaid PX2 Thermal Cycler as follows: (i) primer annealing at 25°C for 10 minutes (ii) strand elongation at 37°C for 1 hour (iii) RT inactivation at 95°C for 5 minutes. The second step allowed Real-Time PCR using the cDNA obtained from the first step. Reactions typically contained 900nM forward and reverse primers, 250nM FAM JFH1 probe, 1x Taqman Fast Universal Mix and 2µl of cDNA template. Reactions were made up to 20µl using dH₂O. Both primers and the probe were complementary to sequences in the 5' UTR of the JFH1 genome. Reactions were performed using an Applied Biosciences 7500 Fast Real-Time PCR System. Reactions were heated to 95°C for 20 seconds to allow denaturation of the cDNA. PCR was then performed as follows: (i) dsDNA strand-separation at 95°C for 3 seconds (ii) primer annealing and strand elongation at 60°C for 30 seconds. Steps (i) and (ii) were repeated 40 times. All RT-PCR reactions were performed in triplicate. The above protocol was also applied to determine cellular GAPDH levels as a control, using GAPDH-specific primers in the second step of the reaction.

2.2.7 Preparation of Mammalian Cell Extracts for SDS-PAGE Analysis

Prior to SDS-PAGE analysis, cells were washed once with PBS (A). Cells were then harvested in 50-100 μ l of 1x boiling mix (dependent on cell culture dish volume) and heated to 100°C for ~10 minutes. For difficult to detect membrane-bound proteins, cellular membrane fractions were isolated by phase extraction. After washing with PBS (A), cells were harvested in 200 μ l phase lysis buffer and transferred to a centrifuge tube. The lysed cells were centrifuged at 8000x G for 5 minutes at room temperature to pellet cellular debris, which was removed from the supernatant. 400 μ l phase separation solution was added to the supernatant and mixed thoroughly by inversion. To separate the detergent and aqueous phases, the solution was centrifuged at 15000x G for 5 minutes at room temperature. The upper aqueous phase was removed, leaving only the oily detergent phase to which 500 μ l cold 100% acetone was added to precipitate protein. Samples were centrifuged at 15000x G for 5 minutes at room temperature to pellet precipitated proteins. The supernatant was removed, the pellet resuspended in 20-50 μ l 1x boiling mix and heated to 100°C for ~10 minutes. Samples were then analysed by SDS-PAGE (see below).

2.2.8 SDS-PAGE Analysis

Proteins were resolved by electrophoresis using Bio-Rad Miniprotein II Apparatus. 10 x 7cm glass plates were assembled using 1.5mm spacers. Resolving gels were prepared using acrylamide (30% acrylamide/bis solution, 37.5:1, 2.6% cross-linker) at a final concentration of 8-12% in 1x resolving gel buffer. Addition of APS (to 0.1%) and TEMED (to 0.08%) initiated polymerisation and the solution was immediately poured into the gel assembly apparatus, leaving a gap of ~2cm at the top. The solution was then overlaid with 1ml of 100% butan-2-ol. When polymerisation was complete, the butan-2-ol was discarded and the gel surface was washed thoroughly with dH₂O. Stacking gels were prepared using acrylamide at a final concentration of 5% in 1x stacking gel buffer. Again, polymerisation was initiated upon the addition of APS (to 0.1%) and TEMED (to 0.08%), before the solution was overlaid onto the resolving gel. A 10-tooth Teflon comb was typically used to form wells in the stacking gel. The gel was allowed to polymerise before removal of the comb. Gels were then loaded into a tank and submerged in tank buffer. Protein samples prepared as described previously (see above) were loaded

into each well. Protein markers (Bio-Rad) were also included for protein size determination and empty wells were filled with an equal volume of boiling mix. Electrophoresis was performed at 120V until the required separation of protein markers and samples was achieved. Gels were then removed from the apparatus for Western blot analysis (see below).

2.2.9 Western Blot Analysis

2.2.9.1 Nitrocellulose Membrane Protein Transfer

Proteins resolved by SDS-PAGE were transferred to a nitrocellulose membrane utilising a Bio-Rad mini-transblot apparatus. The apparatus was set up in the following order, building from bottom to top: fibre pad, blotting paper, gel, nitrocellulose membrane, blotting paper, fibre pad. All materials were soaked in Towbin buffer prior to and during assembly. The materials were transferred to the transblot apparatus, ensuring the membrane was facing the anode. The tank was filled with Towbin buffer, and electrotransfer was performed at 60V for 2 hours.

2.2.9.2 Protein Immunodetection

All washing steps were performed using PBS (A)/0.05% Tween-20. Post-transfer, nitrocellulose membranes were washed briefly, then blocked for ~1 hour using block buffer (Section 2.1.9.4) at room temperature. Membranes were washed for ~5 minutes, then probed overnight at 4°C with the appropriate primary antibody diluted in block buffer and 1% sodium azide. Membranes were washed and probed with the appropriate secondary antibody diluted in block buffer for ~1 hour at room temperature. Membranes were washed before a final wash with PBS (A) to remove any traces of detergent. Proteins were detected utilising the Enhanced Chemiluminescence Plus Western Blotting Detection System (Amersham Biosciences) and a Konica film-processing unit SRX-101a, with Kodak X-OMAT S-film.

2.2.10 Microscopy Techniques and Analysis

2.2.10.1 Indirect Immunofluorescence

Electroporated or transfected cells on 13mm coverslips were fixed for 10 minutes using 100% methanol at -20°C, or 4% paraformaldehyde (PFA) at room

temperature. PFA also contained 0.05% TX-100 for cell permeabilisation. The fixing solution was removed and cells were washed 3 times with PBS (A). Primary antibody was diluted in PBS (A) to the appropriate working concentration and 200µl of diluted antibody was added to cells and incubated at room temperature for ~1 hour. Cells were washed 3 times with PBS (A) and the secondary antibody was diluted into PBS (A) to give the required working concentration. 200µl of this solution was added to the cells and incubated at room temperature for ~1 hour. At this stage, cells were washed 3 times with PBS (A) and nuclei were stained by the addition of DAPI diluted 1/2000 in PBS (A). Cells were then incubated for ~5 minutes at room temperature. Cells were washed with dH₂O to remove residual salt and mounted onto slides using Citifluor glycerol/PBS solution, before sealing with nail varnish. Fluorescence microscopy was performed using a ZEISS LSM510 Meta confocal microscope.

2.2.10.2 Live-Cell Microscopy

For visualising GFP-tagged proteins, cells were seeded onto 35mm live cell dishes (MatTek Cultureware). Prior to microscopy, cells were washed with PBS (A), before the addition of DMEM lacking phenol red. Microscopy was performed using a ZEISS LSM510 Meta confocal microscope, which was fitted with an enclosed stage heated to 37°C and included a supply of 5% CO₂.

2.2.10.3 FRAP Analysis

Cells for FRAP analysis were seeded onto live cells dishes, in the manner described above. For photobleaching, regions of the cell (~38µm² in area) were exposed to 100% laser power (488nm laser line) for 6 iterations. Images were recorded prior to and immediately after bleaching, then every 2 seconds for 2 minutes in order to determine fluorescence recovery. Images were recorded using 2% laser power and all data was corrected against background fluorescence.

2.2.10.4 Activation of PAGFP

Cells were seeded onto live-cell dishes as described previously (Section 2.2.10.2). 100% laser power (405nm laser line) was used to activate NS5A-PAGFP fusion protein molecules in selected intracellular regions. Images were recorded

immediately pre- and post- activation and for periods of up to 15 minutes following activation of PA-GFP.

2.2.11 Assessment of HCV Infectious Virus Production

2.2.11.1 Preparation of Virus

Cells were electroporated as described previously (Section 2.2.5.1), with full-length genomic HCV RNA (strain JFH1). After electroporation of RNA into cells, all procedures were performed under category level 3 (CL3) conditions. Electroporated cells were seeded onto 6-well plates at 8×10^5 cells/well. At 24, 48 and 72 hours, infectious media was removed from cells and centrifuged at 400x G for 2 minutes to pellet cellular debris, before being stored at 4°C.

2.2.11.2 Cell Infection for TCID₅₀, Immunofluorescence and SDS-PAGE Analyses

For TCID₅₀ analysis, naïve Huh-7 cells were seeded at 3×10^3 (in 200µl media) per well in flat-bottomed 96-well plates (Nunc). For immunofluorescence and SDS-PAGE analysis, cells were seeded into 35mm dishes (with 13mm coverslips for IF) at 2×10^5 cells/well. Cells were allowed to settle at 37°C for 24 hours. Cells prepared for TCID₅₀ analysis were inoculated with serial fivefold dilutions of infectious media harvested as described above. Plates were then incubated at 37°C for 72 hours before TCID₅₀ analysis (see below). For immunofluorescence and SDS-PAGE analysis, media was removed from the naïve cells and replaced with 2ml of infectious media diluted 1/2 (1ml infectious media and 1ml fresh media). Plates were then incubated at 37°C for 72 hours. Infected cells were either fixed in 100% methanol (for immunofluorescence) or harvested in 50µl boiling mix (for SDS-PAGE) and then processed as previously described (Sections 2.2.10.1 and 2.2.8 respectively).

2.2.11.3 TCID₅₀ Analysis

72 hours post-infection, cells were fixed in 100% methanol at -20°C for 10 minutes. Methanol was removed and cells were washed 3 times with PBS (A). Hydrogen peroxide was diluted in PBS (A) to a concentration of 0.3% and 50µl of this solution was added to cells for ~30 minutes at room temperature. This step

was necessary to saturate endogenous peroxidases present in the cells. Cells were washed 3 times with PBS (A). Primary antibody (anti-NS5A) was diluted 1/5000 in PBS (A) and 50µl of antibody was added to cells and incubated for ~1 hour at room temperature. Cells were then washed 3 times with PBS (A). Secondary antibody (anti-goat/sheep IgG-peroxidase) was diluted 1/1000 in PBS (A). 50µl of secondary antibody was added to cells, followed by incubation for ~1 hour at room temperature. Cells were washed a final 3 times with PBS (A), before staining with the NovaRED substrate kit for peroxidase (Vector) in accordance with the manufacturers instructions. Positive cells were determined by microscopy, and final TCID₅₀ values were calculated.

2.2.12 siRNA Library Screen

2.2.12.1 siRNA Transfection

Transfections were performed in 24-well plates. For each well, 100µl Optimem-I was mixed with 1µl Lipofectamine RNAiMAX reagent (Invitrogen). The siRNAs were added to the transfection mixture as follows: (i) 1µl control siRNAs at a concentration of 50µM (ii) 0.5µl of the 3 library siRNAs (targeted against the same gene) at a concentration of 50µM each, giving an overall concentration of 75µM. Plates were then incubated at room temperature for 10-20 minutes. Wells were seeded with 7×10^4 Tri-Huh-7 or Tr-U2OS cells/well (cell lines harbouring SGRs containing both luciferase and neomycin genes), in a volume of 900µl. Therefore, the final volume in each well was 1ml, giving a final siRNA concentration of 50nM (control siRNAs) and 75nM (library siRNAs). Plates were incubated at 37°C for 48 hours before cells were harvested to determine luciferase levels (Section 2.2.6.1) and cell viability (see below).

2.2.12.2 Cellular Viability Assay

Cell viability was determined using the Aquabluer Cell-Viability assay (MultiTarget Pharmaceuticals). Aquabluer measures the redox environment in growth medium, where viable cells maintain a reduced environment that is able to convert AquaBluer from a non-fluorescent oxidised form to a reduced fluorescent species, which can be quantified. Therefore, Aquabluer does not require preparation of cell extracts. Experiments using actinomycin D were utilised for authentication of the assay. For the siRNA library screen, plates were removed and assayed for cell

viability 48 hours after siRNA transfection. 1 volume of Aquabluer reagent was added to 9 volumes of fresh DMEM_{Complete} and mixed by pipetting. 100µl of this solution was added to the media in each well and mixed by pipetting. Plates were returned to incubate at 37°C for ~4 hours. Post-incubation, plates were stored in the dark for ~30 minutes to allow media to reach room temperature. 100µl of each sample to be tested was then transferred to a black microwell 96-well plate (nunc) and placed into a HIDEX Chameleon plate reader. Fluorescence intensity was measured at 540ex/590em and all values were corrected for background fluorescence and repeated in duplicate.

3 Live Cell Analysis of the HCV-Encoded NS5A Protein

3.1 Introduction

Similar to other positive-stranded RNA viruses, HCV replication occurs within altered cellular membranes containing all components necessary for replication of the viral genome (Mackenzie, 2005, Salonen et al., 2005). Visualisation of cells harbouring replicating HCV genomes has revealed the presence of punctate foci on the ER membrane, which contain viral NS proteins (Moradpour et al., 2004b, Mottola et al., 2002), viral RNA (El-Hage & Luo, 2003, Gosert et al., 2003, Targett-Adams et al., 2008a) and several host cell factors. Therefore, foci visualised by confocal microscopy are likely to represent viral RCs.

In order to gain insight into the functional organisation of RCs, previous studies have involved conjugating viral proteins to fluorescent molecules such as GFP. This approach has been utilised to examine viral RC components, including NS4B (Elazar et al., 2004, Gretton et al., 2005, Lundin et al., 2006, Lundin et al., 2003) and NS5A (Brass et al., 2002, Kim et al., 1999). Because GFP-tagged proteins can be examined in live cells, further biophysical analysis is possible. For example, mobility analysis has demonstrated that NS4B is more mobile on the ER membrane compared to when it is located at MAFs, believed to represent RCs (Gretton et al., 2005). This type of analysis on other replicase components may be useful to gain a greater understanding of viral RC properties and the interactions occurring within them.

It has been demonstrated that the GFP ORF can be inserted into the C-terminal region of NS5A (Appel et al., 2005b, Liu et al., 2006, Moradpour et al., 2004b). Importantly, GFP could be inserted into NS5A in the context of SGRs derived from the genotype 1b strain Con1, allowing direct visualisation of NS5A in cells actively replicating the viral genome (Moradpour et al., 2004b). Unfortunately the replication levels of such genotype 1 SGRs in cell culture is poor (Appel et al., 2005b). By contrast, SGRs derived from the genotype 2a strain JFH1 sequence replicate far more efficiently (Kato et al., 2003, Targett-Adams & McLauchlan, 2005). Therefore, the initial aim of the project was to insert the GFP ORF into the NS5A coding region of a JFH1-based SGR. It was hoped that this construct would

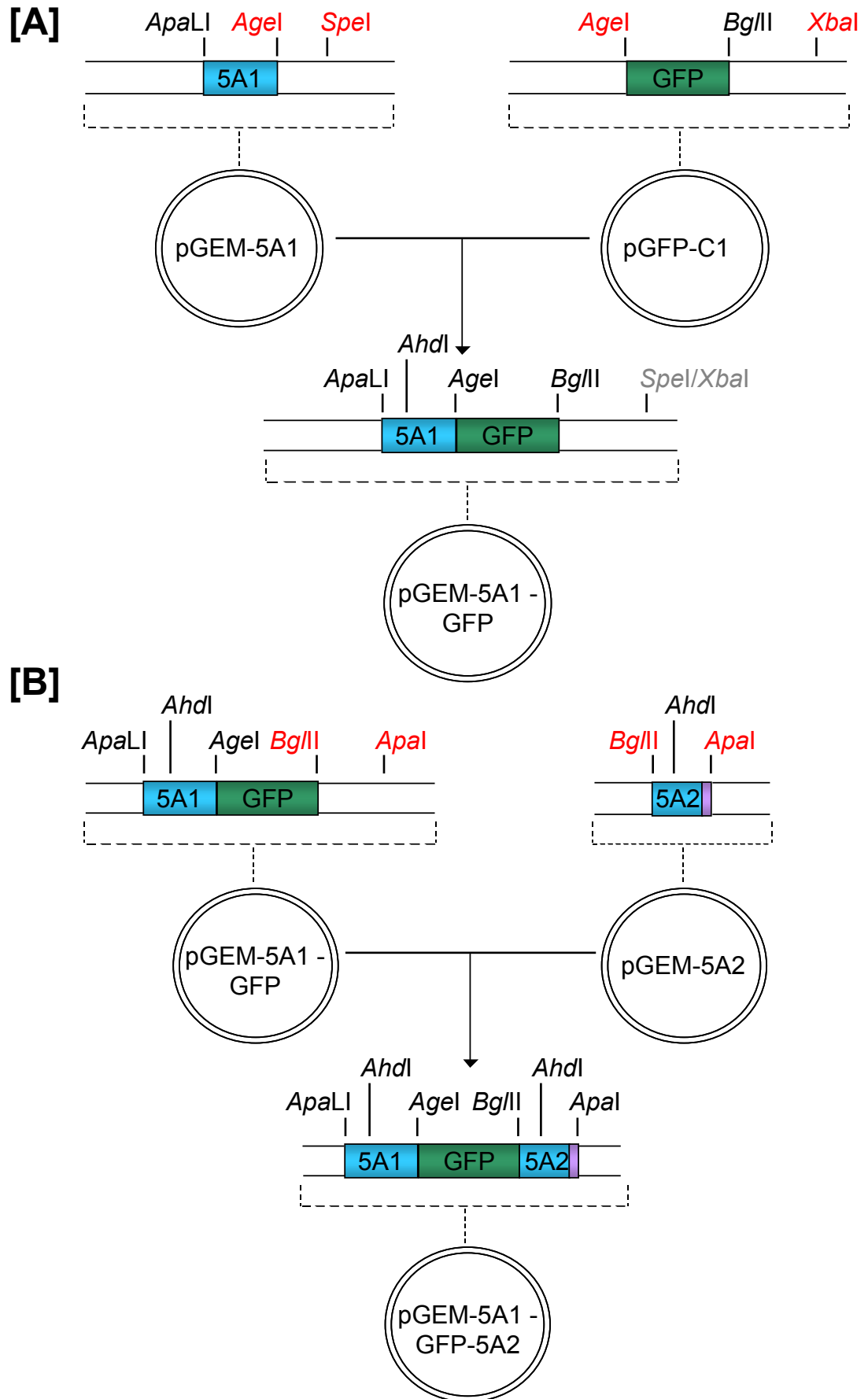


Figure 3.2 Creation of pGEM-5A1-GFP-5A2

[A] The GFP ORF was excised from pEGFP-C1 as an *Agel*/*XbaI* fragment and inserted between the *Agel*/*SpeI* sites in pGEM-5A1. This created pGEM-5A1-GFP and destroyed the *SpeI*/*XbaI* restriction sites. **[B]** The 5A2 coding region was excised using *BglII*/*ApaI* and inserted into the corresponding sites in pGEM-5A1-GFP to create pGEM-5A1-GFP-5A2.

provide a more robust system for studying the characteristics of NS5A in live cells actively replicating viral RNA.

3.2 Creation and Characterisation of the luc-JFH1_{GFP} SGR

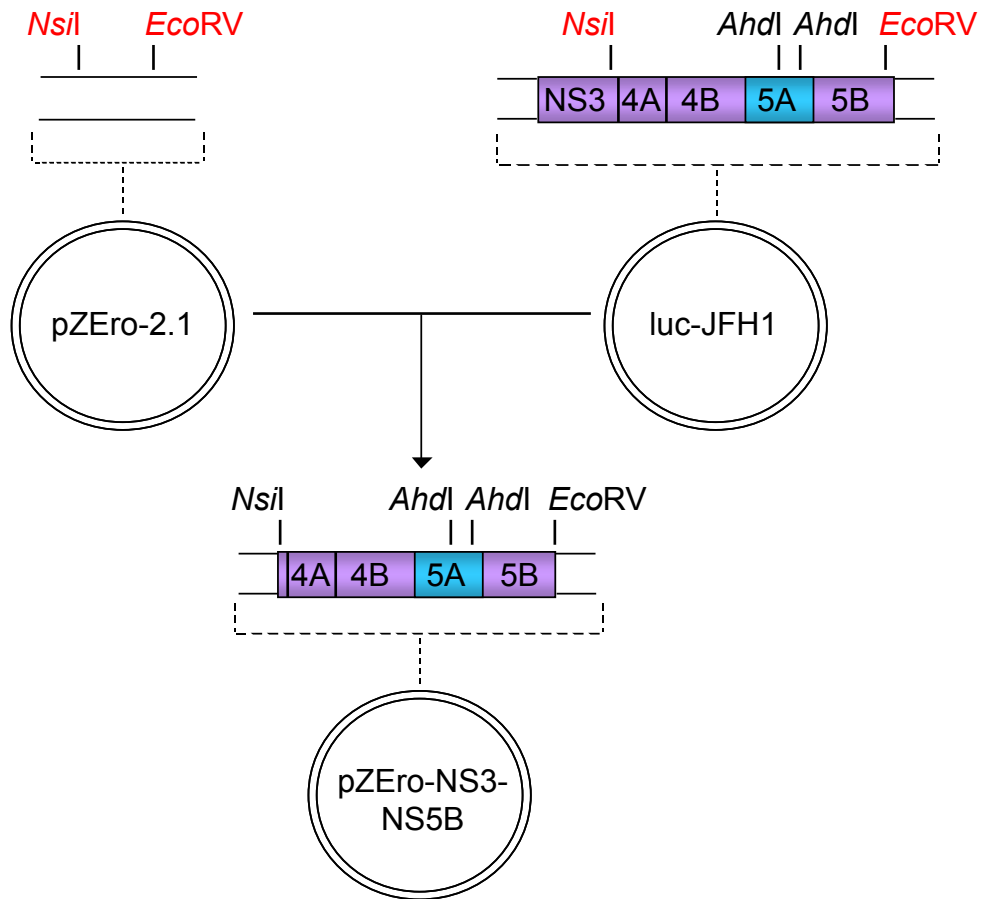
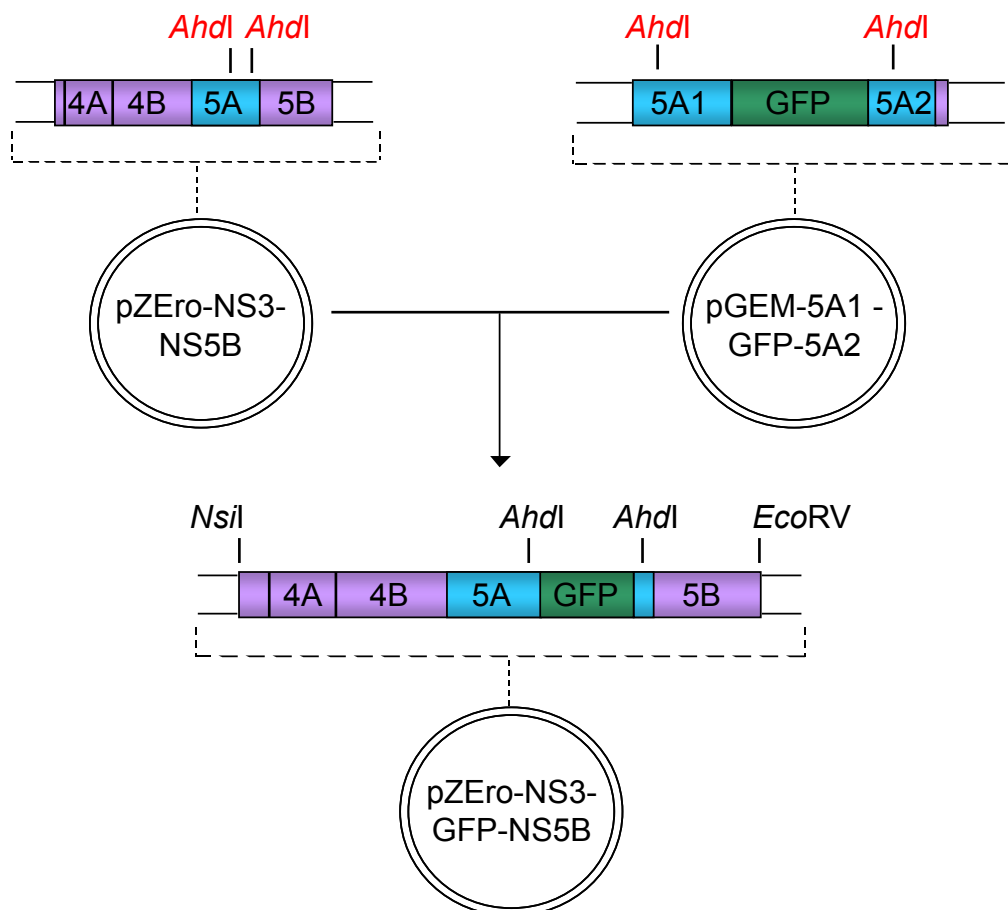
3.2.1 Insertion of GFP into the luc-JFH1 SGR

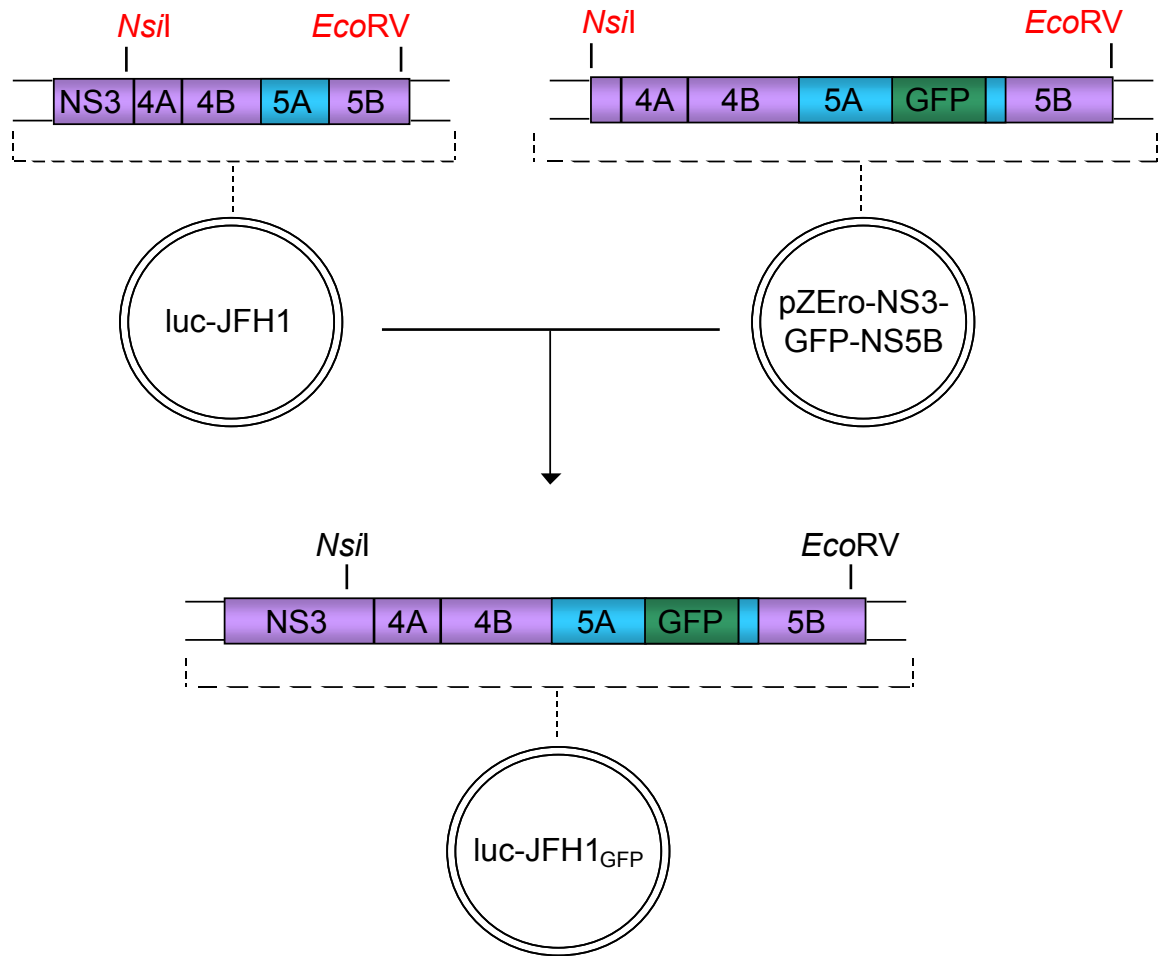
It has been previously established that GFP can be inserted between amino acids 418 and 419 of the Con1 NS5A sequence without abolishing HCV RNA replication (Moradpour et al., 2004b). The stretch of amino acids surrounding this site is identical in the JFH1 NS5A coding region. Therefore, a strategy to insert GFP into the luc-JFH1 SGR at the same position was adopted. Luc-JFH1 is a bi-cistronic SGR (see Figure 1.4), where the first cistron incorporates the firefly luciferase reporter gene and translation is directed by the IRES contained within the JFH1 5' UTR. The second cistron contains the JFH1 NS protein region from NS3 through to NS5B under control of the EMCV IRES (Targett-Adams & McLauchlan, 2005), which permits cap-independent translation initiation of the NS proteins in a manner analogous to that of the HCV IRES. Hence, the proteins within each cistron are presumably translated in equimolar amounts. The 3' terminus of the SGR contains the 3' UTR sequence of JFH1, which is critical for efficient RNA replication and translation (Friebe & Bartenschlager, 2002, Song et al., 2006).

Insertion of the GFP ORF was performed in three cloning stages: (i) PCR amplification of the NS5A sequences flanking the insertion site and introduction of GFP into this region (ii) insertion of the GFP ORF, now flanked by NS5A sequence, into the NS3-NS5B coding region (iii) re-introduction of the NS3-NS5B region (now containing GFP) into the luc-JFH1 SGR sequence. The final SGR was termed luc-JFH1_{GFP}; the cloning strategy is described in detail below, and presented in Figures 3.1-3.3. The generation of luc-JFH1_{GFP}GND, a construct defective for replication, is also described in Section 3.2.1.3.

3.2.1.1 Insertion of the GFP ORF into the NS5A Coding Region

The strategy required insertion of the GFP ORF between the codons for amino acids 418 and 419 of NS5A. Therefore, primers were designed to amplify two fragments (termed 5A1 and 5A2) that flanked this region, using luc-JFH1 as a template (Figure 3.1). Fragment 5A1 was 287bp in length, including the introduced flanking *Apa*LI and *Age*I sites that were employed for cloning purposes. Fragment

[A]**[B]**

[C]**[D]**

$\frac{\text{NS5A}}{\text{....SMPP}}$
 $\frac{\text{GFP}}{\text{LPVAT MVSKG DELYK}}$
 $\frac{\text{NS5A}}{\text{SGLRS LEGE....}}$

Figure 3.3 Creation of *luc-JFH1_{GFP}*

[A] The NS3-NS5B coding region was excised from *luc-JFH1* using *NsiI/EcoRV* and inserted into *pZero-2.1* between the corresponding sites to create *pZero-NS3-NS5B*. **[B]** The 5A1 and 5A2 sequences flanking the GFP sequence in *pGEM-5A1-GFP-5A2* were digested with *AhdI*. This fragment was then inserted between the corresponding *AhdI* sites in *pZero-NS3-NS5B*. **[C]** The NS3-GFP-NS5B coding region was excised from *pZero-NS3-GFP-NS5B* using *NsiI/EcoRV*. This fragment was then inserted between the corresponding sites in *luc-JFH1* to create the final construct *luc-JFH1_{GFP}*. **[D]** Amino acid sequence of the GFP insertion into NS5A. Sequences in black represent NS5A residues whereas those in grey are additional residues flanking the GFP insertion that were introduced as a result of the cloning strategy. Residues in green represent GFP.

5A2 was 250bp in length including the introduced *Bgl*II and *Apa*I sites and also contained the first 91bp of the NS5B coding region. Both fragments were individually ligated into pGEM-T-Easy to create pGEM-5A1 and pGEM-5A2 respectively (Figure 3.2). Following these steps, the pGFP-C1 vector was digested with *Age*I and *Xba*I, thus excising the GFP coding region. GFP was then inserted between the *Age*I and *Spe*I sites of pGEM-5A1, creating pGEM-5A1-GFP and destroying the *Spe*I/*Xba*I sites in the process (Figure 3.2, A). 5A2 was excised from pGEM-5A2 using *Bgl*II and *Apa*I and the fragment was introduced into the corresponding sites of pGEM-5A1-GFP. This resulted in pGEM-5A1-GFP-5A2, with GFP inserted between codons for amino acids 418 and 419 of the original NS5A sequence (Figure 3.2, B).

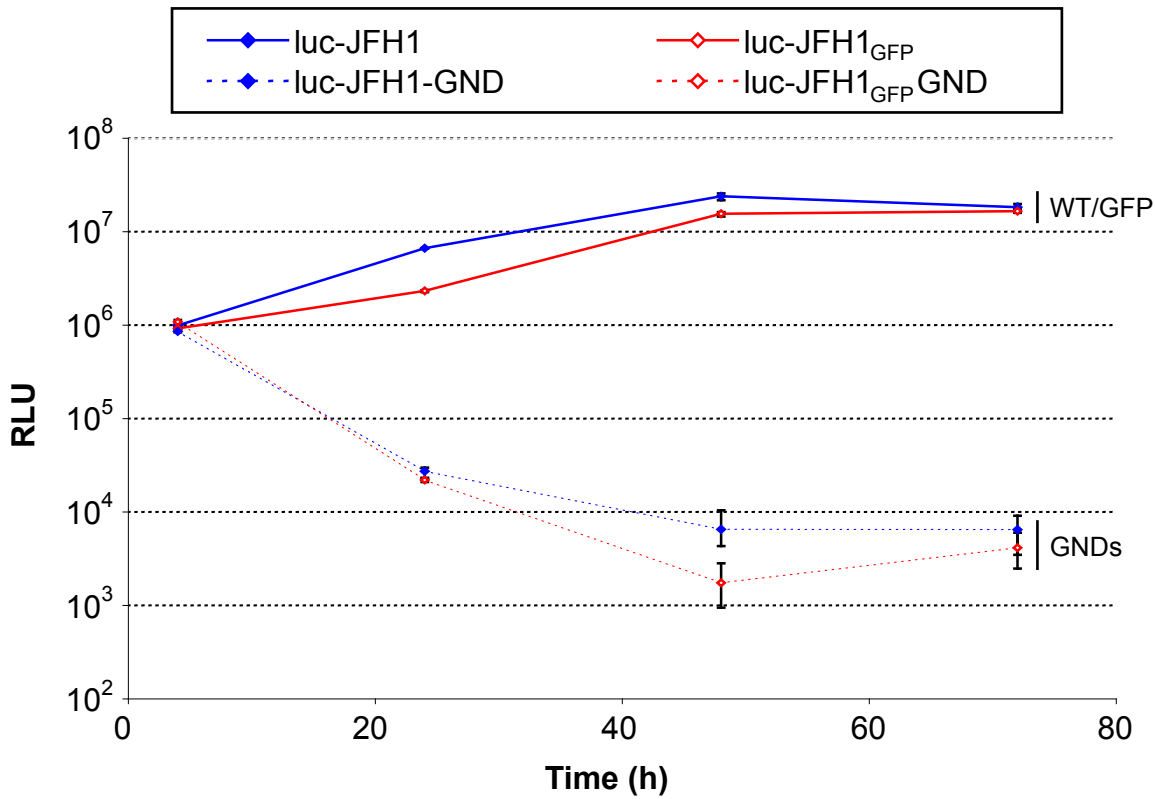
3.2.1.2 Insertion of 5A1-GFP-5A2 into the NS3-NS5B Coding Region

The majority of the 5A1-GFP-5A2 fragment was removed from pGEM-5A1-GFP-5A2 using two existing *Ahd*I sites (Figure 3.3, B). However, the fragment could not be directly inserted into the luc-JFH1 plasmid due to the presence of a third *Ahd*I site within the plasmid backbone. Therefore, a large fragment of the NS coding region from luc-JFH1 was excised using *Nsi*I (in NS3) and *Eco*RV (in NS5B) (Figure 3.3, A). This fragment was termed NS3-NS5B and was inserted between the *Nsi*I and *Eco*RV sites of the pZEro-2.1 vector, creating pZEro-NS3-NS5B (Figure 3.3, A). Thereafter, the 5A1-GFP-5A2 fragment was introduced into pZEro-NS3-NS5B using the corresponding *Ahd*I sites, creating pZEro-NS3-GFP-NS5B (Figure 3.3, B).

3.2.1.3 Creation of luc-JFH1_{GFP} and luc-JFH1_{GFP}GND

With GFP successfully introduced into the C-terminus of NS5A within the context of the NS3-NS5B coding region, pZEro-NS3-GFP-NS5B was digested with *Nsi*I and *Eco*RV. This yielded the NS3-GFP-NS5B fragment, which was introduced into luc-JFH1 using the same sites (Figure 3.3, C). This generated the final construct, luc-JFH1_{GFP}. To create a negative control SGR that incorporated GFP, luc-JFH1-GND (Targett-Adams & McLauchlan, 2005) was digested with *Eco*RV and *Hpa*I. The excised fragment contained the majority of the NS5B coding sequence, including the GND mutation in the viral polymerase sequence that blocks replication. This GND fragment was then introduced into luc-JFH1_{GFP} using the

[A]



[B]

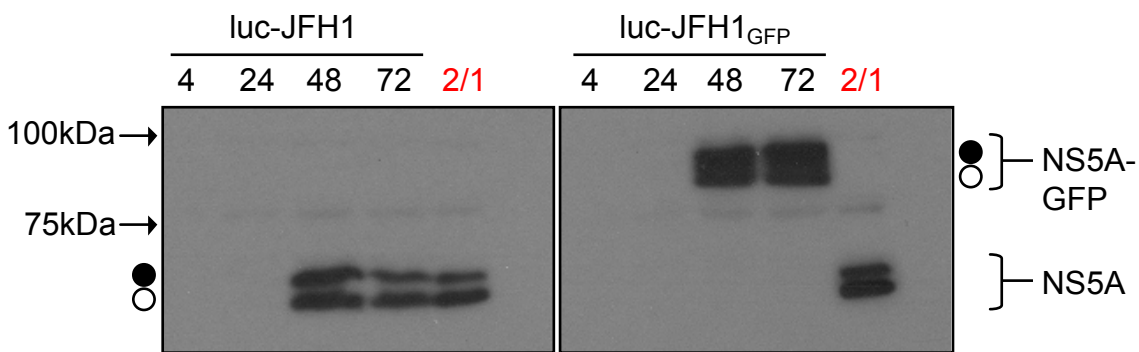


Figure 3.4 luc-JFH1_{GFP} replicates efficiently in Huh-7 cells

[A] Huh-7 cells were electroporated with RNA from luc-JFH1, luc-JFH1_{GFP} and their GND counterparts. Cells were lysed at 4, 24, 48 and 72 hours post-electroporation and extracts were assayed for luciferase activity. Assays were performed in triplicate and the averages are shown. Error bars indicate the range of the values recorded at each time point. **[B]** Huh-7 cells set up in parallel to those described in [A] were harvested for Western blot analysis at 4, 24, 48 and 72 hours post-electroporation. 2/1 cells harbour an autonomously replicating JFH1 SGR and were used as a positive control. The hyper- (closed circles) and hypo- (open circles) phosphorylated species of NS5A are indicated.

corresponding sites, creating luc-JFH1_{GFP}GND. Luc-JFH1_{GFP} and luc-JFH1_{GFP}GND were subsequently linearised and used as templates for *in vitro* transcription of RNA for experimental studies.

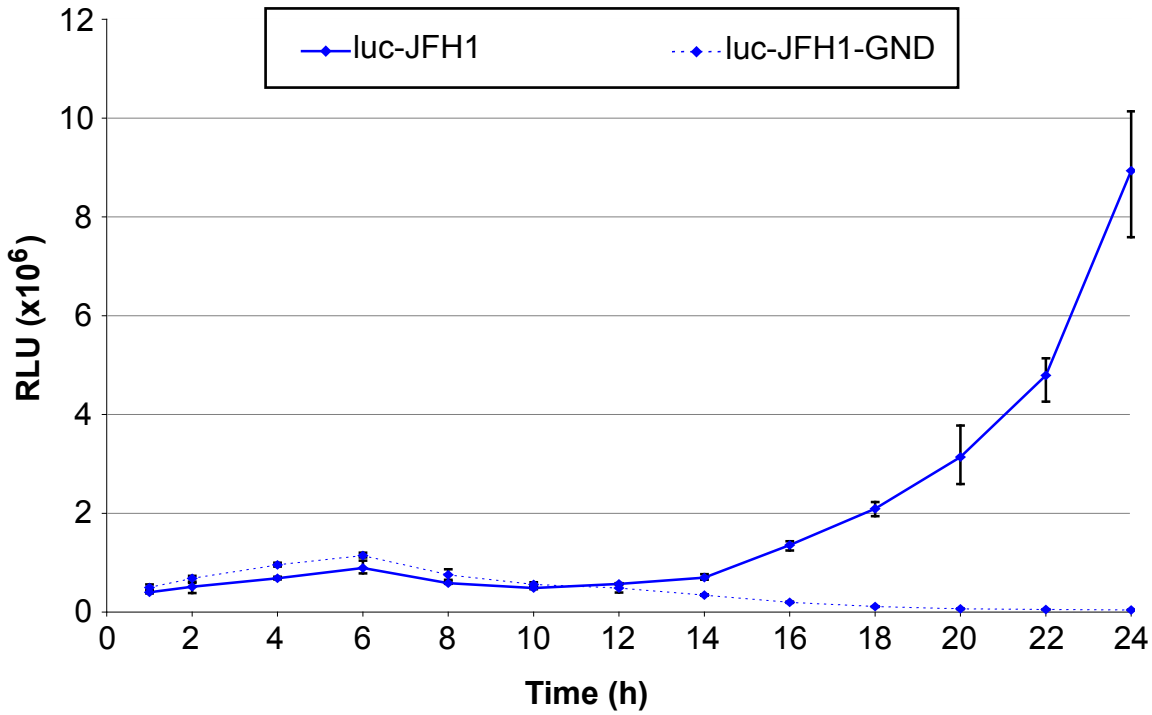
3.2.2 Characterisation of luc-JFH1_{GFP}

3.2.2.1 Luc-JFH1_{GFP} Replicates to Levels comparable to luc-JFH1

To determine the effect of inserting the GFP coding sequence on replication, RNA transcribed from luc-JFH1_{GFP} and luc-JFH1_{GFP}GND was electroporated into Huh-7 cells. RNA encoding luc-JFH1 and luc-JFH1-GND was also electroporated into cells and acted as positive and negative controls respectively. These control constructs do not contain GFP and have previously been shown to replicate efficiently (luc-JFH1) or be incapable of replication (luc-JFH1-GND), as judged by measuring luciferase activity over a 72-hour period (Targett-Adams & McLauchlan, 2005). Upon introduction of RNA into cells, luc-JFH1 replicated robustly and luciferase levels were almost 20-fold higher by 72 hours compared to the 4-hour value (Figure 3.4, A). In contrast, luciferase levels expressed from luc-JFH1-GND were approximately 130-fold lower by 72 hours compared to the 4-hour time point. This result indicated that luc-JFH1-GND RNA did not replicate, in agreement with previous results (Targett-Adams & McLauchlan, 2005). Examination of luciferase levels from luc-JFH1_{GFP} indicated that insertion of GFP into the NS5A coding region did not block replication of the SGR (Figure 3.4, A). However, luc-JFH1_{GFP} did display a delay in replication kinetics and by 24 hours, replication was only 35% of that compared to the unmodified SGR as judged by luciferase activity. Nonetheless, luciferase values increased to 91% of those produced by luc-JFH1 by 72 hours. Therefore, it was concluded that insertion of GFP into NS5A did not significantly impair replication of the SGR. Luc-JFH1_{GFP}GND was deemed incapable of replication, since luciferase activity declined as rapidly as that seen with the control GND SGR (Figure 3.4, A).

To confirm that the NS5A-GFP fusion protein expressed from luc-JFH1_{GFP} could be detected during transient replication, cell extracts prepared over 72 hours were examined by Western blot analysis (Figure 3.4, B). Extracts from cells harbouring luc-JFH1 and both GND SGRs were also analysed. NS5A expressed from luc-JFH1 was detected as two bands, representing the hypo- (56kDa) and hyperphosphorylated (58kDa) species of NS5A (Tanji et al., 1995). Due to the insertion of GFP, two larger species of NS5A-GFP were detected in cells

[A]



[B]

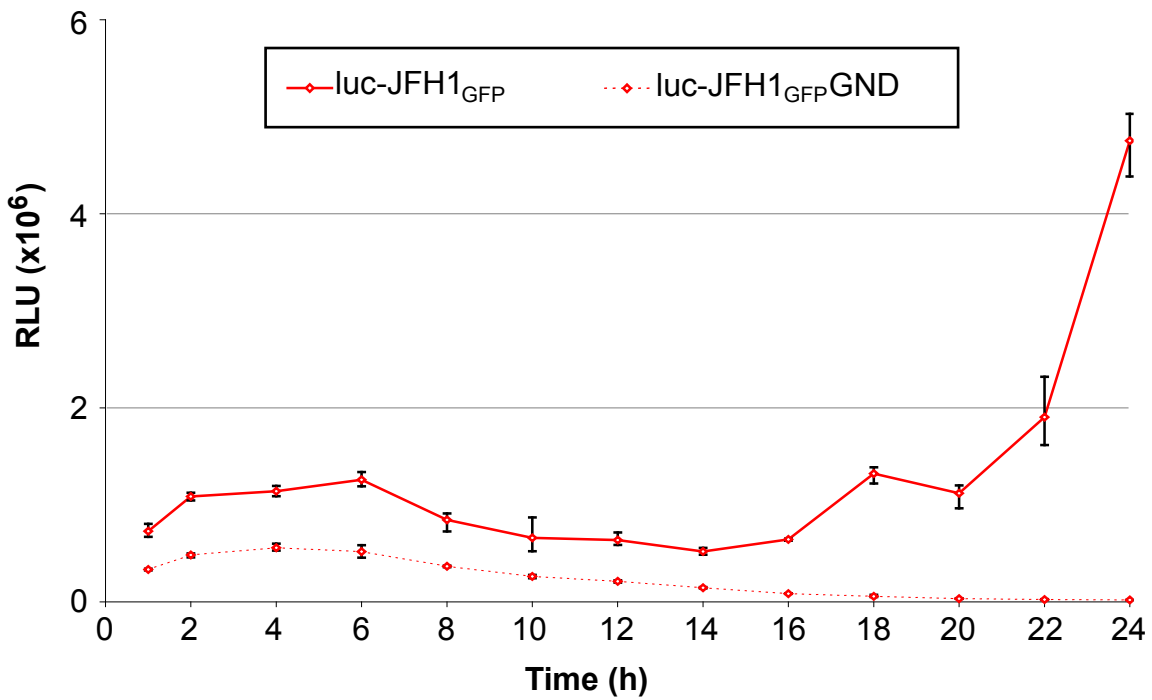


Figure 3.5 Onset of replication by luc-JFH1_{GFP} is delayed compared to luc-JFH1

Huh-7 cells were electroporated with RNA encoding [A] luc-JFH1 [B] luc-JFH1_{GFP}. Both experiments included GND controls. Cells were lysed every two hours and luciferase activity was measured up to and including 24 hours post-electroporation. Assays were performed in triplicate and error bars represent the range of the values recorded at each time point.

harbouring luc-JFH1_{GFP}. These bands were presumed to represent the hypo- (83kDa) and hyperphosphorylated (85kDa) forms of the fusion protein (Figure 3.4, B). Both NS5A and NS5A-GFP were detected at 48 hours post-electroporation and displayed no evidence of proteolytic breakdown (Figure 3.4, B). However, breakdown cannot be firmly excluded in the absence of a Western blot for GFP. In agreement with the luciferase assays, protein levels expressed from both SGRs were comparable by 72 hours post-electroporation. By contrast, no NS5A protein was detected in cells electroporated with either luc-JFH1-GND or luc-JFH1_{GFP}GND (data not shown), emphasising the inability of these SGRs to replicate.

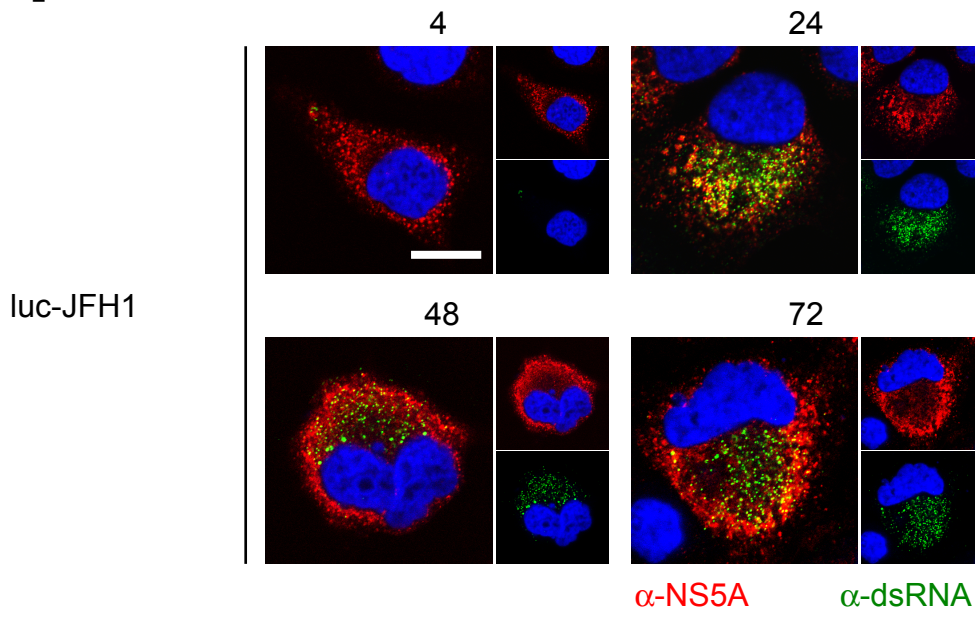
3.2.2.2 Insertion of GFP into luc-JFH1 Delays the Onset of RNA Replication

The results presented in Figure 3.4, A indicated that replication of luc-JFH1_{GFP} RNA was delayed in the first 24 hours post-electroporation compared to unmodified luc-JFH1. To more precisely determine whether this delay occurred, Huh-7 cells were electroporated with RNA from luc-JFH1 and luc-JFH1_{GFP} and luciferase activity was measured every two hours over a period of 24 hours (Figure 3.5, A and B). Luc-JFH1-GND and luc-JFH1_{GFP}GND were included as controls. For all constructs, luciferase activity increased for the first six hours post-electroporation, followed by a subsequent decrease in enzyme levels. Luc-JFH1 luciferase values declined until approximately 12 hours but then increased sharply for the remaining 12 hours (Figure 3.5, A). In contrast, luc-JFH1_{GFP} luciferase levels did not increase until approximately 18 hours post-electroporation but continued to increase thereafter (Figure 3.5, B). Luciferase levels expressed from both GND SGRs decreased after six hours. This result, taken together with those shown previously (Figure 3.4, A), revealed that replication of luc-JFH1_{GFP} was delayed by 4-6 hours compared to unmodified luc-JFH1.

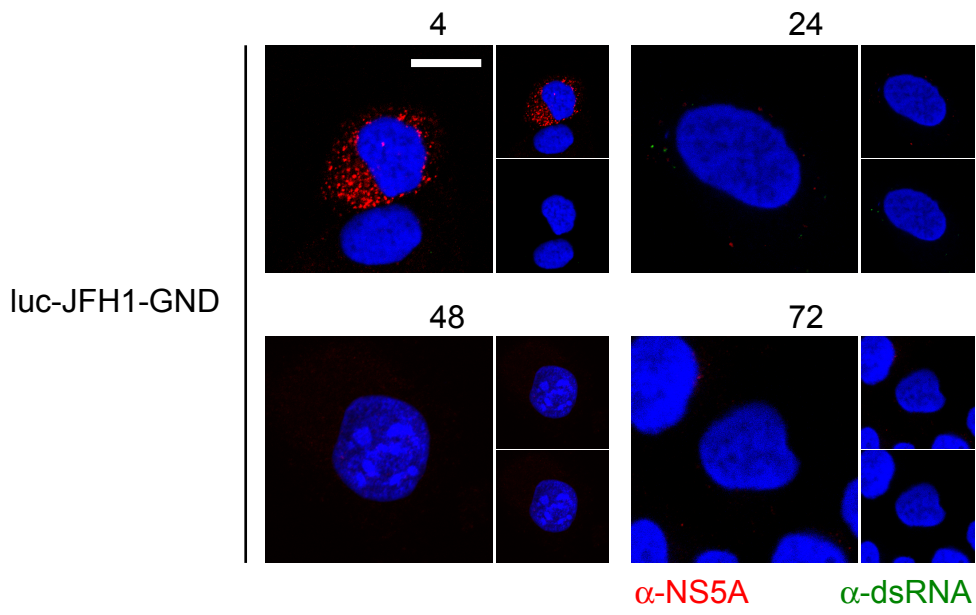
3.2.2.3 Visualisation of NS5A-GFP in Fixed and Live Cells

The incorporation of GFP into NS5A has previously been shown to allow direct visualisation of the protein in electroporated cells (Moradpour et al., 2004b). Therefore, Huh-7 cells were electroporated with RNA encoding luc-JFH1 and luc-JFH1_{GFP}, before being fixed and examined for NS5A and NS5A-GFP over a period of 72 hours (Figure 3.6, A and C). Cells were also probed for dsRNA, an intermediate of viral genome synthesis. Replication of the HCV genome is thought

[A]



[B]



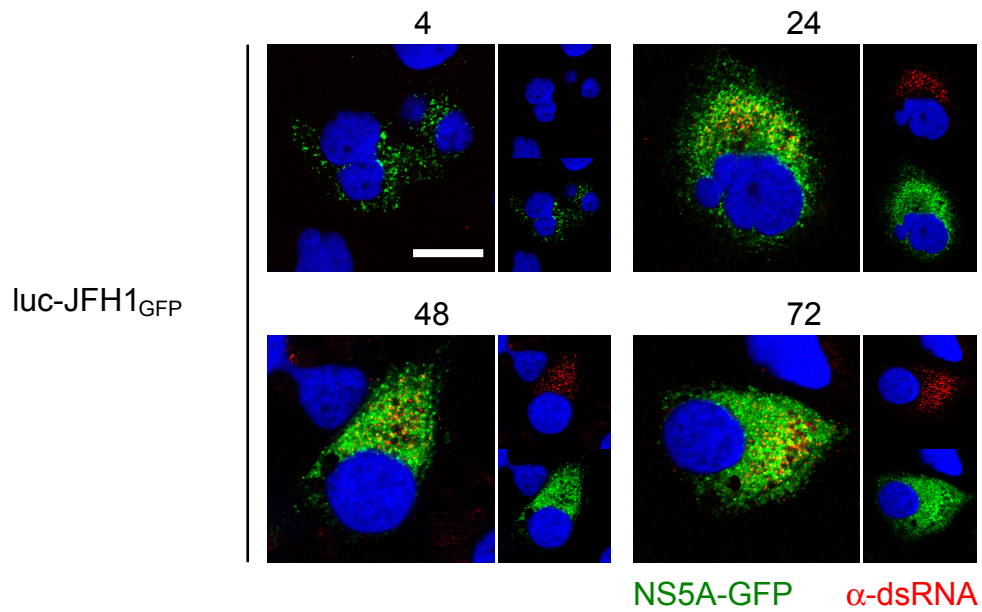
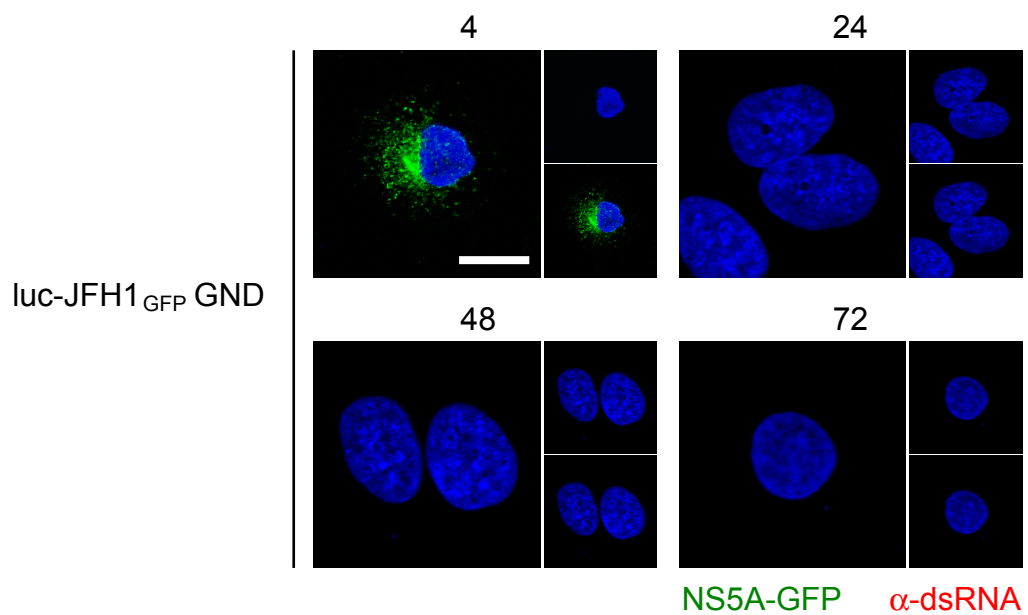
[C]**[D]**

Figure 3.6 Visualisation of NS5A, NS5A-GFP and dsRNA in cells actively replicating luc-JFH1 and luc-JFH1_{GFP} RNA

Huh-7 cells electroporated with RNA from **[A]** luc-JFH1 **[B]** luc-JFH1-GND **[C]** luc-JFH1_{GFP} and **[D]** luc-JFH1_{GFP}GND were fixed and stained for NS5A using NS5A antisera (in **[A]** and **[B]**) and dsRNA using J2 at 4, 24, 48 and 72 hours post-electroporation. In **[C]** and **[D]**, NS5A-GFP was visualised directly. Cell nuclei were stained using DAPI. Scale bars represent 10 μ m.

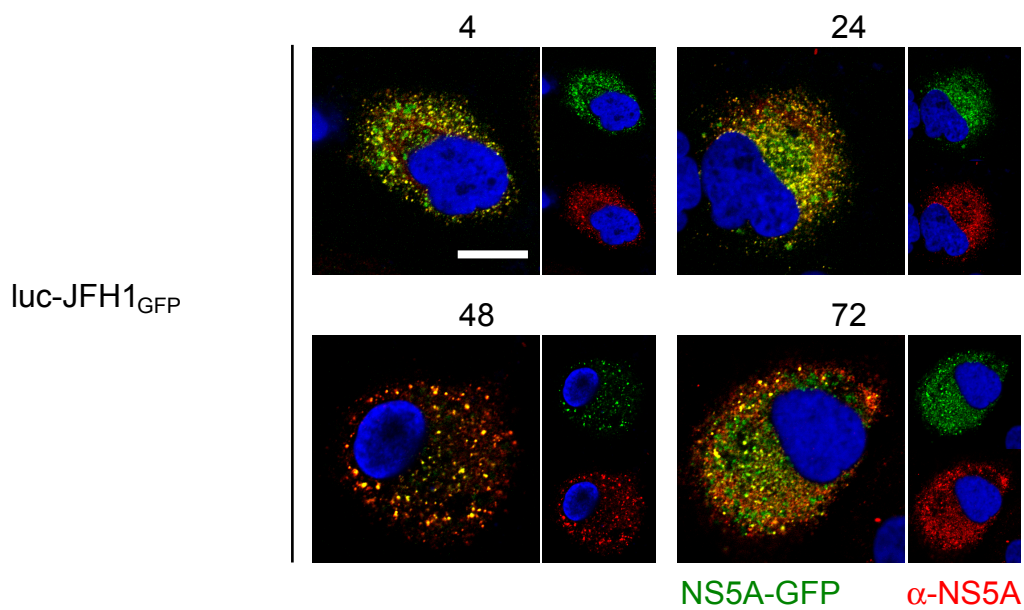
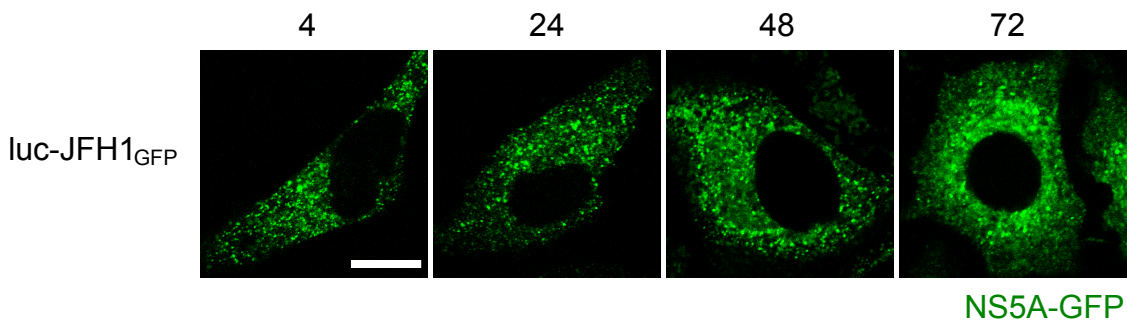
[A]**[B]**

Figure 3.7 NS5A-GFP and NS5A staining coincide, and NS5A-GFP can be directly visualised in live cells actively replicating luc-JFH1_{GFP} RNA

[A] Huh-7 cells electroporated with RNA from luc-JFH1_{GFP} were fixed and stained with NS5A antisera and DAPI at 4, 24, 48 and 72 hours post-electroporation. **[B]** Live Huh-7 cells harbouring luc-JFH1_{GFP} were visualised at 4, 24, 48 and 72 hours post-electroporation. Scale bars represent 10µm.

to occur through production of a negative-strand RNA template, which is used for synthesis of positive-sense RNA molecules (Lohmann et al., 1999, Takehara et al., 1992). A dsRNA duplex is generated by attachment of a positive-strand RNA to the negative-strand template and can be detected using the monoclonal antibody J2 (Targett-Adams et al., 2008a). Visualisation of NS5A expressed from luc-JFH1 required use of NS5A antisera, which revealed an ER-like distribution of the protein that included punctate sites of fluorescence at all time points (Figure 3.6, A). dsRNA was localised exclusively to punctate structures throughout the cytoplasm and these sites shared limited co-localisation with the sites of NS5A fluorescence. For cells electroporated with luc-JFH1_{GFP} RNA, NS5A-GFP was visualised directly and exhibited a cytoplasmic distribution indistinguishable to that of NS5A expressed from the unmodified SGR and sites of dsRNA fluorescence were also similar (Figure 3.6, C). In cells expressing GND constructs, NS5A and NS5A-GFP were detected at 4 hours post-electroporation but were undetectable thereafter, whereas dsRNA could not be visualised at any time point (Figure 3.6, B and D). It is therefore likely that detection of NS5A and NS5A-GFP at the 4-hour time point for all SGRs represented translation of the input RNA, since the absence of a dsRNA signal indicated that replication intermediates were not detected so soon after electroporation.

To confirm that the GFP fluorescence expressed from luc-JFH1_{GFP} accurately represented NS5A protein, cells harbouring luc-JFH1_{GFP} were counter-stained with NS5A antisera (Figure 3.7, A). NS5A-GFP and NS5A displayed a significant degree of overlap at all time points, indicating that GFP provided a representative marker of NS5A distribution in cells. However, it should be noted that areas where these two signals did not overlap were also apparent. To determine whether NS5A-GFP could be visualised under live cell conditions, live cells electroporated with luc-JFH1_{GFP} RNA were examined for the presence of NS5A-GFP over a period of 72 hours (Figure 3.7, B). NS5A-GFP was visualised as early as 4 hours and displayed an ER-like distribution with punctate sites of fluorescence at all time points that was indistinguishable from the pattern observed in fixed cells.

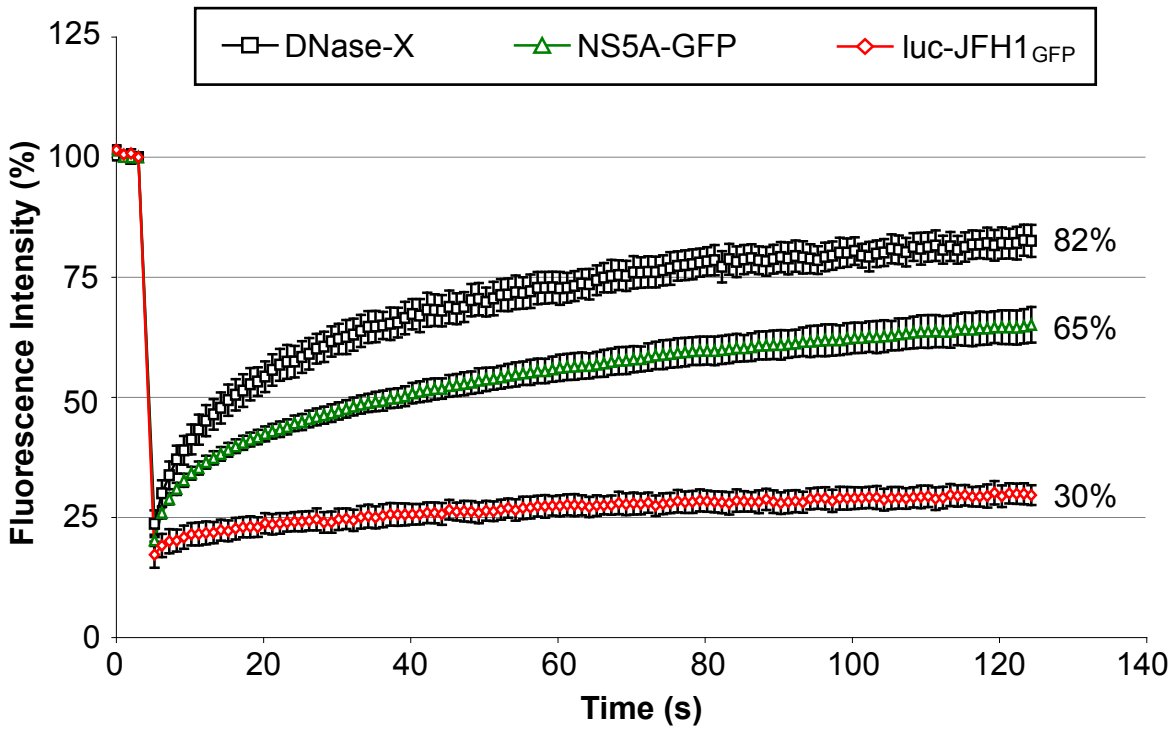
These results, taken together with those presented in Sections 3.2.2.1 and 3.2.2.2, demonstrated that luc-JFH1_{GFP} replicated efficiently and permitted direct visualisation of NS5A in cells. Based on these data, NS5A was further characterised in live cells containing actively replicating HCV RNA.

3.3 The NS Proteins Influence Localisation and Mobility of NS5A

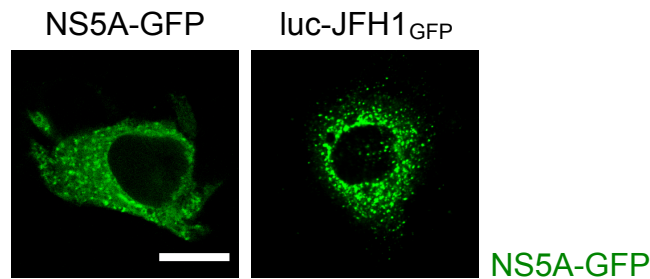
Among the techniques available for analysis of GFP-tagged proteins, FRAP has emerged as a powerful tool for studying the intracellular dynamics of proteins (Reits & Neefjes, 2001). FRAP can also be used to gain insights into protein interactions and the technique has previously demonstrated that HCV-encoded NS4B displays slower movement when localised to small punctate structures on the ER membrane (termed MAFs) compared to when it is localised on the ER membrane (Gretton et al., 2005). To examine the mobility properties of NS5A, cells electroporated with luc-JFH1_{GFP} RNA were examined by FRAP (Figure 3.8, A). For comparative purposes, FRAP was also conducted on cells expressing GFP-DNase-X, a mobile ER protein (Gretton et al., 2005). NS5A-GFP fluorescence was bleached to 17% compared to the pre-bleach value and fluorescence recovery was measured over two minutes. NS5A-GFP fluorescence had recovered to only 30% of the pre-bleach value after two minutes, whereas DNase-X fluorescence had recovered to 82% over the same period of time (Figure 3.8, A). Therefore, NS5A-GFP mobility was limited in cells actively replicating HCV RNA.

To determine whether the low mobility of NS5A-GFP was an inherent characteristic of the fusion protein, the NS5A-GFP ORF was amplified and inserted into pCMV10, creating pCMV-NS5A-GFP (employing the cloning strategy depicted in Figure 3.8, C and D). Cells expressing pCMV-NS5A-GFP were analysed by FRAP at 16-20 hours post-transfection. NS5A-GFP fluorescence was bleached to 20% compared to the pre-bleach value, similar to the bleaching of NS5A-GFP expressed from luc-JFH1_{GFP}. However, after the 2-minute recovery period, fluorescence had recovered to 65% of the pre-bleach value (Figure 3.8, A). NS5A-GFP localisation also differed depending on the context of its expression; when expressed from pCMV-NS5A-GFP, NS5A-GFP exhibited a diffuse ER-like localisation. In contrast, NS5A-GFP expressed from luc-JFH1_{GFP} displayed an ER-like pattern along with punctate sites of fluorescence (compare panels in Figure 3.8, B). This result suggested that one or more of the NS proteins present in luc-JFH1_{GFP} influenced the localisation and mobility of NS5A.

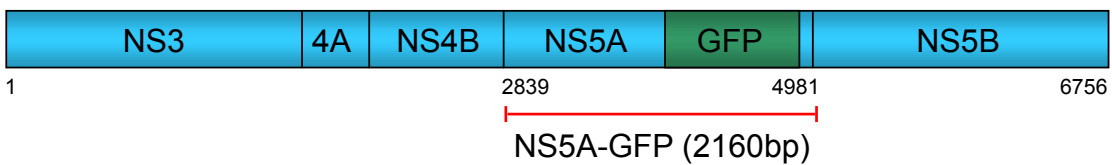
[A]



[B]



[C]



5A-GFP primers

NS5A sequence ²⁸³⁹ TCC GGA TCC TGG CTC CGC GAC GTG

5A-GFP_F 5' CCC GGG ATG TCC GGA TCC TGG CTC CGC GAC GTG 3'
XmaI Start

NS5A sequence GAG GAG GAC GAT ACC ACC GTG TGC ⁴⁹⁸¹

5A-GFP_R 3' CTC CTC CTG CTA TGG TGG CAC ACG ATC GGG CCC 5'
 Stop *XmaI*

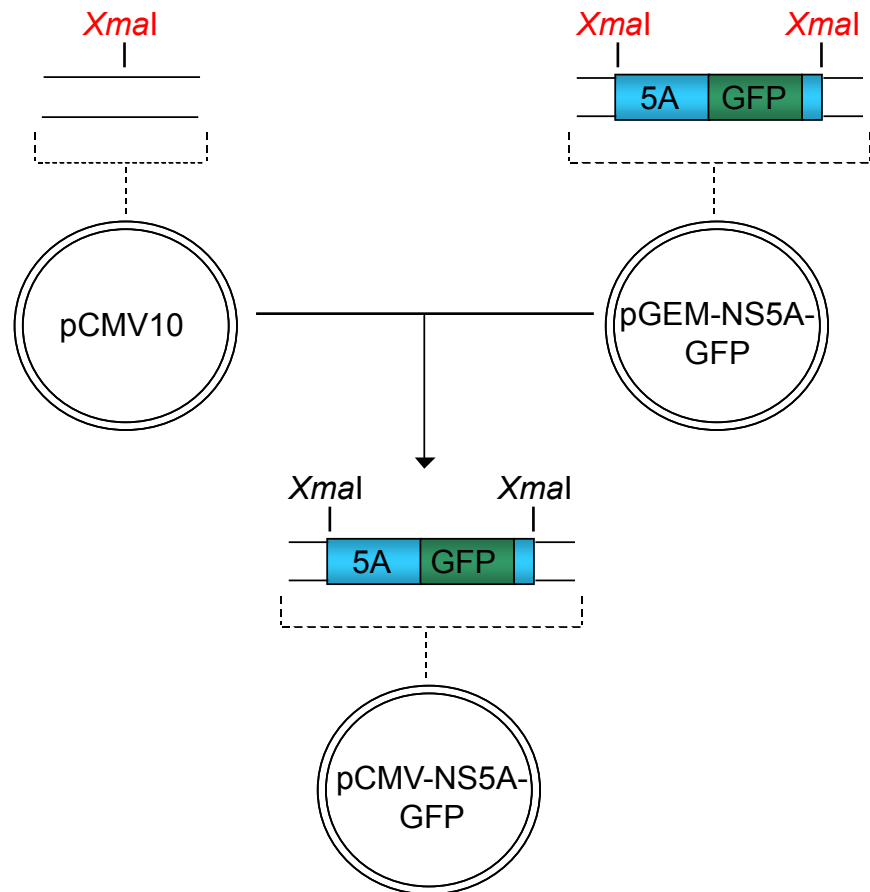
[D]

Figure 3.8 The NS proteins influence the localisation and mobility of NS5A

[A] Cells electroporated with luc-JFH1_{GFP} RNA were analysed by FRAP at 24 hours post-electroporation. Cells transfected with pCMV-NS5A-GFP and GFP-DNase-X were analysed at 16-20 hours post-transfection. Selected areas of 38 μm^2 were bleached using 100% laser power and recovery within these regions was monitored for two minutes at 2% laser power. Values are expressed as a percentage of the pre-bleach value and error bars represent standard errors. **[B]** Huh-7 cells harbouring pCMV-NS5A-GFP (left panel) and luc-JFH1_{GFP} RNA (right panel) were visualised directly at 16-20 hours after transfection (pCMV-NS5A-GFP) or electroporation (luc-JFH1_{GFP}). Scale bar represents 10 μm . **[C]** A schematic representation of the NS3-NS5B coding region of luc-JFH1_{GFP} is shown (top). The positions and sequences of the primers used to amplify the NS5A-GFP region are shown, with introduced non-viral sequences depicted in red. Restriction sites used for cloning purposes and start/stop codons are underlined. The size of NS5A-GFP (2160bp) is inclusive of introduced restriction sites. Nucleotide numbers begin at the NS3 coding region. The NS5A-GFP fragment amplified by PCR was subsequently introduced into the pGEM-T-Easy cloning vector to yield pGEM-NS5A-GFP. **[D]** The NS5A-GFP ORF was excised from pGEM-NS5A-GFP using *Xma*I and introduced into the corresponding site in pCMV10 to generate pCMV-NS5A-GFP.

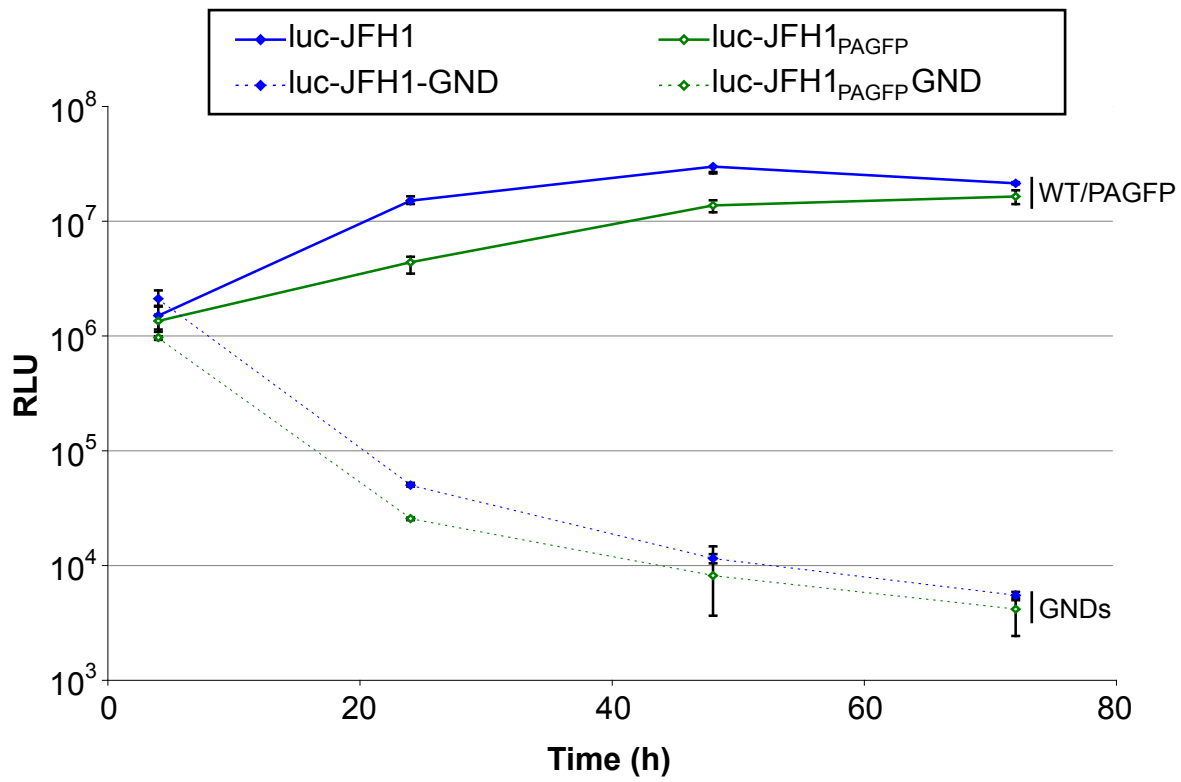
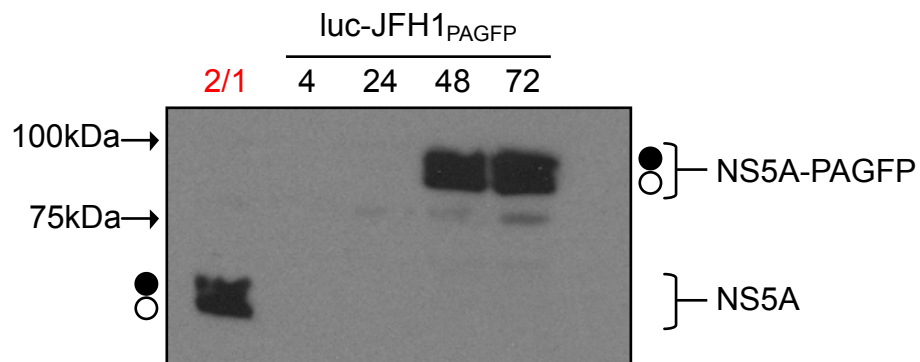
3.3.1 Analysis of NS5A-Photoactivatable GFP (PAGFP)

To confirm the lower mobility of NS5A-GFP expressed from luc-JFH1_{GFP}, the GFP ORF in NS5A was replaced with a photoactivatable form of GFP (termed PAGFP), to generate luc-JFH1_{PAGFP}. PAGFP possesses a Thr to His mutation at amino acid 203 of the protein coding region, which results in increased fluorescence upon photoactivation (see Section 1.7.2). This property allows activation of fluorescence, which is useful for studying protein dynamics within live cells (Patterson & Lippincott-Schwartz, 2002 and 2004). Luc-JFH1_{PAGFP} was created using the same strategy employed for luc-JFH1_{GFP} (Figures 3.1-3.3) and a non-replicating control was also constructed (luc-JFH1_{PAGFP}GND).

3.3.1.1 Luc-JFH1_{PAGFP} Replicates to Levels comparable to luc-JFH1 and luc-JFH1_{GFP}

To ensure luc-JFH1_{PAGFP} was capable of replication, RNA transcribed from Luc-JFH1_{PAGFP} and luc-JFH1_{PAGFP}GND was electroporated into cells and luciferase values were recorded over 72 hours. Cells electroporated with luc-JFH1 and luc-JFH1-GND provided positive and negative controls respectively. In agreement with previous results, luc-JFH1 replicated efficiently, whereas luc-JFH1-GND was incapable of replication (Figure 3.9, A). Luciferase levels from luc-JFH1_{PAGFP}GND declined as quickly as those seen with luc-JFH1-GND, indicating that this SGR was incapable of replicating (Figure 3.9, A). Luc-JFH1_{PAGFP} gave luciferase levels that were only 29% compared to those produced by the unmodified SGR by 24 hours, indicating a delay in the onset of viral RNA synthesis (Figure 3.9, A). However, luciferase activity rose to 77% of the values expressed from luc-JFH1 by 72 hours. This delay in replication was consistent with that observed upon insertion of GFP into the luc-JFH1 genome (Figure 3.4, A). The similarity in replication kinetics between luc-JFH1_{GFP} and luc-JFH1_{PAGFP} is unsurprising, since GFP and PAGFP differ only by a single amino acid.

To confirm that NS5A-PAGFP protein could be detected during transient replication, cell extracts prepared over 72 hours were examined by Western blot analysis (Figure 3.9, B). NS5A-PAGFP was detected in cells at 48 and 72 hours post-electroporation and no evidence of breakdown was apparent, although this could not be confirmed without a Western blot for GFP. In contrast, NS5A-PAGFP was not detected in cells expressing RNA encoding luc-JFH1_{PAGFP}GND (data not shown).

[A]**[B]**

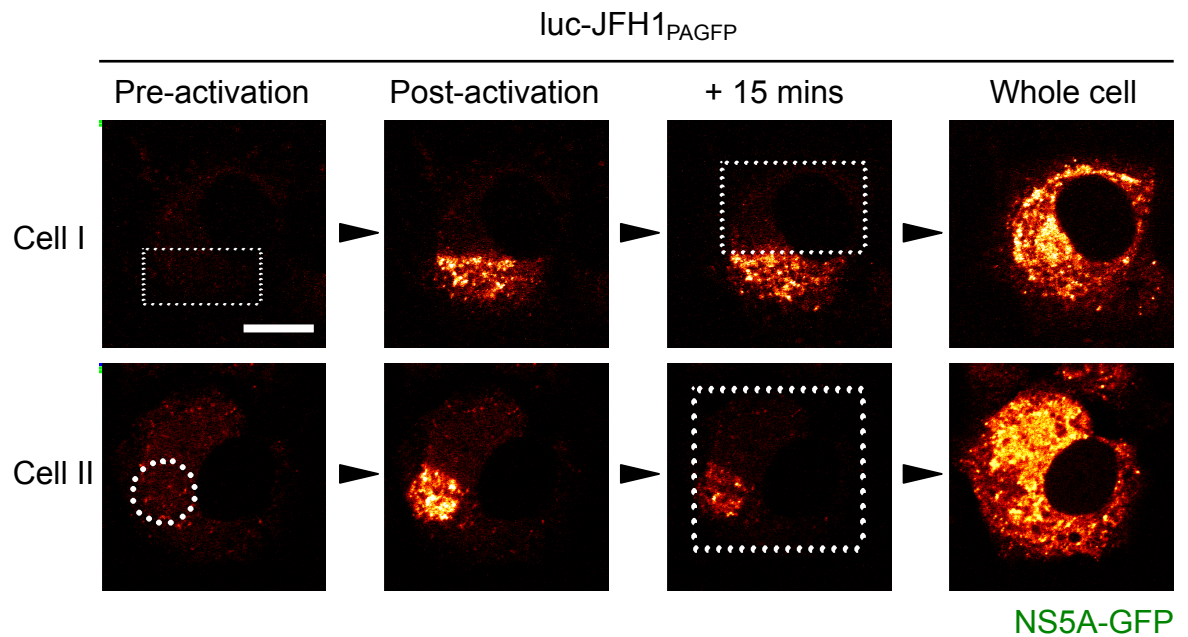
[C]

Figure 3.9 luc-JFH1_{PAGFP} replicates efficiently in Huh-7 cells and NS5A-PAGFP displays a low level of mobility in live cells

[A] Huh-7 cells were electroporated with RNA from luc-JFH1, luc-JFH1_{PAGFP} and their GND counterparts. Cells were lysed at 4, 24, 48 and 72 hours post-electroporation and extracts were assayed for luciferase activity. Assays were performed in triplicate and the averages are shown. Error bars represent the range of the values recorded at each time point. **[B]** Huh-7 cells electroporated with luc-JFH1_{PAGFP} RNA were harvested for Western blot analysis at 4, 24, 48 and 72 hours post-electroporation, and NS5A was detected using NS5A antisera. 2/1 cells were used as a positive control. The hyper- (closed circles) and hypo- (open circles) phosphorylated species of NS5A are indicated. **[C]** Various regions of cells harbouring luc-JFH1_{PAGFP} were activated by exposure to a 405nm laser (indicated by a dotted rectangle [cell I] and circle [cell II]). Post-activation, cells were monitored for 15 minutes to observe any diffusion of fluorescence into the non-activated areas of the cell. Whole cells were then activated by exposure to a 405nm laser. Images are shown in Glow-scale for clarity. Scale bar represents 10 μ m.

3.3.1.2 NS5A-PAGFP Exhibits a Low Level of Mobility in Live Cells

The data obtained from FRAP analysis of luc-JFH1_{GFP} suggested that NS5A-GFP possessed limited mobility in cells (Figure 3.8, A). To further examine this lack of mobility, cells were electroporated with RNA encoding luc-JFH1_{PAGFP} and analysed by confocal microscopy after 24 hours (Figure 3.9, C). Before activation of PAGFP, low fluorescence could be detected in cells, consistent with previous reports (Patterson & Lippincott-Schwartz, 2002). Selected cellular regions were then activated using a 405nm laser, resulting in PAGFP fluorescence. Post-activation, areas of NS5A-PAGFP fluorescence were readily identified (Figure 3.9, C). Cells were monitored for 15 minutes to identify any diffusion of fluorescence that would indicate movement of activated NS5A-PAGFP into non-activated regions of the cell. However, little transfer of the fusion protein was evident in terms of appearance of fluorescence in non-activated regions, although in the second example shown there is some loss of signal intensity in the activated region (Figure 3.9, C). This is a likely consequence of photobleaching over the 15-minute period. To ensure that NS5A-PAGFP molecules were present throughout the cytoplasm, the remaining area of cells was activated. Upon activation, NS5A-PAGFP fluorescence was clearly visible throughout the entire cell and displayed a localisation consistent with that of luc-JFH1_{GFP} (Figures 3.6, B and 3.7). These results confirmed that NS5A exhibits a low level of mobility in cells that harbour actively replicating luc-JFH1_{GFP} and luc-JFH1_{PAGFP} RNA.

3.4 NS5A Localisation and Mobility is Influenced by NS4B

Analysis of NS5A using FRAP and PAGFP indicated that NS5A did not exhibit appreciable mobility in cells containing actively replicating viral genomes. Additionally, NS5A expressed alone gave an ER-like distribution, whereas NS5A produced from luc-JFH1_{GFP} also localised to punctate foci (Figure 3.8, B). These data suggested that one or more of the NS proteins expressed from luc-JFH1_{GFP} could incorporate NS5A into MAF-like structures. This could result in NS5A being tethered at these sites, thereby decreasing protein mobility.

Previous studies have revealed that NS4B induces ER membrane rearrangements, producing discrete structures referred to as the 'membranous web' and MAFs (Egger et al., 2002, Gosert et al., 2003, Gretton et al., 2005).

Other NS proteins (including NS5A) localise to these NS4B-induced structures, presumably creating sites capable of replicating HCV RNA (Elazar et al., 2004, Hugle et al., 2001). Importantly, abolishing NS4B membrane association results in a loss of membrane alteration and consequently, NS proteins cannot localise to these structures in cells expressing subgenomic polyproteins (Elazar et al., 2004). It was therefore predicted that NS4B was at least partly responsible for the differences in NS5A localisation and mobility observed when expressing the protein alone compared to expressing it from a SGR.

To test this hypothesis, NS4B was removed from the NS coding region. Since removal of NS4B from luc-JFH1_{GFP} would abolish replication, the NS3-NS5B coding region was introduced firstly into pCMV10, generating JFH1_{Poly}. This plasmid permitted polyprotein expression in the absence of viral RNA replication and could be used to examine the effect of removal of NS4B on the localisation and mobility of NS5A.

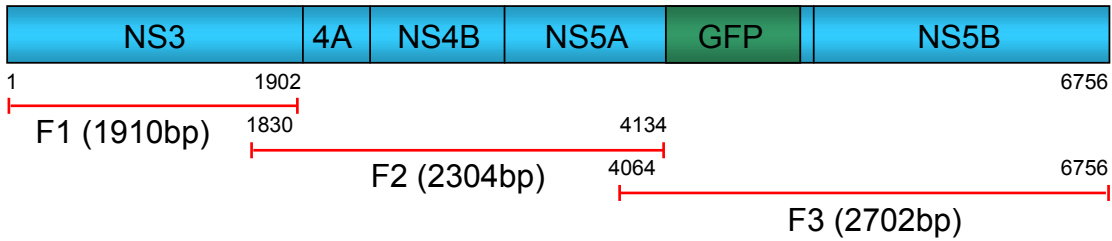
3.4.1 Construction of Plasmids Expressing the HCV NS3-NS5B Coding Region from Strain JFH1

3.4.1.1 Construction of JFH1_{Poly}

The NS3-NS5B coding region (including GFP) was amplified in three fragments (termed F1-F3) using luc-JFH1_{GFP} as a template (Figure 3.10, A). F1 was 1910bp in length and included an introduced *EcoRI* site and ATG initiation codon, the entire NS3 coding region and 7bp of NS4A. F2 was 2304bp in length and incorporated existing *NsiI* (in NS3) and *AgeI* sites (in NS5A, Figure 3.10, A). F3 was 2702bp in length and introduced a *KpnI* site, TAG termination codon and included the entire GFP and NS5B coding regions. F3 also contained 37bp of NS5A sequence upstream from the 5' end of GFP, thus incorporating a pre-existing *AgeI* site (Figure 3.10, A). F1-F3 were introduced into pGEM-T-Easy, producing pGEM-F1, pGEM-F2 and pGEM-F3 respectively (Figure 3.10, B).

These fragments were then excised using *EcoRI/NsiI* (pGEM-F1), *NsiI/AgeI* (pGEM-F2) and *AgeI/KpnI* (pGEM-F3) (Figure 3.10, B). pCMV10 was cut with *EcoRI* and *KpnI* and the four fragments were ligated in a single reaction to create JFH1_{Poly}.

[A]



F1 primers

NS3 sequence 1 GCT CCC ATC ACT GCT TAT GCC CAG

F1_F 5' GAA TTC ATG GCT CCC ATC ACT CGT TAT CGG GAC 3'
EcoRI Start

NS3 sequence CCT TGA GGT CAT GAC CAG CAC GTG¹⁹⁰²

F1_R 3' GGA ACT CCA GTA CTG GTC GTG CAC 5'

F2 primers

NS3 sequence 1830 CCT CAC ACA CCC TGG GAC GAA GTA

F2_F 5' CCT CAC ACA CCC TGG GAC GAA GTA 3'

NS5A sequence GGT GAG CAA GGG CGA GGA GCT GTT⁴¹³⁴

F2_R 3' CCA CTC GTT CCC GCT CCT CGA CAA 5'

F3 primers

NS5A sequence 4064 AGA CAG GTT CGG CCT CCT CTA TGC

F3_F 5' AGA CAG GTT CGG CCT CCT CTA TGC 3'

NS5B sequence CTC TTC CTA CTC CCC GCT CGG⁶⁷⁵⁶

F3_R 3' GAG AAG GAT GAG GGG CGA GCC ATC CCA TGG 5'
 Stop *KpnI*

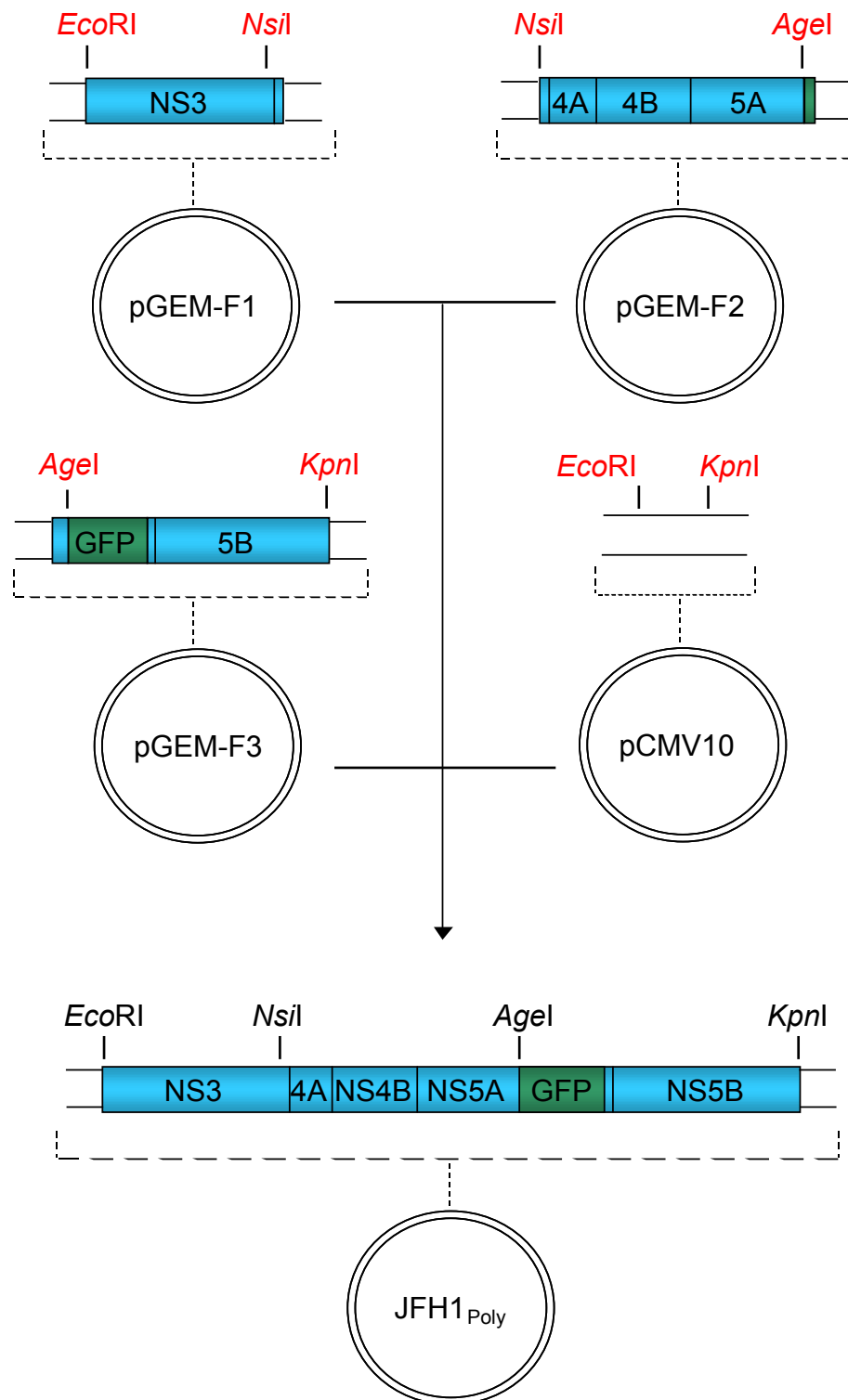
[B]

Figure 3.10 Construction of JFH1_{Poly}

[A] A schematic representation of the NS3-NS5B coding region of luc-JFH1_{GFP} is shown (top). The positions and sequences of the primers used to amplify F1-F3 are indicated, with introduced non-viral sequences depicted in red. Restriction sites used for cloning purposes and start/stop codons are underlined. The sizes of F1 (1910bp), F2 (2304bp) and F3 (2702bp) are inclusive of introduced restriction sites. Nucleotide numbers begin at the NS3 coding region. F1-F3 were subsequently introduced into the pGEM-T-Easy cloning vector, generating pGEM-F1, pGEM-F2 and pGEM-F3. **[B]** F1, F2 and F3 were excised from the corresponding pGEM constructs using *EcoRI/NsiI*, *NsiI/AgeI* and *AgeI/KpnI* respectively. The pCMV10 vector was digested using *EcoRI* and *KpnI* and ligated with F1-F3 in a four-fragment ligation to generate JFH1_{Poly}.

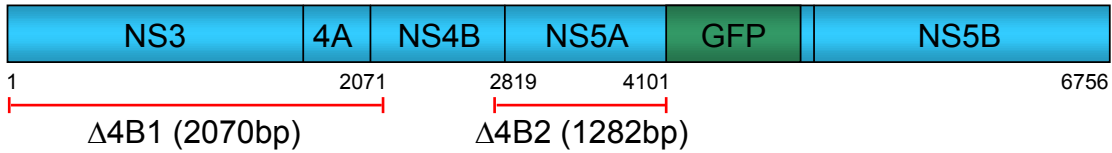
3.4.1.2 Creation of JFH1_{Poly}Δ4B

Removal of NS4B from JFH1_{Poly} required the complete excision of the NS4B coding region in addition to maintenance of NS3 cleavage at the newly created NS4A/NS5A junction. The cleavage sites between the NS4A/NS4B and NS4B/NS5A junctions contain Cys-Ala and Cys-Ser motifs in the P1 and P1' positions respectively (Figure 3.11, B). Cys at P1 and either Ala or Ser at P1' are highly favoured for recognition and cleavage by the NS3 protease (Kim et al., 2000, Zhang et al., 1997). Therefore, removal of NS4B from JFH1_{Poly} would need to maintain an NS4A/NS5A junction that retained a Cys-(Ala/Ser) motif. The cloning strategy utilised primers that introduced *FspI* sites between the NS4A/NS4B and NS4B/NS5A junctions, creating a new NS4A/NS5A junction with a Cys-Ala motif that should be recognised and cleaved by NS3 (Figure 3.11, A and B).

JFH1_{Poly} was used as a template for the amplification of two fragments termed Δ4B1 and Δ4B2 (Figure 3.11, A). Δ4B1 was 2070bp in length and contained the entire NS3 and NS4A coding regions, as well as the first 15bp of NS4B. This incorporated the introduced *EcoRI* site at the start of the NS3 coding region (Figure 3.11, A). The reverse primer for Δ4B1 introduced a nucleotide change (TGCGCC - TGCGCA) that resulted in the creation of an *FspI* site at the NS4A/NS4B junction and retained the cysteine residue marking the end of NS4A. Fragment Δ4B2 was 1282bp in length and included the 3'-terminal 20bp of NS4B and the NS5A coding region, up to and including the *AgeI* site that defined the boundary with GFP (Figure 3.11, A). The forward primer for Δ4B2 introduced two nucleotide changes (TGCTCC-TGCGCA) that resulted in the creation of an *FspI* site at the NS4B/NS5A junction and changed the first serine residue of NS5A to an alanine. The two fragments were subsequently introduced into pGEM-T-Easy, creating pGEM-Δ4B1 and pGEM-Δ4B2 (Figure 3.11, C).

Δ4B1 and the Δ4B2 were excised from pGEM-Δ4B1 and pGEM-Δ4B2 using *EcoRI* and *FspI* and *FspI* and *AgeI* respectively (Figure 3.11, C). JFH1_{Poly} was digested with *EcoRI* and *AgeI* and the resultant backbone was ligated with Δ4B1 and Δ4B2 in a single ligation reaction to produce JFH1_{Poly}Δ4B.

[A]



Δ4B1 primers

NS3 sequence 1 **GAA TTC ATG GCT CCC ATC ACT**

Δ4B1_F 5' **GAA TTC** **ATG** GCT CCC ATC ACT 3'

EcoRI Start

NS4B/4A sequence **ATG GAG GAA TGC GCC TCT AGG GCG GCT** ²⁰⁷¹

Δ4B1_R 3' **TAC CTC CTT** **ACG CGT** **AGA TCC CGC CGA** 5'

FspI

Δ4B2 primers

NS4B/5A sequence

²⁸¹⁹ **AG GAC TGC CCC ATC CCA TGC TCC GGA TCC TGG CTC CGC GAC GT**

Δ4B2_F

5' **AG GAC TGC CCC ATC CCA** **TGC GCA** **GGA TCC TGG CTC CGC GAC GT** 3'

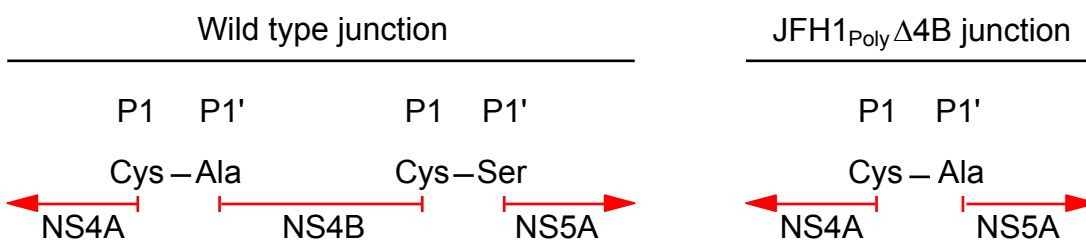
FspI

NS5A sequence **CTC TAT GCC CCC CCT ACC GGT** ⁴¹⁰¹

Δ4B2_R 3' **GAG ATA CGG GGG GGA** **TGG CCA** 5'

AgeI

[B]



[C]

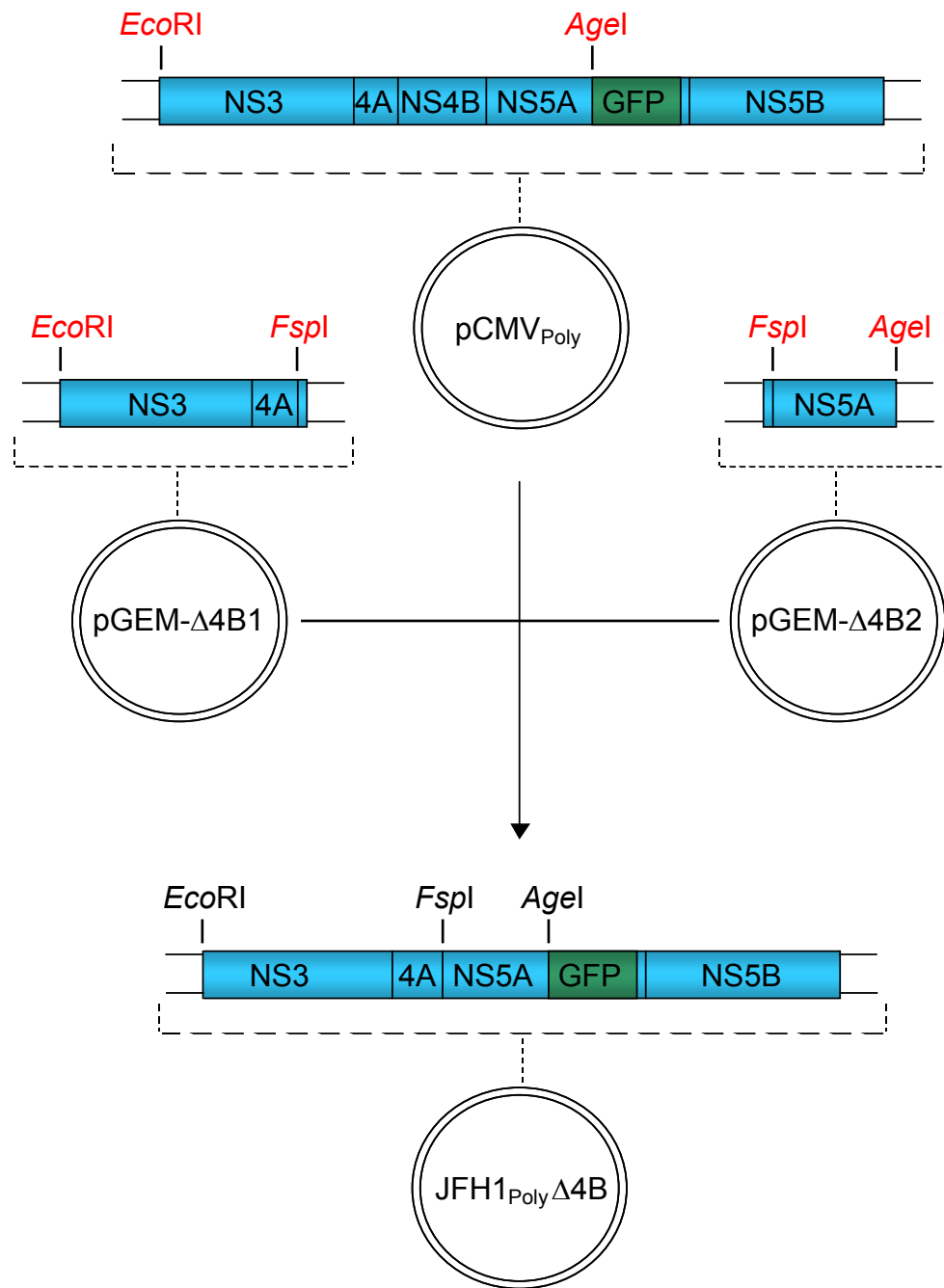


Figure 3.11 Construction of JFH1_{Poly}Δ4B

[A] A schematic representation of the NS3-NS5B coding region of JFH1_{Poly} is shown (top). The positions and sequences of the primers used to amplify Δ4B1 and Δ4B2 are indicated. The introduced nucleotide changes for creation of the *FspI* sites are depicted in red. Restriction sites used for cloning purposes are underlined, as is the start codon in Δ4B1_F. Nucleotide numbers refer to the JFH1_{Poly} sequence, beginning at the NS3 coding region. Δ4B1 and Δ4B2 were subsequently introduced into the pGEM-T-Easy cloning vector, yielding plasmids pGEM-Δ4B1 and pGEM-Δ4B2. **[B]** A schematic representation of the NS4A/NS4B and NS4B/NS5A junctions in a wt polyprotein and the new NS4A/NS5A junction created by deleting NS4B. The amino acids present at the P1 and P1' positions of each junction are shown and cleavage occurs between these residues. **[C]** Δ4B1 and Δ4B2 were excised from pGEM-Δ4B1 and pGEM-Δ4B2 using *EcoRI/FspI* and *FspI/AgeI* respectively. The *EcoRI/AgeI* fragment from JFH1_{Poly} was replaced with Δ4B1 and Δ4B2 in a three-fragment ligation. This resulted in a polyprotein that excluded the NS4B coding region, yet maintained a Cys-Ala cleavage site at the NS4A/NS5A junction.

3.4.2 NS4B Distributes NS5A to Foci

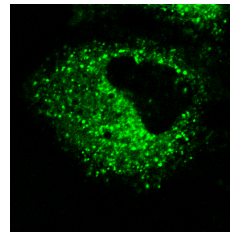
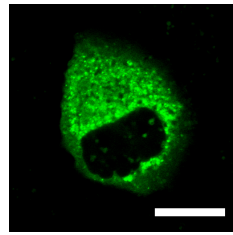
To examine the effect of NS4B removal on localisation of NS5A, cells were transfected with JFH1_{Poly}, pCMV-NS5A-GFP and JFH1_{Poly}Δ4B, and NS5A-GFP distribution was examined. Additionally, examination of NS5A-GFP expressed from both JFH1_{Poly} and luc-JFH1_{GFP} would determine whether viral replication had any influence on NS5A localisation. Therefore, cells electroporated with luc-JFH1_{GFP} RNA were also analysed. At least 250 cells expressing each construct were examined and the localisation of NS5A-GFP was scored into one of two categories: (i) NS5A-GFP predominantly localised to the ER, or (ii) NS5A-GFP predominantly localised to foci (Figure 3.12, A). NS5A-GFP expressed from JFH1_{Poly} was localised to foci in 92% of cells and only 8% of cells displayed a localisation described as being predominantly ER-like (Figure 3.12, A). Luc-JFH1_{GFP} gave a similar profile, where NS5A-GFP was located at foci in 95% of cells. This result suggested that HCV RNA replication had little or no influence on NS5A localisation. By contrast, NS5A-GFP expressed alone or from JFH1_{Poly}Δ4B was localised predominantly on the ER in 97% of cells (Figure 3.12, A). This localisation assay confirmed that NS5A was distributed to foci in the presence of a polyprotein and furthermore, that this distribution was dependent on NS4B but independent of HCV RNA replication.

3.4.3 NS4B Reduces the Mobility of NS5A

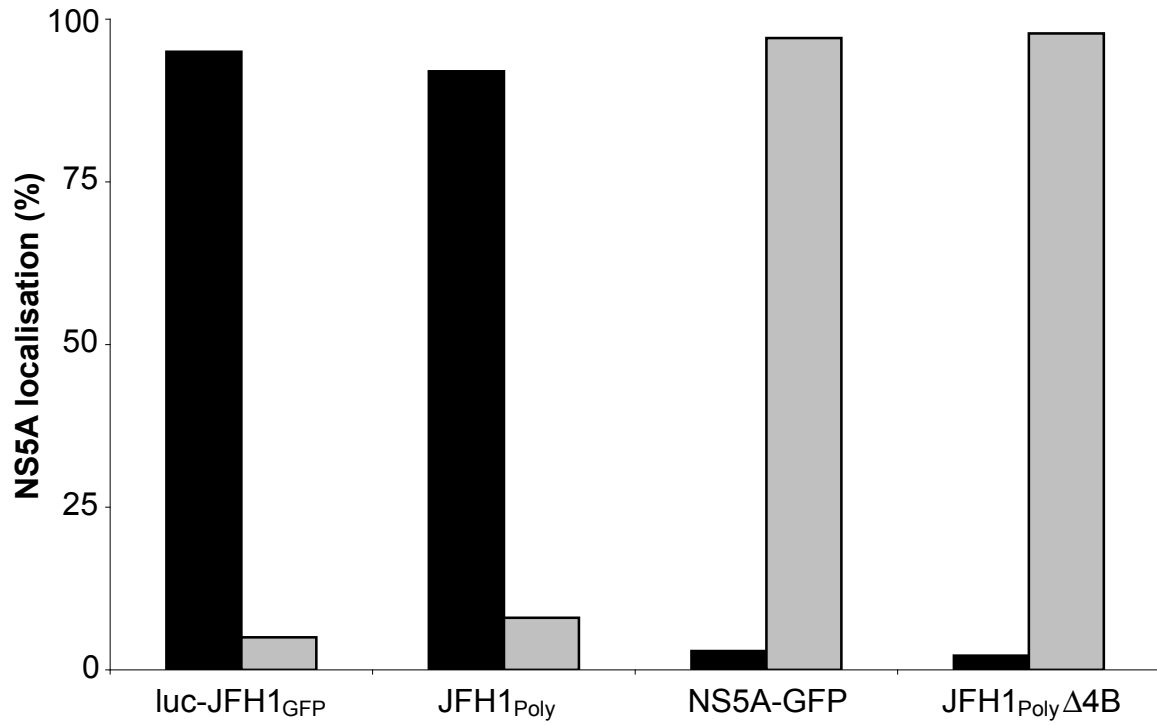
Previous results revealed that NS5A displayed an ER-like distribution and was more mobile when expressed in isolation as compared to expression from luc-JFH1_{GFP} (Figure 3.8, A). An ER-like pattern of NS5A localisation was also observed upon removal of NS4B from the NS3-NS5B polyprotein (Figure 3.12, A). To determine whether removal of NS4B increased NS5A mobility, FRAP analysis was performed on cells harbouring luc-JFH1_{GFP} RNA, or DNA encoding JFH1_{Poly}, JFH1_{Poly}Δ4B and pCMV-NS5A-GFP (Figure 3.12, B). NS5A-GFP expressed from luc-JFH1_{GFP} and JFH1_{Poly} was bleached to 18% and 19% respectively compared to pre-bleach values. Over a two-minute period, fluorescence intensity recovered to 32% (luc-JFH1_{GFP}) and 33% (JFH1_{Poly}, Figure 3.12, B). This low recovery of fluorescence in cells expressing NS5A-GFP from luc-JFH1_{GFP} was identical to that observed previously (Figure 3.8, A). Fluorescence recovery in cells expressing luc-JFH1_{GFP} and JFH1_{Poly} was comparable, suggesting that RNA replication had no influence on NS5A mobility. In contrast, NS5A-GFP fluorescence in cells

[A]

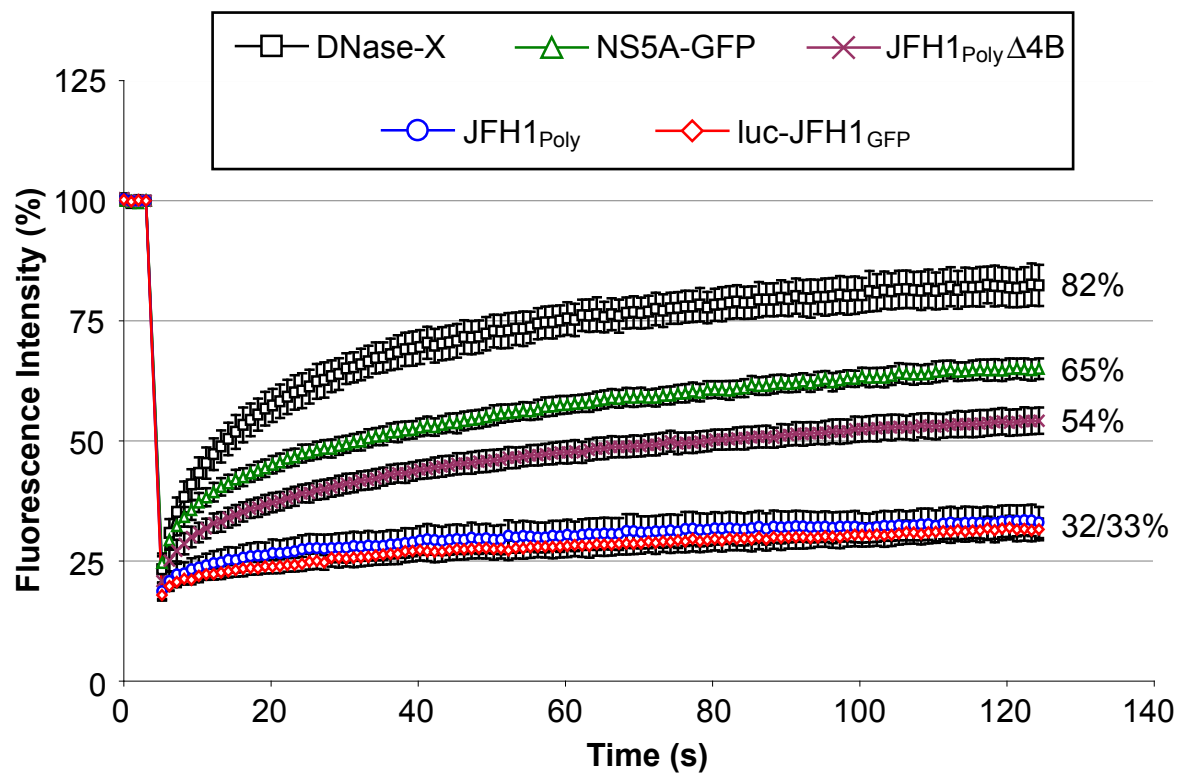
Predominantly ER
 Predominantly foci



NS5A-GFP



[B]



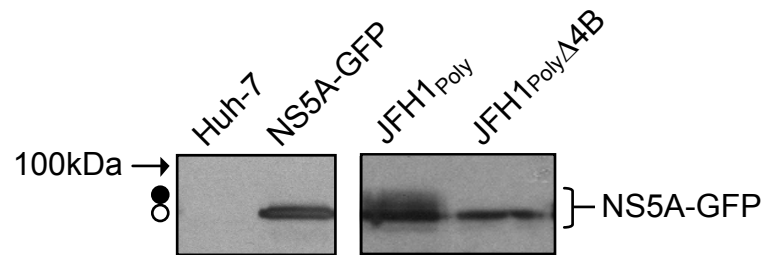
[C]

Figure 3.12 NS4B influences the localisation and distribution of NS5A

[A] Huh-7 Cells were electroporated with luc-JFH1_{GFP} RNA, or transfected with JFH1_{Poly}, pCMV-NS5A-GFP or JFH1_{PolyΔ4B} plasmids, and NS5A-GFP was visualised at 16-20 hours later. At least 250 cells were observed for each construct and scored into either of two categories: (i) NS5A-GFP localised predominantly to the ER (top, left panel) (ii) NS5A-GFP localised predominantly to foci (top, right panel). Cells in each category are expressed as a percentage of the total number counted for each construct. Scale bar represents 10 μ m. **[B]** Huh-7 cells electroporated with luc-JFH1_{GFP} RNA were analysed by FRAP at 24 hours post-electroporation. Cells transfected with plasmids pCMV-NS5A-GFP, GFP-DNase-X, JFH1_{Poly} and JFH1_{PolyΔ4B} were analysed at 16-20 hours post-transfection. Areas of 38 μ m² were bleached using 100% laser power and recovery within these regions was monitored for two minutes at 2% laser power. Values are expressed as a percentage of the pre-bleach value and error bars represent standard errors. **[C]** Lysates from cells transfected with the indicated constructs were examined by Western blot analysis 24 hours post-transfection. NS5A was detected using NS5A antisera. The hyper- (closed circles) and hypo- (open circles) phosphorylated species of NS5A are indicated. Note that hyperphosphorylated NS5A could only be detected in cells expressing JFH1_{Poly}.

expressing JFH1_{Poly}Δ4B recovered to 54% after two minutes. This was substantially greater than the recovery observed for either luc-JFH1_{GFP} or JFH1_{Poly} (Figure 3.12, B). However, this fluorescence recovery was lower compared to that for NS5A-GFP expressed from pCMV-NS5A-GFP (65%). These data indicate that NS4B is a major contributing factor in the low mobility of NS5A-GFP, although other NS proteins also partly account for the low recovery of the fluorescent protein.

To ensure that removal of the NS4B coding region did not affect cleavage at the NS4A/NS5A junction, extracts from cells transfected with pCMV-NS5A-GFP, JFH1_{Poly} and JFH1_{Poly}Δ4B were examined by Western blot analysis for the presence of NS5A-GFP (Figure 3.12, C). NS5A-GFP was detected in all cell extracts at the correct predicted molecular weight of ~83kDa, confirming that cleavage at the NS4A/NS5A junction was not disrupted in JFH1_{Poly}Δ4B. Interestingly, with the exception of cells expressing JFH1_{Poly}, only the hypophosphorylated species of NS5A was detected (Figure 3.12, C). This result is consistent with previous reports stating that hyperphosphorylation of NS5A can only occur in the presence of the other NS proteins and that NS4B is critical to this process (Koch & Bartenschlager, 1999, Neddermann et al., 1999). Overall, these results showed that NS5A is incorporated into foci in the presence of an NS3-NS5B polyprotein and that NS4B is an essential component of this process. Once localised to these structures, NS5A displays a lower mobility compared to protein present on the ER membrane.

3.5 Discussion

Before the discovery of JFH1, genotype 1 SGRs were commonly utilised for investigating HCV RNA replication. Studies with genotype 1 SGRs typically involve indirect measurement of viral RNA replication by determining the colony forming efficiency of cells that stably replicate the SGR under selective pressure (see Section 1.3.2). Efficient replication in these assays is dependent upon the presence of CCAMs within the viral sequence. Even with such mutations however, the replication capacity of these constructs is substantially lower than that of wt JFH1 SGRs, such as luc-JFH1 (Kato et al., 2003, Targett-Adams & McLauchlan, 2005). With luc-JFH1, the level of luciferase produced within electroporated cells is deemed to provide an indirect quantitative measurement of viral genome synthesis. Furthermore, the replication efficiency of JFH1 RNA allows transient

measurement of genome synthesis and bypasses the requirement of cell lines stably replicating HCV SGRs. Therefore, JFH1 SGRs provide a robust system for the study of transient HCV RNA replication.

At the outset of this study, a SGR based on the genotype 1b strain Con1 was used to demonstrate that the C-terminus (domain III) of NS5A could tolerate the insertion of GFP without abolishing viral replication (Moradpour et al., 2004b). This finding was further validated by other groups (Appel et al., 2005b, Liu et al., 2006), and allowed the characterisation of NS5A in live cells. The results presented here show that GFP can also be inserted into the same region of JFH1-encoded NS5A, thus allowing the characterisation of NS5A in the context of an efficiently replicating viral genome. With the Con1 system, GFP insertion into NS5A resulted in a moderate reduction of viral replication (Appel et al., 2005b, Liu et al., 2006, Moradpour et al., 2004b). A similar effect on replication was also evident with luc-JFH1_{GFP}, particularly within the first 24 hours of replication (Figure 3.4, A). Further analysis revealed that active replication of luc-JFH1_{GFP} was delayed by 4-6 hours compared to unmodified luc-JFH1 (Figure 3.5, A and B). Domain III of NS5A is dispensable for RNA replication, as judged by a luciferase assay system similar to that described here (Appel et al., 2008). Therefore, perturbing the structure of domain III through the insertion of GFP would be expected to have no effect on replication. However, it cannot be excluded that the presence of GFP within domain III results in the modification of global NS5A structure, which may be unfavourable for RNA synthesis. Alternatively, it is possible that the delay in luc-JFH1_{GFP} replication is merely a consequence of translating a longer SGR genome. In this respect, it would be interesting to determine whether full-length viral RNA initially exhibit levels of replication that are lower than those displayed by a SGR.

Viral RNA replication is thought to occur rapidly after virus entry and both positive and negative-strand RNAs have been detected using Northern hybridisation at 2-4 hours after introduction of RNA into cells (Binder et al., 2007). It is important to note that the luciferase system used here could not detect viral RNA replication until at least 12 hours post-electroporation (Figure 3.5). This is likely due to the excess luciferase translated directly from the input RNA, resulting in the luciferase signal masking production of the enzyme from replicated genomes. In support of this notion, luciferase values increased up to 6 hours post-electroporation with RNAs harbouring GND mutations that render them incapable of replication (Figure 3.5). Similarly, NS5A expressed from GND mutant RNA can be detected in cells by 4 hours, providing conclusive evidence that a significant level of protein is

produced directly from the RNA introduced by electroporation (Figure 3.6). Therefore, the luciferase system is probably less sensitive for the detection of viral replication at early time points compared to techniques that detect RNA directly.

NS5A-GFP expressed from luc-JFH1_{GFP} could be directly visualised in both fixed and live cells and was distributed on both the ER membrane and to punctate cytoplasmic structures termed foci (Figures 3.6 and 3.7). This pattern of NS5A localisation was also evident in cells expressing photoactivatable NS5A-GFP (Figure 3.9, C). These foci became more abundant over 72 hours and are consistent with those previously identified in cells actively replicating HCV RNA (El-Hage & Luo, 2003, Gosert et al., 2003, Moradpour et al., 2004b, Mottola et al., 2002). Viral RNA co-localises with NS5A in studies utilising FISH (Gosert et al., 2003, Targett-Adams et al., 2008a), BrUTP labelling (El-Hage & Luo, 2003, Moradpour et al., 2004b) and use of an antibody that detects dsRNA intermediates (Targett-Adams et al., 2008a). This result strongly suggests that NS5A foci are indicative of viral RCs. However, NS5A (expressed from luc-JFH1) and NS5A-GFP (expressed from luc-JFH1_{GFP}) were also localised at sites that did not apparently include dsRNA and cells were found to harbour a greater quantity of NS5A (Figure 3.6, A and C). An excess of NS proteins compared to viral RNA has been demonstrated previously and consequently, it is thought that less than 5% of the NS proteins present in cells are actively engaged in RNA replication (Quinkert et al., 2005). Therefore, NS5A distribution alone is not sufficient to identify sites replicating HCV RNA. It is possible that NS5A protein localised at sites distinct from viral RNA is engaged in other roles, such as viral assembly or modulating the host cell response to viral infection (Macdonald & Harris, 2004, Miyanari et al., 2007).

Interestingly, NS5A-GFP no longer localised to foci when expressed in isolation and instead exhibited a more diffuse ER-like distribution, suggesting that NS5A does not inherently form or localise to these sites (Figures 3.8, B and 3.12, A). Furthermore, NS5A-GFP expressed alone was mobile in cells, yet was relatively immobile when expressed in the context of an NS3-NS5B polyprotein (Figure 3.8, A and Figure 3.12, B). Analogous to these results, previous biochemical analysis has shown that NS5A produced from a polyprotein is more tightly associated with membranes compared to NS5A expressed in isolation (Brass et al., 2002). The correlation between the data presented here and that reported by Brass et al. suggests that measurement of protein mobility by FRAP is a plausible alternative approach for examining protein-protein and protein-membrane interactions.

The HCV NS4B protein represented a likely candidate for influencing the localisation and mobility of NS5A. NS4B induces foci formation when expressed in cells and other HCV proteins form a multiprotein complex at these sites (Egger et al., 2002). These structures are assumed to be consistent with the foci seen in confocal microscopy studies, believed to represent sites of viral RNA replication. This assumption is strengthened by additional studies revealing that disruption of NS4B membrane association causes the mis-targeting of other replicase components (including NS5A) to foci, abolishing RNA replication in the process (Elazar et al., 2004). In agreement with these results, removal of the NS4B coding region resulted in a loss of NS5A-GFP localisation to foci and a corresponding increase in mobility of the fusion protein (Figure 3.12, A and B). Therefore, the presence of NS4B is critical for NS5A to associate to foci and, once at these sites, NS5A displays lowered mobility. Other investigations into viral RCs have also highlighted the limited mobility of NS5A within foci (Wolk et al., 2008). These data suggest that RCs likely represent sites that have a relatively static internal architecture that allow limited detectable mobility of the proteins contained within them. It is possible that NS5A and NS4B interact within RCs, resulting in the decreased mobility of NS5A. Indeed, NS4B itself displays no appreciable mobility when located within these structures (Gretton et al., 2005). Interactions involving NS5A and NS4B have been previously identified, although it is unknown whether they associate directly (Dimitrova et al., 2003). Alternatively, NS5A may have a higher affinity for the membrane alterations induced by NS4B, rather than NS4B itself.

4 Mutational Analysis of the NS4B C-terminus

4.1 Introduction

In the previous chapter NS4B was identified as being responsible for influencing both the localisation and mobility of NS5A. This prompted a more detailed investigation into the relationship between these two proteins and the properties of NS4B.

NS4B exhibits the characteristics of an integral ER membrane protein and various biochemical and predictive analyses suggest that the central part of the protein consists of at least four TMDs (Hugle et al., 2001, Lundin et al., 2003). It is therefore believed that the majority of the NS4B protein is tightly buried within the ER membrane and consequently inaccessible to other viral or cellular factors. However, the N- and C-termini as well as a small transmembrane loop linking TMD2 and TMD3 are thought to reside on the cytosolic side of the ER membrane (Figure 4.2). Such orientation of the termini would allow cleavage of NS4B from NS4A and NS5A by the NS3 protease, which itself resides in the cytosol (Lundin et al., 2003). Therefore, these three regions of NS4B may interact with and/or influence other NS proteins residing on the cytosolic side of the ER, including NS5A.

The C-terminus of NS4B is highly conserved among members of the *flaviviridae* family (Welsch et al., 2007), yet has been poorly characterised to date. Of the studies conducted on this region, one study reported that mutating C-terminal Cys residues resulted in impaired NS4B-NS5A interaction (Yu et al., 2006). Thus, the NS4B C-terminus may directly influence NS5A. This prompted a detailed analysis of the C-terminal region of NS4B by mutagenesis and examination of whether this region was responsible for the changes in NS5A localisation and mobility observed in the previous chapter.

4.2 The NS4B C-terminus is well conserved and is predicted to contain two α -helices

Based on structural predictions, the C-terminus of NS4B is defined as the region of 70 amino acids immediately downstream of TMD4 (Hugle et al., 2001, Lundin et al., 2003). To gain further insight into the conservation of the NS4B C-terminus,

[C]

HCV genotype	Number of sequences aligned
1a	11
1b	89
1c	3
2a	13
2b	13
2c	1
3a	4
3b	1
4a	1
5a	2
6a	2
6b	1
Total	141

Figure 4.1 Conservation and predicted secondary structure of the JFH1 NS4B C-terminus

[A] 141 NS4B sequences from the Los Alamos HCV database (<http://hcv.lanl.gov/content/hcv-index>) were aligned using the Jalview Multiple Alignment Editor (<http://www.jalview.org/>). Alignment of the C-terminal region only is shown (aa192 - 261). Bars represent conservation for each amino acid as a percentage and asterisks denote amino acids with 100% conservation. The amino acid sequence shown represents the JFH1 NS4B C-terminus. Region 1 and Region 2 were designated arbitrarily based on the conservation pattern of the C-terminal region as a whole, with Region 1 being highly conserved and Region 2 being less well-conserved. **[B]** Secondary structure prediction of the JFH1 NS4B C-terminus. The sequence was analysed using the PSIPRED Protein Structure Prediction Server (<http://bioinf.cs.ucl.ac.uk/psipred/>). The positions of the two helices (termed H1 and H2) are shown. **[C]** Summary of the HCV genotypes used for the alignment study depicted in [A].

141 HCV NS4B sequences were aligned using the Jalview Multiple Alignment Editor. These sequences were derived from the Los Alamos HCV database and featured strains from all six HCV genotypes (Figure 4.1, C). The alignment revealed a conservation pattern in which the N-terminal half of the C-terminus (defined as Region 1) consisted of highly conserved residues. In contrast, the C-terminal half of the C-terminus (defined as Region 2) displayed lower conservation (Figure 4.1, A).

To complement the data obtained through alignment, the sequence of the JFH1 NS4B C-terminus was analysed using the PSIPRED Protein Structure Prediction Server. This revealed the presence of two potential α -helices, with the first helix (defined as H1, 13 amino acids in length) located within Region 1 and a second longer helix (defined as H2, 27 amino acids in length) within Region 2 (Figure 4.1, B). The positions of these helices agreed with those predicted in other studies on the NS4B C-terminus (Welsch et al., 2007). The intra-helical region and those flanking the two helices were deemed to be unstructured.

4.3 Mutation of the NS4B C-terminus

Utilising the information gained from the conservation and secondary structure prediction data, 15 individual amino acids within the NS4B C-terminal coding region of the luc-JFH1_{GFP} replicon were selected for mutation (Figure 4.2). These residues were distributed along the length of the C-terminal region and incorporated:

- (i) Three mutations in the region upstream of H1 (M1, M2 and M3) that included substitution of an Arg residue at position 192 (M1) involved in RNA binding (Einav et al., 2008a).
- (ii) Two mutations in H1 (M4 and M5).
- (iii) Three mutations in the segment separating H1 and H2 (M6-M8).
- (iv) Six mutations in H2, including substitution of Trp (M13) and Thr (M14) residues at positions 252 and 254 respectively that were previously reported to have a role in HCV RNA replication (Lindstrom et al., 2006).
- (v) One mutation in the segment downstream of H2 at a Cys residue (M15) at position 257 that is believed to be a site for palmitoylation of NS4B (Yu et al., 2006).

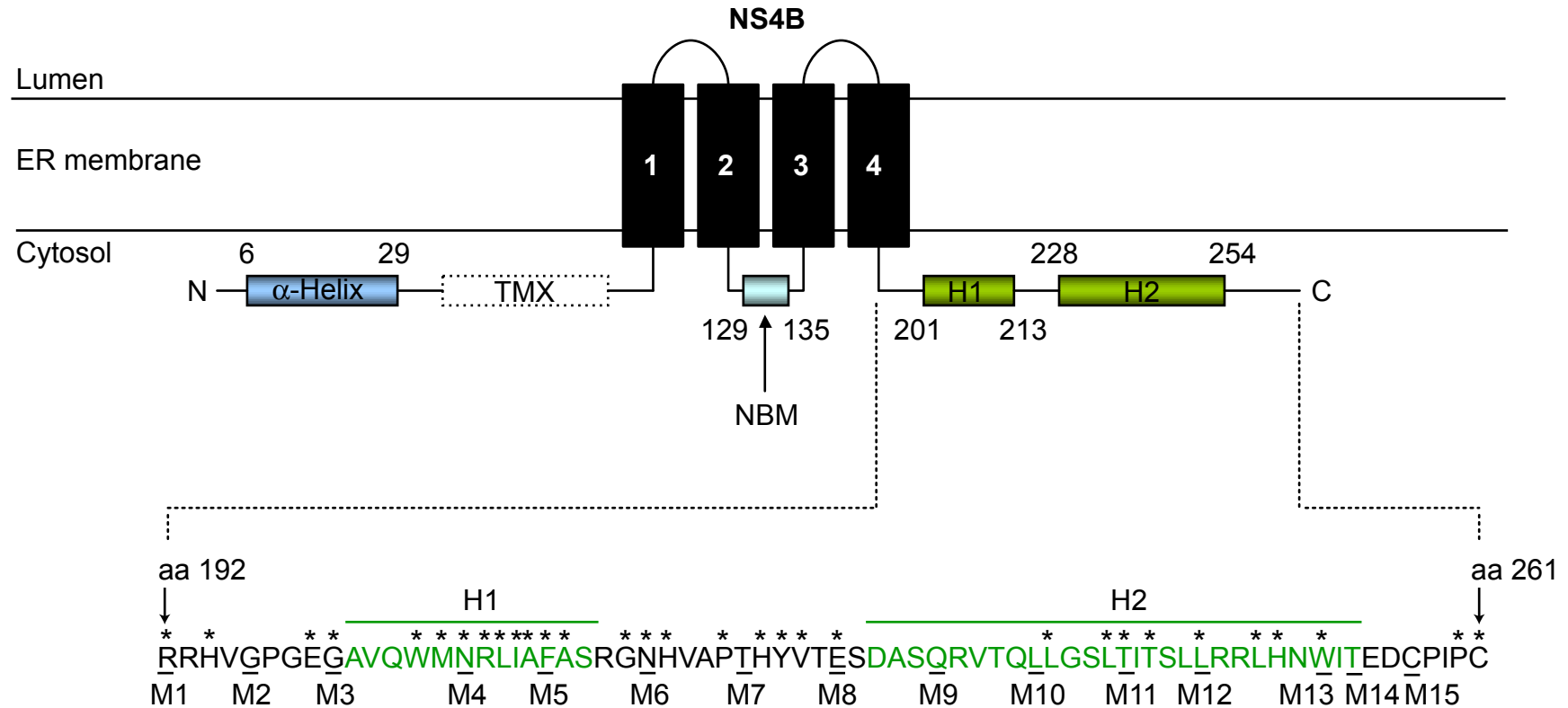


Figure 4.2 Topology of the NS4B protein and mutational analysis of the C-terminal domain

A schematic representation of the predicted topological arrangement of NS4B bound to the ER membrane is shown (top). NS4B is predicted to contain four TMDs (numbered 1-4) that span the ER membrane, where the flanking N- and C- terminal ends are oriented in the cytosol. Positions of previously identified features including the α -helix, TMX domain and the nucleotide binding motif (NBM) are shown. The predicted helices H1 and H2 are also indicated. The amino acid sequence of the C-terminal region of strain JFH1 is presented. Amino acids substituted with alanine are underlined and numbered M1-M15. Amino acids predicted to lie within helices H1 and H2 are overlined and shown in green. Asterisks denote invariant amino acids and residues are numbered in accordance with the N-terminal end of NS4B.

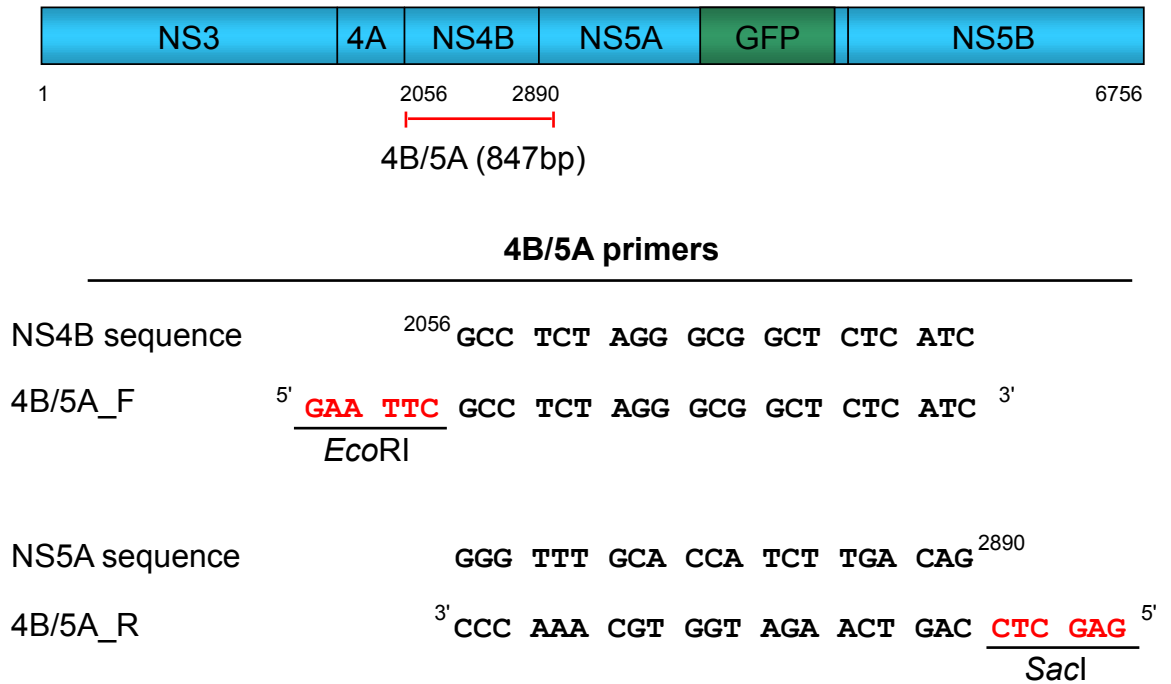
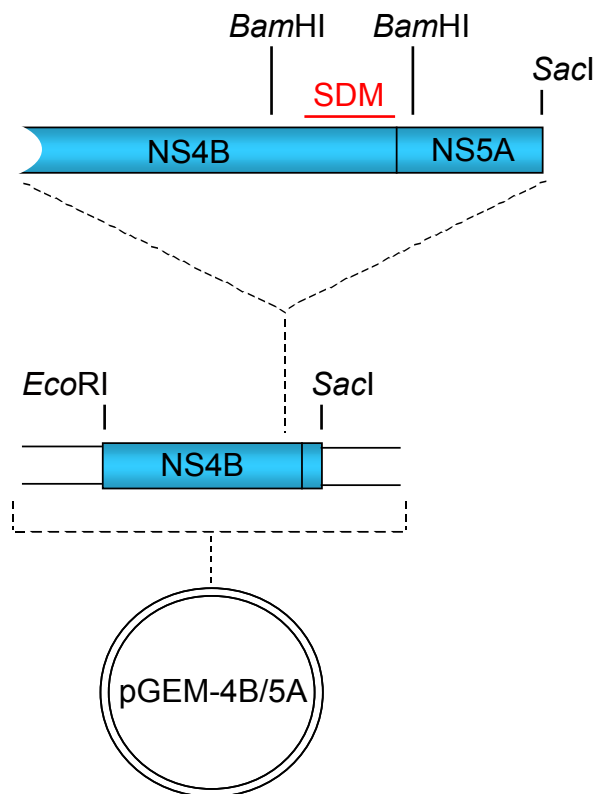
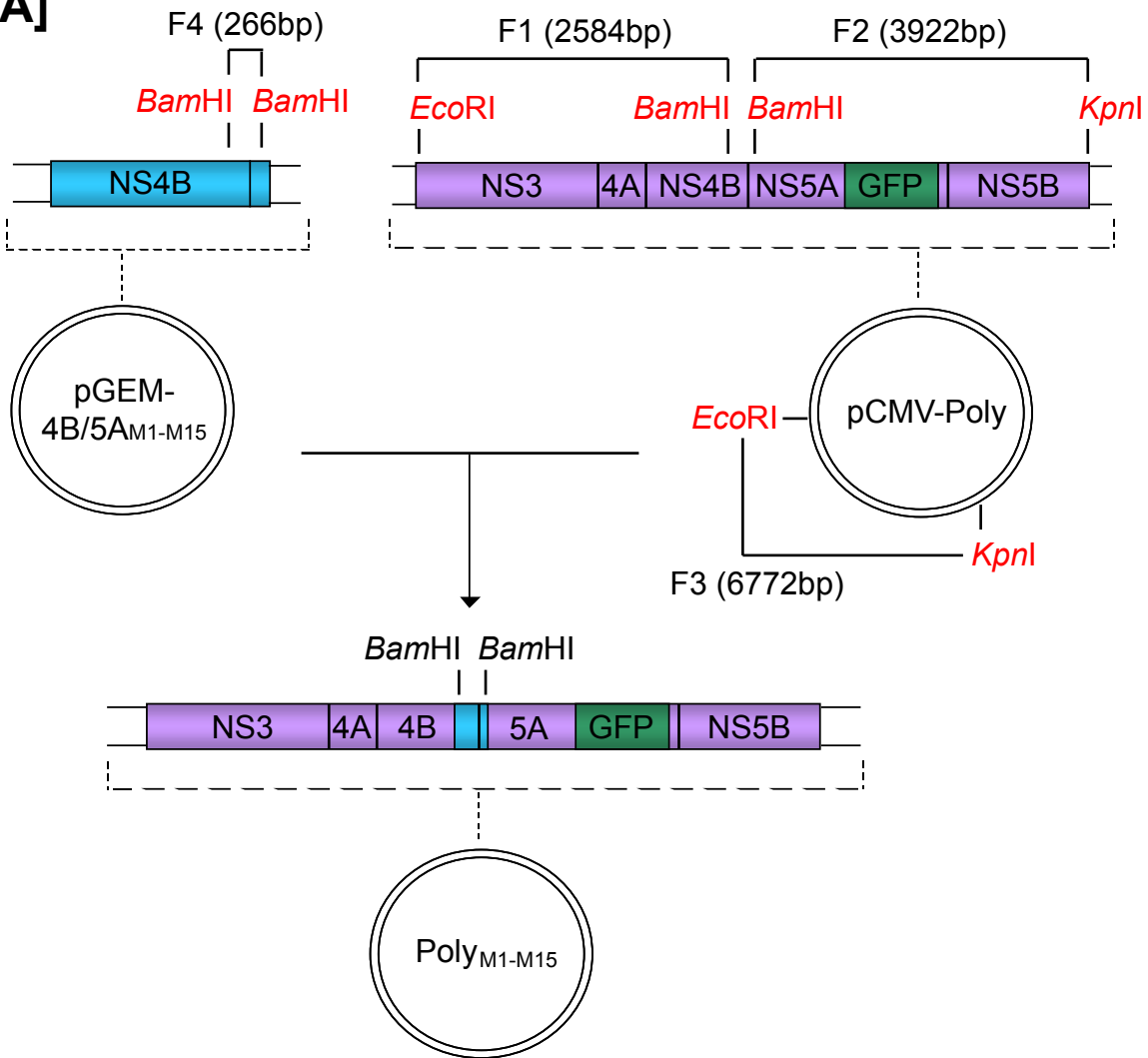
[A]**[B]**

Figure 4.3 Construction of NS4B C-terminal mutants by site-directed mutagenesis

[A] A schematic representation of the NS3-NS5B coding region of luc-JFH1_{GFP} is shown (top) and the position of the amplified fragment is indicated. The primers used to create 4B/5A are shown, with introduced non-viral sequences depicted in red. Restriction sites used for cloning purposes are underlined. The size of 4B/5A (847bp) is inclusive of introduced restriction sites. Nucleotide numbers refer to the JFH1_{Poly} sequence, beginning at the NS3 coding region. 4B/5A was introduced into the pGEM-T-Easy cloning vector to create pGEM-4B/5A. **[B]** pGEM-4B/5A was used for site-directed mutagenesis (indicated by SDM) of the C-terminal region of NS4B between the *Bam*HI sites present in NS4B and NS5A. All 15 mutants were individually introduced in this manner, to generate pGEM-4B/5A_{M1-M15}.

[A]



[B]

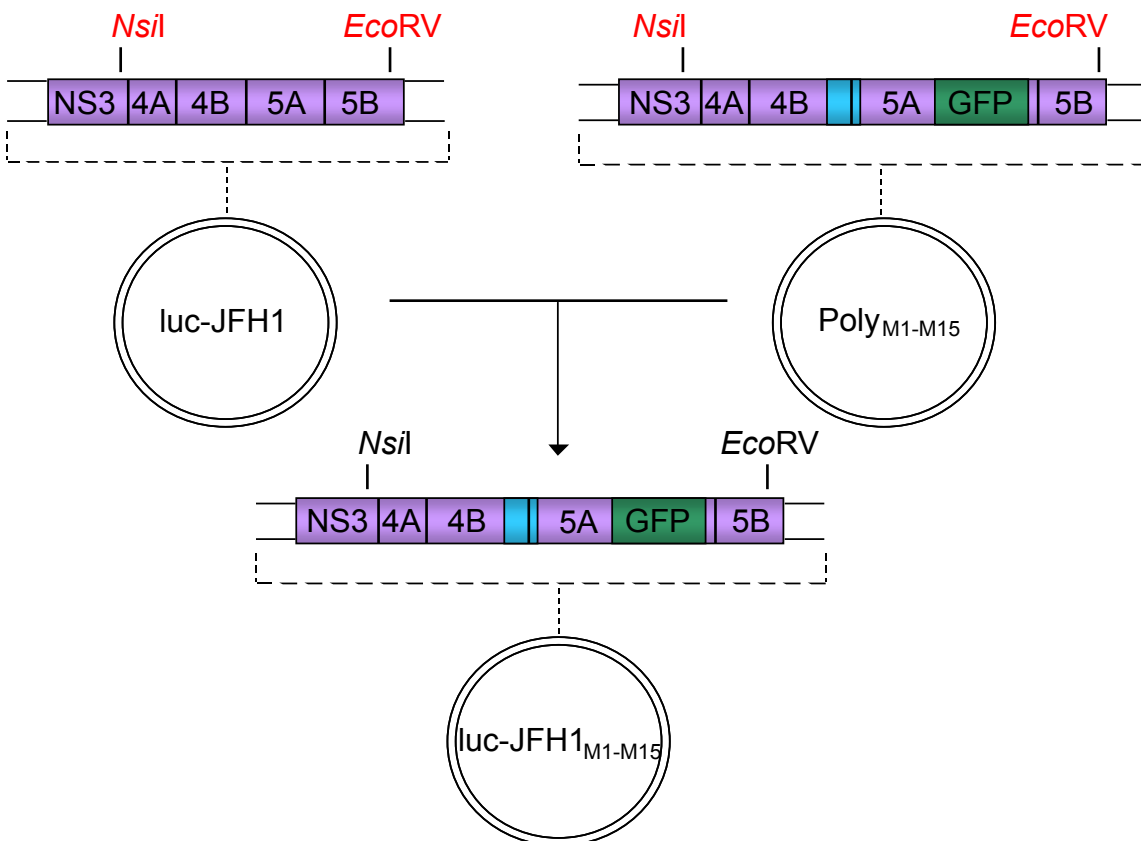


Figure 4.4 Construction of luc-GFP_{M1-M15} and Poly_{M1-M15} NS4B mutants

[A] The NS4B/NS5A fragment harbouring mutations within the C-terminus of NS4B was excised from pGEM-4A/5A_{M1-M15} using *Bam*HI (F4). This fragment could not be directly introduced into luc-JFH1_{GFP} or JFH1_{Poly} due to the presence of a third *Bam*HI site within NS5B. Therefore, JFH1_{Poly} was digested to yield three fragments. F1 was created by digestion with *Eco*RI (marking the start of NS3) and the first *Bam*HI site (in NS4B). F2 was created by digestion with the second *Bam*HI site (in NS5A) and *Kpn*I (marking the end of NS5B). F3 contained plasmid sequence and was created by digestion with *Kpn*I and *Eco*RI. F1 - F4 were then ligated in a four-fragment ligation, to yield Poly_{M1-M15}. All constructs were screened for correct orientation of the *Bam*HI fragment. **[B]** To create luc-GFP_{M1-M15}, the region between *Nsi*I and *Eco*RV was excised from Poly_{M1-M15} and inserted between the corresponding sites in luc-JFH1_{GFP}.

All targeted residues were substituted with Ala, as this amino acid was predicted to have minimal influence on the overall structure of NS4B. Mutations were individually introduced into a 266bp fragment of NS4B by site-directed mutagenesis, before introduction into the luc-JFH1_{GFP} replicon (using the cloning strategy depicted in Figures 4.3 and 4.4). This strategy created mutants luc-M1_{GFP} - luc-M15_{GFP} (Figure 4.2). A list of the primers used to create M1-M15 can be found in Appendix 1.

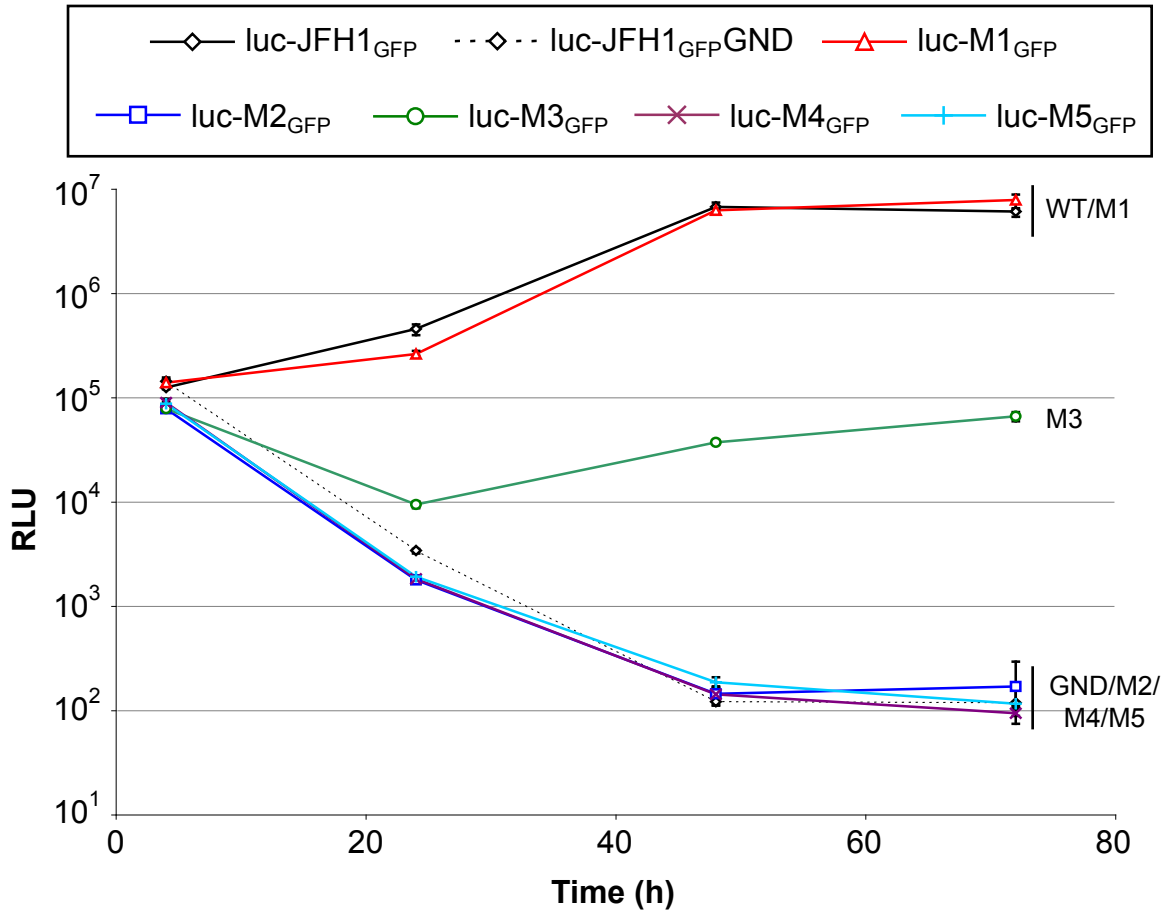
4.4 Characterisation of HCV NS4B Mutants

4.4.1 The C-terminus of NS4B is Involved in HCV RNA Replication

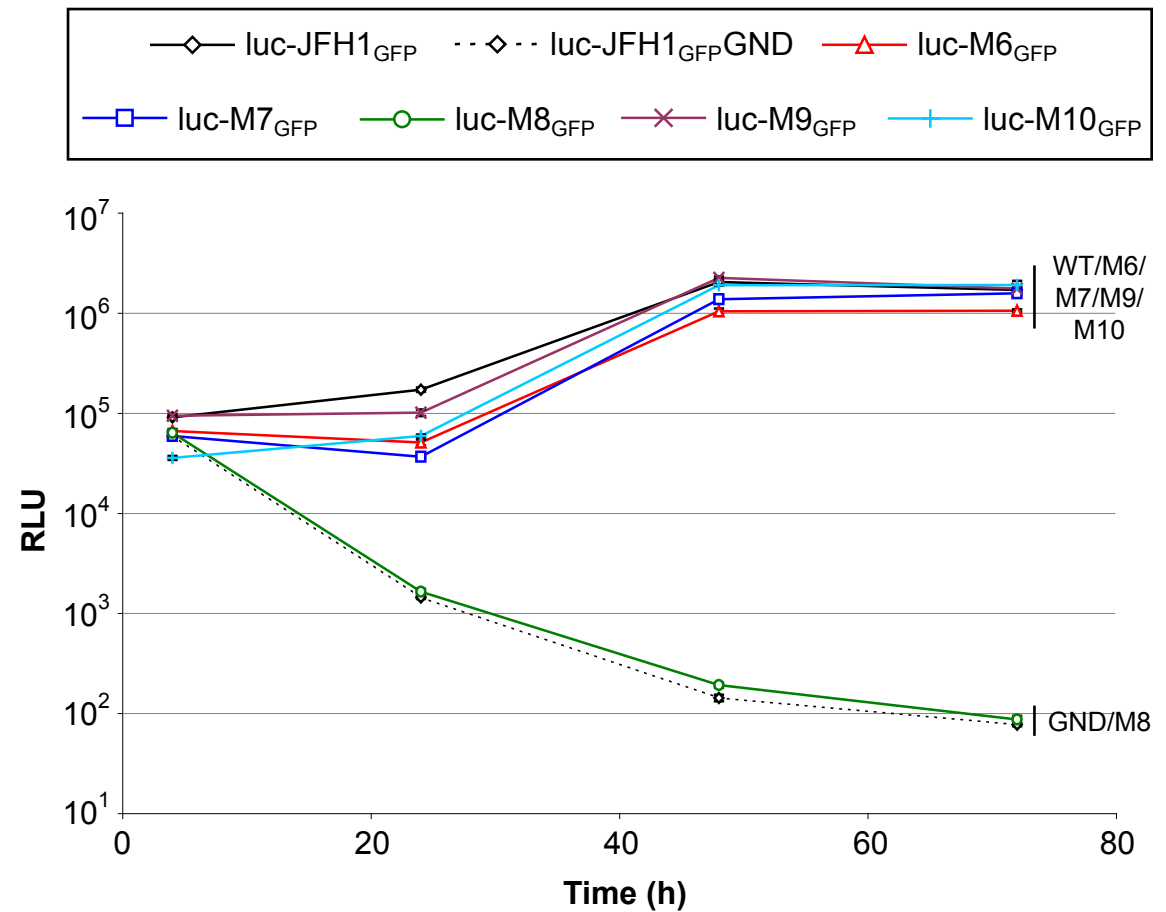
To determine whether any of the 15 mutations within the NS4B C-terminus had an impact on replication, RNA transcribed from luc-M1_{GFP}-luc-M15_{GFP} was electroporated into Huh-7 cells and luciferase activity was measured over a 72-hour period (Figure 4.5, A-C). RNAs encoding luc-JFH1_{GFP} and luc-JFH1_{GFP}GND were also electroporated into cells as positive and negative controls respectively.

In agreement with earlier results (see Section 3.2.2.1), luciferase values indicated that replication of luc-JFH1_{GFP} was impaired within the first 24 hours before increasing over the remaining time points, whereas luc-JFH1_{GFP}GND was incapable of replicating, as judged by determining enzyme activity over the time course (Figure 4.5, A-C). When the 15 mutants were tested in this assay, eight mutants (M1, M6, M7, M9, M10, M12, M14 and M15) gave patterns of luciferase activity comparable to that for luc-JFH1_{GFP}, indicating they retained the capacity to replicate (Figure 4.5, A-C). An attenuated replication phenotype was observed for luc-M3_{GFP} and luc-M11_{GFP} and luciferase levels expressed from these mutants were 48-fold and 63-fold lower respectively compared to the values obtained for luc-JFH1_{GFP} at 24 hours. Although luciferase levels for both mutants increased after this initial decline, values remained considerably lower than those observed with luc-JFH1_{GFP} by 72 hours (Figure 4.5, A and C). Of the 15 mutants tested, luciferase values from five mutants (M2, M4, M5, M8 and M13) declined over the 72-hour period as rapidly as those seen with luc-JFH1_{GFP}GND, indicating that these SGRs did not replicate (Figure 4.5, A-C). Subsequent qRT-PCR analysis confirmed this pattern of replication for all 15 mutant SGRs (B. Flatley, personal communication).

[A]



[B]



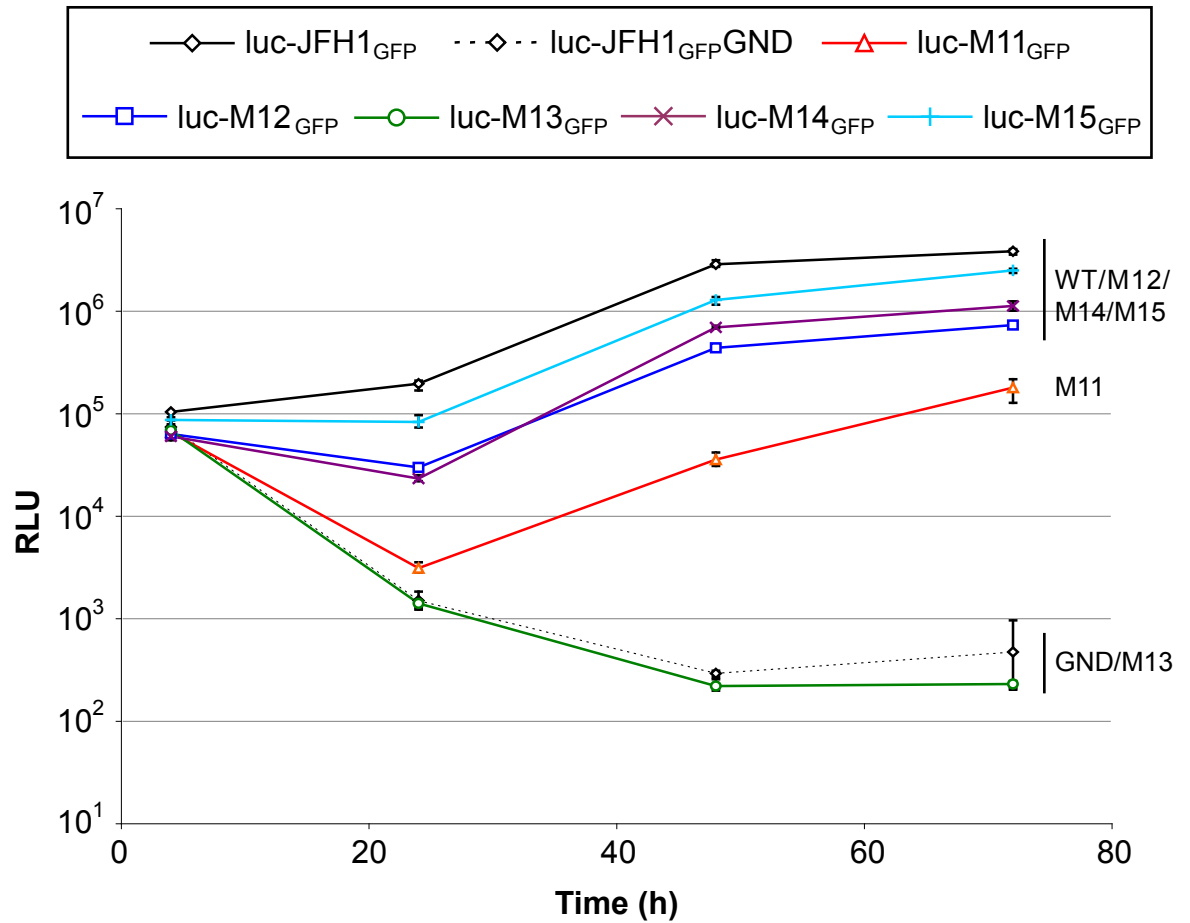
[C]

Figure 4.5 Replication competence of NS4B mutants

Huh-7 cells were electroporated with RNA encoding luc-JFH1_{GFP}, luc-JFH1_{GFP}GND and all 15 mutants, termed luc-M1_{GFP} - luc-M15_{GFP}. Cells were lysed at 4, 24, 48 and 72 hours post-electroporation and extracts were assayed for luciferase activity. Assays were performed in triplicate in three separate experiments: **[A]** luc-M1_{GFP} - luc-M5_{GFP} **[B]** luc-M6_{GFP} - luc-M10_{GFP} **[C]** luc-M11_{GFP} - luc-M15_{GFP}. Average values are shown for each experiment and error bars indicate the range of the values recorded at each time point.

These results revealed five amino acids (G196, N206, F211, E226 and W252) within the C-terminus of NS4B that are critical for HCV RNA replication and a further two residues (G200 and T241) that reduce replication when mutated to Ala. Only one of the residues, W252, has been reported previously as critical for HCV replication (Lindstrom et al., 2006). The remainder of this chapter explores the basis for the block in replication exhibited by the 5 non-replicating mutants.

4.4.2 Foci-Forming Abilities of Non-Replicating NS4B Mutants

When expressed alone in cells, NS4B possesses the intrinsic ability to induce the formation of foci on the ER membrane (Egger et al., 2002, Gosert et al., 2003, Gretton et al., 2005). Replicase components including NS proteins (Moradpour et al., 2004b, Mottola et al., 2002) and viral RNA (El-Hage & Luo, 2003, Gosert et al., 2003, Targett-Adams et al., 2008a) have been shown to localise to these structures, suggesting that foci represent viral RCs. Therefore, the impact of each non-replicating mutant was analysed for effects on foci formation. Each mutant NS4B coding region was amplified and introduced into the pGFP-C1 vector (employing the cloning strategy depicted in Figure 4.6, A and B), creating pNS4B_{M2}GFP, pNS4B_{M4}GFP, etc. Here, each NS4B coding region is tagged to the C-terminus of GFP, allowing NS4B distribution to be determined by analysing GFP fluorescence. This approach has been utilised previously (Egger et al., 2002, Gosert et al., 2003, Gretton et al., 2005). We also examined the impact of each non-replicating mutant on foci formation in the context of JFH1_{Poly}, where NS4B would be cleaved from an authentically processed polyprotein. Hence, all five mutations were introduced into JFH1_{Poly}, creating M2_{Poly}, M4_{Poly}, etc (using the cloning strategy in Figure 4.4, A). With these constructs, NS4B distribution could be determined utilising R1063, an antibody that recognises and binds the NS4B C-terminal sequence.

4.4.2.1 NS4B Proteins from Non-Replicating Mutants form Foci when Expressed in Isolation

Live cells expressing wt NS4B-GFP and each mutant (pNS4B_{M2}GFP, pNS4B_{M4}GFP, etc) were visualised 16-20 hours post-transfection (Figure 4.7, A). Wt NS4B-GFP was predominantly localised to punctate structures on the ER membrane, indicative of the foci reported previously (Egger et al., 2002, Gosert et

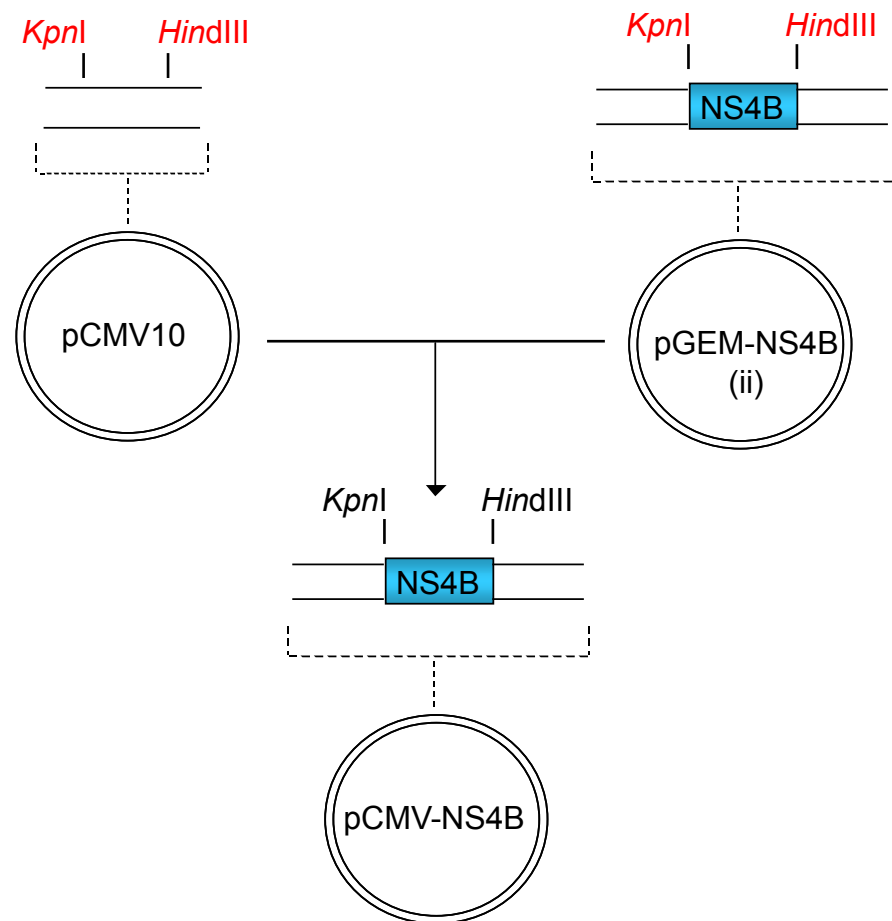
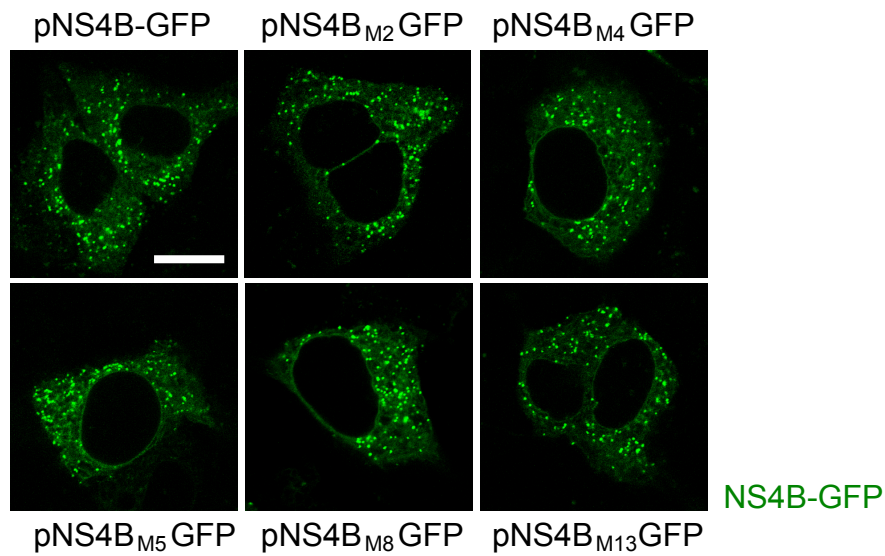
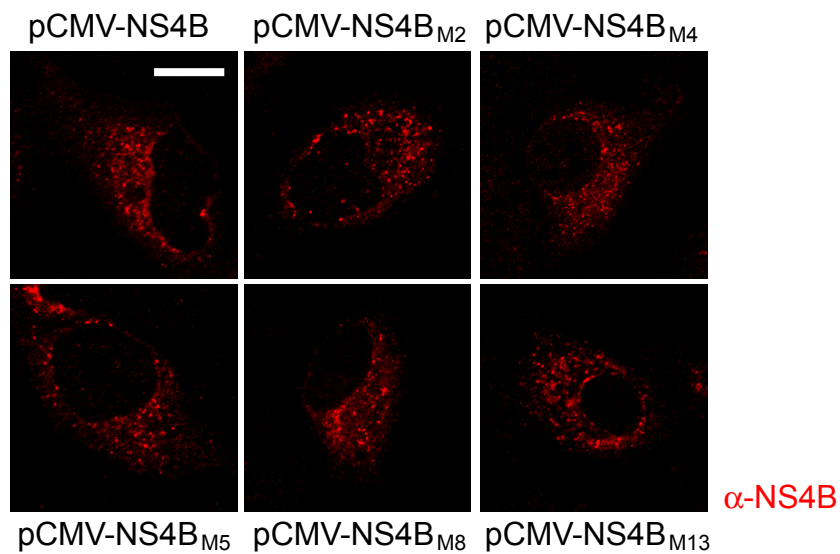
[C]

Figure 4.6 Construction of pNS4B-GFP and pCMV-NS4B

[A] A schematic representation of the NS3-NS5B coding region of luc-JFH1_{GFP} is shown (top). The positions and sequences of the primers used to amplify NS4B are shown, with introduced non-viral sequences depicted in red. Restriction sites used for cloning purposes and start/stop codons are underlined. The size of NS4B (798/801bp) is inclusive of introduced restriction sites and is dependent upon the forward primer used. Nucleotide numbers begin at the NS3 coding region. Primer NS4B_F (i) was used for the introduction of NS4B into the pEGFP-C1 vector and therefore has no start codon. Primer NS4B_F (ii) was used for the introduction of NS4B into the pCMV10 vector and therefore includes a start codon. Reverse primer NS4B_R was used for the amplification of both variants of the NS4B. Both NS4B fragments were subsequently introduced into the pGEM-T-Easy cloning vector, creating pGEM-NS4B (i) and pGEM-NS4B (ii). **[B]** The NS4B ORF was excised from pGEM-NS4B (i) using *Bgl*III and *Hind*III and introduced into pGFP-C1 between the corresponding sites. This resulted in a plasmid encoding a NS4B-GFP fusion protein, with the GFP tag at the N-terminal end of NS4B. **[C]** The NS4B ORF was excised from pGEM-NS4B (ii) using *Kpn*I and *Hind*III and introduced between the corresponding sites of pCMV10, to create pCMV-NS4B.

[A]**[B]****Figure 4.7 NS4B mutants expressed in isolation form foci**

Huh-7 cells were transfected with plasmids encoding **[A]** pNS4B-GFP and the five mutant derivatives, or **[B]** pCMV-NS4B and the five mutant derivatives. 16-20 hours after transfection, NS4B-GFP was visualised in live cells (in the case of **[A]**) or in fixed cells using NS4B antisera R1063 (in the case of **[B]**). Scale bars represent 10 μ M.

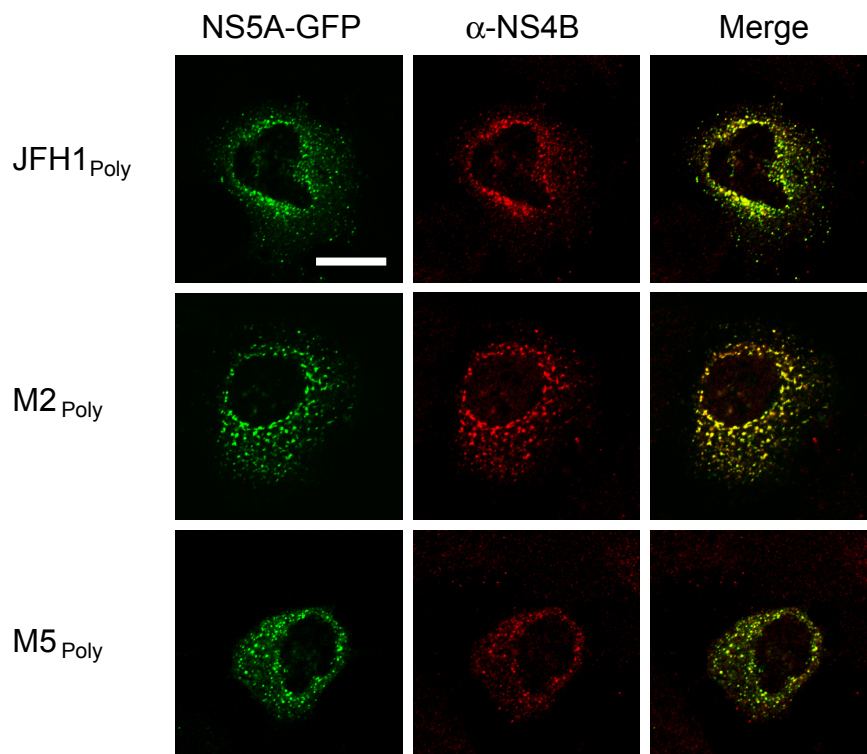
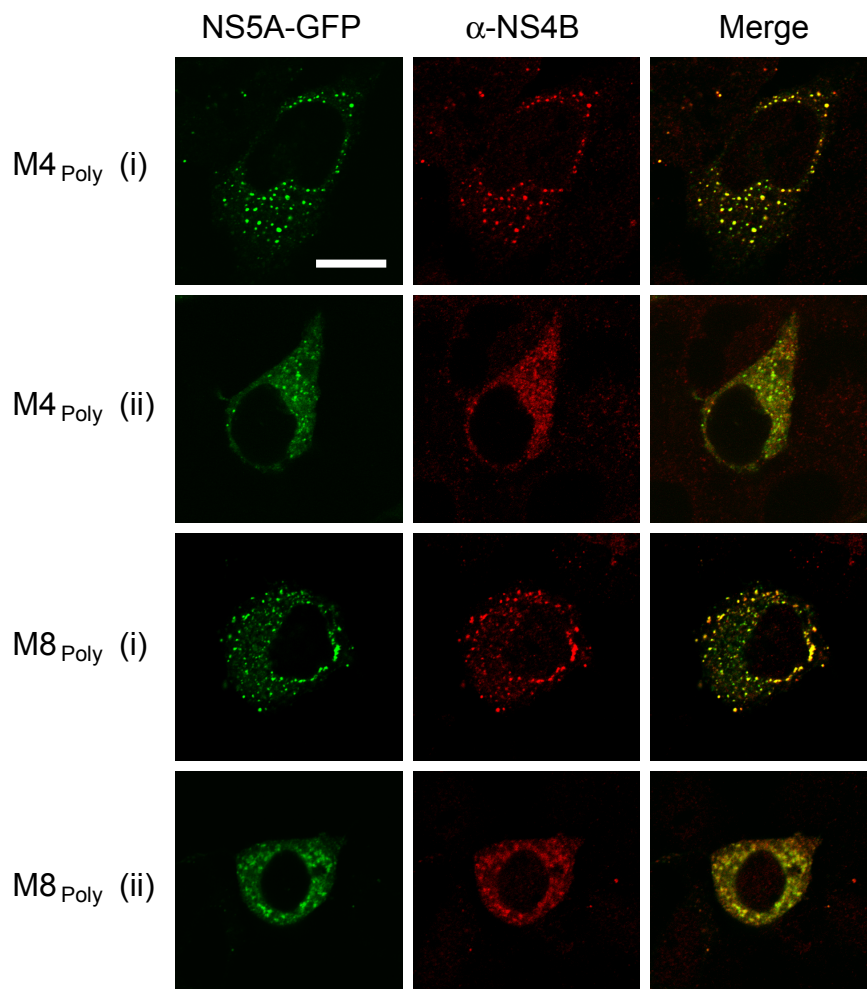
al., 2003, Gretton et al., 2005). In cells expressing NS4B-GFP from each of the non-replicating mutants, the distribution and localisation of the foci were indistinguishable from those seen with wt NS4B (Figure 4.7, A). These data suggested that the mutations did not affect the foci-forming abilities of the NS4B protein.

To exclude the possibility that the GFP tag had an effect on NS4B behaviour, the mutant NS4B coding regions were introduced into pCMV10 (employing the cloning strategy depicted in Figure 4.6, A and C). These constructs (pCMV-NS4B_{M2}, pCMV-NS4B_{M4}, etc) were transfected into cells and NS4B was visualised 16-20 hours later using NS4B antibody R1063 (Figure 4.7, B). In agreement with the results obtained using GFP-tagged proteins, no differences were observed between the foci induced by wt and mutant NS4B proteins.

4.4.2.2 NS4B Proteins from Non-Replicating Mutants Differ in their Ability to form Foci when Expressed from a Polyprotein

The data obtained above suggested that mutations within the C-terminus of NS4B did not affect foci formation. To determine whether the presence of other viral replicase components influenced this observation, JFH1_{Poly} and each mutant derivative (M2_{Poly}, M4_{Poly}, etc.) was transfected into cells and the localisation of NS4B was examined 16-20 hours later using R1063 antibody (Figure 4.8, A - C). Furthermore, the use of JFH1_{Poly} also enabled the localisation of NS5A-GFP to be determined.

In contrast to the results obtained from analysis of the five NS4B mutants in isolation, the mutants now differed in their abilities to form foci and could be divided into three distinct phenotypic categories. Firstly, M2_{Poly} and M5_{Poly} produced foci containing both NS4B and NS5A-GFP, and these foci were indistinguishable from those observed with JFH1_{Poly} (Figure 4.8, A). In the second category, M4_{Poly} and M8_{Poly} exhibited a dual phenotype whereby some cells contained foci to which both NS4B and NS5A-GFP co-localised, while other cells revealed little evidence of either protein being localised to foci (Figure 4.8, B). M13_{Poly} was the sole member of the third category in which both NS5A-GFP and NS4B were rarely detected in foci and the ER-like pattern of NS5A-GFP distribution was identical to that seen with JFH1_{Poly}Δ4B (Figure 4.8, C).

[A]**[B]**

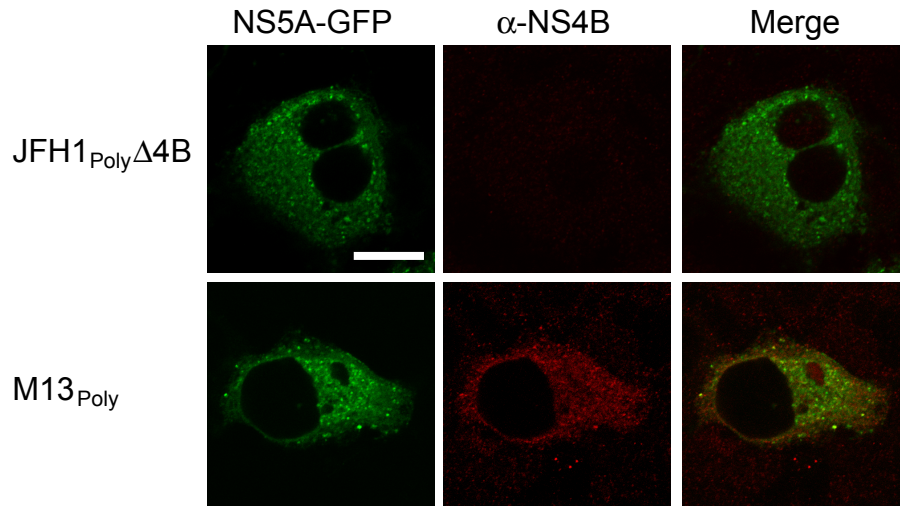
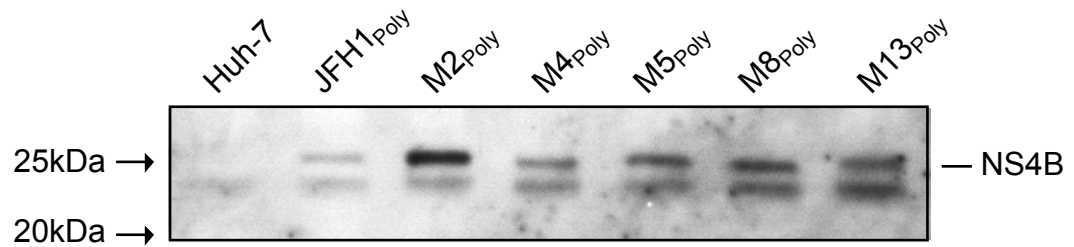
[C]**[D]**

Figure 4.8 The NS4B C-terminus contains determinants for foci formation

Huh-7 cells were transfected with plasmids encoding JFH1_{Poly}, JFH1_{Poly} Δ 4B and each JFH1_{Poly} NS4B mutant. 16-20 hours post-transfection, cells were fixed and NS4B was visualised using R1063, while NS5A-GFP was observed directly. Localisation patterns for both proteins were divided into three phenotypic categories: **[A]** proteins predominantly localised to foci, **[B]** proteins localise to foci in some cells (i) but display an ER-like distribution in others (ii), **[C]** both proteins display an ER-like distribution only. Scale bars represent 10 μ m. **[D]** Huh-7 cells transfected in parallel to those described in [A] - [C] were harvested for Western blot analysis at 20 hours post-transfection and the membrane was probed with R1063 antisera.

To confirm that introducing mutations into NS4B had not decreased the stability of the protein or influenced polyprotein processing, cells expressing each mutant were harvested approximately 20 hours post-transfection and subjected to Western blot analysis (Figure 4.8, D). In all cases NS4B was detected at the correct size of ~27kDa and revealed no evidence of degradation or altered cleavage.

4.4.2.3 The NS4B C-terminus Influences Localisation of NS5A to Foci and the Number of Foci in Cells

Studies on the five NS4B mutants revealed that three (M4, M8 and M13) were compromised in their ability to form foci at the ER membrane. In order to acquire a quantitative assessment of NS5A localisation with these mutants, at least 250 cells expressing JFH1_{Poly}, JFH1_{Poly}Δ4B and each mutant JFH1_{Poly} construct were analysed and the localisation of NS5A-GFP was scored into one of two categories: (i) NS5A-GFP predominantly localised to the ER, or (ii) NS5A-GFP predominantly localised to foci (Figure 4.9, A). This approach revealed that NS5A-GFP expressed from JFH1_{Poly} was localised to foci in a high proportion of the cells examined (94%), whereas the majority of cells expressing JFH1_{Poly}Δ4B gave an ER-like distribution of NS5A-GFP (98%, Figure 4.9, A). Examination of cells expressing M2_{Poly} and M5_{Poly} revealed that NS5A-GFP was localised to foci in 94% and 92% of cells respectively, confirming that these mutant NS4B proteins produced foci indistinguishable from those of wt NS4B. M4_{Poly} and M8_{Poly} exhibited a dual phenotype of NS5A-GFP distribution, with 48% and 50% of the fusion protein respectively being localised to foci, while the remaining 52% and 50% of cells displayed an ER-like distribution of the protein (Figure 4.9, A). Finally, NS5A-GFP expressed from M13_{Poly} gave a distribution consistent with an ER-like pattern in 85% of cells examined.

To confirm further the impact of NS4B mutations on foci formation, cells expressing each construct were examined using software that allowed the number of NS5A-GFP foci per cell to be counted (Figure 4.9, B). Approximately ten cells were counted for each construct and the average number of foci per cell was calculated. This analysis revealed that constructs capable of producing foci (JFH1_{Poly}, M2_{Poly} and M5_{Poly}) gave similar numbers of foci (116-128 foci per cell). Mutants that impaired foci formation (M4_{Poly} and M8_{Poly}) had a lower number of foci per cell (82 and 90 foci respectively). (Figure 4.9, B). M13_{Poly} and JFH1_{Poly}Δ4B

[A]

 Predominantly ER
 Predominantly foci

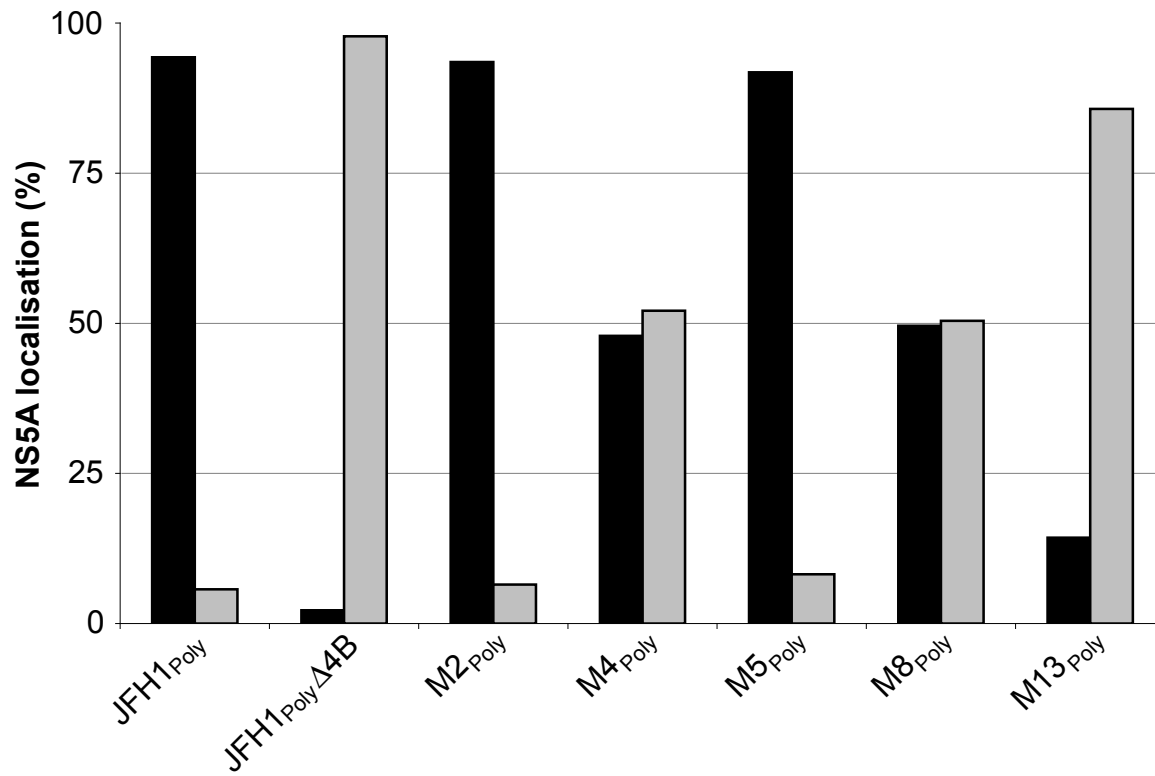
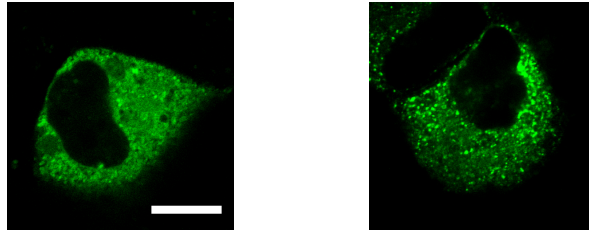
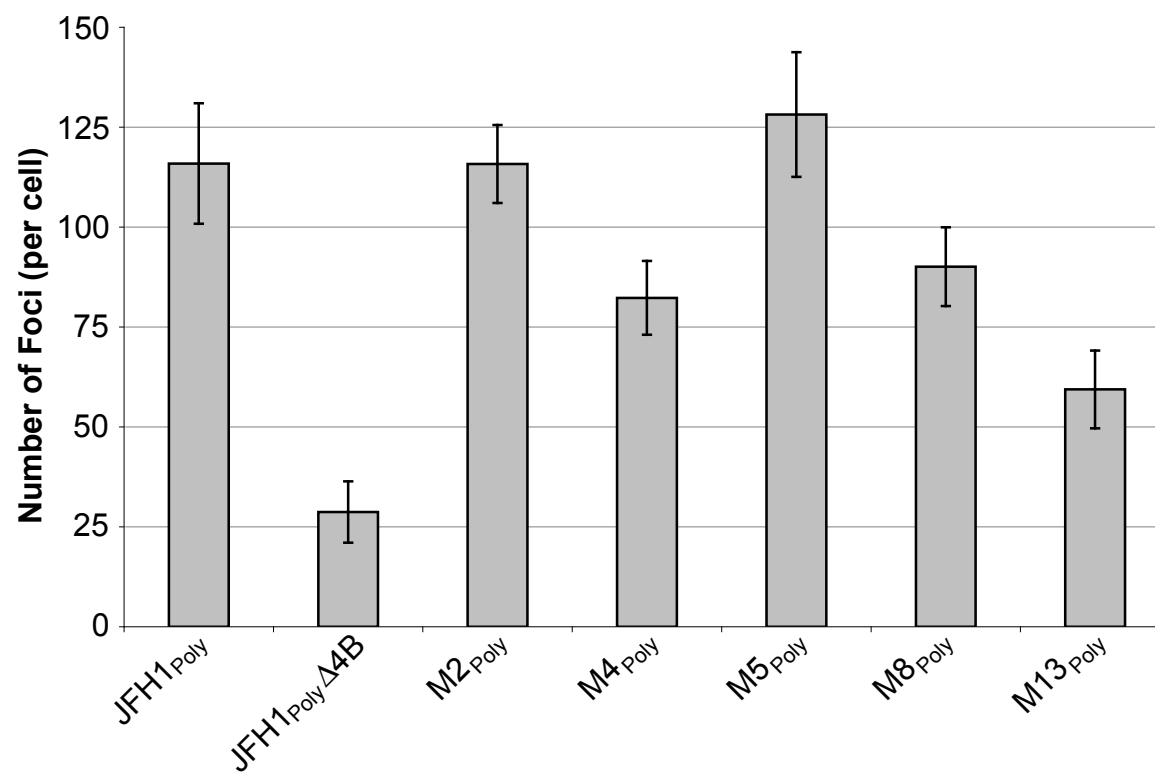
**[B]**

Figure 4.9 The NS4B C-terminus influences NS5A-GFP localisation to foci and the number of foci in cells

Huh-7 cells were transfected with JFH1_{Poly}, JFH1_{Poly}Δ4B and each JFH1_{Poly} NS4B mutant. 16-20 hours post-transfection, cells were fixed and NS5A-GFP was visualised directly. **[A]** At least 250 cells were observed for each construct and scored into a category dependent on NS5A-GFP localisation: (i) NS5A-GFP localised predominantly to the ER (top, left panel) (ii) NS5A-GFP localised predominantly to foci (top, right panel). Cells in each category are expressed as a percentage of the total number counted for each construct. **[B]** The number of foci were counted in approximately 10 cells per construct and the averages are shown. Error bars represent standard errors.

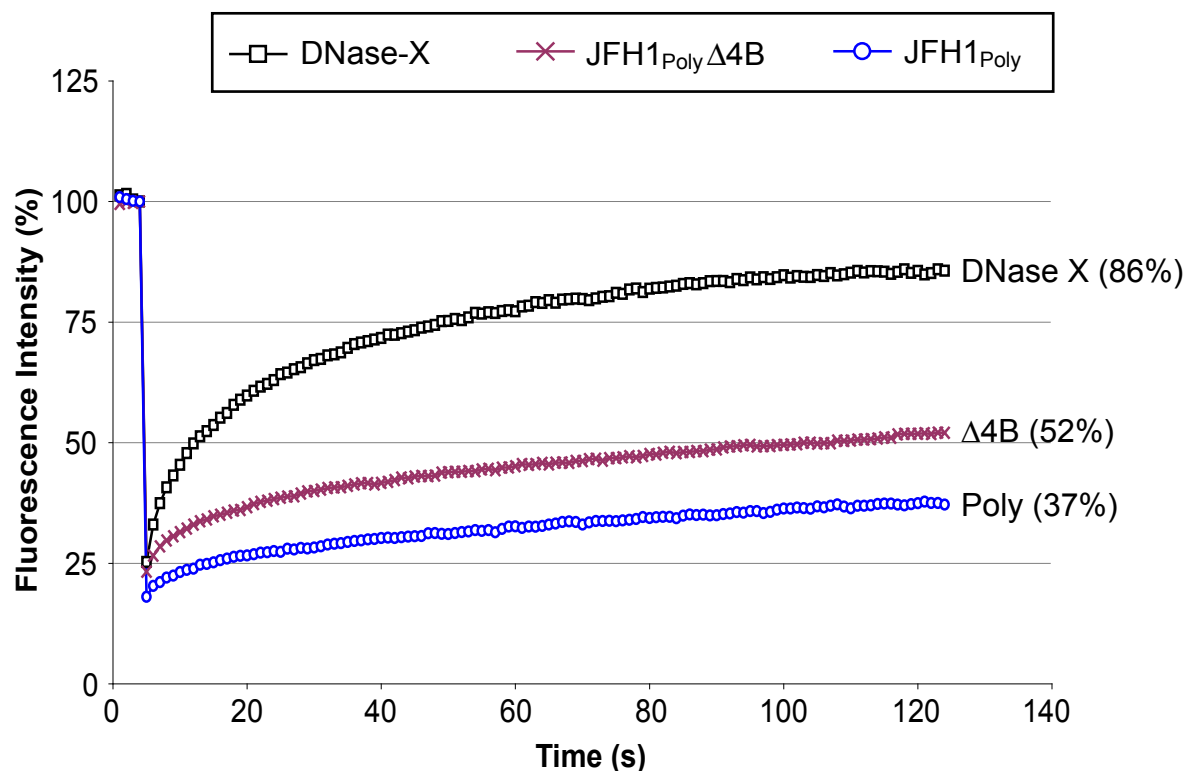
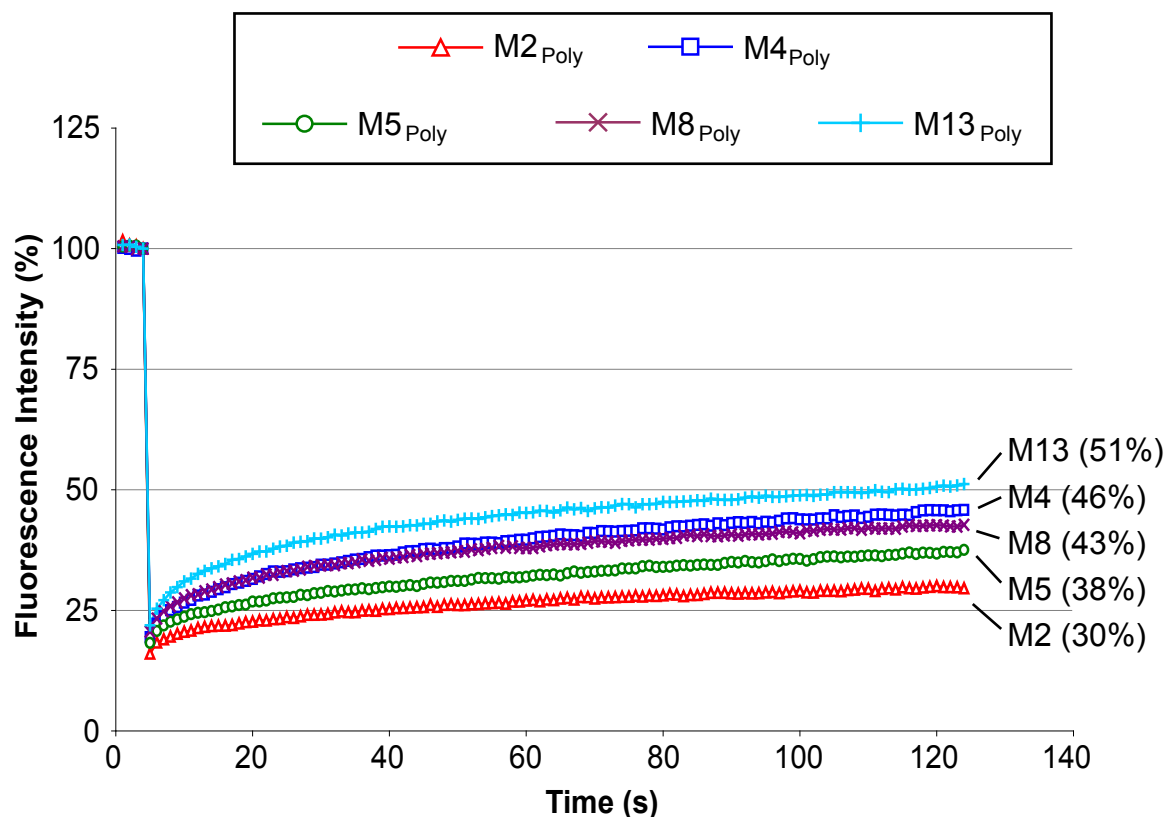
[A]**[B]**

Figure 4.10 The NS4B C-terminus influences NS5A-GFP mobility

Huh-7 cells transfected with **[A]** GFP-DNase-X, JFH1_{Poly} and JFH1_{Poly}Δ4B or **[B]** each NS4B mutant were analysed by FRAP at 16-20 hours post-transfection. Selected areas of 38μm² were bleached using 100% laser power and recovery within these regions was monitored for two minutes at 2% laser power. Values are expressed as a percentage of the pre-bleach value. Error bars have been removed for clarity.

only produced 29 and 59 foci per cell respectively in this assay, confirming the impaired ability of these mutants to generate foci.

Taken together, these results indicated that amino acids N206 (M4), E226 (M8) and particularly W251 (M13) were important for the ability of NS4B to generate foci and for the incorporation of NS5A at these sites. In contrast, residues G196 (M2) and F211 (M5) were apparently unimportant for these functions.

4.4.3 The NS4B-C-terminus Influences NS5A Mobility

In the previous chapter, it was found that the NS5A-GFP fusion protein was more mobile on the ER membrane compared to when it was localised at foci (see Section 3.3). Furthermore, the presence of NS4B was responsible for NS5A-GFP distributing to foci, lowering mobility of the fusion protein in the process (see Sections 3.4.2 and 3.4.3). Given that NS5A-GFP mobility was measurably different in the presence and absence of NS4B and since three of the five non-replicating NS4B mutants were able to reduce the amount of NS5A-GFP located at foci, NS5A-GFP mobility was examined when expressed from these mutants. Cells harbouring JFH1_{Poly}, JFH1_{Poly}Δ4B and each JFH1_{Poly} NS4B mutant were examined by FRAP analysis at 16-20 hours post-transfection (Figure 4.10, A and B). FRAP was also conducted on cells transfected with GFP-DNase-X, which served as a positive control for mobility. NS5A-GFP fluorescence was bleached to 18% - 23% in all cases, compared with pre-bleach values. In agreement with earlier results (see Section 3.4.3), NS5A-GFP fluorescence recovery over a two-minute period was greater in cells expressing JFH1_{Poly}Δ4B (52%) compared to those harbouring JFH1_{Poly} (37%), which expressed the entire NS3-NS5B coding region (Figure 4.10, A). Upon examination of cells expressing the NS4B mutants, it was evident that mutants M2_{Poly} and M5_{Poly}, which did not affect foci formation, also had little impact on NS5A-GFP mobility and the fusion protein expressed from these mutants recovered to 30% and 38% respectively (Figure 4.10, B). These rates of recovery were comparable to that seen with JFH1_{Poly}. However, mutants that caused a loss of foci formation in cells (M4_{Poly} and M8_{Poly}) exhibited increased NS5A-GFP mobility and FRAP analysis revealed fluorescence recoveries of 46% and 43% respectively when expressed from these mutants (Figure 4.10, B). Most strikingly, NS5A-GFP expressed from M13_{Poly} recovered to 51%, comparable to the recovery displayed by JFH1_{Poly}Δ4B (Figure 4.10, A and B).

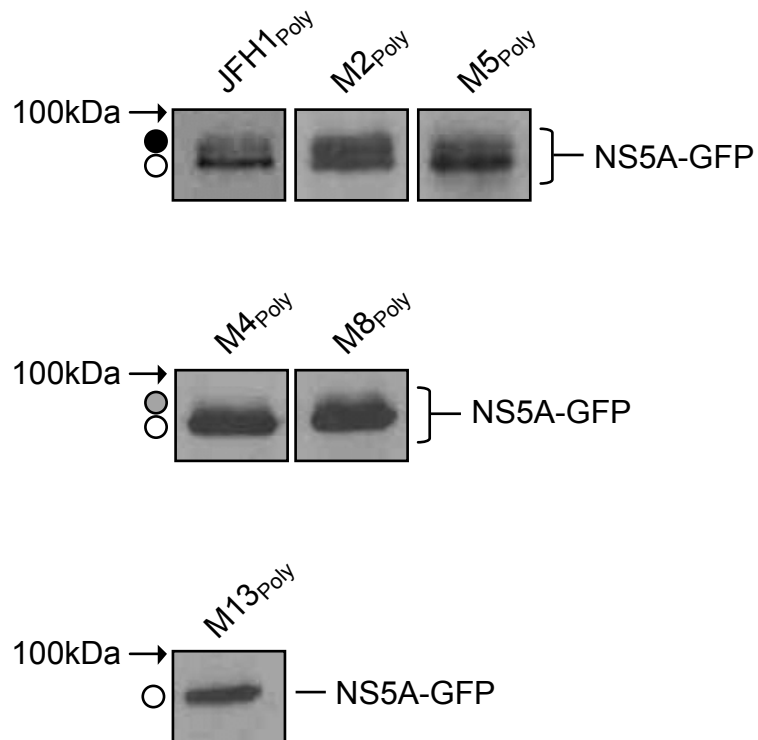


Figure 4.11 The NS4B C-terminus Influences NS5A-GFP phosphorylation

Lysates from cells transfected with JFH1_{Poly} and each NS4B mutant were analysed by Western blot at 16-20 hours post-transfection. The membrane was probed with NS5A antisera. The hyper- (closed circles) and hypo- (open circles) phosphorylated species of NS5A are indicated. Wild-type (black circle) and diminished (grey circle) levels of hyperphosphorylated NS5A are also shown. The gels are different exposures from the same Western blot.

The FRAP analysis results revealed that NS5A-GFP fluorescence recovery correlates with the ability of each mutant to form foci; foci-forming mutants (M2_{Poly} and M5_{Poly}) displayed a low level of fluorescence recovery, while mutants incapable of forming foci (M13_{Poly}) exhibited recovery values comparable to when NS4B was absent from the polyprotein.

4.4.4 The NS4B C-terminus Influences Hyperphosphorylation of NS5A

NS5A exists as two phosphorylated species of 56kDa (hypophosphorylated NS5A) and 58kDa (hyperphosphorylated NS5A, Tanji et al., 1995), and previous work has shown that the presence of NS4B is essential for NS5A hyperphosphorylation (Koch & Bartenschlager, 1999, Neddermann et al., 1999). This requirement for NS4B was confirmed by comparing NS5A-GFP expressed from JFH1_{Poly} and JFH1_{Poly}Δ4B, where hyperphosphorylation was not detected in the absence of NS4B (see Section 3.4.3). In light of this observation, NS5A-GFP phosphorylation was examined in cells expressing each non-replicating NS4B mutant (Figure 4.11). Western blot analysis of NS5A-GFP expressed from M2_{Poly} and M5_{Poly} confirmed that the fusion protein was detected as two bands, presumed to be the hypo- and hyperphosphorylated species (Figure 4.11). The Western blot profile of these two mutants was indistinguishable from that seen with JFH1_{Poly}. However, the abundance of the hyperphosphorylated form of NS5A-GFP was decreased for M4_{Poly} and M8_{Poly}, where a seemingly greater amount of the hypophosphorylated form was detected. Furthermore, the hyperphosphorylated species of NS5A-GFP was not detected in cells harbouring M13_{Poly} (Figure 4.11).

Taken together with the mobility data and examination of foci formation, these results establish a correlation between NS5A localisation, mobility and phosphorylation, and also reveal that amino acids within the C-terminus of NS4B can influence these characteristics. The results from this chapter are summarised in Figure 4.12.

4.5 Discussion

The hydrophobic nature of NS4B has restricted structural studies on the protein and consequently, predictive analysis has been an important tool for identifying structured regions within NS4B. Such analyses have predicted several important

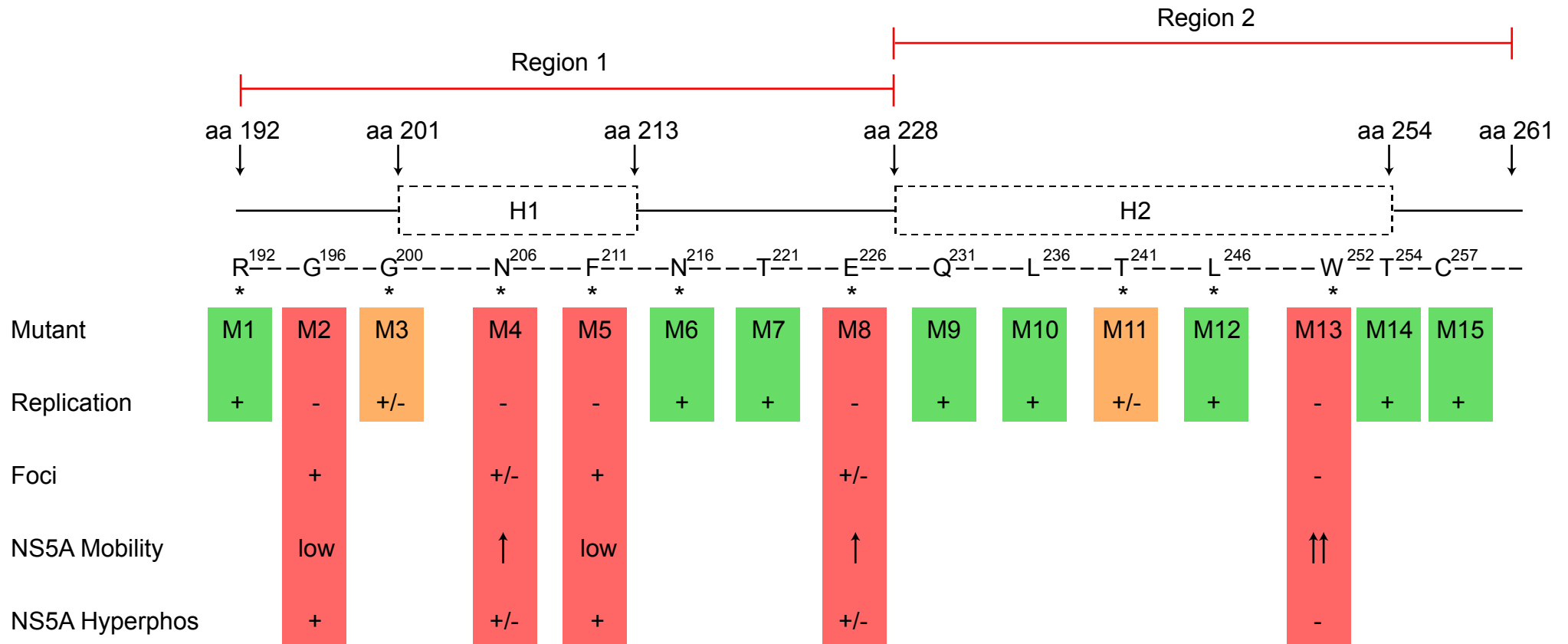


Figure 4.12 Summary of the characteristics of the mutants at the C-terminus of NS4B

A schematic representation of the NS4B C-terminus is shown. Region 1 (highly conserved), Region 2 (less conserved compared to Region 1), the positions of both predicted helices (H1 and H2) and the locations of the 15 mutations are depicted. Invariant amino acids are denoted by an asterisk and are numbered with respect to the N-terminal end of NS4B. Mutations that did not effect (green), attenuated (orange) or abolished (red) replication are highlighted. Results with the five non-replicating NS4B mutants are also summarised.

features, including the four TMDs in the central portion of the protein (Hugle et al., 2001, Lundin et al., 2003). However, only one study has examined the presence of putative structured regions within the C-terminal region of NS4B (Welsch et al., 2007). The results in this chapter represent an attempt to gain a greater insight into the C-terminal region of NS4B by utilising conservation studies, protein structure prediction and mutagenic analyses.

An alignment of 141 HCV sequences revealed that the C-terminus of NS4B could be broadly divided into two segments; Region 1 (36 amino acids, 58% of which were invariant) and Region 2 (34 amino acids, 29% of which were invariant, (Figure 4.1, A). These different levels of conservation suggest that the first half of the NS4B C-terminus is under a high level of selective pressure, possibly indicating an important function for this region in the HCV life cycle. Indeed, four of the five mutations that abolished HCV replication targeted amino acids within Region 1, three of which were invariant (Figures 4.12). It is therefore possible that Region 1 makes a greater contribution to viral RNA replication compared to Region 2. By contrast, only one mutation within Region 2 (W251A, M13) abolished replication (Figure 4.5, C). The sequence alignment data revealed that this Trp residue was invariant across HCV genotypes and a previous report has shown it to be critical for replication of genotype 1b HCV replicons (Lindstrom et al., 2006). Therefore this residue is likely to be essential for genome synthesis in all strains of HCV. In the same study, N254 was identified as important for the replication and mutation of this Asn to Asp resulted in decreased RNA replication (Lindstrom et al., 2006). The amino acid at position 254 is not fully conserved and is replaced by Thr in JFH1 (Figure 4.1, A). Interestingly, mutation of this residue to Ala (M14) in our mutagenic study had no effect on HCV RNA replication (Figure 4.5, C). Analysis of the HCV sequences used for alignment revealed that other amino acids occurred naturally at this position and it is therefore likely that Thr, Ala and Asn are all compatible with functional NS4B in viral replication. In contrast, Asp is an acidic amino acid that may alter the conformation of the C-terminus and thereby block the function of NS4B.

Protein structure prediction analysis of the JFH1 NS4B C-terminus predicted two α -helical elements (termed H1 and H2, Figure 4.1, B) and the positions of these helices correlated with those predicted previously (Welsch et al., 2007). H1 was predicted to reside within the highly conserved Region 1, while H2 encompassed the majority of the more variable Region 2. Data from the alignment of HCV sequences revealed that 69% of the residues constituting H1 were invariant,

compared to only 30% of those within H2. Interestingly, both mutations introduced into H1 (N206A, M4 and F211A, M5) abolished replication, whereas only one of the five mutations introduced into H2 (W251A, M13) had this effect (Figure 4.5, A and C). These results imply that H1 may be critical as a structural element for NS4B function, whereas H2 is more genetically flexible. Confirmation of the existence of these helices and any additional insight into their function warrants further study.

NS4B possesses the intrinsic ability to re-arrange cellular ER membranes into structures that permit assembly of complexes capable of replicating viral RNA (Egger et al., 2002, Gosert et al., 2003, Mottola et al., 2002). These altered membranes are thought to be analogous to foci, small punctate structures on the ER membrane that contain replicase components including NS proteins (Moradpour et al., 2004b, Mottola et al., 2002), viral RNA (El-Hage & Luo, 2003, Gosert et al., 2003, Targett-Adams et al., 2008a) and several documented host cell factors critical to replication. Therefore, the ability of each non-replicating NS4B mutant to induce foci was investigated. Expressing NS4B proteins in isolation from each mutant resulted in the production of foci that were indistinguishable from those produced by a wt protein (Figure 4.7, A and B). However, expressing mutant NS4B sequences in the context of a polyprotein highlighted differences in the foci-forming characteristics of the mutants (Figure 4.8, A-C). The reason for this discrepancy in results is unclear. One possibility is that the presence of the other NS proteins may be required in order for NS4B to form interactions essential for authentic foci generation. Indeed, direct interactions between NS4B and NS3, NS4A and NS5A have been demonstrated in the past (Dimitrova et al., 2003, Gao et al., 2004) and it is thought that NS4B can form complexes with NS5B via its interaction with NS5A (Gao et al., 2004). Therefore, the 'foci' seen when expressing NS4B in the absence of the other NS proteins may not represent functional replicase units but rather aggregates of NS4B protein. The fact that the properties of NS4B seemingly differ depending on the context of its expression means that examining HCV proteins expressed as part of a polyprotein is likely to increase the relevance of the results obtained, especially since NS4B would be expressed in this manner during HCV infection.

C-terminal residues N206 (M4), E226 (M8) and particularly W251 (M13), were integral to the foci-forming ability of NS4B (Figure 4.8, B and C). Furthermore, loss of these foci resulted in changes to NS5A-GFP mobility and phosphorylation (Figures 4.10, B and 4.11). Results presented previously revealed that NS5A is

more mobile on the ER membrane compared to when localised to foci (see Section 3.3), suggesting that NS5A possesses a more rigid association with foci. This hypothesis is strengthened by the fact that NS4B mutations resulting in a loss of foci also increased the mobility of NS5A-GFP. NS5A is phosphorylated on multiple Ser and Thr residues and exists as hypo- and hyperphosphorylated forms (Tanji et al., 1995). Although the functional importance of both forms is unclear, reduction of the hyperphosphorylated form of NS5A increases RNA replication in genotype 1 SGRs (Appel et al., 2005b, Neddermann et al., 2004), yet decreases virion assembly and release of HCVcc (Tellinghuisen et al., 2008a). Hence, it has been proposed that the phosphorylation status of NS5A may act as a switch between genome synthesis and the latter stages of the virus life cycle (Evans et al., 2004b). Hyperphosphorylation of NS5A requires expression of the protein from a RNA molecule encoding an intact NS3-NS5A polyprotein (Koch & Bartenschlager, 1999, Neddermann et al., 1999). In agreement with these reports, removal of NS4B from a polyprotein resulted in loss of the hyperphosphorylation of NS5A-GFP (see Section 3.4.3). Furthermore, there was a correlation between the ability of NS4B to form foci and the hyperphosphorylation of NS5A, where prevention of foci formation (W251A, M13) resulted in a loss of NS5A-GFP hyperphosphorylation (Figure 4.11). These results suggest that hyperphosphorylation of NS5A can only occur when foci are correctly formed and that replication at these sites is not required for this process. It is possible that RCs formed by functionally intact NS4B results in the increased contact of NS5A with cellular kinases such as CKII- α (Quintavalle et al., 2006 and 2007). Hence, NS5A hyperphosphorylation may only occur within intact RCs. Alternatively, NS5A may be hyperphosphorylated in the cytoplasm but protection from cellular phosphatases may only be offered when the protein is localised to intact RCs. Such a scenario could be possible, since the contents of RCs have previously been shown to be protected from both protein and RNA degradation (Aizaki et al., 2004, El-Hage & Luo, 2003, Yang et al., 2004).

Aside from providing an environment for replication to occur, any additional contributions of NS4B to viral replication are poorly understood. Importantly, the mutational analysis presented here identified two mutations, G196A (M2) and F211A (M5), that abolished replication yet had no effect on the ability of NS4B to form RCs on the ER membrane (Figure 4.8, A). Furthermore, the localisation, mobility and phosphorylation of NS5A were all unaffected by mutation of these two residues (Figures 4.10 and 4.11). This result possibly indicates that NS4B

contributes a further undefined function to the synthesis of viral genomes, beyond the induction of membranous changes. Alternatively, it cannot be ruled out that the foci induced by these mutant proteins could be altered in a manner too subtle to be detected by the microscopy studies used here.

5 Trans-Complementation Studies Utilising NS4B and NS5A Mutant SGRs

5.1 Introduction

In order to gain insight into the functional organisation of HCV RCs and their components, *trans*-complementation assays utilising defective and helper SGRs have been established (Appel et al., 2005a, Tong & Malcolm, 2006). These assays have shown that NS5A can be complemented *in trans*, whereas replication cannot be restored to SGRs containing deleterious mutations within the NS3, NS4B or NS5B coding regions (Appel et al., 2005a, Evans et al., 2004a, Tong & Malcolm, 2006). These data imply that the majority of the NS proteins must be derived from the same polyprotein in order to function, or that they are incapable of exchange between RCs. Such a scenario is plausible, since NS3 (via NS4A), NS4B and NS5B are tightly anchored to the ER by hydrophobic domains, possibly restricting their mobility (Ivashkina et al., 2002, Lundin et al., 2003, Wolk et al., 2000). In contrast, NS5A associates with the ER post-translationally via an N-terminal amphipathic α -helix (Brass et al., 2002) and therefore may have a looser association with membranes that facilitates its transfer between sites of replication (Appel et al., 2005a).

Previous studies investigating *trans*-complementation of HCV proteins were performed using stable cell lines and genotype 1 SGRs harbouring CCAMs (Appel et al., 2005a, Evans et al., 2004a, Tong & Malcolm, 2006), which replicate poorly in comparison to SGRs derived from JFH1 (Kato et al., 2003, Targett-Adams & McLauchlan, 2005). Furthermore, a limited set of mutations were tested for each NS protein, particularly in the case of NS4B (Appel et al., 2005a, Tong & Malcolm, 2006). Thus, it was possible that *trans*-complementation of NS proteins other than NS5A may be detected using an expanded set of mutants in the context of a JFH1 SGR.

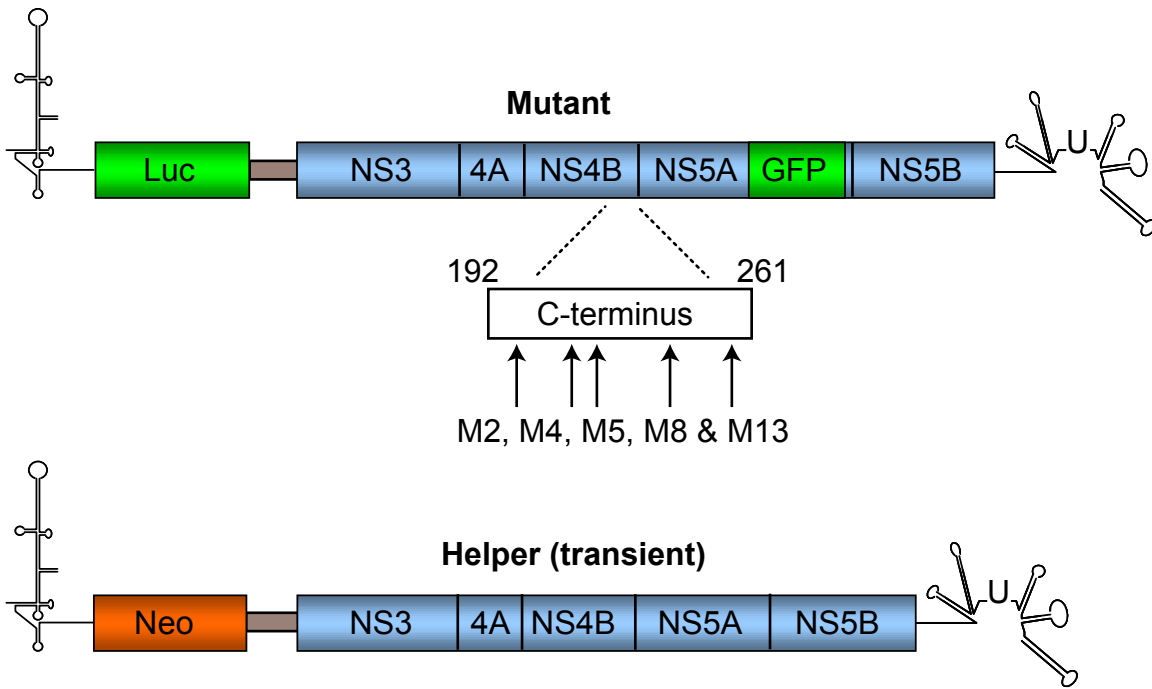
To test this hypothesis, *trans*-complementation of NS4B was re-examined using the five non-replicating luc-JFH1_{GFP} mutants harbouring mutations within the C-terminus of NS4B that were deleterious for RNA replication.

5.2 Non-Replicating NS4B Mutant SGRs can be Complemented *in trans*

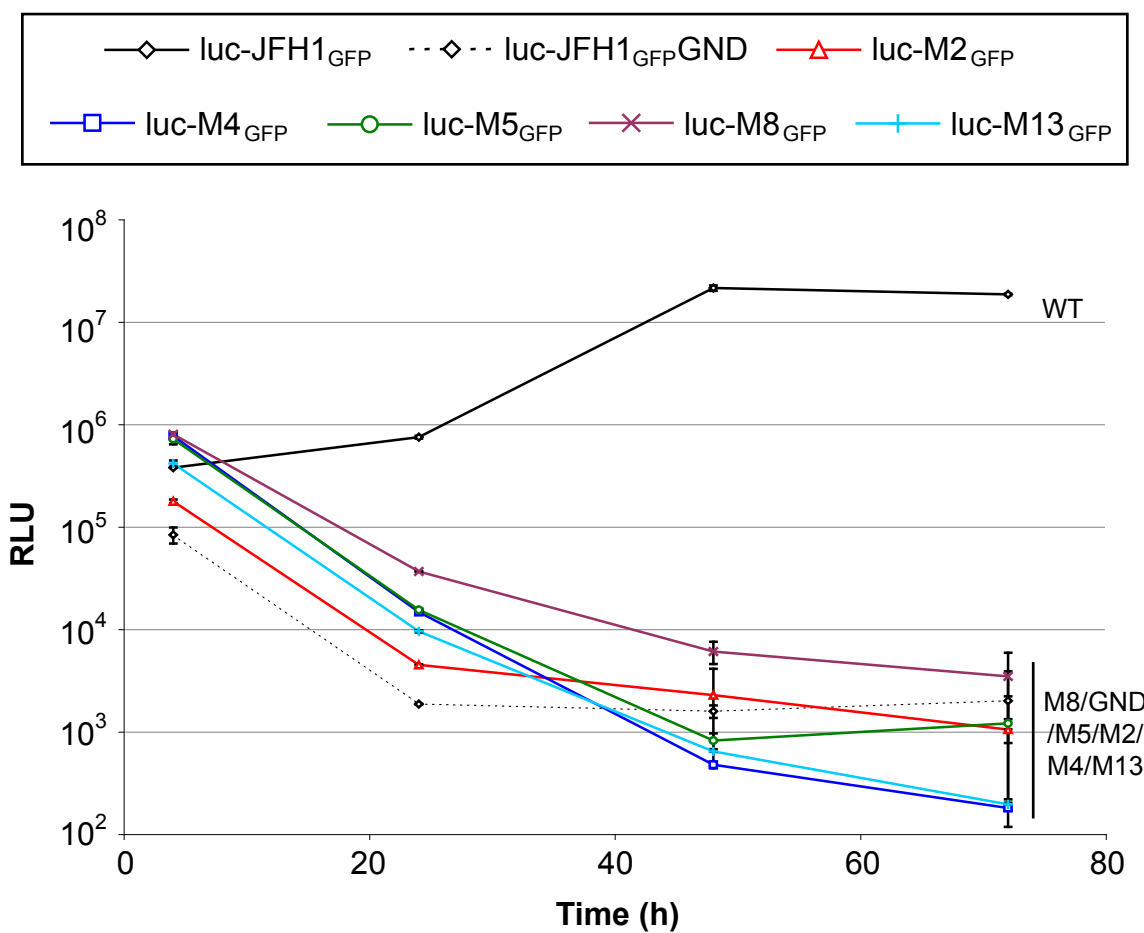
Results in the previous chapter revealed that SGRs containing five of the 15 NS4B mutants (M2, M4, M5, M8 and M13) were incapable of replicating when electroporated into Huh-7 cells. To determine whether replication of these mutants could be restored by the presence of functional NS4B, RNA from each mutant (luc-M2_{GFP}, luc-M4_{GFP}, etc) was electroporated into Huh-7 cells with (Figure 5.1, C) or without (Figure 5.1, B) helper RNA encoding neo-JFH1 and luciferase activity was measured over 72 hours. The ability to *trans*-complement defective replicons has been investigated previously by co-electroporating SGRs in this manner (Evans et al., 2004a). Neo-JFH1 is a SGR analogous to luc-JFH1 but harbours a selectable antibiotic resistance marker in place of the luciferase gene (Figure 5.1, A). Therefore, any detected luciferase activity in this assay would result from replication of the NS4B mutant RNA rather than the neo-JFH1 helper RNA. Cells were also electroporated with RNA encoding luc-JFH1_{GFP} and luc-JFH1_{GFP}GND along with neo-JFH1 to provide positive and negative controls respectively.

Upon introduction of mutant RNA into cells in the absence of neo-JFH1 helper RNA, luciferase values from each of the five NS4B mutants declined almost as rapidly as for the GND control; these data are in agreement with the results in Chapter 4 and indicate that the mutants were incapable of replicating in Huh-7 cells (Figure 5.1, B). In contrast, luciferase levels from luc-JFH1_{GFP} increased over the 72-hour time period. Interestingly, luc-JFH1_{GFP} displayed a different pattern of luciferase activity when introduced simultaneously with RNA from neo-JFH1; enzyme activity remained at similar levels up to 48 hours and then declined by 72 hours (Figure 5.1, C). This result suggested that luc-JFH1_{GFP} replication was partially attenuated in the presence of the second SGR, neo-JFH1. Competition between SGRs has been identified previously and the presence of one replicon has been demonstrated to reduce the capacity of a second to replicate (Evans et al., 2004a). Hence, it was possible that luc-JFH1_{GFP} replication was lowered due to competition from the neo-JFH1 SGR. Among the mutants, luciferase values from luc-M2_{GFP}, luc-M8_{GFP} and luc-M13_{GFP} at 72 hours post-electroporation were higher compared to luc-M4_{GFP}, luc-M5_{GFP} and the GND control (Figure 5.1, C). However, since attenuation of these mutants by neo-JFH1 may occur in a similar manner to that for luc-JFH1_{GFP}, *trans*-complementation was assessed in an alternative system.

[A]



[B]



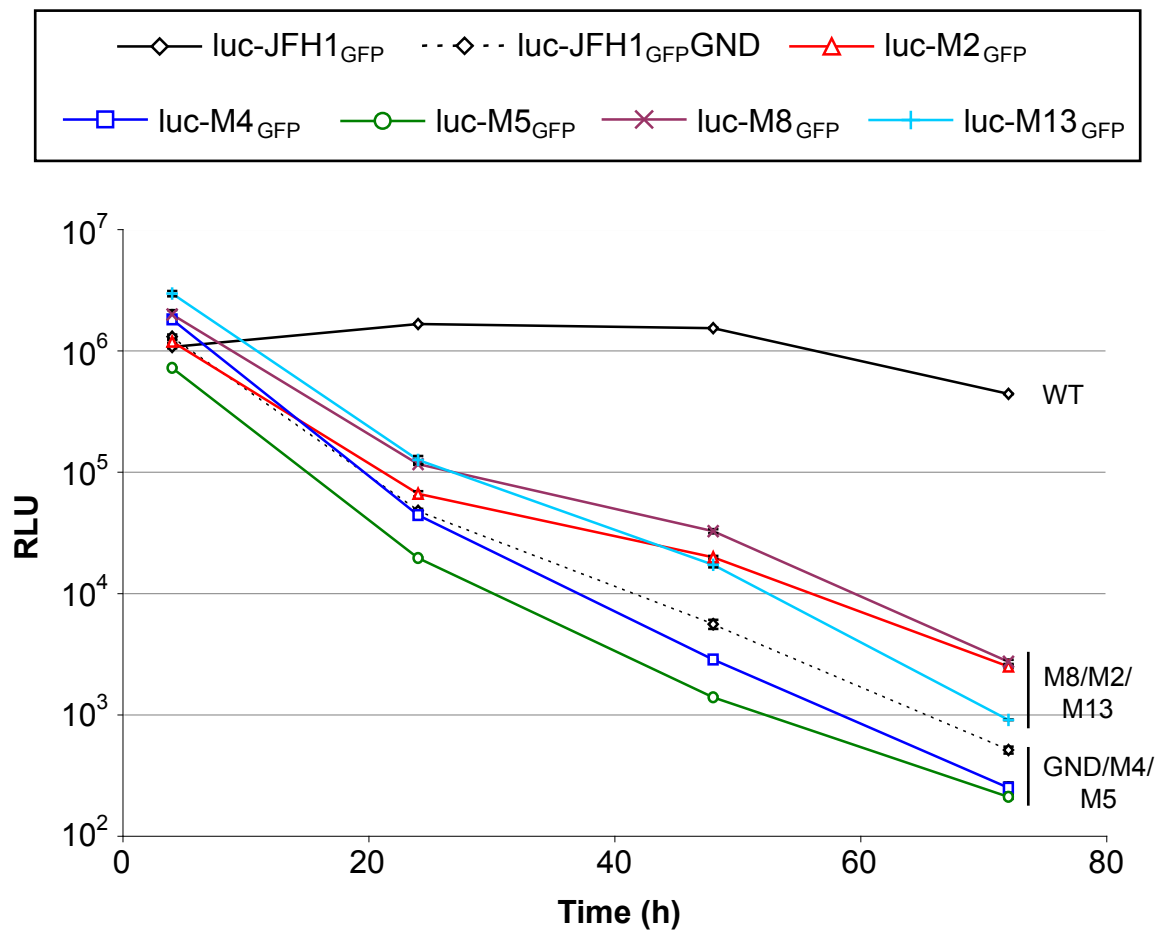
[C]

Figure 5.1 Transient *trans*-complementation of non-replicating NS4B mutant SGRs

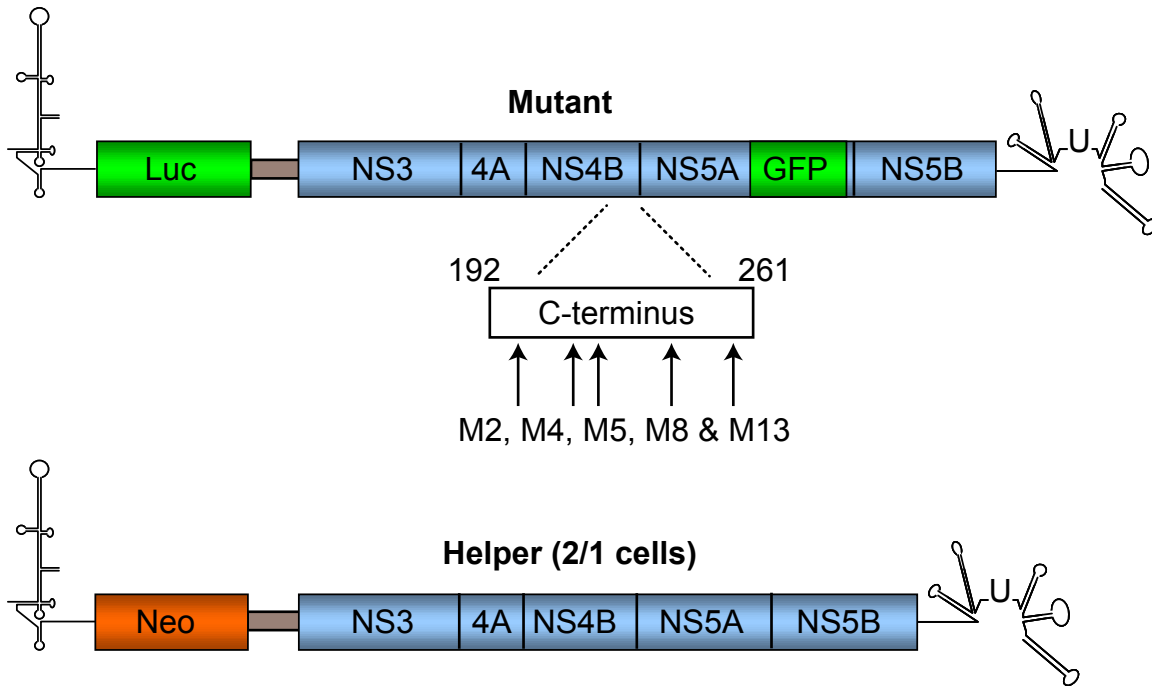
[A] Schematic representation of the non-replicating NS4B mutant SGRs (M2, M4, M5, M8 and M13, top) and the helper SGR, Neo-JFH1 (bottom). Each NS4B mutant contains the luciferase reporter gene and encodes the NS5A-GFP fusion protein. Neo-JFH1 encodes the Neo gene and an untagged NS5A protein. RNA from luc-JFH1_{GFP}, luc-JFH1_{GFP}GND and each NS4B mutant (luc-M2_{GFP}, luc-M4_{GFP}, etc) was **[B]** electroporated into Huh-7 cells **[C]** co-electroporated with RNA encoding Neo-JFH1 into Huh-7 cells. Cells were lysed at 4, 24, 48 and 72 hours post-electroporation and extracts assayed for luciferase activity. All assays were performed in duplicate and average values are shown for each experiment. Error bars represent the range of the values recorded at each time point.

Trans-complementation of the five non-replicating NS4B mutants was next attempted by electroporating RNA into 2/1 cells, a Huh-7 cell line that autonomously replicates the neo-JFH1 SGR. In this situation, the helper RNA is already present in cells and is not introduced simultaneously with the mutant RNAs, as with the previous system. 2/1 cells were also electroporated with RNA from luc-JFH1_{GFP} and luc-JFH1_{GFP}GND and luciferase activity was assessed over 72 hours.

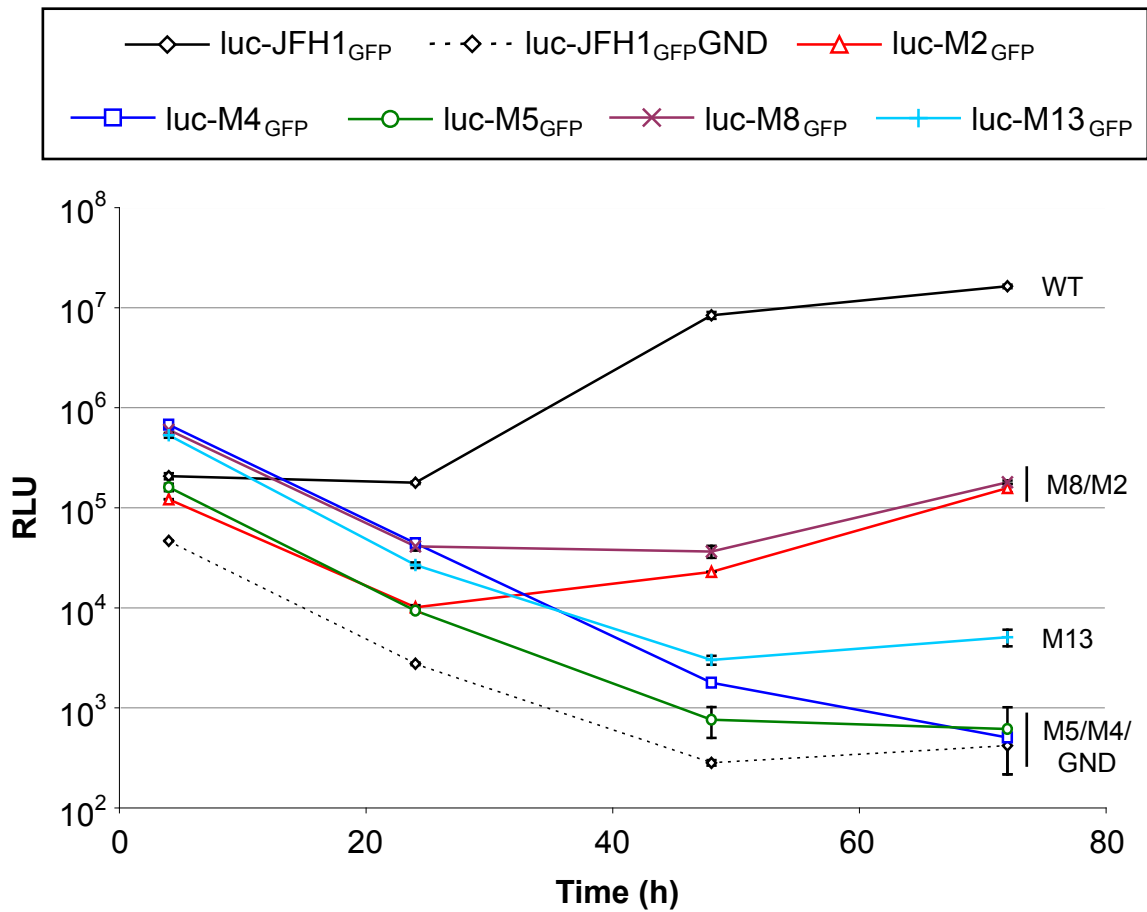
In contrast to results from the previous assay, luciferase values from luc-JFH1_{GFP} in 2/1 cells were approximately 50-fold higher by 72 hours compared to the 4-hour time point, indicating that efficient replication occurred in the presence of the helper RNA (Figure 5.2, B). A decrease in luciferase activity was observed over the first 24 hours in 2/1 cells harbouring each NS4B mutant. However, luc-M2_{GFP} and luc-M8_{GFP} exhibited increases in luciferase levels between 24 and 72 hours, indicating partial restoration of replication for these mutant SGRs (Figure 5.2, B). Luc-M13_{GFP} also displayed an increase in enzyme activity, although this was delayed to between 48 and 72 hours. In contrast, luciferase levels provided no evidence of replication for luc-M4_{GFP}, luc-M5_{GFP} or the GND control (Figure 5.2, B). By 72 hours post electroporation, luciferase levels for luc-M2_{GFP} and luc-M8_{GFP} were approximately 100-fold lower compared to luc-JFH1_{GFP} and enzyme activity from luc-M13_{GFP} was more than 3500-fold lower. However, these levels were significantly greater than the values obtained with luc-M4_{GFP}, luc-M5_{GFP} and luc-JFH1_{GFP}GND, which all gave luciferase values in excess of 30000-fold lower by 72 hours compared to luc-JFH1_{GFP}. Therefore, luc-M2_{GFP}, luc-M8_{GFP} and to a lesser extent, luc-M13_{GFP}, were considered capable of a low level of *trans*-complementation.

To confirm that the partial restoration of luciferase activity for three of the five non-replicating NS4B mutants was also reflected in rises in HCV protein expression, 2/1 cells electroporated with each mutant RNA were fixed at 72 hours and examined for the presence of NS5A-GFP. Since the SGR present in 2/1 cells encodes a wt NS5A protein, any detected NS5A-GFP would confirm expression from the input mutant RNA (Figure 5.2, C). Cells were stained also for NS5A that would be produced by neo-JFH1. NS5A was detected in a high proportion of the 2/1 cells, representing expression by the autonomously replicating neo-JFH1 SGR. However, for cells electroporated with luc-JFH1_{GFP}, luc-M2_{GFP} and luc-M8_{GFP}, NS5A-GFP was also visualised (Figure 5.2, C, white arrowheads and shown enlarged in D). A low proportion of cells expressing NS5A-GFP was evident

[A]



[B]



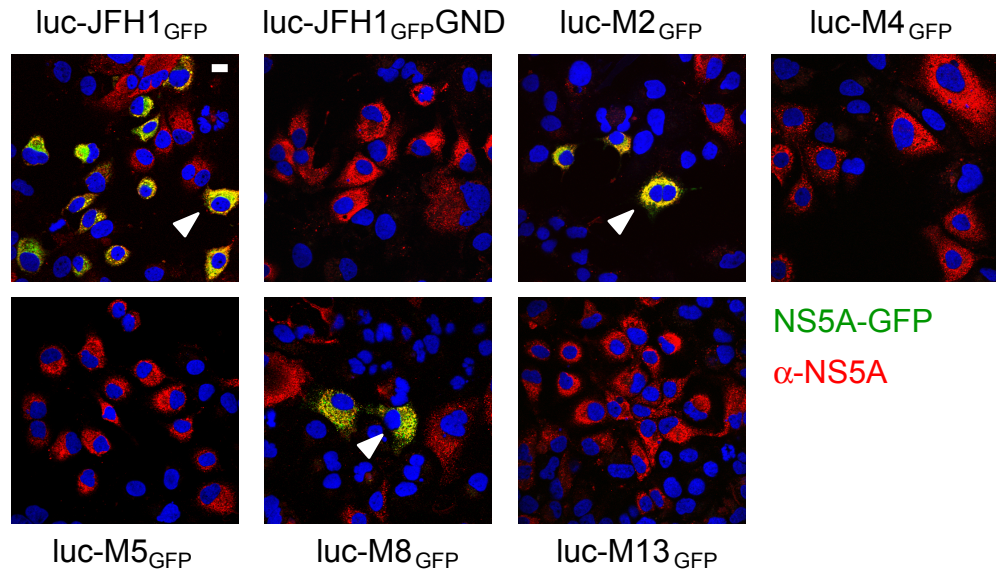
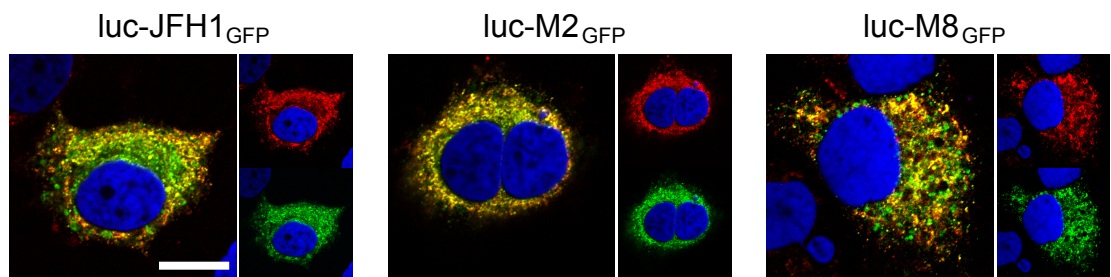
[C]**[D]**

Figure 5.2 Non-replicating NS4B mutant SGRs can be *trans*-complemented

[A] Schematic representation of the non-replicating NS4B mutant SGRs (M2, M4, M5, M8 and M13, top) and the helper SGR, which replicates autonomously within the 2/1 cell line (bottom). Each NS4B mutant contains the luciferase reporter gene and encodes the NS5A-GFP fusion protein. The 2/1 helper SGR encodes the Neo gene and wt NS5A. **[B]** RNA from luc-JFH1_{GFP}, luc-JFH1_{GFP}GND and each NS4B mutant (luc-M2_{GFP}, luc-M4_{GFP}, etc) was electroporated into 2/1 cells. Cells were lysed at 4, 24, 48 and 72 hours post-electroporation and extracts assayed for luciferase activity. All assays were performed in duplicate and average values are shown for each experiment. Error bars indicate the range of the values recorded at each time point. **[C]** Cells electroporated in parallel to those described in [B] were fixed at 72 hours post-electroporation and NS5A was visualised using NS5A antisera. Cells were also stained with DAPI and NS5A-GFP was visualised directly. The detection of NS5A-GFP indicated replication of the NS4B mutant SGR and cells with this phenotype are indicated (white arrowheads) and shown in closer detail in **[D]**. Scale bars represent 10 μ m.

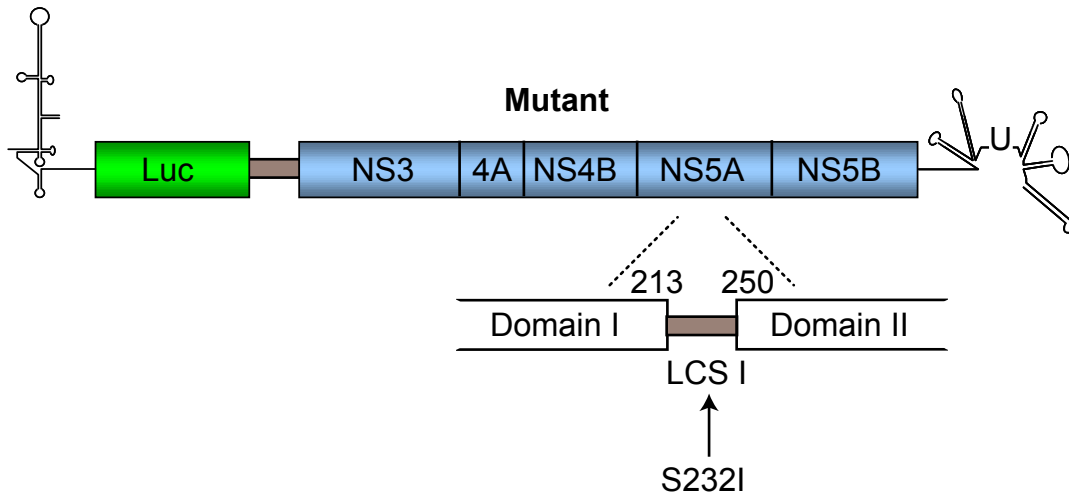
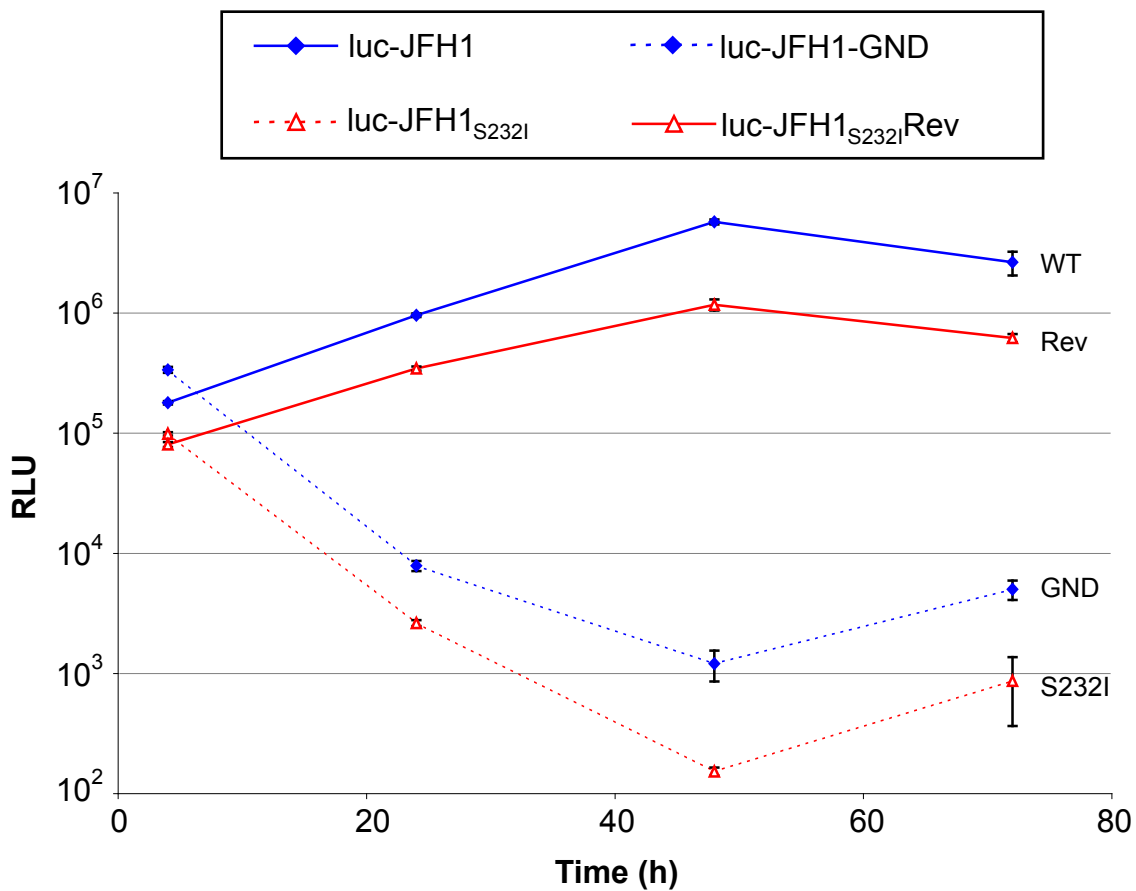
[A]**[B]**

Figure 5.3 A Ser to Ile change at amino acid 232 abolishes luc-JFH1 replication

[A] Schematic representation of the luc-JFH1_{S232I} replicon, with the position of the S232I mutation within NS5A depicted beneath. luc-JFH1_{S232I} contains the luciferase reporter gene and encodes an untagged NS5A protein. **[B]** RNA from luc-JFH1, luc-JFH1-GND, luc-JFH1_{S232I} and luc-JFH1_{S232I}Rev was electroporated into Huh-7 cells. Cells were lysed at 4, 24, 48 and 72 hours post-electroporation and extracts assayed for luciferase activity. All assays were performed in duplicate and average values are shown for each experiment. Error bars indicate the range of the values recorded at each time point.

for luc-M2_{GFP} and luc-M8_{GFP} in comparison to luc-JFH1_{GFP}, most likely as a consequence of the decreased replication efficiency of these mutants as indicated by luciferase measurements. NS5A-GFP could not be detected in cells expressing luc-M4_{GFP}, luc-M5_{GFP}, the GND control or luc-M13_{GFP}, despite this mutant displaying a slight increase in replication by 72 hours (Figure 5.2, C). However, it is probable that this level of replication was too low for visualisation of NS5A-GFP.

Taken together, the results revealed that the replication of some, but not all SGRs harbouring mutations within the NS4B coding region could be rescued by the presence of a replicating helper RNA, most likely through *trans*-complementation of NS4B.

5.3 A Non-Replicating NS5A Mutant SGR can be Complemented *in trans*

In the previous chapter, it was demonstrated that the processes of foci formation and NS5A hyperphosphorylation were linked, and NS4B mutants that were compromised in their ability to create foci only produced the basally phosphorylated species of NS5A. Originally, we sought to determine whether phosphorylation acted as a determinant of NS5A localisation, where hyperphosphorylation might result in the trafficking of NS5A to foci. To explore this hypothesis, a Ser to Ile change at amino acid 232 was introduced into the NS5A coding region of luc-JFH1 by site directed mutagenesis, since introduction of the same mutation into a genotype 1b strain Con1 SGR (referred to as amino acid 2204 in Lohmann et al., 2001) reduced the level of hyperphosphorylated NS5A. This SGR was called luc-JFH1_{S232I} (Figure 5.3, A). Surprisingly, electroporation of RNA from luc-JFH1_{S232I} into Huh-7 cells resulted in luciferase levels that followed the same pattern as those observed for luc-JFH1-GND, indicating that luc-JFH1_{S232I} was incapable of replicating (Figure 5.3, B). Construction of a revertant (termed luc-JFH1_{S232I}Rev) confirmed that this single amino acid change was sufficient to completely abolish replication, since reversion of the Ile to Ser at position 232 resulted in RNA replication that paralleled luc-JFH1 (Figure 5.3, B). Therefore, luc-JFH1_{S232I} represented a non-replicating SGR.

NS5A is capable of *trans*-complementation and the replication of SGRs containing mutations within its coding region can be restored in the presence of functional NS5A supplied by a helper RNA (Appel et al., 2005a, Tong & Malcolm, 2006). To

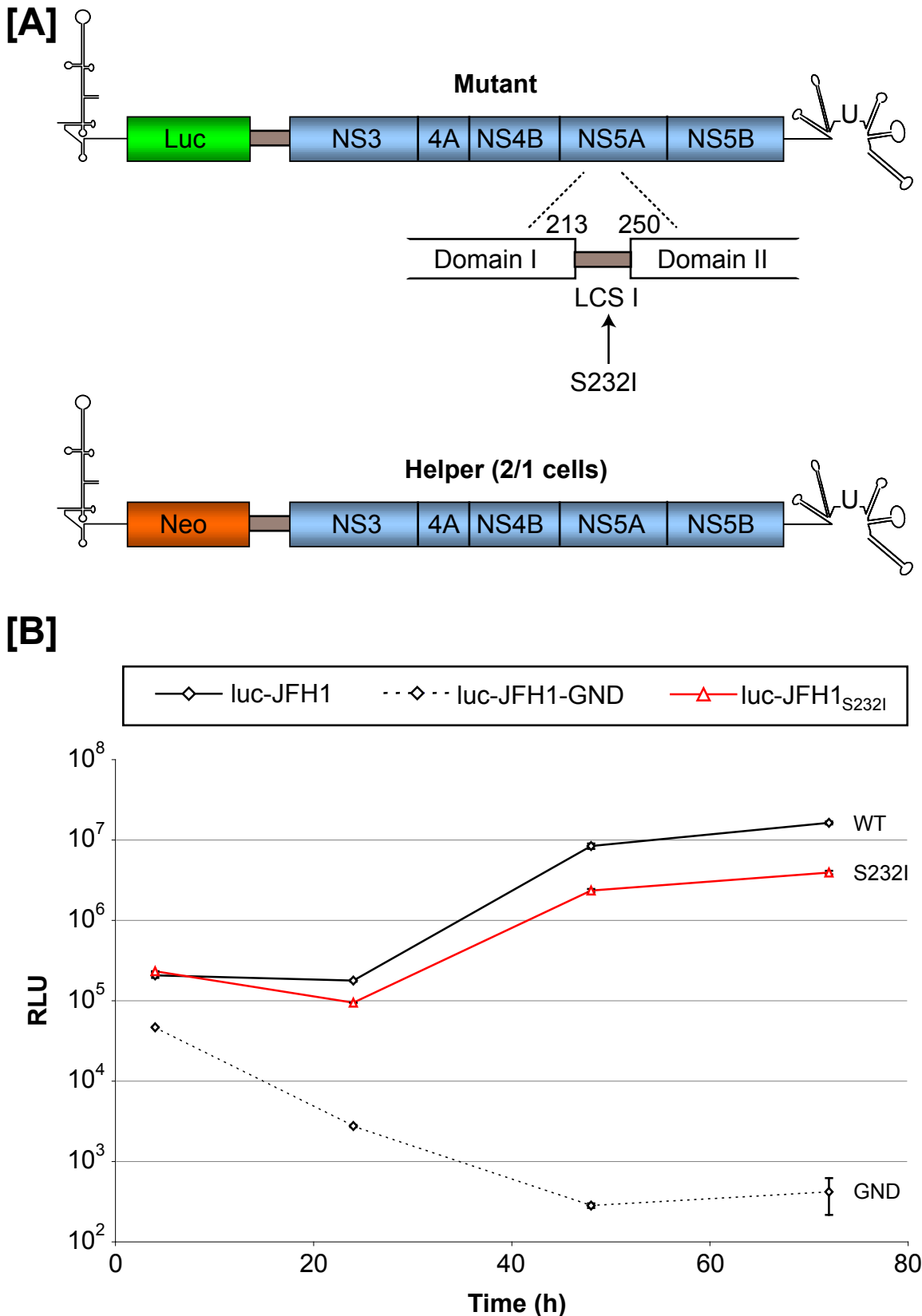


Figure 5.4 luc-JFH1_{S232I} RNA replication can be *trans*-complemented

[A] Schematic representation of the luc-JFH1_{S232I} replicon (top) and the helper SGR, which replicates autonomously within the 2/1 cell line (bottom). luc-JFH1_{S232I} contains the luciferase reporter gene, while the 2/1 helper SGR encodes the Neo gene. Both SGRs harbour untagged NS5A proteins. **[B]** RNA from luc-JFH1, luc-JFH1-GND and luc-JFH1_{S232I} was electroporated into 2/1 cells. Cells were lysed at 4, 24, 48 and 72 hours post-electroporation and extracts were assayed for luciferase activity. All assays were performed in duplicate and average values are shown for each experiment. Error bars represent the range of the values recorded at each time point.

determine whether replication of luc-JFH1_{S232I} could be restored in the same manner, luc-JFH1_{S232I} was electroporated into 2/1 cells and luciferase activity was measured over 72 hours (Figure 5.4, B). In 2/1 cells, luc-JFH1_{S232I} exhibited luciferase values at the 72-hour time point that were only four-fold lower than those displayed by luc-JFH1 (Figure 5.4, B). In contrast, no increases in luciferase activity were observed in 2/1 cells electroporated with luc-JFH1-GND. This result indicated that replication of the luc-JFH1_{S232I} SGR could be restored in the presence of the functional SGR present in 2/1 cells, presumably by *trans*-complementation of NS5A.

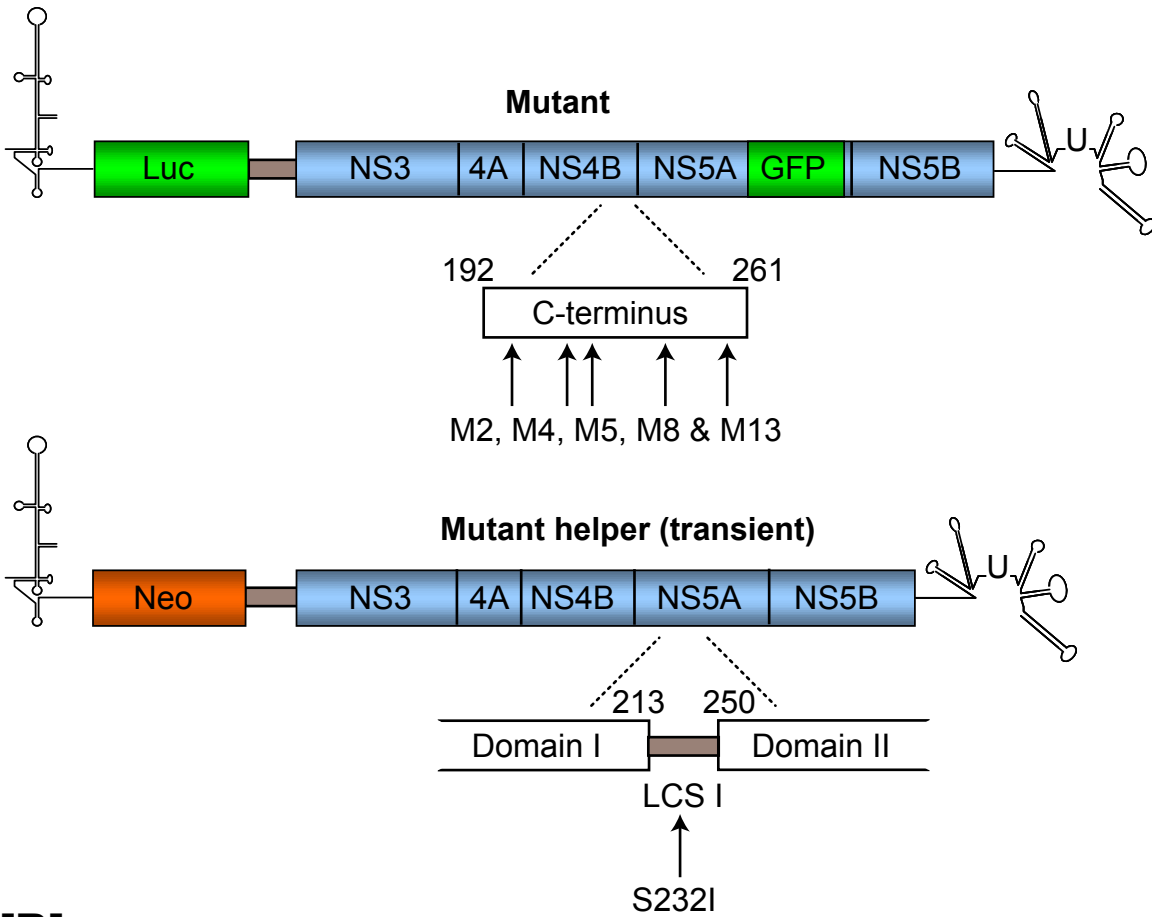
5.4 Reconstitution of Replication from Non-Replicating NS4B and NS5A Mutant SGRs

5.4.1 Detection of NS4B Mutant SGR Replication

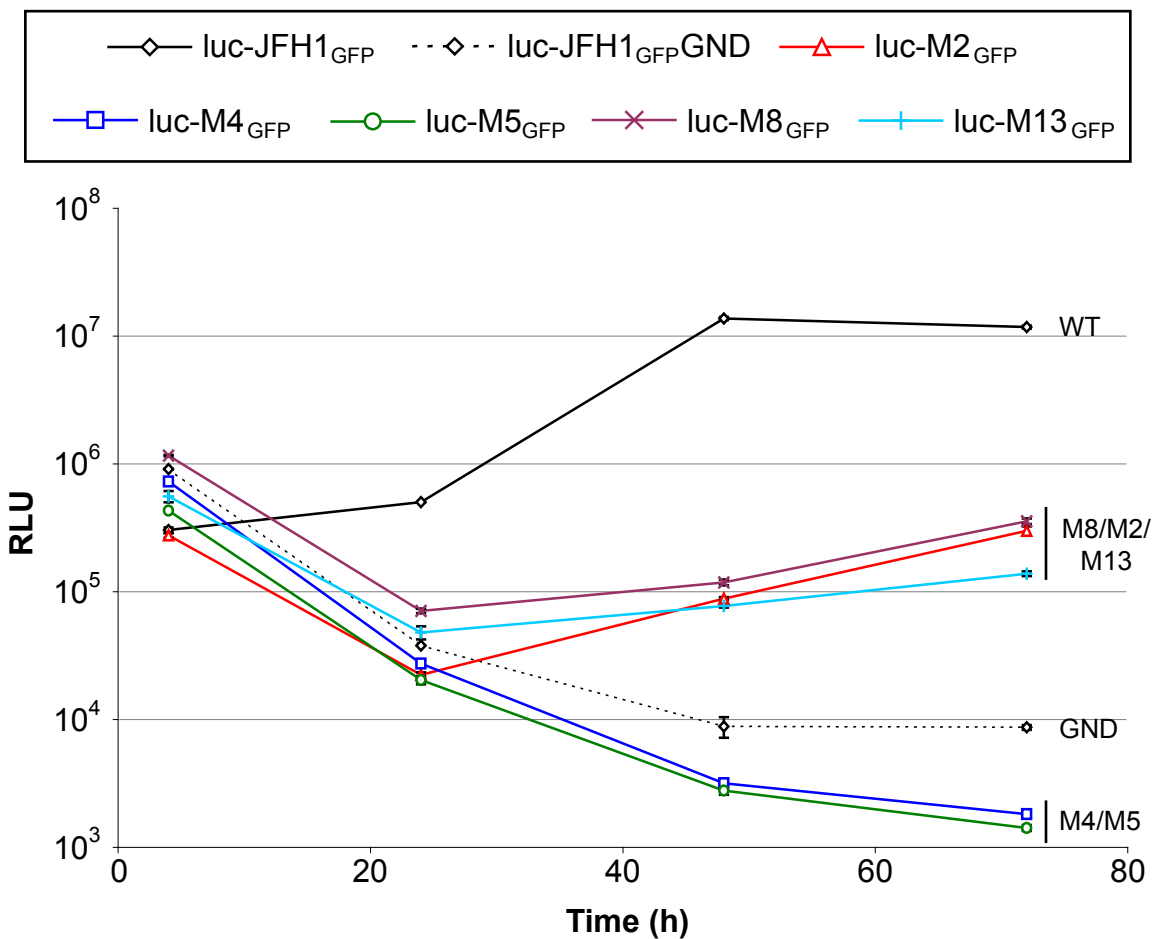
The results described thus far confirmed that a functional helper RNA could rescue the replication of SGRs harbouring mutations in both NS4B and NS5A. We next sought to determine whether the replication of each NS4B mutant could be *trans*-complemented using a helper RNA harbouring the deleterious S232I mutation within NS5A (Figure 5.5, A). Huh-7 cells were co-electroporated with neo-JFH1_{S232I} and each NS4B mutant (luc-M2_{GFP}, luc-M4_{GFP}, etc) and luciferase activity was recorded over 72 hours (Figure 5.5, B). Interestingly, luciferase levels increased between 24 and 72 hours post-electroporation for luc-M2_{GFP}, luc-M8_{GFP} and luc-M13_{GFP}, indicating that replication was partially restored for these mutants. *Trans*-complementation had previously been demonstrated for these three mutants using a functional helper SGR in 2/1 cells (Figure 5.2, B). Here however, *trans*-complementation seemed more efficient, and luciferase levels were 40-fold (luc-M2_{GFP}), 33-fold (luc-M8_{GFP}) and 85-fold (luc-M13_{GFP}) lower than those exhibited by luc-JFH1_{GFP} by 72 hours (Figure 5.5, B). Again, luc-M4_{GFP}, luc-M5_{GFP} and the GND control exhibited decreases in luciferase levels over the time course, confirming that these mutants could not be rescued by *trans*-complementation.

To confirm that replication was restored in cells containing two non-functional SGRs, cells set up in parallel to those described above were examined for the presence of NS5A-GFP and dsRNA (Figure 5.5, C). Each NS4B mutant encodes NS5A-GFP, thus detection of the fusion protein would indicate replication of the mutant SGR. Similarly, the detection of dsRNA would confirm that active

[A]



[B]



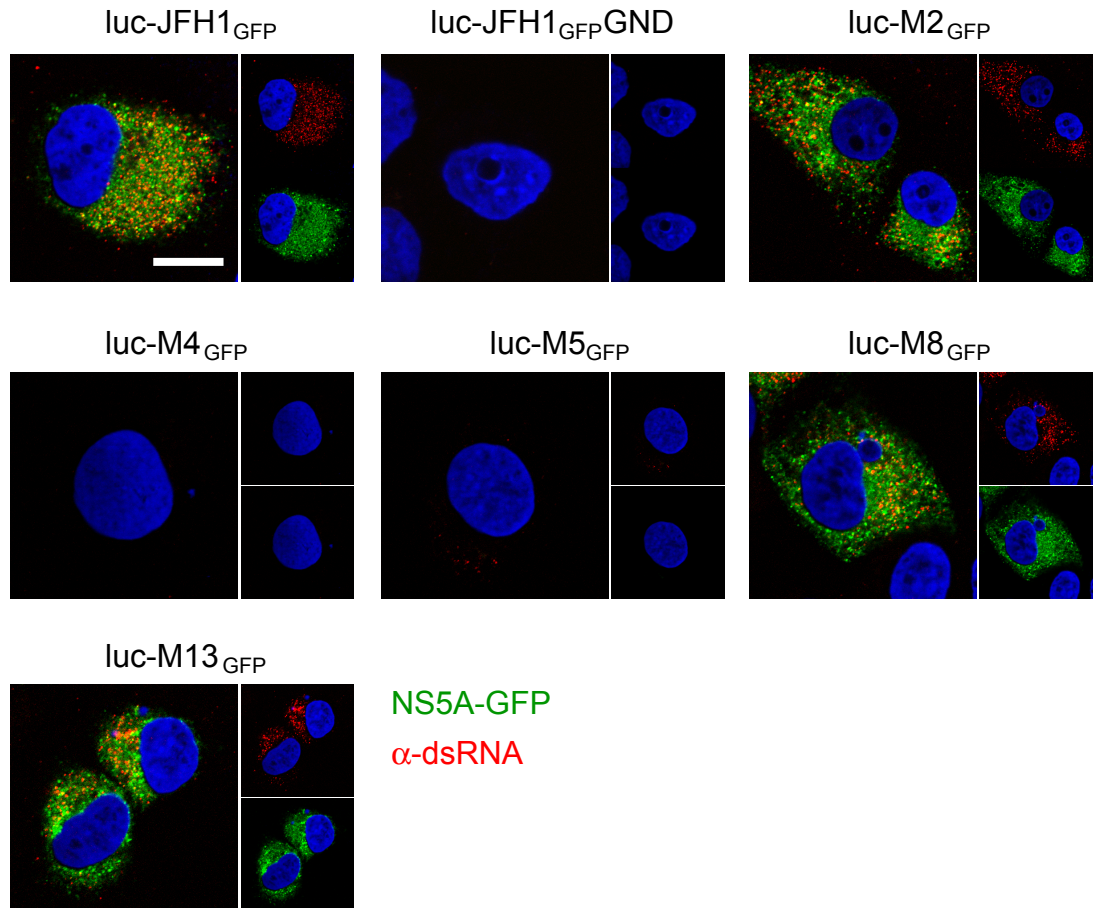
[C]

Figure 5.5 Reconstitution of replication from non-replicating NS4B and NS5A mutant SGRs

[A] Schematic representation of the non-replicating NS4B mutant SGRs (M2, M4, M5, M8 and M13, top) and the defective 'helper' Neo-JFH1_{S232I} SGR, which itself cannot replicate (bottom). Each NS4B mutant contains the luciferase reporter gene and encodes the NS5A-GFP fusion protein, whereas Neo-JFH1_{S232I} encodes the Neo gene and an untagged NS5A protein. **[B]** RNA from luc-JFH1_{GFP}, luc-JFH1_{GFP}GND and each NS4B mutant (luc-M2_{GFP}, luc-M4_{GFP}, etc) was co-electroporated with RNA encoding neo-JFH1_{S232I} into Huh-7 cells. Cells were lysed at 4, 24, 48 and 72 hours post-electroporation and extracts were assayed for luciferase activity. All assays were performed in duplicate and average values are shown for each experiment. Error bars represent the range of the values recorded at each time point. **[C]** Cells electroporated in parallel to those in [B] were fixed at 72 hours post-electroporation and dsRNA was visualised using J2 antibody. Cells were also stained with DAPI and NS5A-GFP was visualised directly. Scale bars represent 10µm.

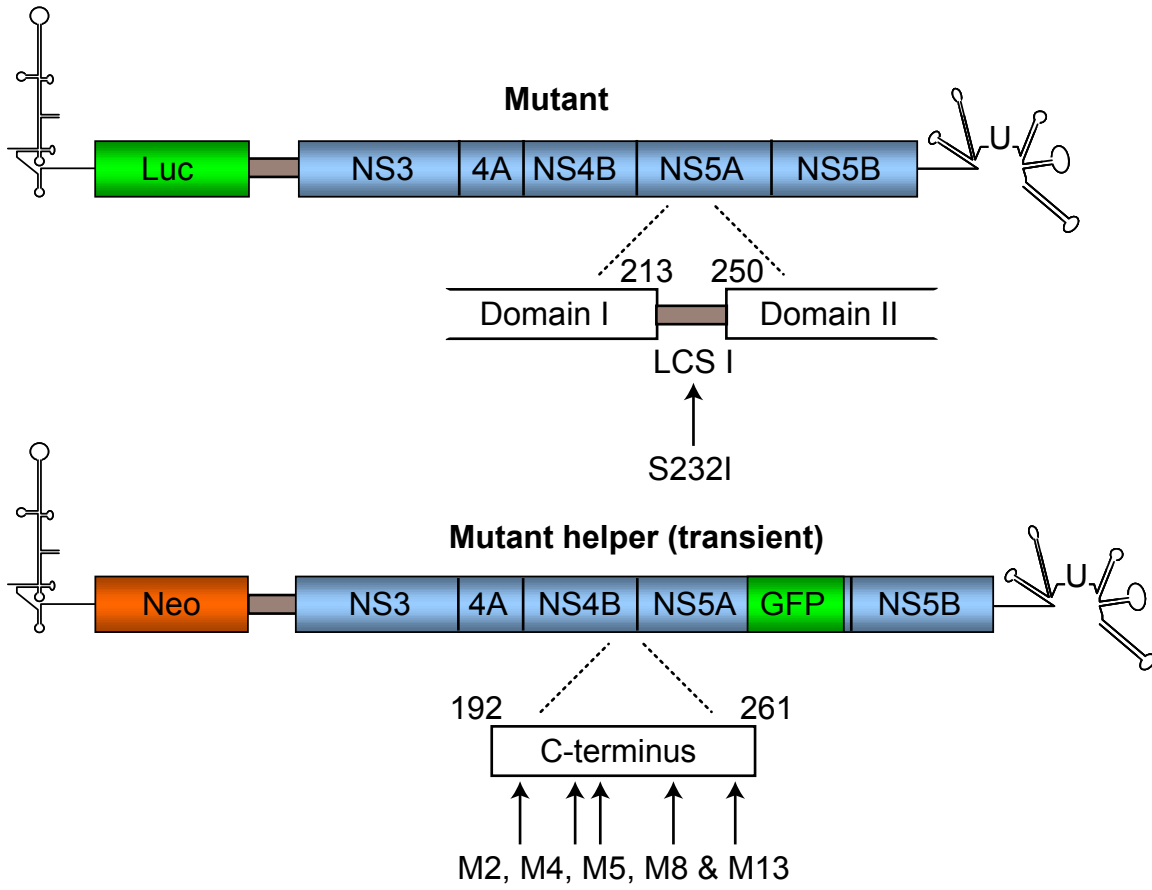
replication had occurred. Upon examination of cells, both NS5A-GFP and dsRNA were present in cells co-electroporated with luc-JFH1_{GFP} and neo-JFH1_{S232I}, consistent with the increase in luciferase activity seen over 72 hours with this construct (Figure 5.5, C). In contrast, neither NS5A-GFP nor dsRNA could be visualised in cells containing a combination of luc-M4_{GFP}, luc-M5_{GFP} and neo-JFH1_{S232I} RNAs. However, NS5A-GFP and dsRNA were observed in a low number (~1%) of cells co-electroporated with luc-M2_{GFP}, luc-M8_{GFP} and neo-JFH1_{S232I}, and both signals were also detected occasionally (<1% of cells) with the luc-M13_{GFP} mutant (Figure 5.5, C).

5.4.2 Detection of NS5A Mutant SGR Replication

The data described above indicated that luc-M2_{GFP}, luc-M8_{GFP} and luc-M13_{GFP} could all be *trans*-complemented by a non-functional helper RNA harbouring a deleterious NS5A mutation. This prompted an investigation into whether neo-JFH1_{S232I} could, in turn, be *trans*-complemented by the NS4B mutants. To examine this possibility, neo-JFH1_{S232I} was replaced with luc-JFH1_{S232I}, therefore allowing the replicative ability of this SGR to be quantified by measuring luciferase activity. Similarly, the luciferase gene present in the NS4B mutants (luc-M2_{GFP}, luc-M4_{GFP}, etc) was replaced with the neo gene (Figure 5.6, A). Thus, the experiment was essentially identical to that presented in Figure 5.5, B, except measurement of luciferase activity would now reveal whether *trans*-complementation was restoring replication of the NS5A mutant SGR as opposed to the NS4B mutant SGRs. Each NS4B mutant (neo-M2_{GFP}, neo-M4_{GFP}, etc) was co-electroporated into cells along with luc-JFH1_{S232I} and luciferase activity was monitored over 72 hours (Figure 5.6, B). Interestingly, luciferase levels expressed from luc-JFH1_{S232I} increased between 48 and 72 hours when electroporated into cells with neo-M2_{GFP}, neo-M8_{GFP} and neo-M13_{GFP} (Figure 5.6, B). In contrast, luc-JFH1_{S232I} could not replicate when combined with neo-M4_{GFP}, neo-M5_{GFP} or when introduced individually into cells.

The results presented in Section 5.4.1 indicate that the replication of S232I leads to production of functional NS4B that can *trans*-complement M2, M8 and M13, restoring their replicative ability. In turn, data shown in this section suggest that the functional NS5A-GFP protein from M2, M8 and M13 can *trans*-complement the non-replicating S232I mutant, restoring its capacity to replicate. Taken together, the conclusion from these experiments is that NS4B and NS5A mutant SGRs are mutually dependent for their replication.

[A]



[B]

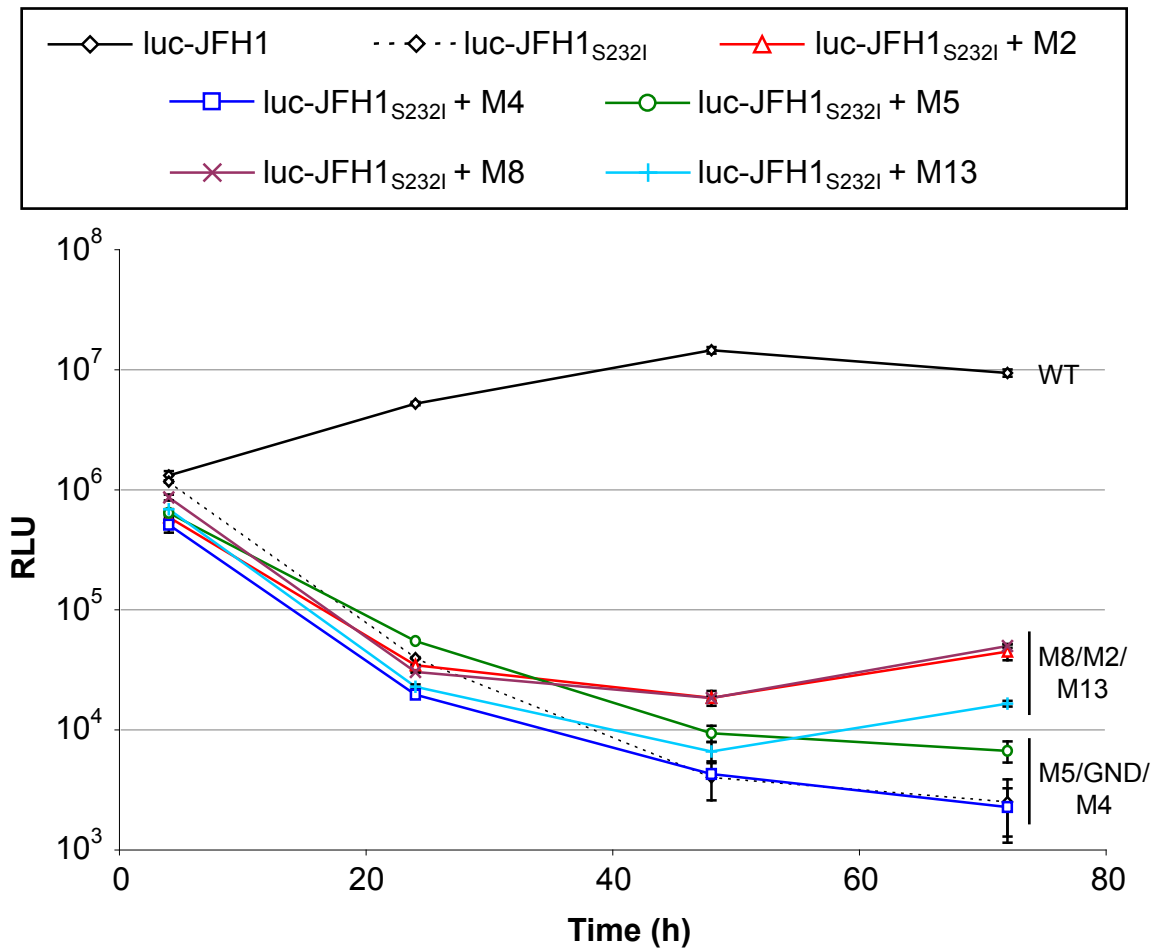


Figure 5.6 *Trans*-complementation of a defective SGR with a NS5A mutation by non-replicating SGRs expressing mutant NS4B

[A] Schematic representation of the non-replicating luc-JFH1_{S232I} SGR (top) and the defective 'helper' NS4B mutant SGRs (M2, M4, M5, M8 and M13), which themselves cannot replicate (bottom). Each NS4B mutant contains the Neo gene and encodes the NS5A-GFP fusion protein, whereas Neo-JFH1_{S232I} encodes the luciferase reporter gene and an untagged NS5A protein. **[B]** RNA from luc-JFH1_{GFP} and luc-JFH1_{S232I} was co-electroporated with RNA encoding each NS4B mutant (Neo-M2_{GFP}, Neo-M4_{GFP}, etc) into Huh-7 cells. Cells were lysed at 4, 24, 48 and 72 hours post-electroporation and extracts were assayed for luciferase activity. All assays were performed in duplicate and average values are shown for each experiment. Error bars indicate the range of the values recorded at each time point.

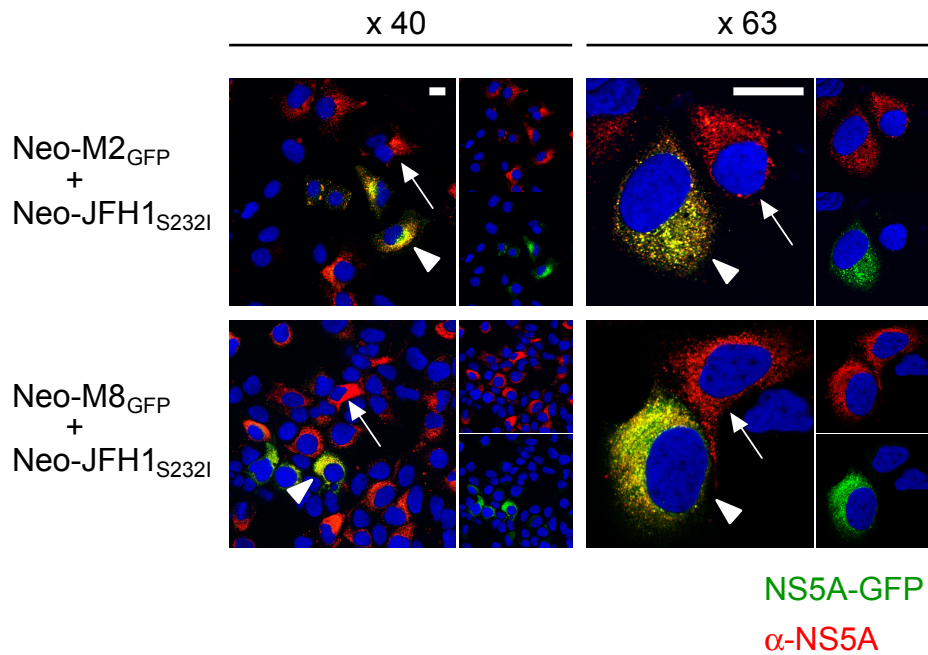
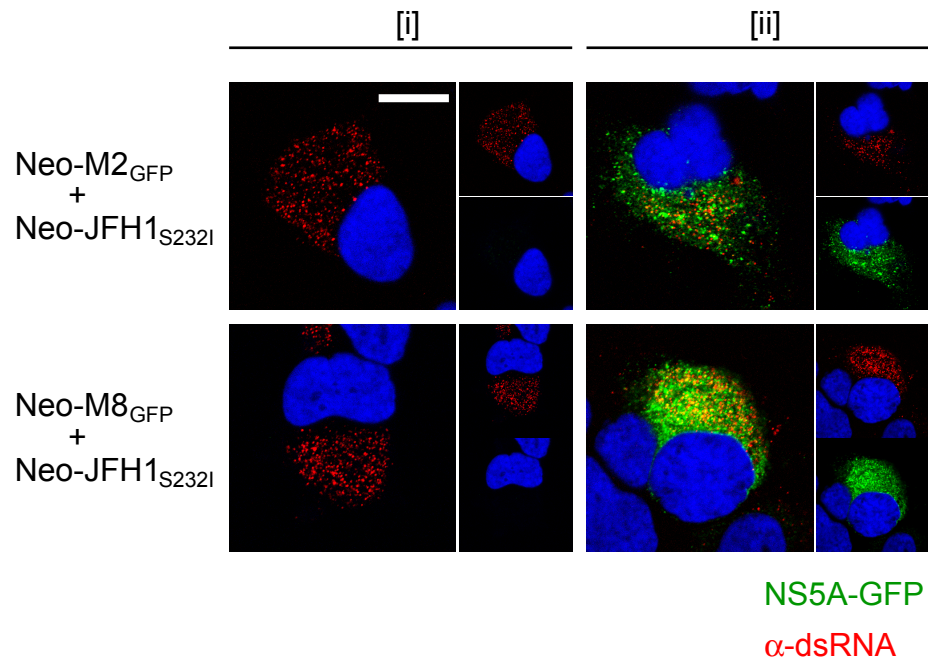
[A]**[B]**

Figure 5.7 Generation of cell lines from non-replicating NS4B and NS5A mutant SGRs

Huh-7 cells were co-electroporated with RNA from Neo-JFH1_{S232I} and either Neo-M2_{GFP} or Neo-M8_{GFP}, before being passaged for several weeks in the presence of G418. Cells were fixed and NS5A-GFP was visualised directly along with **[A]** NS5A, using NS5A antisera or **[B]** dsRNA, using J2 antibody. Cells were also stained using DAPI. In **[A]**, cells exhibiting NS5A-GFP (white arrowheads) and NS5A (white arrows) are depicted. Similarly in **[B]**, cell populations harbouring either dsRNA alone [i], or dsRNA and NS5A-GFP [ii] are shown. Scale bars represent 10µm.

5.4.3 Creation of a Cell Line from Non-Replicating NS4B and NS5A Mutant SGRs

The above results indicate that transient replication could be reconstituted in cells electroporated with two non-replicating SGRs. However, it was not clear whether this mutual *trans*-complementation would sustain replication of both mutants over an extended period of time. Therefore, we next attempted to create cell lines harbouring stably replicating NS4B and NS5A mutants. The first cell line was generated by co-electroporating Huh-7 cells with RNA encoding neo-M2_{GFP} and neo-JFH1_{S232I}, while the second cell line contained neo-M8_{GFP} and neo-JFH1_{S232I}. Thus, each cell line would harbour two distinct SGRs; one with a non-functional NS4B and the other with a non-functional NS5A. A cell line utilising M13 was not attempted since previous results had suggested that this mutant was *trans*-complemented less efficiently than M2 and M8 (Figure 5.2, B). All cells were permitted to grow for 72 hours post-electroporation before the addition of G418, since data in Sections 5.4.1 and 5.4.2 had revealed that mutant RNA replication had initiated by this point. G418 selection was maintained for several weeks before each cell line was examined by fluorescence microscopy.

Firstly, each cell line was stained using NS5A antisera to allow detection of both NS5A (neo-JFH1_{S232I}) and NS5A-GFP (neo-M2_{GFP} and neo-M8_{GFP}, Figure 5.7, A). NS5A-GFP was also visualised directly in both cell lines. After G418 selection, it was expected that cells would contain both the NS4B and NS5A mutants and that their mutual *trans*-complementation would sustain replication, conferring G418 resistance to the cells. Consequently, cells should exhibit expression of both NS5A and NS5A-GFP. As expected, NS5A could be detected in the majority of cells from both cell lines. However, not all of the NS5A-positive cells visibly expressed NS5A-GFP (Figure 5.7, A, white arrows), although a low number of cells expressing NS5A and NS5A-GFP were detected (Figure 5.7, A, white arrowheads). Both cell lines were examined for the presence of dsRNA to confirm that they produced replicated HCV RNA and NS5A-GFP was also visualised (Figure 5.7, B). As expected, both cell lines exhibited cells that contained both NS5A-GFP and dsRNA (Figure 5.7, B, [ii]). Once again however, cells were frequently found that displayed no detectable NS5A-GFP, yet exhibited a dsRNA signal (Figure 5.7, B, [i]).

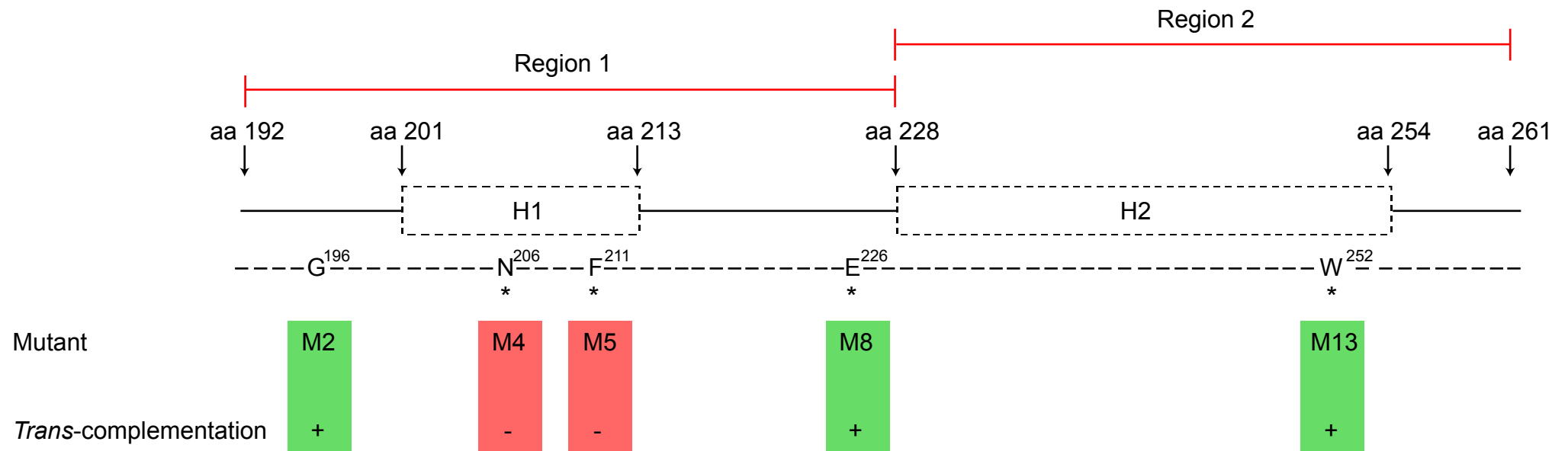


Figure 5.8 Summary of the *trans*-complementation data for non-replicating NS4B mutant SGRs

A schematic representation of the NS4B C-terminus is shown. Region 1 (highly conserved), Region 2 (less conserved compared to Region 1), the positions of both predicted helices (H1 and H2) and the positions of the five mutations that abolish replication are depicted. Invariant amino acids are denoted by an asterisk and are numbered with respect to the N-terminal end of NS4B. Mutations that could (green) or could not be (red) *trans*-complemented are highlighted.

These results confirmed that cell lines could be established from the selection of two non-functional SGRs and the interpretation of these results will be discussed below. A summary of the NS4B *trans*-complementation data from this chapter is presented in Figure 5.8.

5.5 Discussion

A hallmark of positive-strand RNA viruses is their ability to rearrange internal cellular membranes, ultimately creating structures that are capable of supporting viral RNA replication (Mackenzie, 2005, Salonen et al., 2005). For HCV, these membrane-derived RCs have been shown to contain NS proteins and viral RNA that are protected from degradation by RNase or protease treatment (Aizaki et al., 2004, El-Hage & Luo, 2003, Yang et al., 2004). These data suggest that RCs are enclosed structures that permit little exchange of material between the internal and external environments of the complex and therefore, RCs may include all components necessary for replication upon formation. However, RCs cannot be entirely enclosed since replicated viral RNA is thought to be transported to LDs for packaging into virus particles (Miyanari et al., 2007).

Previous investigations into the functional organisation of HCV replicase proteins within RCs utilised genotype 1 SGRs harbouring CCAMs and examined the ability to complement non-functional NS3, NS4B and NS5A proteins (Appel et al., 2005a, Tong & Malcolm, 2006). It was concluded from these experiments that NS5A was the only HCV NS protein involved in RNA replication that can be supplied *in trans*. In the case of NS4B however, a limited set of mutants was tested for their ability to be complemented. The mutants tested included a single mutation at Val 186 (referred to as 1897 in Appel et al., 2005), in addition to two large deletions spanning amino acids 71-110 and 194-222 (referred to as Δ 1782-1821 and Δ 1905-1933 respectively in Appel et al., 2005). SGRs harbouring these large deletions or the Val point mutation were not complemented *in trans*. However, V186 is predicted to reside within TMD4, while the deletions would encompass the majority of TMDs 1 and 2 (Δ 71-110) and the entirety of predicted Helix 1 within the C-terminal domain (Δ 194-222). Hence, the mutations tested would either severely disrupt the overall structure of NS4B, or its membrane-binding properties. Therefore, we re-investigated the ability to *trans*-complement NS4B using efficiently replicating JFH1-based SGRs along with the five non-replicating mutants that were characterised in Chapter 4. These mutants harboured single

amino acid changes within the C-terminus of the protein, which is predicted to reside on the cytosolic side of the ER and may therefore be accessible by functional NS4B supplied *in trans*.

The results presented in this chapter show for the first time that replication can be at least partially restored to non-functional SGRs (M2, M8 and M13) by *trans*-complementation of the NS4B protein (Figure 5.2). In contrast, M4 and M5 were incapable of being complemented in this manner. With no available structural data on the C-terminal region of NS4B, it is unclear why some NS4B mutants can be complemented whereas others are not. Both N206 (M4) and F211 (M5) are completely conserved across all HCV isolates and cannot be complemented. However, E226 (M8) is also invariant, yet can be complemented (Figure 5.2). Therefore, mutation of highly conserved amino acids is not predictive of whether NS4B complementation is possible. M2, M8 and M13 also exhibited varying effects on the ability of NS4B to form foci as well as NS5A localisation and phosphorylation (see Section 4.3), meaning there is no clear correlation between these data and the complementation results. However, it is interesting that N206 (M4) and F211 (M5) both reside within Helix 1 (Figure 5.8), an α -helical structure determined by secondary structure prediction. It has been previously demonstrated that mutations within NS5A that abolish the amphipathic nature of the N-terminal α -helix results in the production of NS5A that cannot be complemented *in trans* (Appel et al., 2005a, Evans et al., 2004a). It is therefore tempting to speculate that a similar scenario may occur with NS4B, in which mutations M4 and M5 interfere with the secondary structure of Helix 1. In contrast, mutations within unstructured regions of NS4B (M2 and M8) can be *trans*-complemented (Figure 5.8). Investigation into the structural organisation of the NS4B C-terminus would allow further insights into this hypothesis.

Introduction of three non-replicating NS4B mutants and one non-replicating NS5A mutant into 2/1 cells led to restoration of replication, presumably due to the *trans*-complementation of NS4B and NS5A respectively. However, the efficiency of complementation was lower for the NS4B mutants compared to that observed with the NS5A S232I mutant. By 72 hours post-electroporation, *trans*-complementation of NS5A restored the replication of luc-JFH1_{S232I} to 24% compared to luc-JFH1_{GFP} (using the luciferase values in Figure 5.4, B). In contrast, complementation of NS4B restored replication of luc-M2_{GFP} and luc-M8_{GFP} to only 1% compared with luc-JFH1_{GFP}, and luc-M13_{GFP} was lower still at 0.05% (using the luciferase values

in Figure 5.2, B). The difference between NS4B and NS5A complementation efficiencies may arise from differing mechanisms by which the proteins are able to provide their functions *in trans*. The membrane association of NS5A is governed by an N-terminal amphipathic α -helix, whereas NS4B is an integral membrane protein that is tightly anchored to the ER by its four TMDs (Brass et al., 2002, Lundin et al., 2003). It has been speculated that the looser association of NS5A with membranes may facilitate its exchange between distinct RCs located at different intracellular sites, whereas such a scenario may not arise for NS4B (Appel et al., 2005a). Indeed, NS4B exhibits a low level of mobility when localised to intracellular foci (Gretton et al., 2005). Hence, complementation of NS4B may occur within individual sites of viral RNA replication and we propose a model in which more than one genome can be incorporated into a single RC (Figure 5.9). Such an event may be rare and could account for the lower efficiency of NS4B complementation compared to NS5A. The incorporation of two distinct SGRs into a single RC might create a local pool of viral components, a combination of which could reconstitute active replication (Figure 5.9). Therefore, the replication of both SGRs would be mutually dependent and rely on the continuous reciprocal *trans*-complementation of functional proteins from both genomes. It is unlikely that replication of the input mutant RNA occurs in RCs formed by the functional SGR already present in cells (as with 2/1 cells), since detection of replication should then be possible for all NS4B mutants. Similarly, SGRs harbouring the GND mutation within NS5B should be replicated if this were the case. Recombination between the two SGRs is also unlikely, since this event would be expected to occur with all mutants tested.

The wt luc-JFH1_{GFP} SGR exhibited efficient levels of replication when electroporated into 2/1 cells containing a replicating helper JFH1 SGR (Figure 5.2, B). In contrast, luc-JFH1_{GFP} replication was partially attenuated when introduced into Huh-7 cells simultaneously with the same helper JFH1 SGR (Figure 5.1, C). These results suggest that competition occurs when two replication-competent SGRs are introduced simultaneously into a cell. Previous studies have shown that Huh-7 cells containing a replicating SGR are refractory to replication of a second SGR (Evans et al., 2004a). Furthermore, SGR replication efficiency is inversely correlated with the amount of SGR RNA introduced into a cell (Lohmann et al., 2003). The conclusion from both studies was that host cell components necessary for RC formation and/or function might be limiting in Huh-7 cells. The data presented in this chapter suggest SGRs introduced simultaneously into cells may

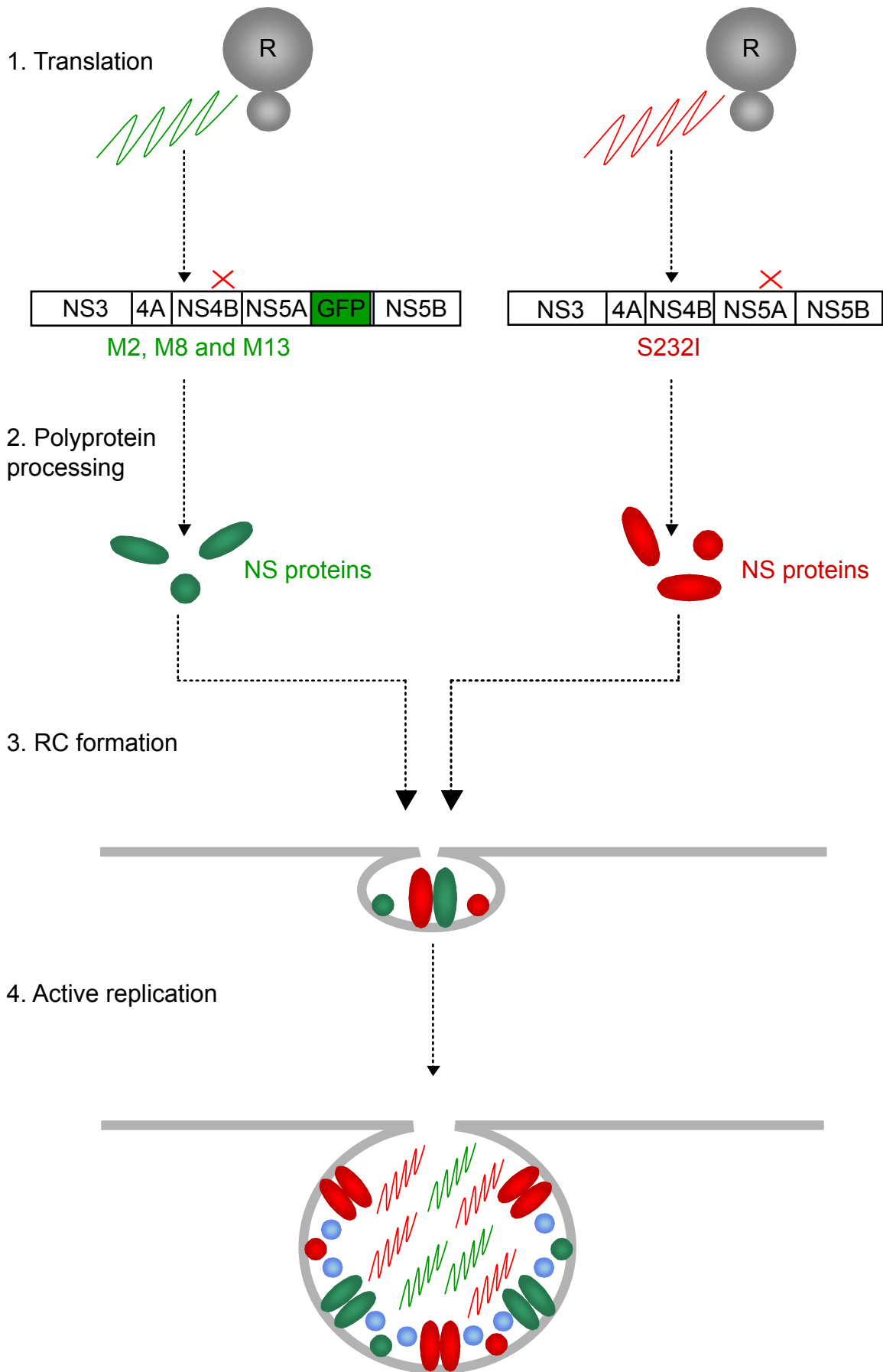


Figure 5.9 Proposed model for NS4B *trans*-complementation and reconstitution of active RNA replication

The translation of the two non-replicating RNA genomes results in two species of subgenomic polyprotein; one encoding non-functional NS4B (M2, M8 and M13, shown in green) and the other encoding non-functional NS5A (S232I, shown in red). The non-functional proteins in each case are depicted with a red cross. Alone, these SGRs are incapable of forming RCs that replicate viral RNA. However, co-electroporation of both SGRs into cells may result in a pool of NS proteins from each genome. It is possible that a combination of proteins from each SGR may be able to form a hybrid RC that contains functional NS4B (from the S232I SGR) and functional NS5A (from the M2, M8 and M13 SGRs), in addition to the other NS proteins and host cell factors (shown in light blue) required for viral RNA replication. These hybrid RCs would therefore be functional and replication of two distinct mutant genomes (shown in green and red) might occur within a single complex. Hence, each SGR would be mutually dependent on the other for replication.

compete for limiting host cell factors involved in the formation of RCs. However, this competition was not observed upon introduction of an SGR into cells that already contained actively replicating viral RNA. This result raises at least two possibilities. Firstly, limiting host factors may be required for the formation of RCs but not the process of RNA replication. Hence, these factors would be released from RCs formed by the first SGR, making them available to the second SGR. Secondly, limiting host cell factors may be retained within formed RCs and therefore synthesis of these factors may have to exceed a threshold level in order for a second SGR to create sites capable of replicating viral RNA. Alternatively, 2/1 cells have been shown to harbour lower levels of viral RNA compared to cells that have been electroporated transiently with RNA from a SGR (B. Flatley and P. Domingues, personal communications). It is therefore possible that excess viral RNA that is introduced into cells by electroporation sequesters limiting host cell factors and that this sequestration does not occur in 2/1 cells where a lower level of viral RNA is present.

The data obtained from the cell lines harbouring non-replicating SGRs revealed that NS5A could be detected in the majority of cells, whereas fewer cells contained NS5A-GFP (Figure 5.7, A). This result was surprising, since all cells were expected to contain NS5A (expressed from neo-JFH1_{S232I}) and NS5A-GFP (expressed from neo-M2_{GFP} and neo-M8_{GFP}). NS5A-GFP should *trans*-complement neo-JFH1_{S232I}, restoring replication of this SGR. In turn, replication of neo-JFH1_{S232I} would provide functional NS4B that could *trans*-complement neo-M2_{GFP} or neo-M8_{GFP}. In other words, the mutual dependency of each SGR relies on the presence of functional NS5A-GFP, since the untagged NS5A produced by neo-JFH1_{S232I} is defective. The detection of cells expressing dsRNA (Figure 5.7, B) and NS5A but not NS5A-GFP could indicate that neo-JFH1_{S232I} replicates but neo-M2_{GFP} and neo-M8_{GFP} do not. At least two possibilities could explain these results. Firstly, NS5A-GFP may be present in all cells replicating viral RNA but at a level too low to be detected by direct visualisation. This hypothesis is plausible since NS5A can be *trans*-complemented efficiently in comparison to NS4B and therefore a very low level of NS5A-GFP could be sufficient to restore replication of neo-JFH1_{S232I}. Alternatively, the S232I mutation may have reverted, or other compensatory mutations within neo-JFH1_{S232I} could have arisen. Such mutations could permit neo-JFH1_{S232I} to replicate in the absence of either neo-M2_{GFP} or neo-M8_{GFP}. Sequence analysis of RNA extracted from both cell lines is necessary to distinguish between these possibilities.

In HCV-infected patients, quasispecies represent a heterogeneous spectrum of mutant genomes that arise due to the lack of proofreading ability possessed by the HCV-encoded NS5B polymerase (Martell et al., 1992). The finding that replication can be reconstituted from non-replicating genomes (Figures 5.5 and 5.6) could have implications for the maintenance of quasispecies pools in infected patients. For example, the infection of a single hepatocyte with two non-replicating HCV quasispecies may result in *trans*-complementation and therefore the formation of sites active in viral RNA synthesis. Additionally, recent studies have shown that release of virus can be rescued by complementation of the NS2 protein (Jirasko et al., 2008) and furthermore, that subgenomic genomes can be packaged by supplying the HCV structural proteins *in trans* (Ishii et al., 2008, Steinmann et al., 2008). Therefore, *trans*-complementation may provide a mechanism to permit replication and packaging of quasispecies that harbour deleterious mutations. A further understanding of the interactions between distinct HCV genomes, detailing which mutations can and cannot be *trans*-complemented, may provide further insight into the replication strategies of quasispecies within infected patients.

6 NS4B Influences the Production of Infectious Virus Particles

6.1 Introduction

It has become increasingly apparent that the HCV NS proteins do not function solely in viral RNA replication but are also engaged in virus production. Assembly of viral particles is thought to initiate at LDs, intracellular storage sites for triacylglycerols and cholesterol esters (Miyahari et al., 2007). The viral capsid is composed of HCV core protein (see Section 1.2.2.2), whose association with LDs is critical for the production of infectious virus progeny (Boulant et al., 2007, Shavinskaya et al., 2007, Targett-Adams et al., 2008b). However, the recruitment of both NS proteins and viral RNA by core to LDs requires NS5A and disruption of NS5A-core association leads to a severe decline in infectious particle production (Masaki et al., 2008, Miyahari et al., 2007). Furthermore, the helicase domain of NS3 is important for a pre-assembly step in virus production that is independent of its role in viral replication (Ma et al., 2008). Thus, NS proteins such as NS5A and NS3 do not solely facilitate RNA replication but extend their roles to the latter stages of the virus life cycle.

To date, no role for the NS4B protein in virus production has been established. Therefore, our aim was to determine whether mutations within the NS4B C-terminus, which did not affect replication, had any influence on the production of infectious HCV particles.

6.2 TCID₅₀ Analysis of JFH1 Mutants Harboring Mutations Within the C-terminus of NS4B

The mutagenic screen of the NS4B C-terminus had revealed 10 mutant SGRs that retained their ability to replicate viral RNA (see Section 4.3.1). Eight of these mutants (M1, M6, M7, M9, M10, M12, M14, M15) replicated to levels equivalent to a wt SGR and two mutants (M3 and M11) exhibited attenuated RNA replication, as judged by luciferase assay. To determine whether NS4B influenced virion production, each mutation was introduced into JFH1, a cDNA construct encompassing the entire viral genome that is capable of producing infectious virus particles (Wakita et al., 2005, Zhong et al., 2005). All 10 JFH1 mutants were

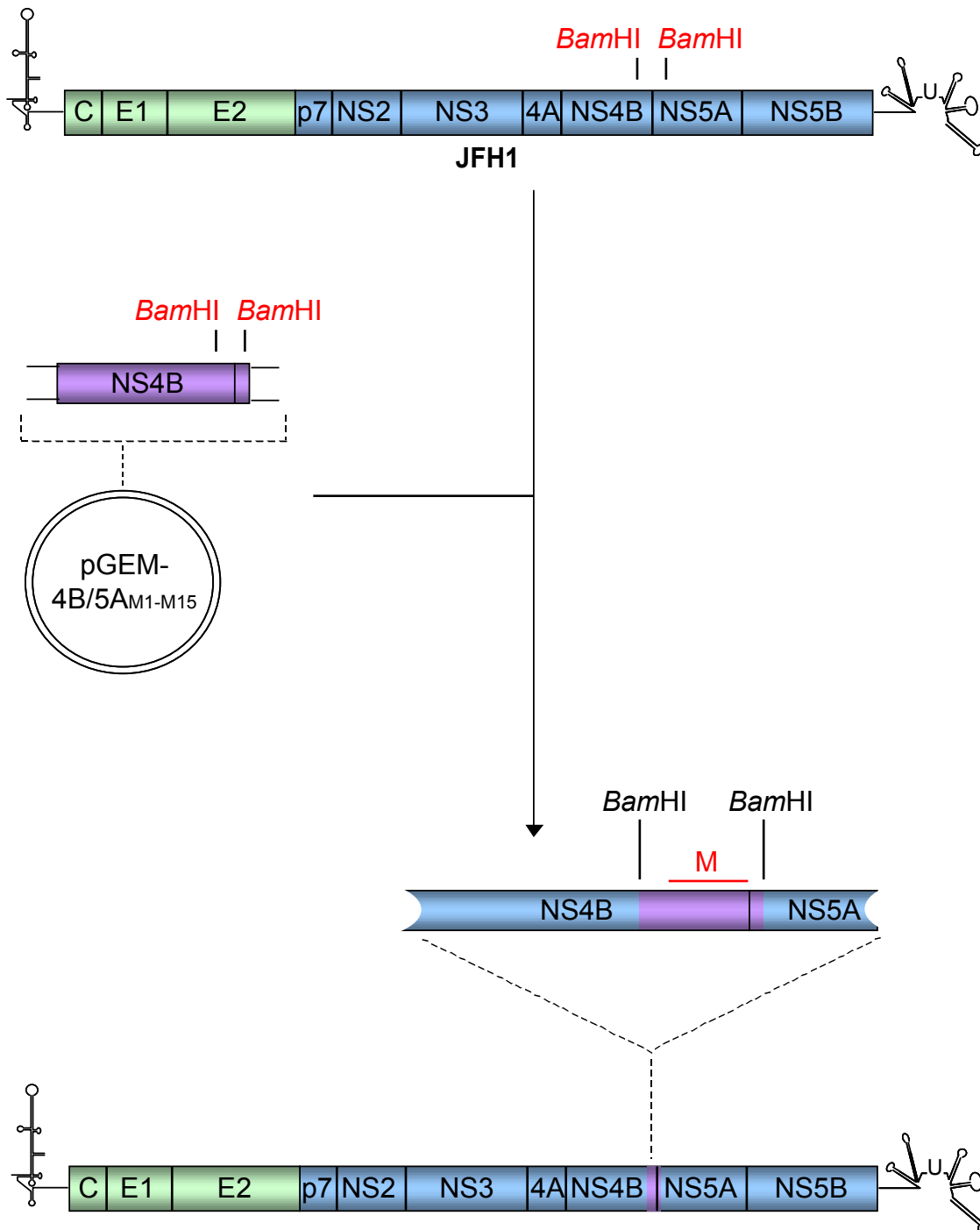


Figure 6.1 Insertion of NS4B C-terminal mutations into the genomic JFH1 cDNA

The 266bp NS4B/NS5A fragment containing the mutations within the C-terminus of NS4B was released from the pGEM-4A/5A_{M1-M15} plasmid series using *Bam*HI. The fragments were directly inserted between the corresponding restriction sites in JFH1, which contained the genome-length cDNA for strain JFH1. All constructs were screened for correct orientation of the *Bam*HI fragment. This method was used to create 10 mutants containing individual mutations within the C-terminus of NS4B (depicted with a red M above). These JFH1 mutants were termed JFH1_{M1}, JFH1_{M3}, etc.

created by excision of 266bp *Bam*HI fragments from the pGEM-4B/5A_{M1-M15} plasmid series (see Section 4.2 and Figure 4.4, A), followed by insertion and orientation of the fragment between the corresponding sites in pJFH1 (Figure 6.1). RNA encoding the 10 mutants (JFH1_{M1}, JFH1_{M3}, etc) was electroporated into cells. The supernatant was removed from electroporated cells at 24, 48 and 72 hours and used to infect naïve cells. Cells were also electroporated with RNA from wt JFH1 (hereafter referred to as JFH1) and JFH1_{ΔE1/E2}, a JFH1 mutant that is incapable of producing infectious virus particles due to an in-frame deletion of the E1 and E2 glycoprotein coding regions. These RNAs served as positive and negative controls respectively. Production of infectious virus was determined by TCID₅₀ (median tissue culture infective dose) analysis, an assay determining the amount of pathogenic agent required to produce pathological change in 50% of the cells inoculated (Figure 6.2). TCID₅₀ analysis revealed that cells electroporated with JFH1 RNA produced approximately 1.6×10^4 infectious particles/ml by 72 hours, consistent with previous reports (Pietschmann et al., 2006, Zhong et al., 2005). In contrast, cells harbouring JFH1_{ΔE1/E2} RNA produced barely detectable levels of infectious particles and the TCID₅₀ value for this mutant remained at the detection limit of 2.24 particles/ml over the 72-hour period (Figure 6.2). Seven of the JFH1 NS4B mutant RNAs (M1, M7, M9, M10, M12, M14 and M15) produced levels of infectious virus that were comparable to JFH1 and the amount of secreted virus steadily increased over the 72-hour time period. JFH1_{M3} and JFH1_{M11} RNAs produced approximately 2.4×10^3 and 3.1×10^3 infectious particles/ml respectively by 72 hours post-electroporation, almost seven- and five-fold lower respectively than the titres produced by JFH1 RNA at the same time point (Figure 6.2). The reduced level of virus release exhibited by these two mutants is likely a consequence of attenuated viral replication, as observed previously (see Section 4.3.1). Interestingly, cells electroporated with JFH1_{M6} RNA generated approximately 7.9×10^4 infectious particles/ml by 72 hours, five-fold greater than the levels observed with JFH1 RNA, and increased virus production was evident at all time points tested (Figure 6.2). The increased level of virus production exhibited by JFH1_{M6} was confirmed in several repeat experiments (data not shown). These data suggested that the Asn residue at amino acid 216 of the NS4B C-terminus influenced processes involved in the production of infectious virus particles.

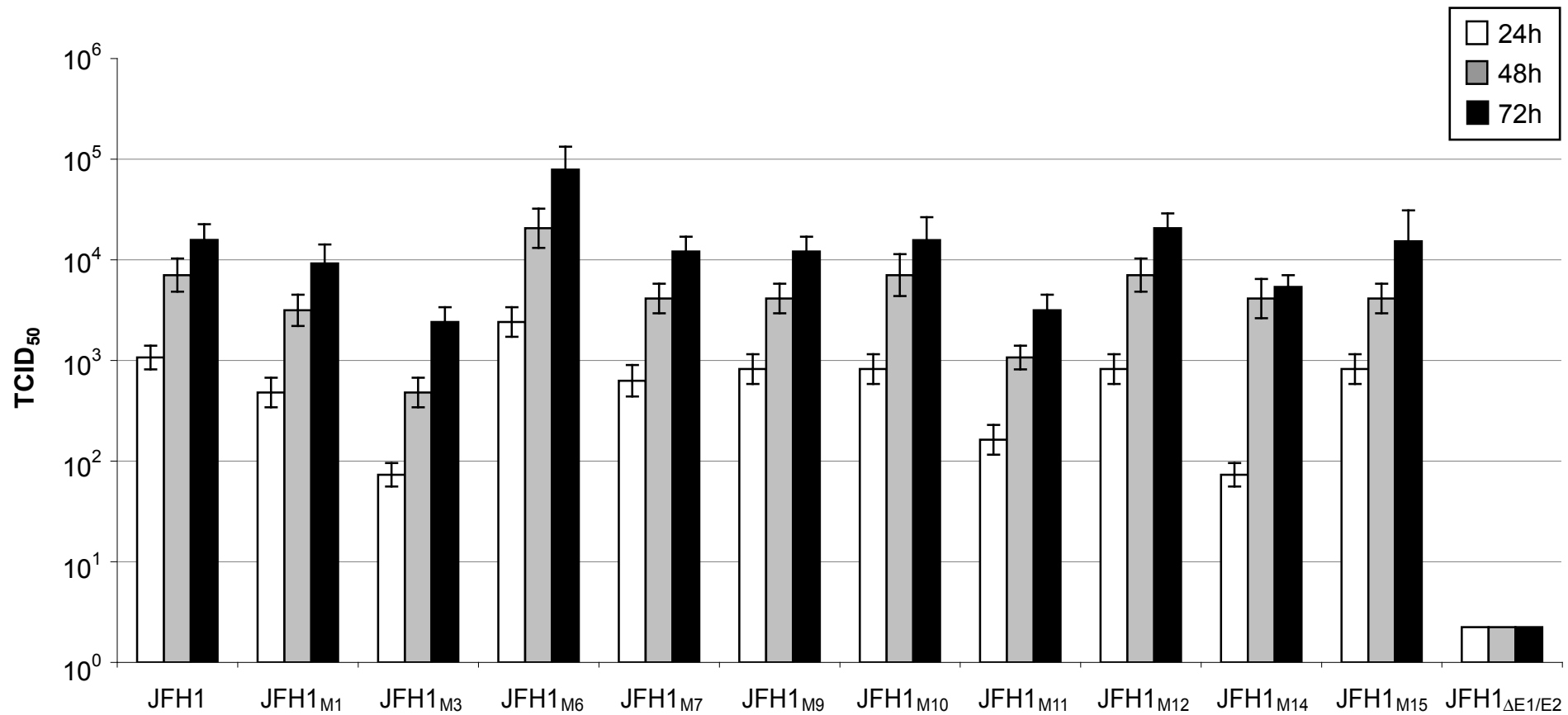


Figure 6.2 TCID₅₀ analysis of JFH1 harbouring mutations within the C-terminus of NS4B

Huh-7 cells were electroporated with RNA from JFH1, JFH1_{ΔE1/E2} and each JFH1 NS4B mutant (JFH1_{M1}, JFH1_{M3}, etc). At 24, 48 and 72 hours post-electroporation, cell culture medium was removed and 1ml was added to naïve Huh-7 cells for 72 hours. Infectious virus particle release from supernatants harvested at 24 (white), 48 (grey) and 72 (black) hours was determined for each construct by TCID₅₀ analysis. The values shown are an average of six data sets and error bars indicate standard errors.

6.3 Characterisation of JFH1_{M6}

6.3.1 JFH1_{M6} Enhances the Production of Infectious Virus Particles

TCID₅₀ analysis had revealed that JFH1_{M6} enhanced the production of infectious HCV virions to a level greater than that observed using JFH1. To confirm this result, cells electroporated with RNA from JFH1 and JFH1_{M6} were harvested for Western blot analysis at 24, 48 and 72 hours. Additionally, the supernatant (containing virus particles) was removed from electroporated cells at 24, 48 and 72 hours and 1ml of supernatant medium was used to infect naïve cells. As additional controls, cells were also infected with supernatant taken from cells electroporated with mutants that abolished (JFH1_{ΔE1/E2}), decreased (JFH1_{M3}), or had no effect (JFH1_{M1}) on virus production (Figure 6.2). 72 hours post-infection, cells were harvested and NS5A was detected in both electroporated and infected cells using NS5A-specific antisera (Figure 6.3, A).

NS5A could be detected at approximately equal levels for all viruses in RNA-electroporated cells at 24, 48 and 72 hours, including the replication-attenuated JFH1_{M3} mutant. In infected cells, JFH1_{M1} produced levels of NS5A indistinguishable from those seen with JFH1, indicating that an equivalent level of infection was achieved with both viruses (Figure 6.3, A). In contrast, a diminished NS5A signal was observed in cells infected with JFH1_{M3} and NS5A was undetectable in cells inoculated with media harvested from JFH1_{ΔE1/E2}. Importantly, NS5A was detected at all time points in cells infected with JFH1_{M6} and in greater quantities than observed for JFH1 (Figure 6.3, A).

As further support for this result, cells infected in parallel to those used for Western blot analysis were probed using NS5A antisera and protein was visualised at 48 hours-post infection (Figure 6.3, B). NS5A was observed in all virus-infected cells, with the exception of JFH1_{ΔE1/E2}. Approximately equal numbers of infected cells were visualised for JFH1 and JFH1_{M1}, while fewer NS5A-expressing cells could be detected with JFH1_{M3}. However, a greater number of infected cells were visualised with JFH1_{M6} (Figure 6.3, B). The data obtained collectively through TCID₅₀, Western blot and IF analyses confirmed that cells electroporated with JFH1_{M6} RNA produced an increased level of infectious virus particles compared to JFH1 RNA.

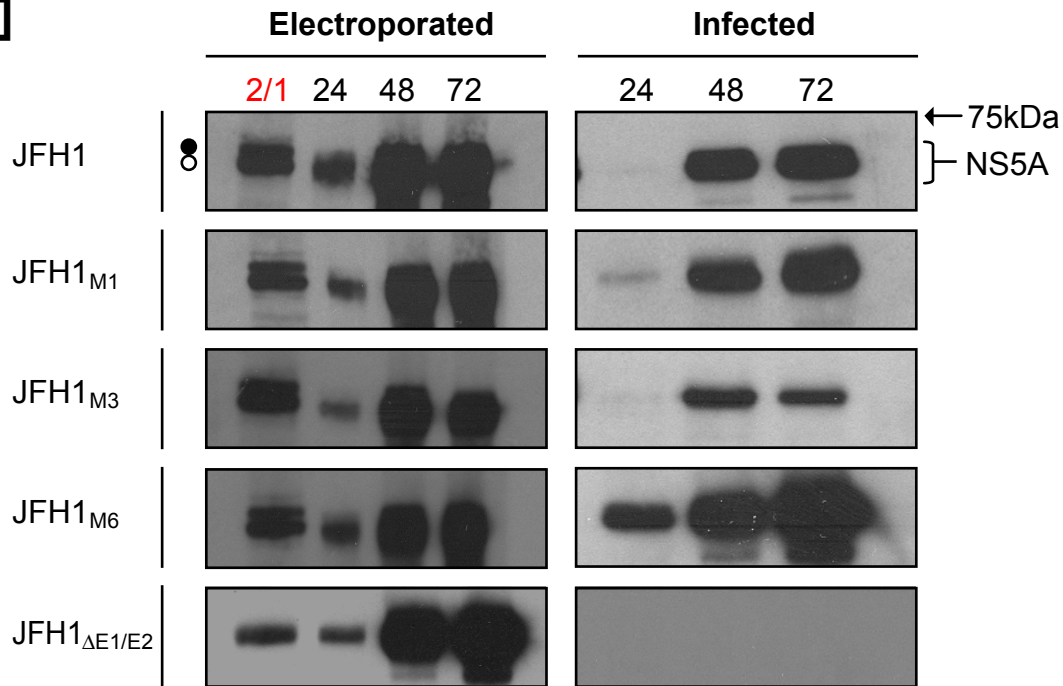
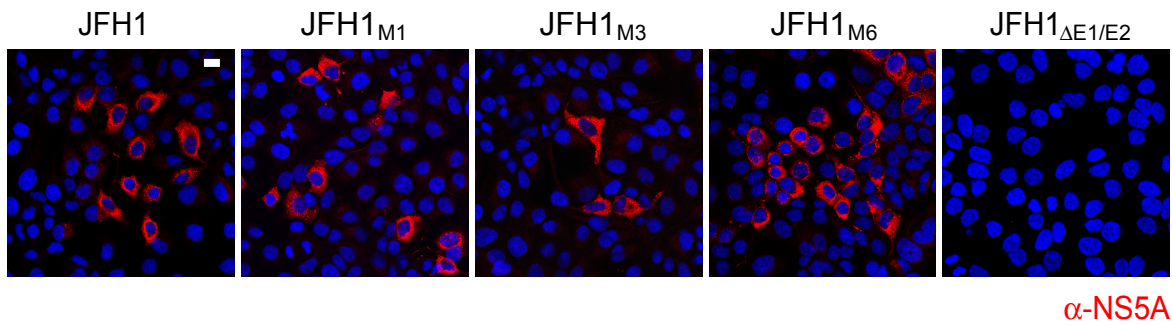
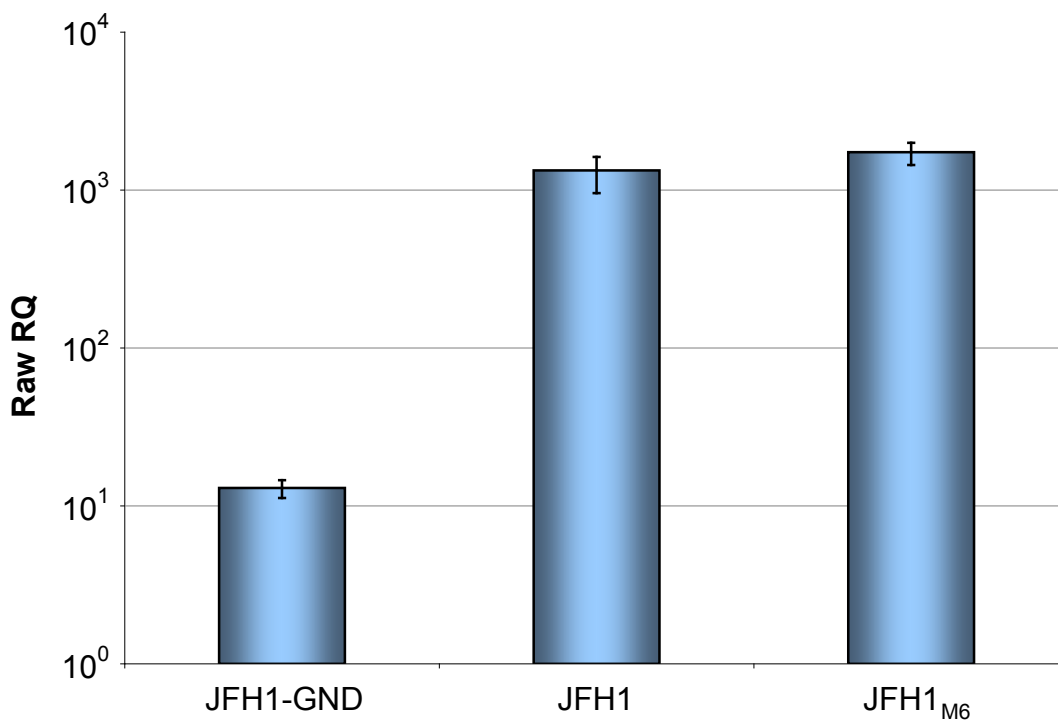
[A]**[B]** α -NS5A**[C]**

Figure 6.3 JFH1_{M6} enhances the production of infectious virus particles

[A] Huh-7 cells were electroporated with RNA encoding JFH1 NS4B mutants that decreased (JFH1_{M3}), enhanced (JFH1_{M6}) or had no effect on infectious virus production (JFH1_{M1}). Cells electroporated with JFH1 and JFH1 Δ E1/E2 were also included as controls. At 24, 48 and 72 hours post-electroporation, cells were harvested for Western blot analysis with anti-NS5A antisera and 1ml of cell culture medium was removed and added to naïve Huh-7 cells. 72 hours after incubation, the infected cells were also harvested for Western blot analysis. 2/1 cells harbour an autonomously replicating JFH1 SGR and were used as a positive control for NS5A detection. The hyper- (closed circles) and hypo- (open circles) phosphorylated species of NS5A are indicated.

[B] Cells infected in the same manner described in [A] were fixed and stained using NS5A antisera and DAPI. Cells infected using 48-hour time point media are shown. Scale bar represents 10 μ M.

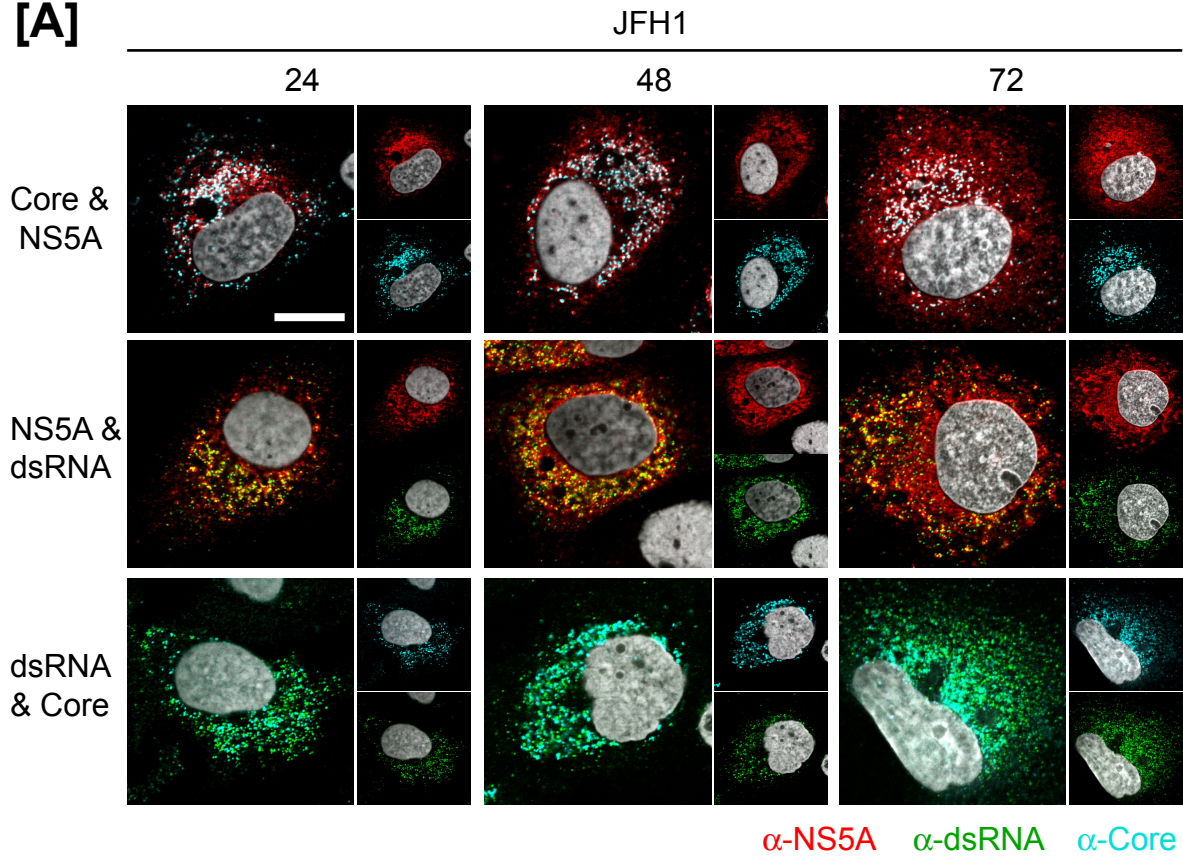
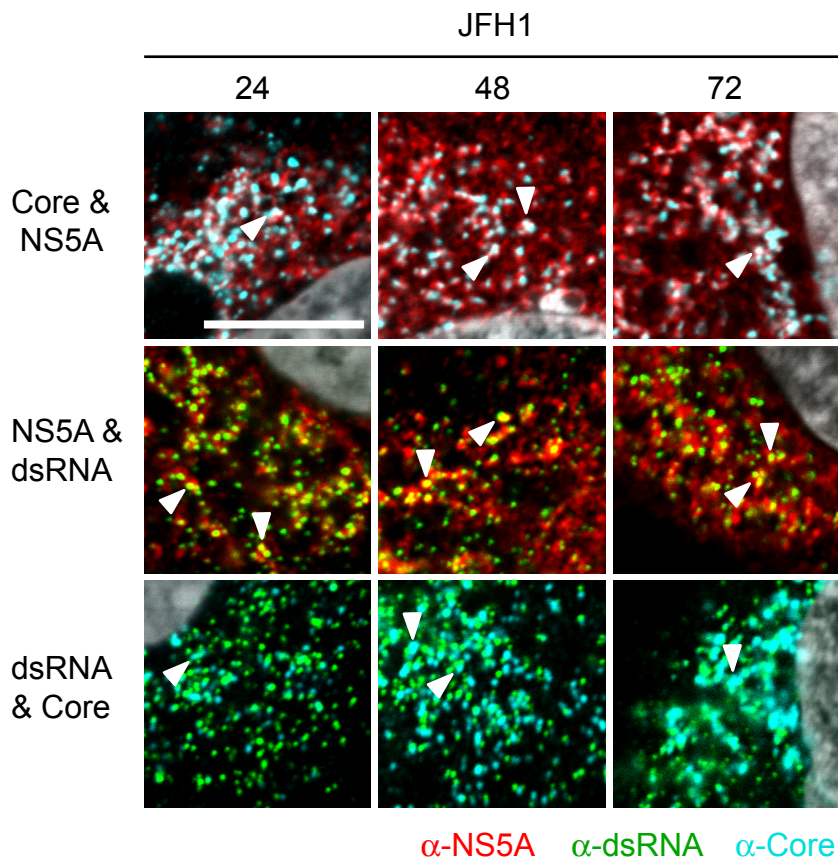
[C] Huh-7 cells electroporated with RNA from JFH1, JFH1_{M6} and JFH1-GND were trypsinised and re-seeded 48 hours post-electroporation and cultured for a further 72 hours. Total RNA was then extracted from the cells and HCV RNA was quantified by qRT-PCR. The relative quantification (raw RQ) values represent a comparison of the level of viral RNA across the samples tested. The data in part [C] was kindly provided by G.Hope and P. Domingues.

6.3.2 Replication of JFH1_{M6} RNA is not Enhanced in Electroporated Cells

Measurement of luciferase activity had previously shown that the subgenomic version of JFH1_{M6}, luc-M6_{GFP}, displayed no increase in replication compared to luc-JFH1_{GFP} (see Section 4.3.1). However, it was possible that the M6 mutation may increase RNA replication in the context of a full-length genome that did not contain GFP within the NS5A coding region. Such an increase in genome synthesis may account for the enhanced production of infectious progeny, meaning JFH1_{M6} may not influence virus production directly. To examine this possibility, total RNA was extracted from cells electroporated with JFH1 and JFH1_{M6} RNAs and HCV RNA was quantified by qRT-PCR (Figure 6.3, C). HCV RNA was measured in cells electroporated with JFH1-GND RNA (a full-length genome incapable of viral RNA replication) and Huh-7 cellular RNA was included as a further negative control. JFH1 and JFH1_{M6} RNA levels were greater than those measured in cells harbouring JFH1-GND (by 134-fold) and naive Huh-7 cells (by 1700-fold) respectively, indicating that the detected RNA resulted from active viral replication (Figure 6.3, C). In agreement with previously shown luciferase data (see Section 4.3.1), the quantity of viral RNA in cells electroporated with JFH1 and JFH1_{M6} genomes was approximately equal (Figure 6.3, C). Therefore, the enhancement of virus production observed with JFH1_{M6} was not a consequence of increased RNA replication.

6.3.3 JFH1_{M6} does not Alter the Localisation of NS5A, Core or dsRNA in Infected Cells

NS5A is thought to be responsible for the transfer of NS proteins and viral RNA to core protein situated at the surface of LDs (Miyanari et al., 2007). It is therefore possible that the rate and/or quantity of RNA distributed to core by NS5A could be a determining factor in the levels of infectious virus produced. To determine whether JFH1_{M6} altered the trafficking of RNA to core, the intracellular localisation of core, NS5A and dsRNA was examined in cells electroporated with RNA encoding JFH1 and JFH1_{M6} at 24, 48 and 72 hours post-electroporation (Figure 6.4). At each time point in cells electroporated with JFH1 RNA, sites of co-localisation were observed for core, NS5A and dsRNA in the cytoplasm (Figure 6.4, A and B). Upon examination of cells harbouring JFH1_{M6} RNA, the localisation

[A]**[B]**

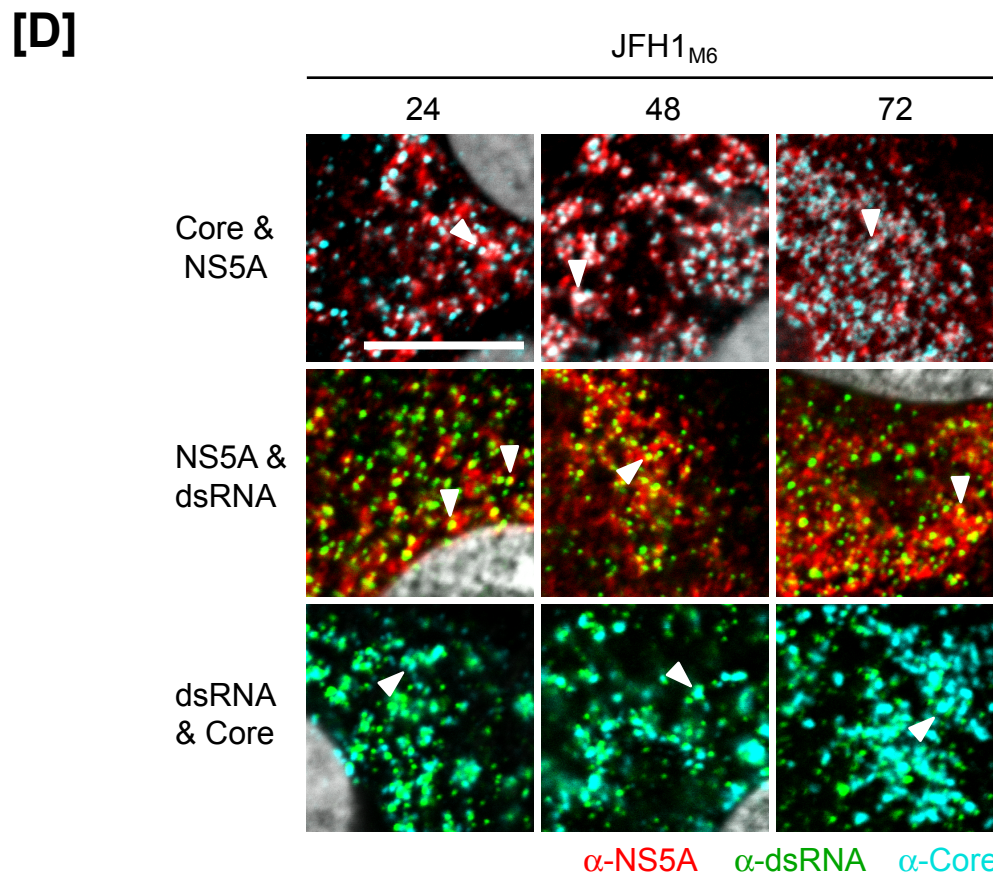
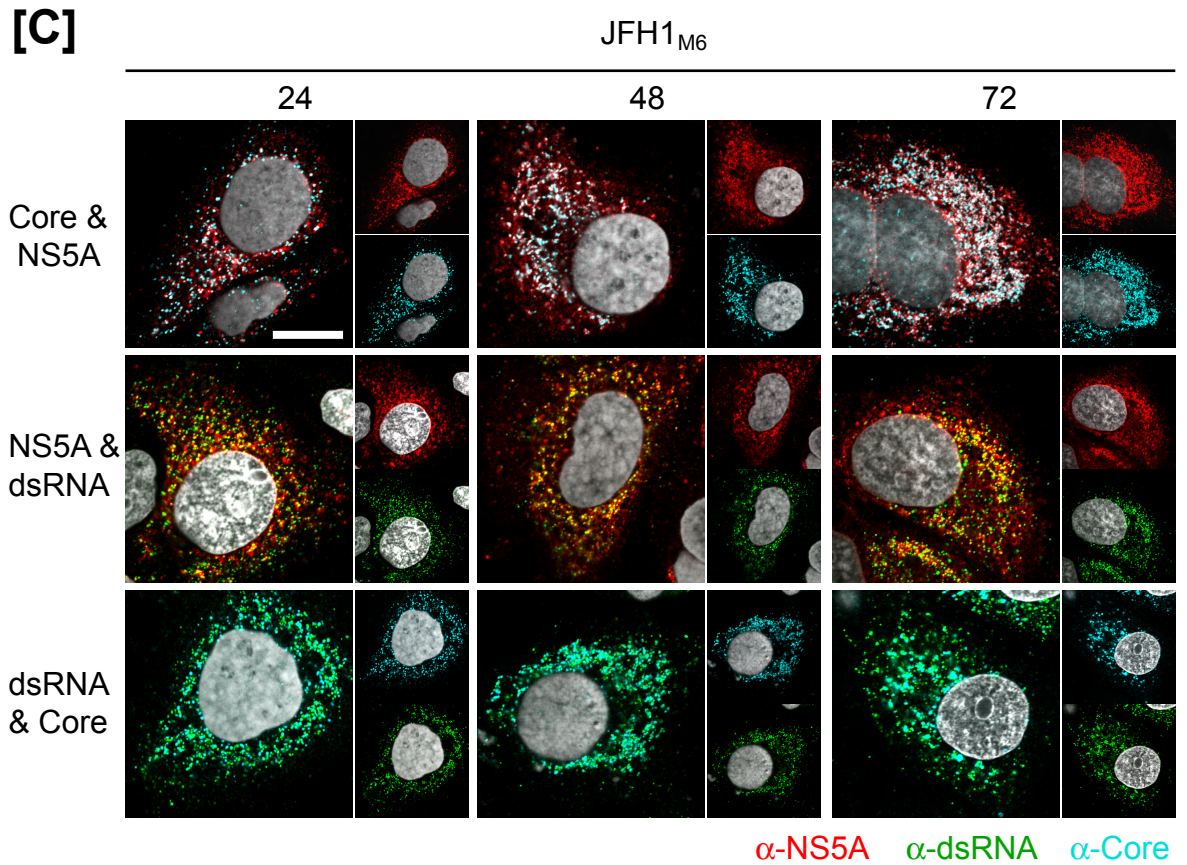


Figure 6.4 JFH1_{M6} does not alter the localisation of NS5A, core or dsRNA

Huh-7 cells electroporated with RNA from **[A]** JFH1 and **[C]** JFH1_{M6} were fixed and probed using core and NS5A antiserum, J2 to detect dsRNA and DAPI at 24, 48 and 72 hours post-electroporation. Enlarged regions for **[B]** JFH1 and **[D]** JFH1_{M6} are shown and areas of co-localisation are indicated by white arrowheads. Scale bars represent 10 μ m.

pattern of core, NS5A and dsRNA at each time point was indistinguishable from that seen for JFH1 (Figure 6.4, C and D). Therefore, the enhanced production of infectious virus by JFH1_{M6} was not apparently attributed to an increase in the NS5A-dependent distribution of viral RNA to sites of core localisation.

6.4 Introduction of mutation M6 into J6-JFH1

6.4.1 Characterisation of J6-JFH1

J6-JFH1 is a chimeric virus in which the coding sequences incorporating JFH1 core to the loop region between TMDs 1 and 2 in NS2 is replaced with the corresponding sequence from genotype 2a strain HC-J6 (Figure 6.5, A). This virus is identical to a chimeric construct called Jc1, which produces virus titres that are significantly greater than those obtained with JFH1 (Pietschmann et al., 2006). To determine whether, like Jc1, J6-JFH1 displayed increased production of infectious virus compared to JFH1, cells electroporated with JFH1 and J6-JFH1 RNAs and growth medium supernatants were analysed by TCID₅₀. Consistent with data published on Jc1, J6-JFH1 produced approximately 68- and five-fold more infectious virus compared to JFH1 at 24 and 72 hours respectively, and produced a peak titre of approximately 5×10^5 infectious particles/ml (Figure 6.5, B). This increase in virus production was also evident upon examination of cell extracts by Western blot analysis, since a much greater level of NS5A was detected in cells infected with J6-JFH1, as compared to JFH1 (Figure 6.5, C, right-hand panel). Therefore, J6-JFH1 provided another infectious clone for further study of the role of NS4B in virus production.

6.4.2 Introduction of M6 into J6-JFH1 Represses Infectious Particle Production

Introduction of the M6 mutation into JFH1 increased the production of infectious viral particles by approximately five-fold by 72 hours post-electroporation (Figure 6.2). To determine whether this increase in virus production could be transferred to a chimeric virus, M6 was introduced into J6-JFH1, generating J6-JFH1_{M6} (Figure 6.6, A). RNA encoding J6-JFH1 and J6-JFH1_{M6} was electroporated into cells and infectious particles released into the supernatant at 24, 48 and 72 hours were used to infect naïve cells. 72 hours later, infected cells were analysed using the TCID₅₀ method to determine virus titre (Figure 6.6, B). As found previously, J6-

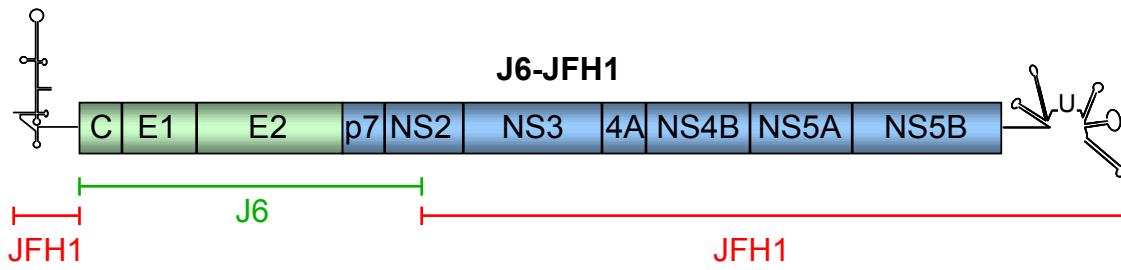
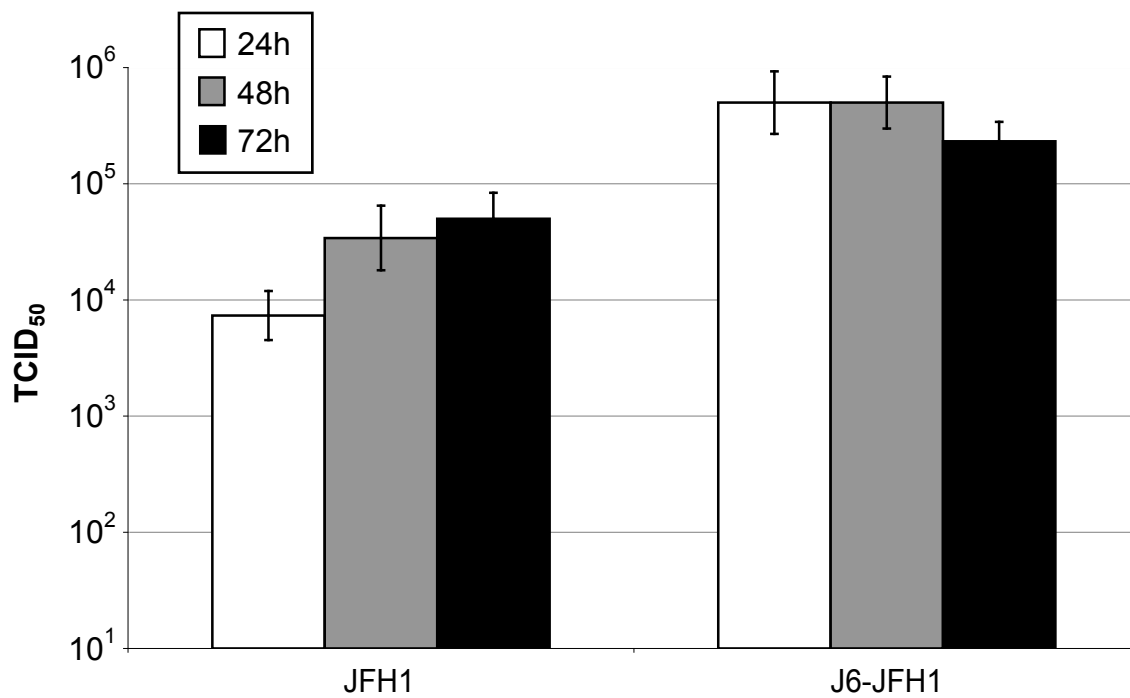
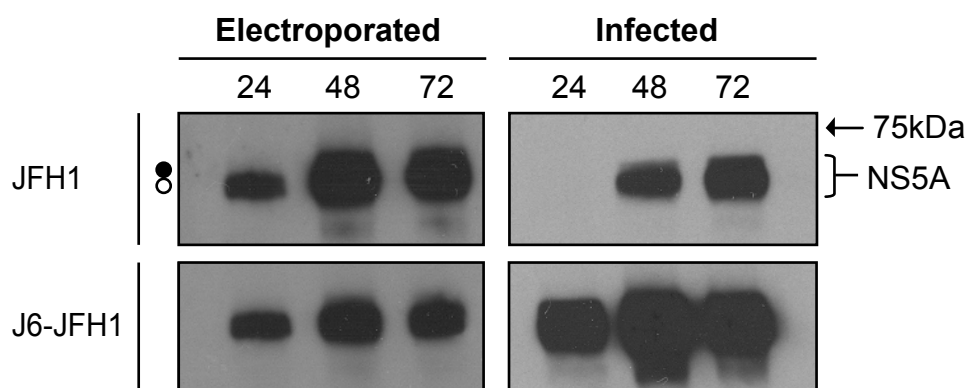
[A]**[B]****[C]**

Figure 6.5 Characterisation of J6-JFH1

[A] Schematic representation of the chimeric virus J6-JFH1. In J6-JFH1, the JFH1 sequence from core to the loop region between TMDs 1 and 2 in NS2 (amino acids 1-864 in the JFH1 polyprotein sequence) is replaced with the corresponding sequence from the genotype 2a strain HC-J6. **[B]** Huh-7 cells were electroporated with RNA from JFH1 and J6-JFH1. At 24, 48 and 72 hours post-electroporation, cell culture medium was removed and 1ml was added to naïve Huh-7 cells for 72 hours. Infectious virus particle release at 24 (white), 48 (grey) and 72 (black) hours was determined for each construct by TCID₅₀ analysis. The values shown are an average of six data sets and error bars indicate standard errors. **[C]** At 24, 48 and 72 hours post-electroporation, cells set up in parallel to those described in [B] were harvested for Western blot analysis using anti-NS5A antisera and 1ml of cell culture medium was removed and added to naïve Huh-7 cells for 72 hours. The infected cells were then harvested for Western blot analysis. The hyper- (closed circles) and hypo- (open circles) phosphorylated species of NS5A are indicated.

Figure 6.6 Introduction of M6 into J6-JFH1 reduces production of infectious virus particles

[A] Schematic representation of the chimeric virus J6-JFH1_{M6}, highlighting the position of the M6 mutation within the NS4B coding region. **[B]** Huh-7 cells were electroporated with RNA from J6-JFH1 and J6-JFH1_{M6}. At 24, 48 and 72 hours post-electroporation, cell culture medium was removed and 1ml was added to naïve Huh-7 cells for 72 hours. Infectious virus particle release at 24 (white), 48 (grey) and 72 (black) hours was determined for each construct by TCID₅₀ analysis. The values shown are an average of six data sets and error bars indicate standard errors. **[C]** At 24, 48 and 72 hours post-electroporation, cells set up in parallel to those described in [B] were harvested for Western blot analysis using anti-NS5A antisera and 1ml of cell culture medium was removed and added to naïve Huh-7 cells for 72 hours. Infected cells were then harvested for Western blot analysis. The hyper- (closed circles) and hypo- (open circles) phosphorylated species of NS5A are indicated.

JFH1 produced high viral titres that peaked at approximately 2.3×10^5 infectious particles/ml by 48 hours. Surprisingly, cells electroporated with J6-JFH1_{M6} RNA produced lower levels of virus at each time point compared to J6-JFH1 RNA and produced a peak titre of only 2.7×10^4 infectious particles/ml, almost nine-fold lower than observed with the unmodified chimeric virus (Figure 6.6, B). Western blot analysis of cells electroporated with J6-JFH1 and J6-JFH1_{M6} RNAs revealed an indistinguishable level of NS5A, suggesting that replication of J6-JFH1_{M6} was not attenuated in comparison to J6-JFH1 (Figure 6.6, C). However, NS5A was less readily detected in cells infected with J6-JFH1_{M6} compared to those infected with J6-JFH1. Thus, J6-JFH1_{M6} was apparently compromised in its ability to produce infectious virus.

The results presented in this chapter demonstrate that a single amino acid mutation at position 216 in the NS4B C-terminus can increase the production of infectious virus from JFH1. By contrast, a decrease in virus production is observed upon insertion of the same mutation into the chimeric viral genome J6-JFH1.

6.5 Discussion

Several investigations into members of the *flaviviridae* family, including BVDV, YFV, DV and KV, have contributed to a growing body of evidence demonstrating that the NS proteins encoded by these viruses contribute significantly to virus production (Murray et al., 2008). Recently, analysis of the latter stages of the HCV life cycle has become possible with the discovery that full-length genomes derived from JFH1 are capable of producing infectious virus particles *in vitro* (Lindenbach et al., 2005, Wakita et al., 2005, Zhong et al., 2005). Since that time, it has become increasingly apparent that, like other members of the *flaviviridae*, the HCV NS proteins are not only engaged in viral RNA replication, but also the production of virus particles. For example, NS3 (Ma et al., 2008, Yi et al., 2007) and NS5A (Appel et al., 2008, Masaki et al., 2008, Miyanari et al., 2007, Tellinghuisen et al., 2008a) are required for viral replication, and are essential for, or at least contribute towards, the production of infectious virus particles. The results presented here reveal that NS4B also contributes towards virus production.

In JFH1, mutation of a single asparagine residue at position 216 of NS4B was sufficient to increase production of virus by up to five-fold (Figure 6.2) and this effect was not due to increased replication of the viral genome (Figure 6.3, C). NS4B is a component of viral RCs, which provide the environment for RNA

replication and are recruited to core-coated LDs during infection (Miyanari et al., 2007). RC components can modulate virus production, since amino acid changes within another RC protein, NS3, are able to rescue virus production in chimeric replicons that are otherwise defective in this process (Ma et al., 2008, Yi et al., 2007). Virus assembly is likely to involve the engagement of viral RNA with core protein for packaging, a process that may be influenced by NS4B located within RCs. This influence could be direct, where NS4B may modulate RNA export from RCs to core situated on LDs. This hypothesis is strengthened by a study reporting that NS4B binds to viral RNA (Einav et al., 2008). Alternatively, the contribution of NS4B to virus production could be achieved indirectly, by influencing the behaviour of another protein such as NS5A. NS5A is a RNA-binding protein (Huang et al., 2005) and the transfer of RNA from RCs to LDs is mediated in an NS5A-dependent manner (Miyanari et al., 2007). Hence, the M6 mutation within NS4B may enhance the RNA transfer activity of NS5A, leading to increased assembly of infectious virions at LDs. While no differences in the localisation of core, NS5A or dsRNA was observed for JFH1_{M6} (Figure 6.4), the distribution of these proteins could be altered in a manner too subtle to be detected by IF analysis. Finally, phosphorylation of a single serine residue within domain III of NS5A is important for virus production (Tellinghuisen et al., 2008a) and the C-terminus of NS4B can influence this modification of NS5A (see Section 4.3.4). Consequently, it is possible that the M6 mutation within NS4B modulates NS5A phosphorylation and thereby enhances virus production. Again, while no differences in NS5A phosphorylation were observed (Figure 6.3, A), the nature of any subtle differences in NS5A phosphorylation may not be detected by the methods used in this study.

Although M6 leads to an increase in infectious virus production, the stage at which the mutation exerts its effect is unclear. There are at least three possible scenarios that could result in an enhanced level of infectious virions. Firstly, JFH1_{M6} may possess an increased rate of assembly compared to JFH1 and consequently more viral particles are secreted into the supernatant to infect naïve cells. Secondly, the same number of particles may be assembled for both viruses but those produced by JFH1_{M6} may be more readily secreted into the supernatant. Finally, it is possible that JFH1 and JFH1_{M6} assemble and secrete the same number of HCV virions but those secreted by JFH1_{M6} infect naïve cells more effectively. The egress of HCV virions from infected cells is a poorly understood process but is thought to be dependent upon the cellular machinery responsible for VLDL

secretion (Gastaminza et al., 2008, Huang et al., 2007a). Currently, no role for NS4B in this process has been established. Similarly, it is unclear whether any of the NS proteins actually form part of the secreted HCV virion itself, and therefore be capable of modulating virus entry. However, further investigation into the mechanism by which M6 enhances virus production could be conducted in future studies. For example, quantification of the ratio of intracellular and extracellular levels of infectious virus may provide clues as to whether JFH1_{M6} exhibits either increased assembly or increased secretion of virus compared to JFH1. Such analyses have demonstrated that p7 and NS2 are essential for virus production at a pre-assembly step (Jones et al., 2007).

J6-JFH1 (also known as Jc1, Pietschmann et al., 2006) is a chimeric virus in which the core to the loop region between TMDs 1 and 2 in NS2 of JFH1 is replaced with the corresponding sequence from the genotype 2a strain HC-J6. J6-JFH1 is capable of producing a significantly greater titre of infectious virus compared to JFH1, particularly at early time points (Figure 6.5). The combination of J6 core and p7 increases the kinetics of viral release compared to a virus containing J6 core and JFH1 p7, suggesting that genotype-specific interactions between core and p7 are important for virus production and release (Shavinskaya et al., 2007). Interactions between the structural and NS proteins may be generally important, since virus production can be restored in genotype 1a/2a chimeras (which are usually incapable of producing infectious virus) by introduction of compensatory mutations into NS2 and NS3 (Yi et al., 2007). These mutations are hypothesised to correct incompatibilities between the proteins of different HCV genotypes at sites of critical protein-protein interactions required for virus production (Yi et al., 2007). Interestingly, introducing M6 into J6-JFH1 resulted in lower infectious virus production (Figure 6.6), whereas the same mutation enhanced virus production in JFH1 (Figure 6.2). Hence, our results suggest that mutations within the NS coding region can modulate virus production depending on the composition of the structural coding region. The conclusion drawn from introducing M6 into both JFH1 and J6-JFH1 is that a genotype-specific interaction between the C-terminus of NS4B with core, E1, E2, p7 or the N-terminal region of NS2 is important for modulation of virus production. Further investigation into this hypothesis is necessary. For example, serial passaging of J6-JFH1_{M6} virus in cell culture may lead to compensatory mutations within the structural proteins that circumvent incompatibilities with NS4B. This would further define the importance of structural-NS protein interactions for the production of infectious virus particles.

7 Identification of Cellular Genes that Influence HCV RNA Replication

7.1 Introduction

Small RNA viruses such as HCV encode a limited set of proteins within their genome, and thus rely on host cell factors to facilitate their replicative cycle (Moriishi & Matsuura, 2007). One method of identifying genes that influence HCV genome replication is to determine whether the silencing of individual genes by siRNAs has any effect on the level of HCV RNA synthesis. The use of siRNAs has revealed many proteins from a wide range of protein families that contribute to the HCV life cycle (Ng et al., 2007, Xue et al., 2007).

To expand the scope of the project beyond studies on viral components, it was decided that a library of siRNAs (supplied by Ambion) targeting genes encoding cellular nucleotide-binding proteins would be chosen and screened. This class of proteins was selected in an attempt to identify cellular components that influenced replication and/or translation of HCV RNA. Thus, a siRNA library targeting 299 cellular genes was selected (see Appendix 2). These genes principally encoded translation factors, ribosomal proteins, RNA-binding proteins and proteins involved in the IFN response pathway, since IFN reduces replication of the JFH1 SGR in Huh-7 cells (Targett-Adams & McLauchlan, 2005). For exploratory purposes, genes in other categories were also selected and included genes encoding proteins involved in cell cycle control and the cellular degradation pathway. By including genes from a wide range of cellular pathways, we hoped to identify novel processes involved in modulating HCV RNA replication.

7.2 Production of a System Suitable for Screening a siRNA Library

7.2.1 Selection and Characterisation of a Positive Control siRNA

7.2.1.1 Selection of a Positive Control siRNA

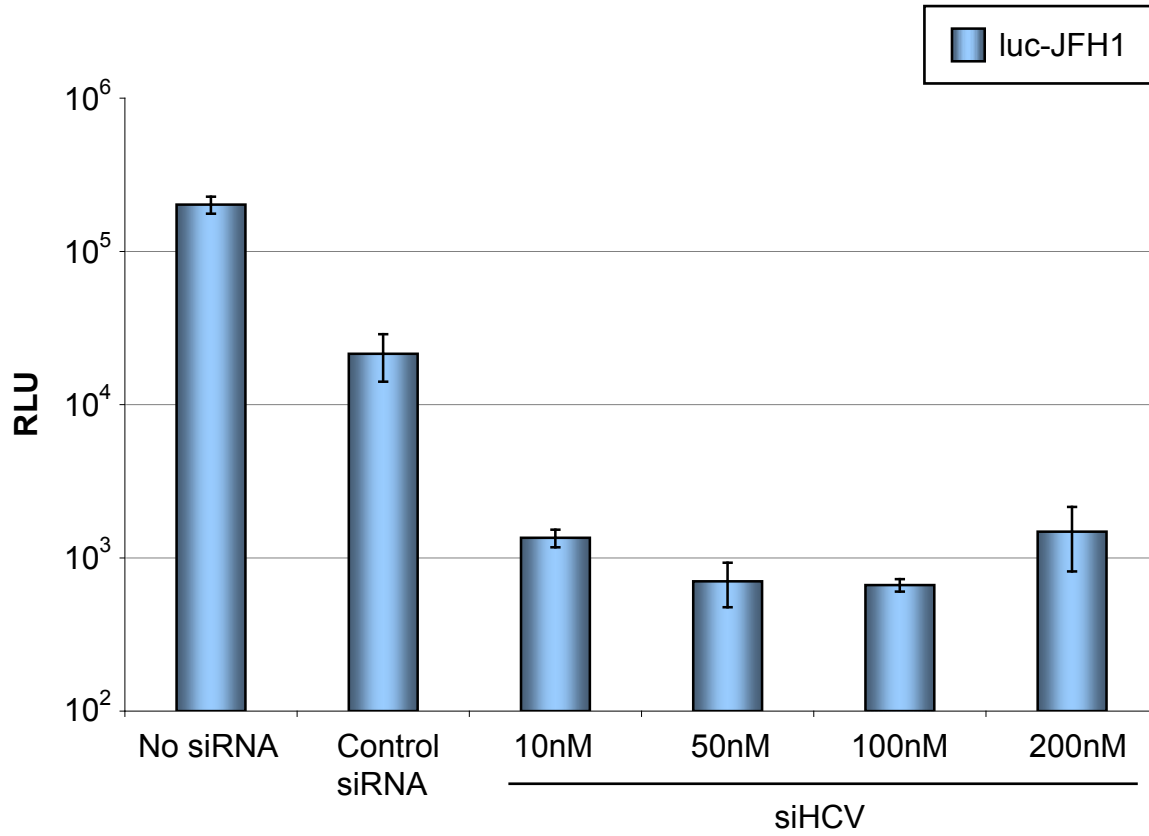
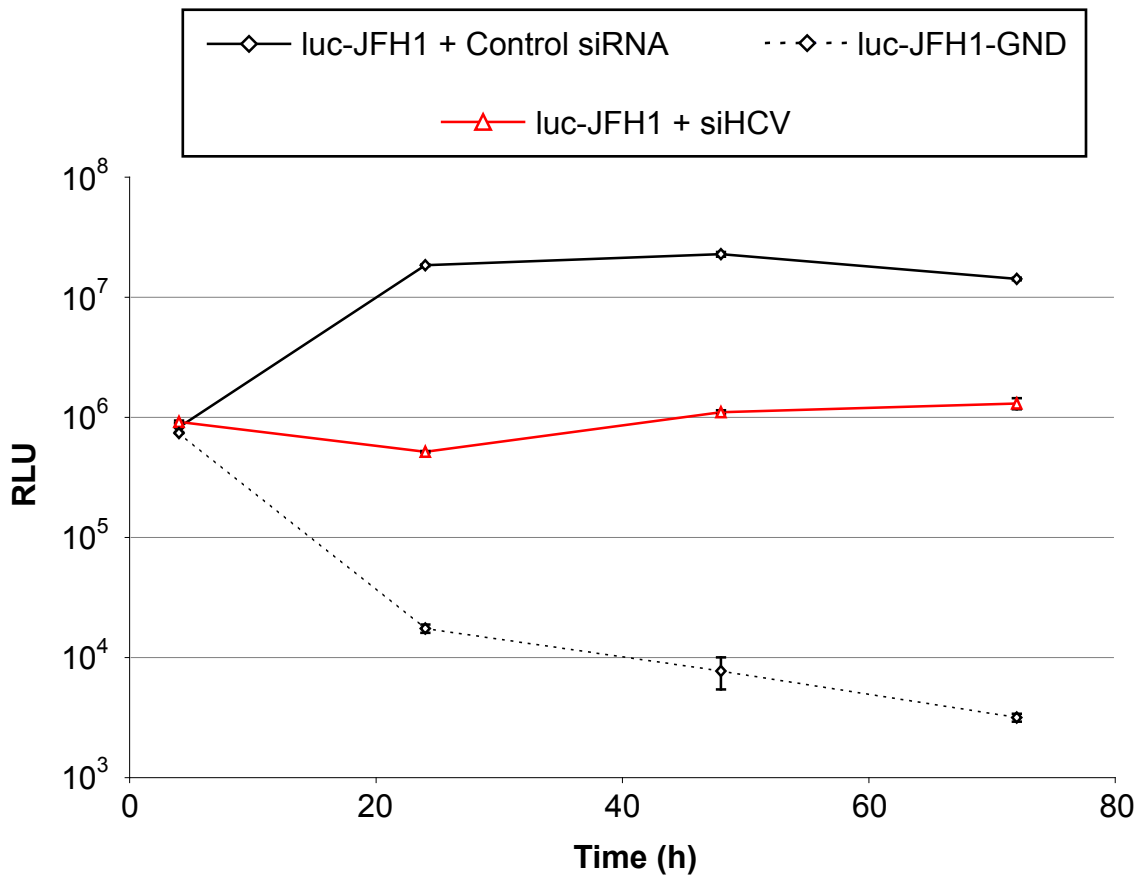
To verify the impact on HCV RNA replication resulting from the knockdown of cellular genes, it was important to establish a robust system for quantifying any effects. Previous investigations utilising siRNA technology have revealed that viral

replication is most effectively repressed when the RNA genome is targeted by siRNAs directed against the regions encoding NS3 (Kapadia et al., 2003, Prabhu et al., 2005), NS5B (Kapadia et al., 2003, Ng et al., 2007, Prabhu et al., 2005) or the 5' UTR (Chevalier et al., 2007, Kanda et al., 2007, Kronke et al., 2004, Ng et al., 2007, Seo et al., 2003, Yokota et al., 2003). These regions harbour highly conserved sequences that are essential for their roles in polyprotein cleavage (NS3), RNA replication (NS5B and the 5' UTR) and translation (the 5' UTR). Hence, siRNAs targeting these sequences work more effectively than those targeting more variable HCV coding regions.

The 5' UTR is the most conserved part of the HCV genome and contains the viral IRES, a structure critical for cap-independent initiation of HCV polyprotein translation (Figure 7.1). The IRES harbours secondary and tertiary RNA structures and can be divided into four domains (termed I-IV). A siRNA that targets domain III/IV (termed si313) has been shown to be particularly effective at reducing HCV RNA replication (Chevalier et al., 2007). Furthermore, this region is conserved across several HCV genotypes, including JFH1. Therefore, a siRNA identical in sequence to si313 was synthesised and termed siHCV. The sequence of siHCV and the IRES region to which it would anneal are shown in Figure 7.1.

7.2.1.2 siHCV Reduces Transient HCV RNA Replication

To determine the optimal concentration of siHCV required to reduce viral RNA replication, RNA transcribed from luc-JFH1 was electroporated into Huh-7 cells. Immediately post-electroporation, cells were transfected with 50nM of a scrambled control siRNA or increasing concentrations (10-200nM) of siHCV siRNA and any effect on HCV replication was determined by luciferase assay 48 hours later (Figure 7.2, A). Introduction of the control siRNA resulted in an approximately 10-fold decrease in luciferase values compared to untreated cells, likely due to cellular toxicity resulting from simultaneous electroporation and transfection. However, enzyme activity was reduced by a further 15- to 32-fold upon introduction of siHCV compared to cells transfected with the control siRNA. (Figure 7.2, A). The most effective reduction in luciferase levels was observed with 50nM and 100nM of siHCV, which displayed 30- and 32-fold reductions in enzyme activity respectively (Figure 7.2, A). Based on these data, 50nM of siHCV was used in further experiments.

[A]**[B]**

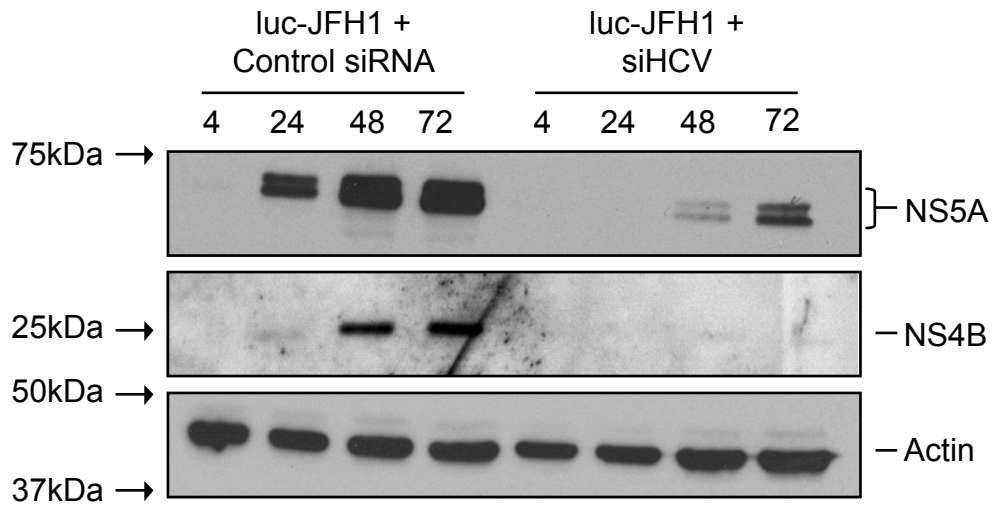
[C]

Figure 7.2 siHCV reduces transient HCV RNA replication in Huh-7 cells

[A] Huh-7 cells were electroporated with RNA encoding luc-JFH1, followed by immediate transfection with increasing concentrations of siHCV. Electroporated cells alone (no siRNA), or cells transfected with 50nM of a scrambled siRNA sequence (control siRNA) were also included and served as controls. At 48 hours post-electroporation/transfection, cells were lysed and extracts were assayed for luciferase activity. **[B]** Huh-7 cells electroporated with luc-JFH1 were set up in duplicate; one set of cells was transfected with 50nM of siHCV, while the second set was transfected with 50nM of a control siRNA. Cells electroporated with luc-JFH1-GND were also included as a negative control of HCV replication. Cells were lysed at 4, 24, 48 and 72 hours post-electroporation and extracts were assayed for luciferase activity. For [A] and [B], all assays were performed in duplicate and average values are shown for each experiment. Error bars indicate the range of the values recorded at each time point. **[C]** Cells set up in parallel to those described in [B] were harvested for Western blot analysis at 4, 24, 48 and 72 hours post-electroporation. Extracts from each time point were probed for NS5A (with NS5A antisera), NS4B (with R1063) and actin detection served as a loading control.

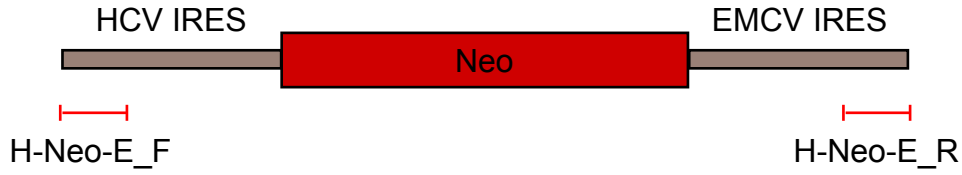
To confirm that siHCV was effective over a longer time period, Huh-7 cells were electroporated with RNA encoding luc-JFH1 or luc-JFH1-GND and cells harbouring luc-JFH1 were immediately transfected with 50nM of siHCV or the control siRNA. Luciferase assays were then determined over a 72-hour period (Figure 7.2, B). In cells transfected with the control siRNA, luc-JFH1 expressed luciferase values that were 20-fold higher by 24 hours compared to the four-hour time point and enzyme levels remained high for the duration of the time course, indicating efficient replication of this RNA (Figure 7.2, B). By contrast, luciferase values at 24 hours were almost half of those displayed at four hours in cells treated with siHCV and, although luciferase values increased thereafter, they remained 10-fold lower compared to control siRNA-treated cells by 72 hours (Figure 7.2, B). Luciferase values for luc-JFH1-GND decreased over the entire 72-hour period, indicating that this construct was incapable of replicating.

To demonstrate further the effect of siHCV on replication of luc-JFH1, extracts prepared over 72 hours from cells set up in parallel to those described above were analysed by Western blot analysis (Figure 7.2, C). Cell lysates were examined for HCV-encoded NS5A and NS4B proteins and actin detection served as a loading control. NS5A was detected by 24 hours in cells containing luc-JFH1 and the control siRNA and NS4B became detectable by 48 hours post-electroporation/transfection (Figure 7.2, C). In contrast, NS5A was not detected until 48 hours in cells harbouring luc-JFH1 and siHCV and was present in reduced amounts at 72 hours compared to results obtained with the control siRNA. NS4B was not detected throughout the time course (Figure 7.2, C). This reduction in HCV-encoded proteins was not due to differences in sample loading, as confirmed by probing for actin. Taken together, these results confirmed that siHCV was a potent inhibitor of transient HCV RNA replication in Huh-7 cells.

7.2.2 Creation and Characterisation of a Tri-cistronic JFH1 Replicon

The results gained through siHCV optimisation experiments suggested that electroporating and transfecting cells simultaneously was sufficient to decrease HCV RNA replication compared to those cells that were electroporated but not transfected (Figure 7.2, A, compare 'no siRNA' with 'control siRNA'). Both electroporation and transfection are cytotoxic and the observed reduction in luciferase levels by the scrambled siRNA was likely due to the combined effect of both processes. Therefore, transfection of a cell line already harbouring a HCV

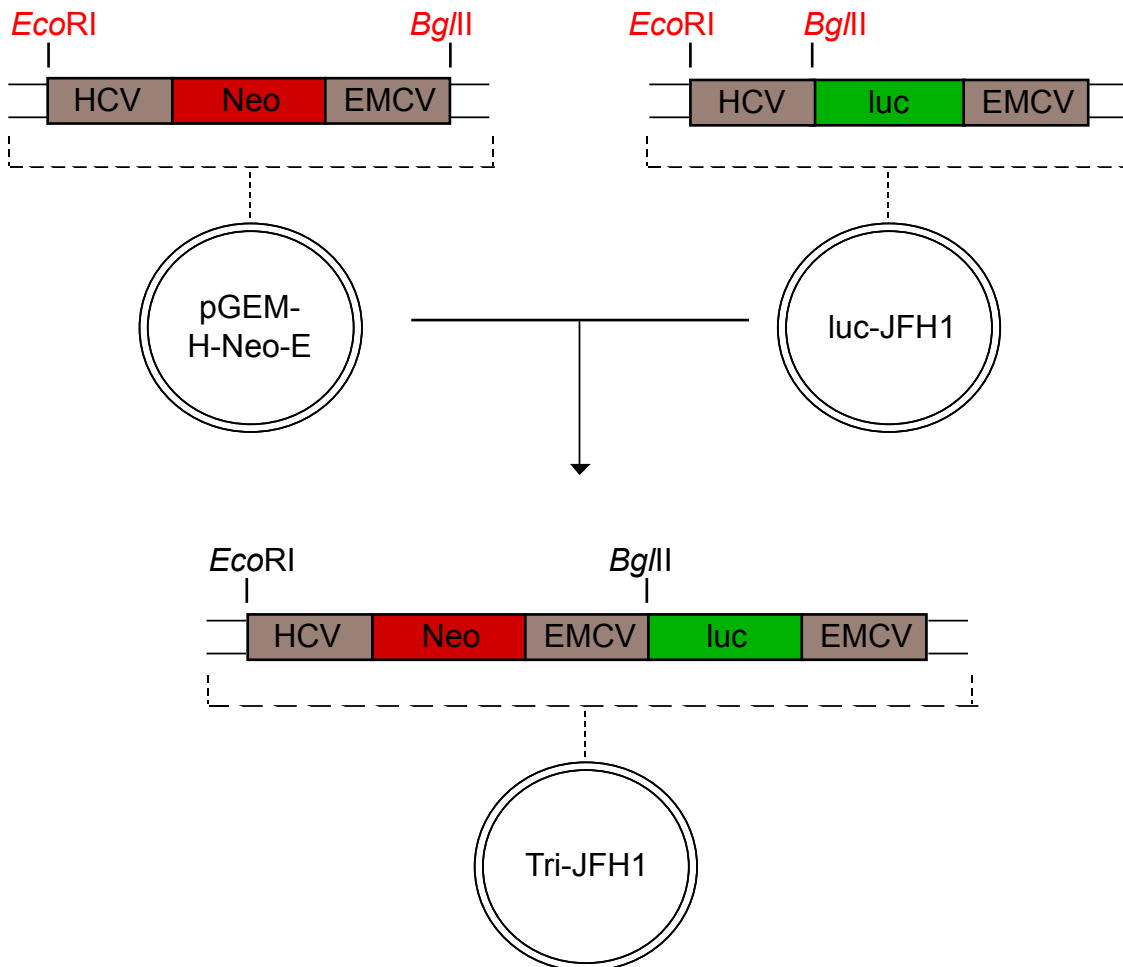
[A]



H-Neo-E primers

HCV IRES sequence	GAA TTC TAA TAC GAC TCA CTA
H-Neo-E_F	5' <u>GAA TTC TAA TAC GAC TCA CTA</u> 3' EcoRI
EMCV IRES sequence	CTG GGC GCC ATA GTG GTG AGT
H-Neo-E_R	3' GAC CCG CGG TAT CAC CAC TCA <u>TCT AGA</u> 5' BgII

[B]



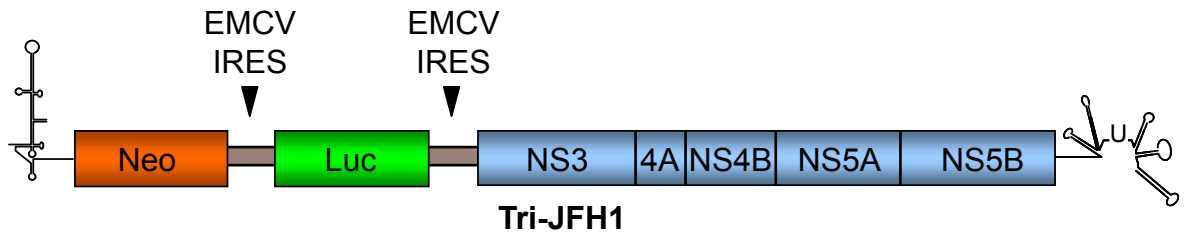
[C]

Figure 7.3 Creation of Tri-JFH1

[A] A schematic representation of the region encoding the Neo gene flanked by the HCV and EMCV IRES is shown (top) and the positions and sequences of the primers used to amplify the fragment (termed H-Neo-E) are indicated, with introduced non-viral sequences depicted in red. Restriction enzyme sites used for cloning purposes are underlined. H-Neo-E was subsequently introduced into the pGEM-T-Easy cloning vector, generating pGEM-H-Neo-E. **[B]** The H-Neo-E fragment was released from pGEM-H-Neo-E using *EcoRI* and *BglII*. Luc-JFH1 was also digested with *EcoRI* and *BglII*, thus removing the HCV IRES preceding the luciferase gene. H-Neo-E was then inserted between these restriction sites, creating Tri-JFH1. **[C]** A schematic representation of the Tri-JFH1 SGR. Translation of the Neo gene is directed by the HCV IRES, whereas the luciferase gene and the NS coding region are each translated via an EMCV IRES.

replicon would be preferable, thereby bypassing the need for electroporation. Optimally, this cell line should contain a SGR harbouring a gene for drug selection as well as a reporter for quantification of viral RNA replication. Such cell lines have previously been established using HCV Con1 SGRs (so called tri-cistronic replicons, Supekova et al., 2008). Furthermore, pFK-I389neo/luc/Ns3-3'/5.1 (a tri-cistronic replicon harbouring the neomycin gene, luciferase gene and Con1 NS region NS3-5B) was suitable for screening a siRNA library (Supekova et al., 2008). Using an identical strategy, a tri-cistronic replicon encoding the JFH1 NS proteins was generated and termed Tri-JFH1. Tri-JFH1 was firstly characterised in transient assays to determine its replication properties compared to luc-JFH1, the bi-cistronic SGR. The tri-cistronic replicon was then stably introduced into cells to yield cell lines that gave constitutive RNA replication.

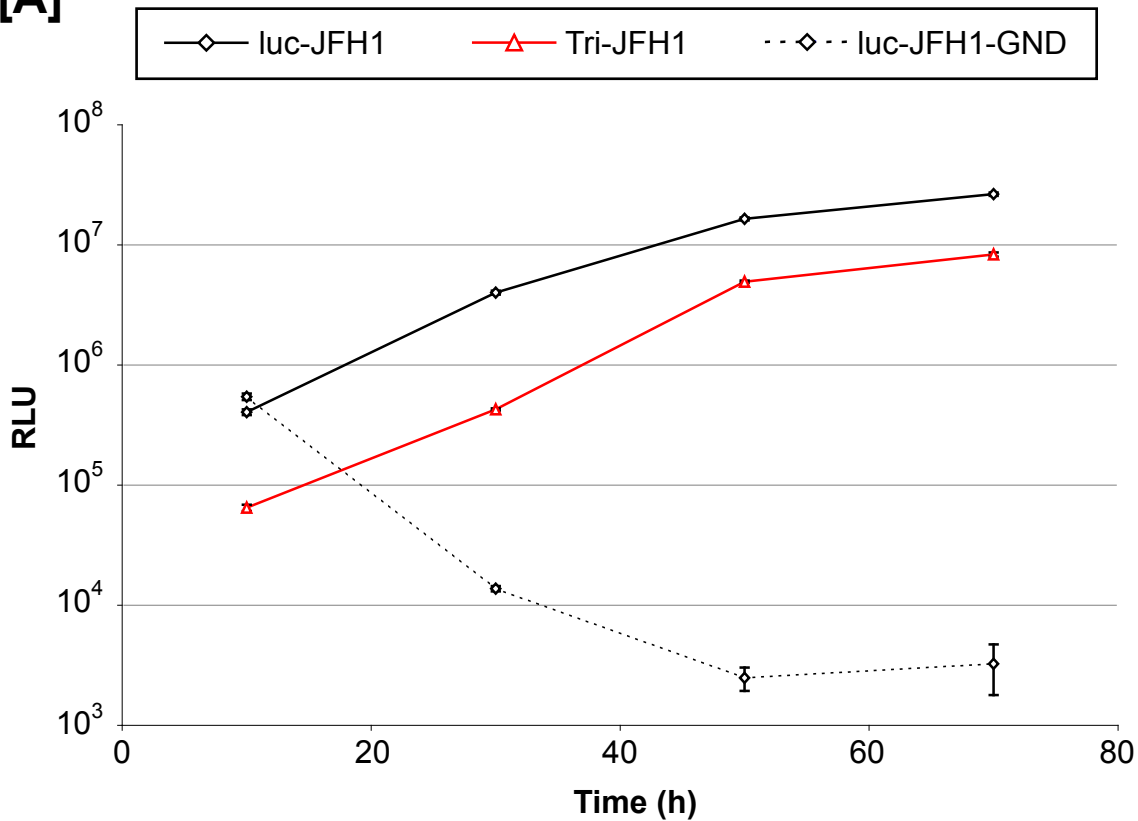
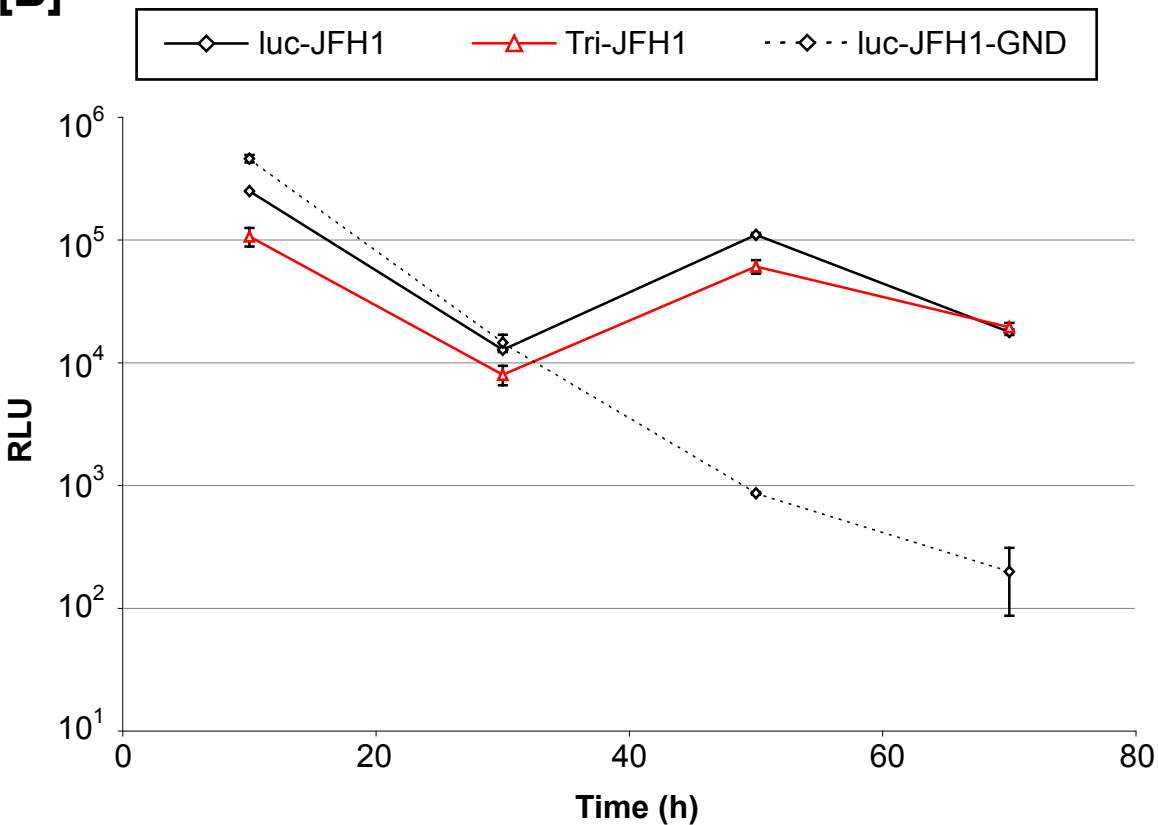
7.2.2.1 Creation of Tri-JFH1

Tri-JFH1 required both the neomycin resistance gene and the luciferase reporter gene to be positioned upstream of the JFH1 NS3-5B coding region. Therefore, the HCV IRES, neomycin gene and EMCV IRES were amplified using neo-JFH1 as a template (Figure 7.3, A). This fragment (termed H-Neo-E) incorporated an existing *EcoRI* site at the beginning of the HCV IRES and harboured a novel *BglII* site at the end of the EMCV IRES. H-Neo-E was inserted into pGEM-T-Easy, producing pGEM-H-Neo-E (Figure 7.3, B).

The luc-JFH1 replicon harbours a HCV IRES that drives translation of the luciferase reporter gene. The plasmid containing the replicon was digested using *EcoRI* and *BglII*, thus excising the HCV IRES. H-Neo-E was then released from pGEM-H-Neo-E using *EcoRI* and *BglII* and this fragment was inserted between the corresponding sites of luc-JFH1 (Figure 7.3, B). This strategy produced Tri-JFH1, in which the HCV IRES directs translation of the neomycin resistance gene and translation of both the luciferase reporter gene and the JFH1 NS coding region is directed by two separate EMCV IRES sequences (Figure 7.3, C).

7.2.2.2 Characterisation of Tri-JFH1

To determine whether Tri-JFH1 replicated, *in vitro* transcribed RNA from the construct was electroporated into both Huh-7 and U2OS cells. U2OS cells are derived from an osteosarcoma and support replication of luc-JFH1, although with a

[A]**[B]****Figure 7.4 Tri-JFH1 replicates transiently in both Huh-7 and U2OS cells**

RNAs encoding luc-JFH1, luc-JFH1-GND and Tri-JFH1 were electroporated into **[A]** Huh-7 cells and **[B]** U2OS cells. Cells were lysed at 4, 24, 48 and 72 hours post-electroporation and extracts were assayed for luciferase activity. All assays were performed in duplicate and average values are shown for each experiment. Error bars represent range of the values recorded at each time point.

lower efficiency than Huh-7 cells (Targett-Adams & McLauchlan, 2005). U2OS cells were included in the characterisation of Tri-JFH1 as a possible alternative cell line for screening the siRNA library. Cells were also electroporated with RNA encoding bi-cistronic control replicons luc-JFH1 and luc-JFH1-GND, and luciferase activity was measured over 72 hours (Figure 7.4). As expected, luciferase levels derived from luc-JFH1 were 65-fold higher by 72 hours compared to the 4-hour time point, indicating efficient replication of this RNA in Huh-7 cells. By contrast, luc-JFH1-GND did not replicate (Figure 7.4, A). In U2OS cells, luc-JFH1 exhibited luciferase levels that never increased beyond those observed at 4 hours but did not decrease as rapidly as those seen with the GND control (Figure 7.4, B). Therefore, U2OS cells supported luc-JFH1 replication but to lower levels compared with Huh-7 cells, consistent with previously described data (Targett-Adams & McLauchlan, 2005). Importantly, enzyme activity from Tri-JFH1 indicated a pattern of replication that paralleled luc-JFH1 in both cell lines, although luciferase values were slightly lower at each time point (Figure 7.4, A and B). These data indicated that Tri-JFH1 replicated transiently in two cell lines known to support HCV viral replication.

7.2.3 Characterisation of Cell Lines Supporting Autonomous Replication of Tri-JFH1

In parallel studies, it had been demonstrated that U2OS cells were more efficient for siRNA transfection compared to Huh-7 cells. For example, the siRNA-mediated knockdown of adipocyte differentiation-related protein (ADRP) was more efficient in U2OS cells compared to Huh-7 cells (J. McLauchlan, personal communication). Therefore, a U2OS cell line that supported HCV replication could be more sensitive for screening the siRNA library compared to a Huh-7 cell line. Hence, RNA encoding Tri-JFH1 was electroporated into both Huh-7 and U2OS cells, which were passaged in the presence of G418 for several weeks. These cell lines were termed Tri-Huh-7 and Tri-U2OS.

To examine whether Tri-JFH1 replication could be detected after several weeks of passage, both cell lines were fixed and probed for the presence of NS5A and dsRNA (Figure 7.5, A). NS5A and dsRNA were detected in >95% of cells for both cell lines, indicating that Tri-JFH1 replicated following G418 selection in a high proportion of cells. Interestingly, some Tri-U2OS cells displayed a dsRNA signal only (Figure 7.5, A, bottom panel), whereas Tri-Huh-7 cells typically contained

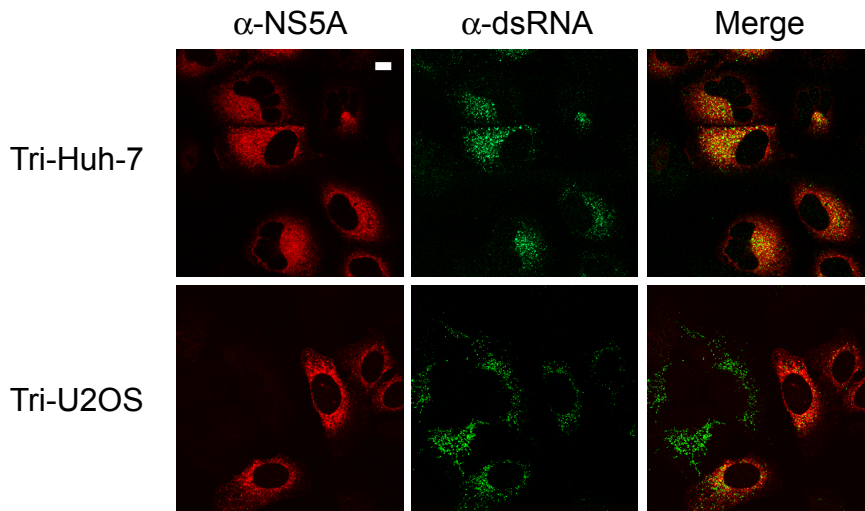
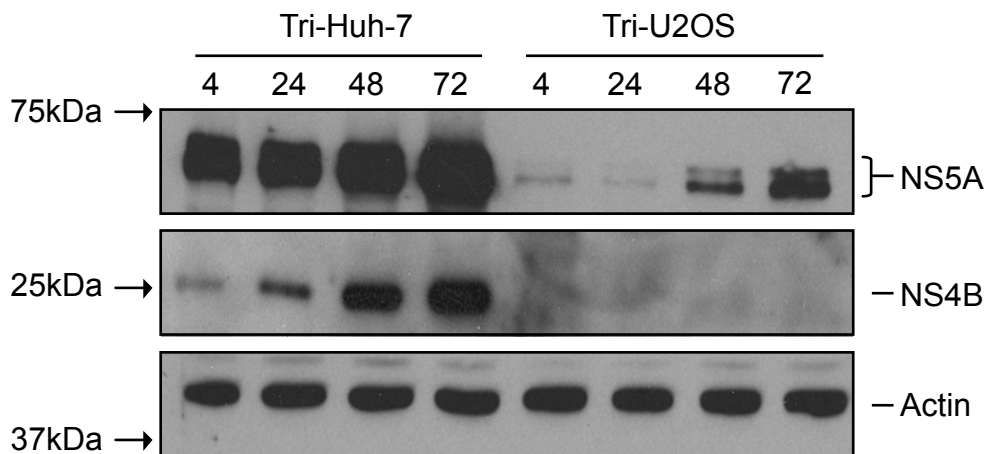
[A]**[B]**

Figure 7.5 Generation of two cell lines; Tri-Huh-7 and Tri-U2OS

RNA from Tri-JFH1 was electroporated into both Huh-7 and U2OS cells and cells were passaged for several weeks in the presence of G418. These cell lines were termed Tri-Huh-7 and Tri-U2OS. **[A]** Tri-Huh-7 and Tri-U2OS cells were fixed and probed using NS5A antisera and J2 to detect NS5A and dsRNA respectively. Scale bar represents 10 μ m. **[B]** Tri-Huh-7 and Tri-U2OS cell extracts prepared at 4, 24, 48 and 72 hours were subjected to Western blot analysis for the presence of NS5A (using NS5A antisera), NS4B (using R1063) and actin.

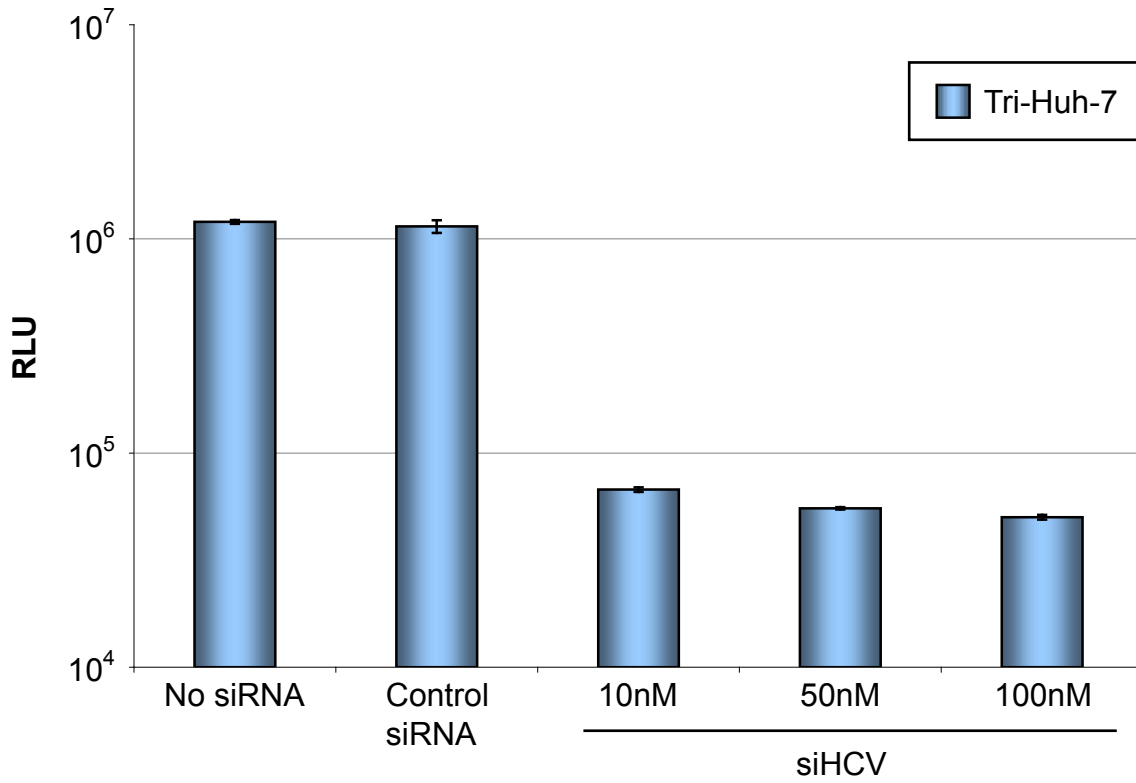
both dsRNA and NS5A (Figure 7.5, A, top panel). To confirm this result, cell extracts from Tri-Huh-7 and Tri-U2OS cells harvested at different times up to 72 hours were examined by Western blot analysis for the presence of viral NS4B and NS5A proteins (Figure 7.5, B). Both proteins were detected at all time points in Tri-Huh-7 cells and increased in abundance over the 72-hour period, likely resulting from cell growth. In contrast, a substantially lower level of NS5A was detected in Tri-U2OS cells and NS4B could not be observed at any time point (Figure 7.5, B). The different levels of protein expressed from each cell line were not a consequence of inaccurate sample loading as demonstrated by the detection of actin (Figure 7.5, B). The lower amount of viral proteins detected is consistent with the reduced level of transient HCV replication observed in U2OS compared to Huh-7 cells (Figure 7.4, B).

These data indicated that the Tri-U2OS cell line gave a lower level of Tri-JFH1 RNA replication compared to Tri-Huh-7 cells. Nonetheless, both cell lines supported constitutive replication of the Tri-JFH1 SGR.

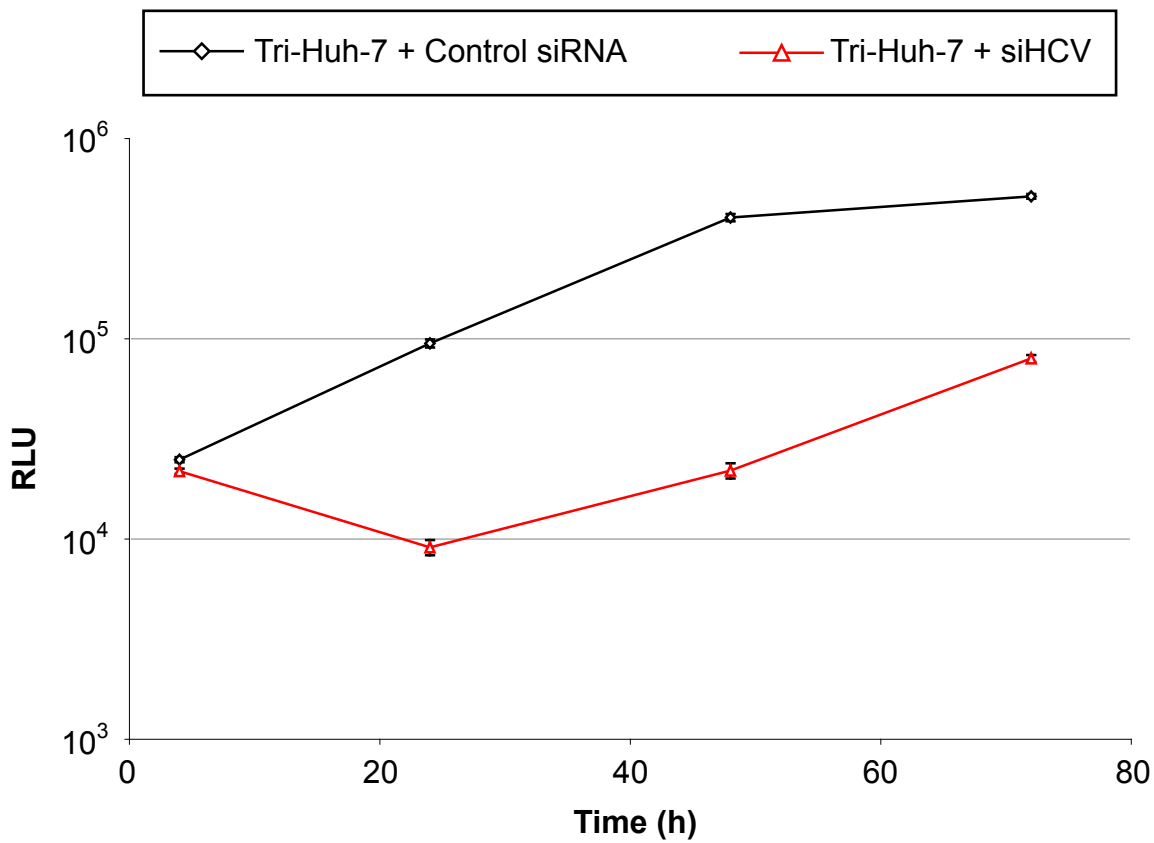
7.2.4 siHCV Reduces Tri-JFH1 Replication in Tri-Huh-7 and Tri-U2OS Cells

Previously, 50nM of siHCV had been sufficient to reduce HCV RNA replication by 30-fold compared to cells treated with a control siRNA (Figure 7.2, A). To test whether this concentration of siHCV was also effective for reducing viral replication in the newly established cell lines, both Tri-Huh-7 and Tri-U2OS cells were transfected with 50nM of scrambled siRNA, or increasing concentrations (10nM-100nM) of siHCV and HCV replication was determined by luciferase assay 48 hours later (Figures 7.6 and 7.7, A). Importantly, no reduction in HCV RNA replication was observed in Tri-Huh-7 cells treated with the control siRNA compared to those that were untreated (Figure 7.6, A, compare 'no siRNA with 'control siRNA'). This result indicated that the reduction in luciferase values observed with the control siRNA in transient assays (Figure 7.2, A) did not occur upon transfection into cells that gave constitutive HCV RNA replication. As found previously, 10nM, 50nM and 100nM of siRNA all potently inhibited HCV RNA replication in Tri-Huh-7 and Tri-U2OS cells (Figures 7.6, A and 7.7, A). Upon transfection of Tri-Huh-7 cells with 50nM of siHCV, a 20-fold decrease in luciferase activity was observed compared to control siRNA-treated cells (Figure 7.6, A).

[A]



[B]



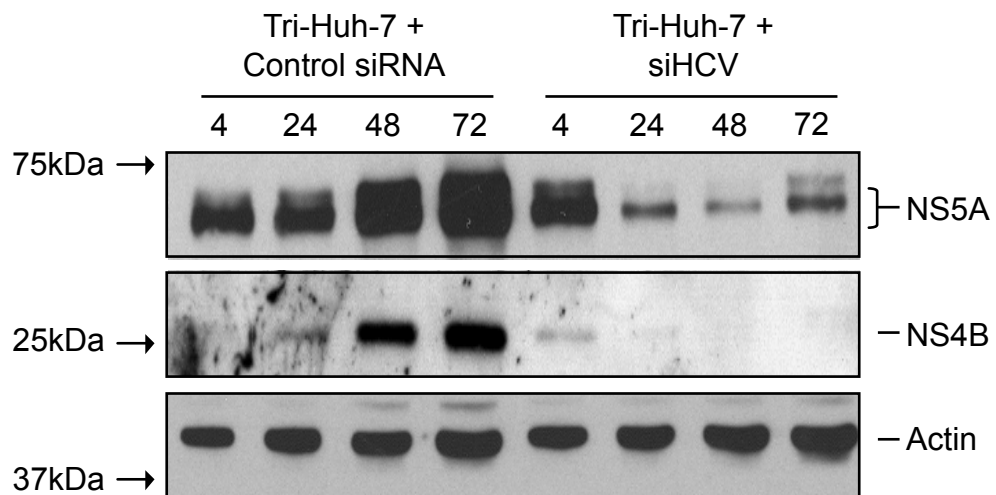
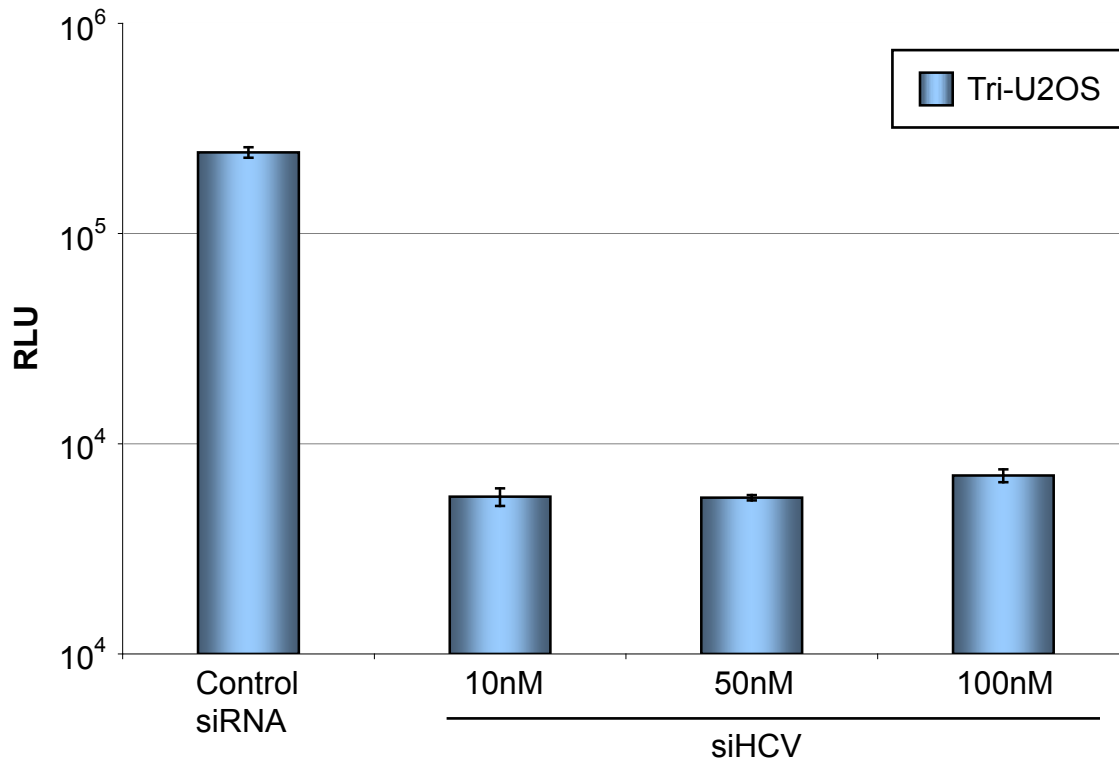
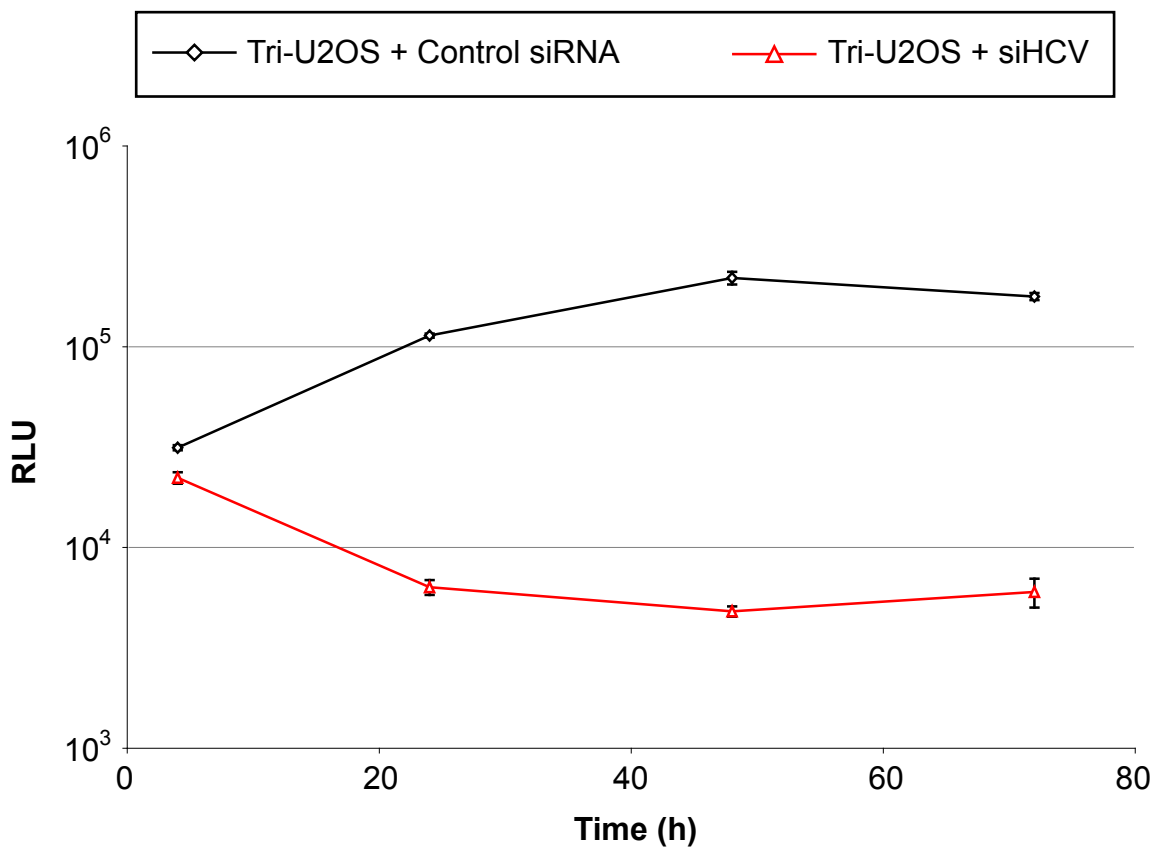
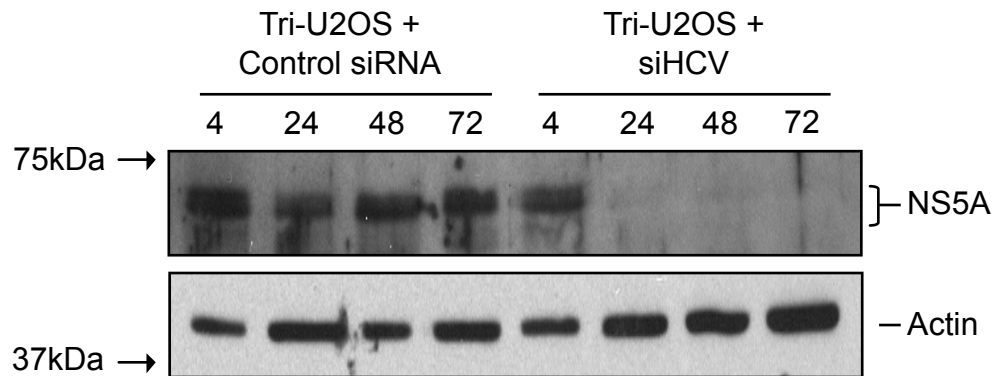
[C]

Figure 7.6 siHCV reduces viral RNA replication in Tri-Huh-7 cells

[A] Tri-Huh-7 cells were transfected with increasing concentrations of siHCV. Tri-Huh-7 cells that were not transfected (no siRNA) or transfected with 50nM of a scrambled siRNA sequence (control siRNA) were also included and served as controls. At 48 hours post-transfection, cells were lysed and extracts were assayed for luciferase activity. **[B]** Tri-Huh-7 cells were set up in duplicate; one set of cells was transfected with 50nM of siHCV, while the second set was transfected with 50nM of the control siRNA. Cells were lysed at 4, 24, 48 and 72 hours post-transfection and extracts were assayed for luciferase activity. For [A] and [B], all assays were performed in duplicate and average values are shown for each experiment. Error bars indicate the range of the values recorded at each time point. **[C]** Cells set up in parallel to those described in [B] were harvested for Western blot analysis at 4, 24, 48 and 72 hours post-electroporation. Extracts from each time point were probed for the presence of viral NS5A (using NS5A antisera), NS4B (using R1063) and actin detection served as a loading control.

[A]**[B]**

[C]**Figure 7.7 siHCV reduces viral RNA replication in Tri-U2OS cells**

[A] Tri-U2OS cells were transfected with increasing concentrations of siHCV, or 50nM of a scrambled siRNA sequence (control siRNA). At 48 hours post-transfection, cells were lysed and extracts were assayed for luciferase activity. **[B]** Tri-U2OS cells were set up in duplicate; one set of cells was transfected with 50nM of siHCV, while the second set was transfected with 50nM of the control siRNA. Cells were lysed at 4, 24, 48 and 72 hours post-transfection and extracts were assayed for luciferase activity. For **[A]** and **[B]**, all assays were performed in duplicate and average values are shown for each experiment. Error bars represent the range of the values recorded at each time point. **[C]** Cells set up in parallel to those described in **[B]** were harvested for Western blot analysis at 4, 24, 48 and 72 hours post-electroporation. Extracts from each time point were probed for the presence of viral NS5A using anti-NS5A antisera and actin detection served as a loading control.

Remarkably, 50nM of siHCV reduced enzyme activity by 45-fold in Tri-U2OS cells, more than double the reduction observed in Tri-Huh-7 cells (Figure 7.7, A).

To determine the effect of siHCV over a time course, Tri-Huh-7 and Tri-U2OS cells were transfected with 50nM of siHCV or scrambled siRNA and luciferase levels were measured over 72 hours (Figures 7.6 and 7.7, B). Luciferase levels were consistently lower in both cell lines treated with siHCV compared to those treated with the control siRNA from 24 hours onwards. The greatest relative decrease in replication for both cell lines was at 48 hours post-transfection. At this time point, luciferase levels expressed from Tri-Huh-7 cells were 20-fold lower compared to control cells (Figure 7.6, B). Once again, luciferase activity was reduced to a greater extent in Tri-U2OS cells, where a 45-fold knockdown was detected in siHCV-treated cells at 48 hours (Figure 7.7, B). Furthermore, the effects of siHCV were sustained over a longer time period in Tri-U2OS cells compared to Tri-Huh-7 cells. By 72 hours, luciferase values had recovered to only six-fold lower in Tri-Huh-7 cells treated with siHCV compared to those treated with a scrambled siRNA (Figure 7.6, B). In contrast, Tri-U2OS cells expressed luciferase values that were still 30-fold lower than control cells by 72-hours (Figure 7.7, B). This result was reflected by Western blot analysis of extracts prepared from cells set up in parallel to those described above. Levels of NS5A (and NS4B in the case of Tri-Huh-7 cells) were reduced in both cell lines when treated with siHCV (Figures 7.6 and 7.7, C). Despite knockdown of viral replication, NS5A was still detected at each time point in Tri-Huh-7 cells. In contrast, NS5A was observed at four hours with treated Tri-U2OS cells, but was not detected thereafter (Figures 7.7, C).

Combined, the data from luciferase and Western blot analyses revealed that viral RNA replication could be effectively and reproducibly reduced in siHCV-treated cell lines. Moreover, it was evident that the effects of siHCV were more potent in Tri-U2OS cells compared to the Tri-Huh-7 cell line.

7.2.5 Knockdown of CKI- α Reduces Tri-JFH1 Replication in Tri-Huh-7 and Tri-U2OS Cells

Before screening with the siRNA library directed against cellular genes, both Tri-Huh-7 and Tri-U2OS cell lines were validated further using a siRNA that targeted a cell gene implicated in HCV RNA replication. The cellular kinase CKI- α is involved in NS5A hyperphosphorylation and furthermore, knockdown of CKI- α by siRNA

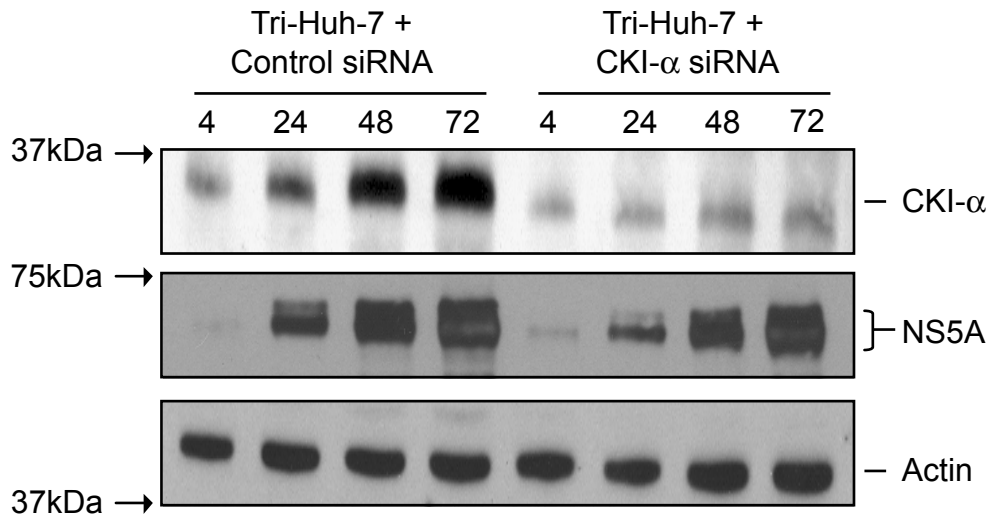
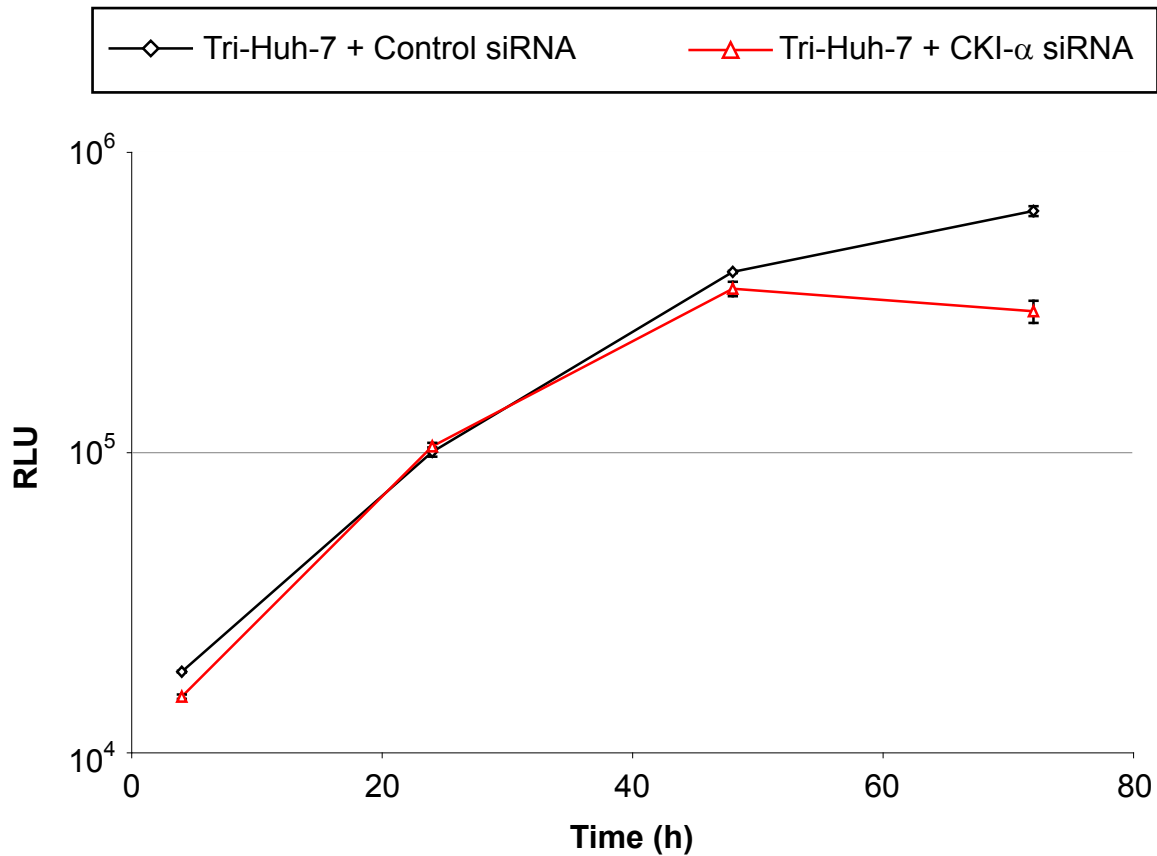
treatment reduces both NS5A hyperphosphorylation and viral RNA replication (Quintavalle et al., 2006 and 2007). Hence, Tri-Huh-7 and Tri-U2OS cells were transfected with a siRNA targeting CKI- α and cell extracts were prepared for Western blot and luciferase assay analyses over a period of 72 hours (Figure 7.8).

Levels of CKI- α were reduced in both cell lines transfected with CKI- α siRNA compared to those transfected with a control siRNA and the protein was more potently silenced in Tri-U2OS cells (Figure 7.8, A and C). Interestingly, although NS5A seemed unaffected in Tri-Huh-7 cells, a lower abundance of the hyperphosphorylated species of NS5A was detected in Tri-U2OS cells treated with the CKI- α siRNA compared to those treated with the scrambled siRNA (Figure 7.8, C). This result is in agreement with the notion that CKI- α is involved in NS5A hyperphosphorylation (Quintavalle et al., 2006 and 2007). Upon examination of the luciferase levels expressed by Tri-Huh-7 cells, HCV replication was unaffected by CKI- α siRNA treatment until 72 hours post-transfection. At this time point, luciferase activity decreased by two-fold (Figure 7.8, B). By contrast, luciferase levels were reduced by 48 hours post-transfection in CKI- α siRNA-treated Tri-U2OS cells, indicating that Tri-JFH1 replication was inhibited earlier in this cell line. The decrease in enzyme activity was greater still by 72 hours and luciferase values were reduced by seven-fold compared to cells transfected with scrambled siRNA (Figure 7.8, D).

These results confirmed that CKI- α is involved in HCV RNA replication, likely through disruption of NS5A hyperphosphorylation. Moreover, the data indicated that Tri-JFH1 replication could be reduced in both cell lines by a siRNA targeting a cellular gene. However, the effects on HCV RNA replication were more pronounced in Tri-U2OS cells. It is likely that two factors contribute to this observation. Firstly, a higher degree of RNA replication is detected in Tri-Huh-7 cells as compared to Tri-U2OS cells. Secondly, Tri-U2OS cells are more efficiently transfected with siRNAs than Tri-Huh-7 cells.

7.3 Screening of the siRNA Library in Tri-Huh-7 and Tri-U2OS Cells

Following the above validation, the siRNA library was screened in both Tri-Huh-7 and Tri-U2OS cell lines. Individual genes were targeted by three siRNAs complementary to different regions of their coding sequence and each siRNA was

[A]**[B]**

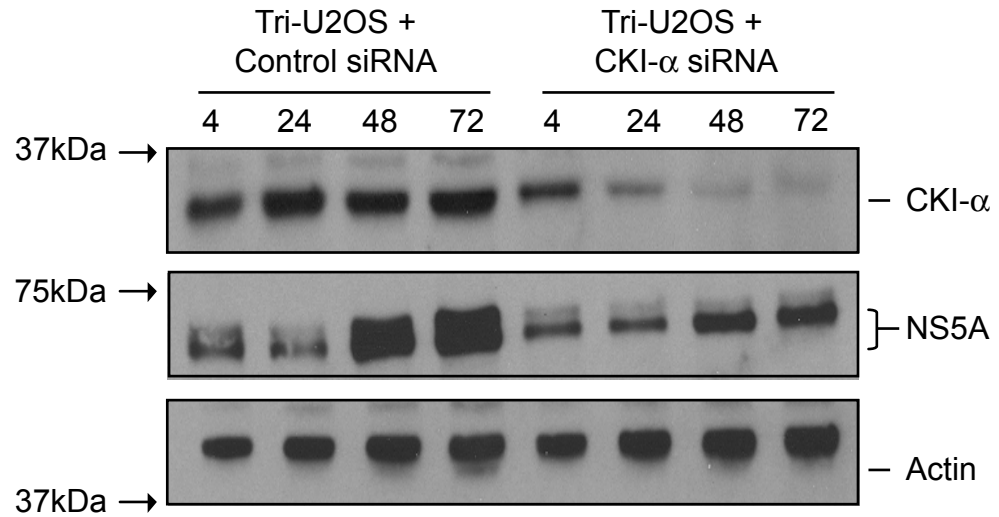
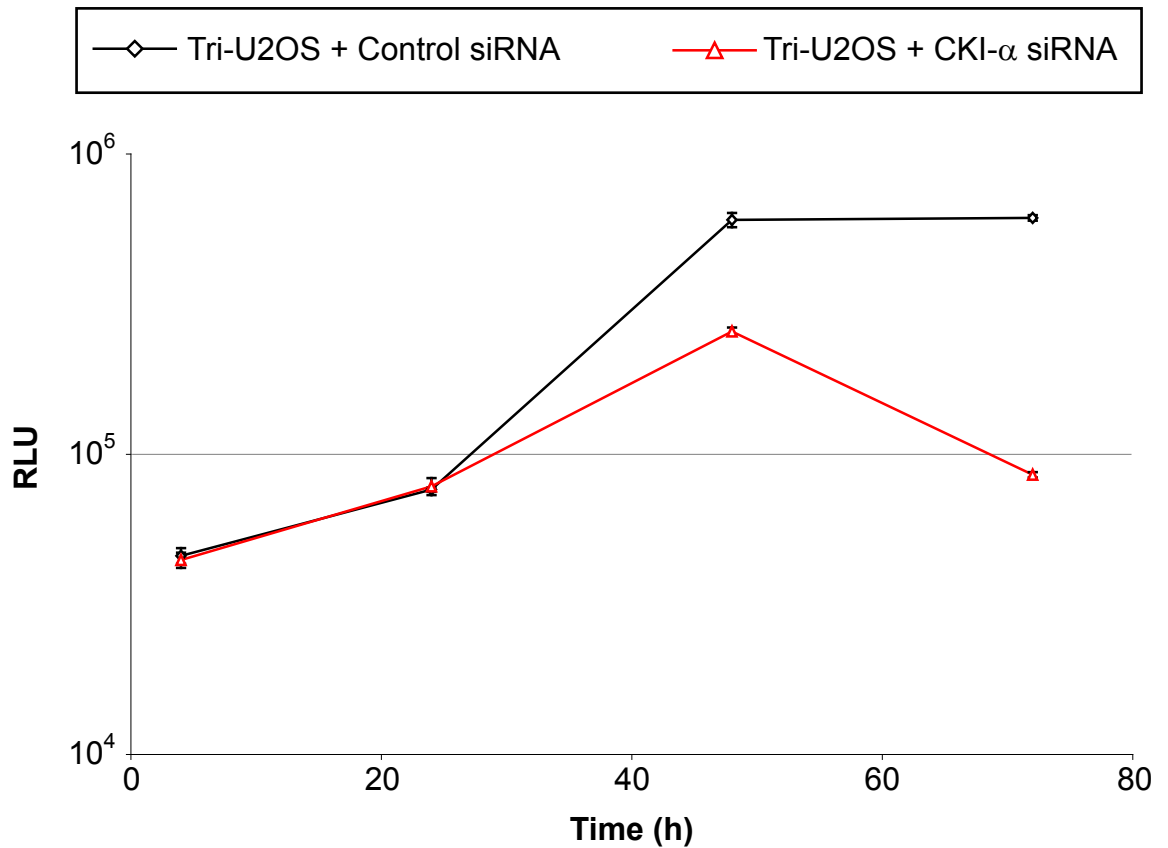
[C]**[D]**

Figure 7.8 Knockdown of CKI- α in Tri-Huh-7 and Tri-U2OS cells

[A] Tri-Huh-7 cells or **[C]** Tri-U2OS cells were set up in duplicate; one set of cells was transfected with 50nM of an siRNA targeting the cellular kinase CKI- α , while the second set was transfected with 50nM of the control siRNA. Cells were harvested for Western blot analysis at 4, 24, 48 and 72 hours post-transfection. Extracts from each time point were probed for the presence of CKI- α , NS5A and actin detection served as a loading control. **[B]** and **[D]** Cells set up in parallel to those described in **[A]** and **[C]** were lysed at 4, 24, 48 and 72 hours post-transfection and extracts were assayed for luciferase activity. All assays were performed in duplicate and average values are shown for each experiment. Error bars indicate the range of the values recorded at each time point.

transfected at a concentration of 25nM. Therefore, the final overall concentration of siRNAs targeting each cellular mRNA was 75nM. siRNAs were transfected into both Tri-Huh-7 and Tri-U2OS cells seeded on 24-well plates (see Section 2.2.12.1). Preliminary studies were conducted using a smaller number of cells seeded on 96-well plates. However, the results obtained using this approach were highly variable. The siRNA screen was performed in duplicate for both cell lines and luciferase activity was measured to quantify effects on replication and/or translation of the Tri-JFH1 SGR harboured within cells. 24-well plates included both positive (siHCV) and negative (scrambled siRNA) controls, each at a final concentration of 50nM. Cell viability was also measured for all siRNA-transfected cells using AquaBluer (see Section 2.2.12.2).

The complete data set from the screen in both cell lines is shown in Appendix 2. In general and consistent with results presented earlier, luciferase values were altered by siRNAs to a greater extent in Tri-U2OS cells compared to Tri-Huh-7 cells. For example, silencing of XRN1 (5'-3' exoribonuclease 1) increased luciferase activity by ~50% in Tri-Huh-7 cells and 3.5-fold in Tri-U2OS cells (Table 6) compared to controls. This observation agrees with the higher transfection efficiency achieved in U2OS cells. Given the difference in transfection efficiencies between the two cell lines, changes (either increases or decreases) in luciferase activity of >50% in Tri-U2OS cells and >25% in Tri-Huh-7 cells were selected as criteria for identifying siRNA-targeted genes that influenced viral replication/translation. Using these criteria, 65 genes were identified (Tables 1-8) and the average values for luciferase activity and cell viability are shown. For luciferase activities, the range of the values from which the average was derived is also depicted. All values are expressed as a percentage of the values obtained for cells treated with the scrambled siRNA. Silencing of these genes had a variety of effects and luciferase levels decreased (genes in red), increased (genes in green) or had opposing effects (genes in blue) in the two cell lines when they were siRNA-treated. However, the knockdown of many genes also decreased cellular viability, which was often more pronounced in the Tri-U2OS cell line. For example, silencing of RPL37 (ribosomal protein L37, Table 1) reduced cell viability to only 81% in Tri-Huh-7 cells. However, knockdown of the same gene in Tri-U2OS cells lowered cell viability to 43.4% (Table 1). From the 65 genes shown, silencing of RPS7 (ribosomal protein S7) caused the greatest reduction in Tri-Huh-7 cell viability (52.1%, Table 2), whereas Tri-U2OS cell viability was reduced to as low as 34.4% when UBB (Ubiquitin B) was knocked down by siRNA treatment (Table

6). Therefore, those siRNAs that maintained cell viability values of >80% after siRNA treatment were selected as having specific effects on the Tri-JFH1 SGR. This reduced the list of cellular genes affecting luciferase activity in both cell lines to 15. These genes are depicted (shaded grey) in Tables 1-8.

Gene	Accession No. (NM_)	Plate Position	Tri-Huh-7		Tri-U2OS	
			Luciferase (%)	Viability (%)	Luciferase (%)	Viability (%)
RPL5	000969	P1_E7	17.1 (+/-) 0.2	82.6	32.8 (+/-) 13.6	68.1
RPL7	000971	P1_E9	16.7 (+/-) 0.7	66	42.4 (+/-) 8.8	45.5
RPL11	000975	P1_F3	38.6 (+/-) 6.5	71.4	32 (+/-) 7.2	51.9
RPL12	000976	P1_F4	59.6 (+/-) 5.2	78.4	25.2 (+/-) 5	58.7
RPL13	033251	P1_F5	33.5 (+/-) 6.6	76	25.4 (+/-) 4.4	56.8
RPL14	001034996	P2_F2	19.1 (+/-) 2.3	84.1	46.9 (+/-) 10.2	48.1
RPL23a	000984	P1_G1	16.5 (+/-) 3.7	70.3	37.6 (+/-) 11.5	52.5
RPL24	000986	P1_G2	31.2 (+/-) 3.3	80.8	28.5 (+/-) 9.6	46.2
RPL27	000988	P1_G4	11.8 (+/-) 1.6	69.5	44.2 (+/-) 12.6	51.5
RPL27a	000990	P1_G6	17.6 (+/-) 9.4	79.5	23.2 (+/-) 1.4	71.8
RPL30	000989	P1_G5	19.5 (+/-) 11.1	70	26.8 (+/-) 10.1	51.5
RPL31	000993	P1_G9	31.1 (+/-) 13.7	78.6	42.3 (+/-) 7.3	51.8
RPL37	000997	P1_H2	43.1 (+/-) 10	81	38.4 (+/-) 10.6	43.4
RPLP2	001004	P1_H6	18 (+/-) 8.2	63.7	9.3 (+/-) 5.5	52

Table 1 Ribosomal proteins (large)

Gene	Accession No. (NM_)	Plate Position	Tri-Huh-7		Tri-U2OS	
			Luciferase (%)	Viability (%)	Luciferase (%)	Viability (%)
RPS2	002952	P1_H7	30 (+/-) 12.6	66.6	22.6 (+/-) 8.5	65.2
RPS3	001005	P1_H8	14 (+/-) 7.2	59.1	14.6 (+/-) 7.4	55.8
RPS3A	182777	P1_H9	11.3 (+/-) 6.9	67.1	14.4 (+/-) 7.6	44.5
RPS5	001009	P1_H10	22.1 (+/-) 9.6	77.4	20 (+/-) 10.3	52.5

RPS7	001011	P1_H11	11.3 (+/-) 5.9	52.1	35.8 (+/-) 1.8	54.3
RPS8	001012	P2_A1	3.9 (+/-) 0.1	75.4	9.8 (+/-) 2.5	62.4
RPS9	001013	P2_A2	21.9 (+/-) 1.7	108.5	5.6 (+/-) 2	66.8
RPS11	001015	P2_A3	34.1 (+/-) 12.4	95.5	15.2 (+/-) 3.9	57.9
RPS14	005617	P2_A4	6.6 (+/-) 0.1	83.8	12.5 (+/-) 3	84
RPS15	001018	P2_A5	9.7 (+/-) 1.4	84.7	9 (+/-) 2	45.5
RPS15A	001030009	P2_A6	4.4 (+/-) 0.4	92.3	8.8 (+/-) 0.2	61.2
RPS16	001020	P2_A7	2.5 (+/-) 0.3	82.2	6.5 (+/-) 2	63.6
RPS17	001021	P2_A8	7.7 (+/-) 0.1	84.7	8.3 (+/-) 1.6	56.1
RPS18	022551	P2_A9	4.4 (+/-) 0.6	75.8	7.6 (+/-) 0.1	51.1
RPS19	001022	P2_A10	5.6 (+/-) 0.8	73.9	8 (+/-) 0.6	48.7
RPS20	001023	P2_A11	8.4 (+/-) 3.2	74.7	4.7 (+/-) 2	55.5
RPS21	001024	P2_B1	7 (+/-) 2.5	73.3	14 (+/-) 3.5	57.9
RPS23	001025	P2_B2	7.7 (+/-) 2.3	88.9	8.8 (+/-) 2.3	49.2
RPS24	033022	P2_B3	5.6 (+/-) 1.4	78	9.8 (+/-) 2.9	42.9
RPS26	001029	P2_B4	6.6 (+/-) 0.8	73.3	7.4 (+/-) 2.4	61.6
RPS27A	002954	P2_B6	4.1 (+/-) 0.9	82.5	6.6 (+/-) 2.6	67
RPS28	001031	P2_B7	5.8 (+/-) 1.4	84.9	8.2 (+/-) 3.3	55.8

Table 2 Ribosomal proteins (small)

Gene	Accession No. (NM_)	Plate Position	Tri-Huh-7		Tri-U2OS	
			Luciferase (%)	Viability (%)	Luciferase (%)	Viability (%)
EIF4A2	001967	P1_B3	165 (+/-) 5.4	109	232 (+/-) 18.8	83.6
EIF4G2	001418	P1_B9	138.6 (+/-) 13.3	98	207 (+/-) 1.8	145.2
EFTUD1	024580	P3_F4	136 (+/-) 14.6	93.4	257.3 (+/-) 26.1	75.4
EIF3B	003751	P2_E2	14.5 (+/-) 4.5	92.4	34.1 (+/-) 8.3	79.1
EIF3I	003757	P2_E6	35.6 (+/-) 6.3	106.1	8.3 (+/-) 1.2	59.1
EIF3FP2	031943	P3_F8	60.9 (+/-) 7.3	82.4	49.2 (+/-) 13.3	75.4

Table 3 Translation factors

Gene	Accession No. (NM_)	Plate Position	Tri-Huh-7		Tri-U2OS	
			Luciferase (%)	Viability (%)	Luciferase (%)	Viability (%)
RNPS1	006711	P2_H9	129.6 (+/-) 0.6	99.4	209 (+/-) 41.1	82.7
RBM25	021239	P3_E5	35.7 (+/-) 3	70.3	32.4 (+/-) 8.6	72.7
HNRNPD	031370	P1_C6	58.9 (+/-) 11.1	89.1	34.3 (+/-) 2.3	103.6
RBMS2	002898	P1_E5	64.2 (+/-) 14.2	100.5	29.7 (+/-) 6.4	99.9
SRP14	003134	P2_C2	57.7 (+/-) 10.4	102.8	40.8 (+/-) 8.3	74.5
RBM7	016090	P2_G7	128.2 (+/-) 19.5	92.4	47.5 (+/-) 0.3	75.2
CPEB1	030954	P3_E11	55 (+/-) 7.7	78	168.5 (+/-) 9	53.9

Table 4 RNA-binding proteins

Gene	Accession No. (NM_)	Plate Position	Tri-Huh-7		Tri-U2OS	
			Luciferase (%)	Viability (%)	Luciferase (%)	Viability (%)
ISG15	005101	P2_F10	127.5 (+/-) 9	102.9	354 (+/-) 57	92.6
ISG20L2	030980	P3_F6	132.9 (+/-) 14	93.2	181.6 (+/-) 8.8	85.9
PRKRA	003690	P2_D11	74.7 (+/-) 4.6	97.2	47.6 (+/-) 15.5	62.8

Table 5 Proteins involved in IFN induction

Gene	Accession No. (NM_)	Plate Position	Tri-Huh-7		Tri-U2OS	
			Luciferase (%)	Viability (%)	Luciferase (%)	Viability (%)
XRN1	019001	P3_D3	154.7 (+/-) 4.9	99.3	350.7 (+/-) 26.4	94.7
UBA52	003333	P2_C8	24.9 (+/-) 9.3	77.9	12.2 (+/-) 2.4	51.9
UBB	018955	P2_C9	11.8 (+/-) 4.7	76.2	1.6 (+/-) 0.2	34.4
UBC	021009	P2_C10	34.4 (+/-) 13.1	96	10 (+/-) 0.3	46.1

Table 6 Degradation pathway proteins

Gene	Accession No. (NM_)	Plate Position	Tri-Huh-7		Tri-U2OS	
			Luciferase (%)	Viability (%)	Luciferase (%)	Viability (%)
RBBP6	032626	P1_E1	52.4 (+/-) 11.5	90	44.9 (+/-) 6.7	81.6
PDCD4	145341	P3_C2	58.9 (+/-) 11.8	105.5	27.3 (+/-) 4.6	87.1

Table 7 Cell cycle control proteins

Gene	Accession No.	Plate Position	Tri-Huh-7		Tri-U2OS	
			Luciferase (%)	Viability (%)	Luciferase (%)	Viability (%)
ACAP2	NM_012287	P3_B1	134.7 (+/-) 4.5	99.8	155.4 (+/-) 19.2	96.7
ZNF575	NM_174945	P4_A5	42.9 (+/-) 6.7	64.8	22.8 (+/-) 1.4	43.4
ZNF653	NM_138783	P3_G7	59.8 (+/-) 12.3	84.9	40 (+/-) 4.1	84.4
-	XM_203320	P4_A6	69.3 (+/-) 0.3	85.6	26.1 (+/-) 2.1	60
-	XM_497121	P4_C7	63.2 (+/-) 7.2	86.9	46.8 (+/-) 5.3	93.2
TRMT6	NM_015939	P3_C10	136.1 (+/-) 20.6	96	48.2 (+/-) 4.6	93.9
-	XM_498389	P3_G10	74.8 (+/-) 12.1	84.2	164 (+/-) 22.2	83.8

Table 8 Non-assigned proteins

7.3.1 Genes That Increased Luciferase Activity In Both Cell Lines

From the 15 identified genes, silencing of seven resulted in increased luciferase activity in both Tri-Huh-7 and Tri-U2OS cells. This result suggests that these genes encode proteins that are involved in inhibiting the replication and/or translation of HCV RNA and that this repression is relieved by gene silencing. The largest increases in luciferase levels were observed when targeting ISG15 (ISG15 ubiquitin-like modifier, Table 5) and XRN1 (Table 6). In both cases, enzyme activity was increased more dramatically in Tri-U2OS compared to Tri-Huh-7 cells and luciferase values were increased by ~3.5-fold compared to control Tri-U2OS cells. Silencing of other genes increased luciferase activity to a lesser extent and included RNSP1 (RNA binding protein S1 serine rich domain, Table 4), ISG20L2

(IFN-stimulated exonuclease gene 20kDa-like 2, Table 5), ACAP2 (ArfGAP with coiled-coil, ankyrin repeat and PH domains 2, Table 8), EIF4A2 and EIF4G2 (Table 3).

7.3.2 Genes That Decreased Luciferase Activity In Both Cell Lines

Conversely to those described above, knockdown of seven of the 15 genes led to a reduction in luciferase enzyme levels, implying that these genes promoted HCV RNA replication and/or translation. Although all of the small ribosomal proteins were apparently important, knockdown of RPS14 (ribosomal protein S14) dramatically reduced luciferase activity without lowering cell viability to less than 80% in both Tri-Huh-7 and Tri-U2OS cells (Table 2). In addition, silencing RBMS2 (RNA binding motif, single-stranded interacting protein 2, Table 4) and HNRNPD (heterogeneous nuclear ribonucleoprotein D, Table 4) led to significant decreases in luciferase levels with little effect on cellular viability. This effect was especially evident with RBMS2, where siRNA treatment decreased enzyme levels to 64.2% and 29.7% (in Tri-Huh-7 and Tri-U2OS cells respectively), yet cell viability barely deviated from 100%. Other proteins implicated in aiding HCV replication included RBBP6 (retinoblastoma binding protein 6, Table 7), PDCD4 (programmed cell death 4, Table 7), ZNF653 (zinc finger protein 653, Table 8) and an as yet undefined gene (Table 8).

7.3.3 Genes that had Opposing Effects on Luciferase Activity

One gene, TRMT6 (tRNA methyltransferase 6 homolog, Table 8) had opposing effects on luciferase activity upon silencing. Luciferase activity increased by 36% in Tri-Huh-7 cells treated with siRNAs targeting TRMT6 but was reduced by ~50% in Tri-U2OS cells treated in the same manner. This was the only example of a gene that had opposing effects in the two different cell lines without reducing cell viability to less than 80%.

7.4 Knockdown of ISG15 and XRN1 can Increase HCV RNA Replication in Transient Assays

As stated above, silencing of two genes, XRN1 and ISG15, led to the greatest increases in luciferase levels using Tri-U2OS cells, and enzyme activity also rose

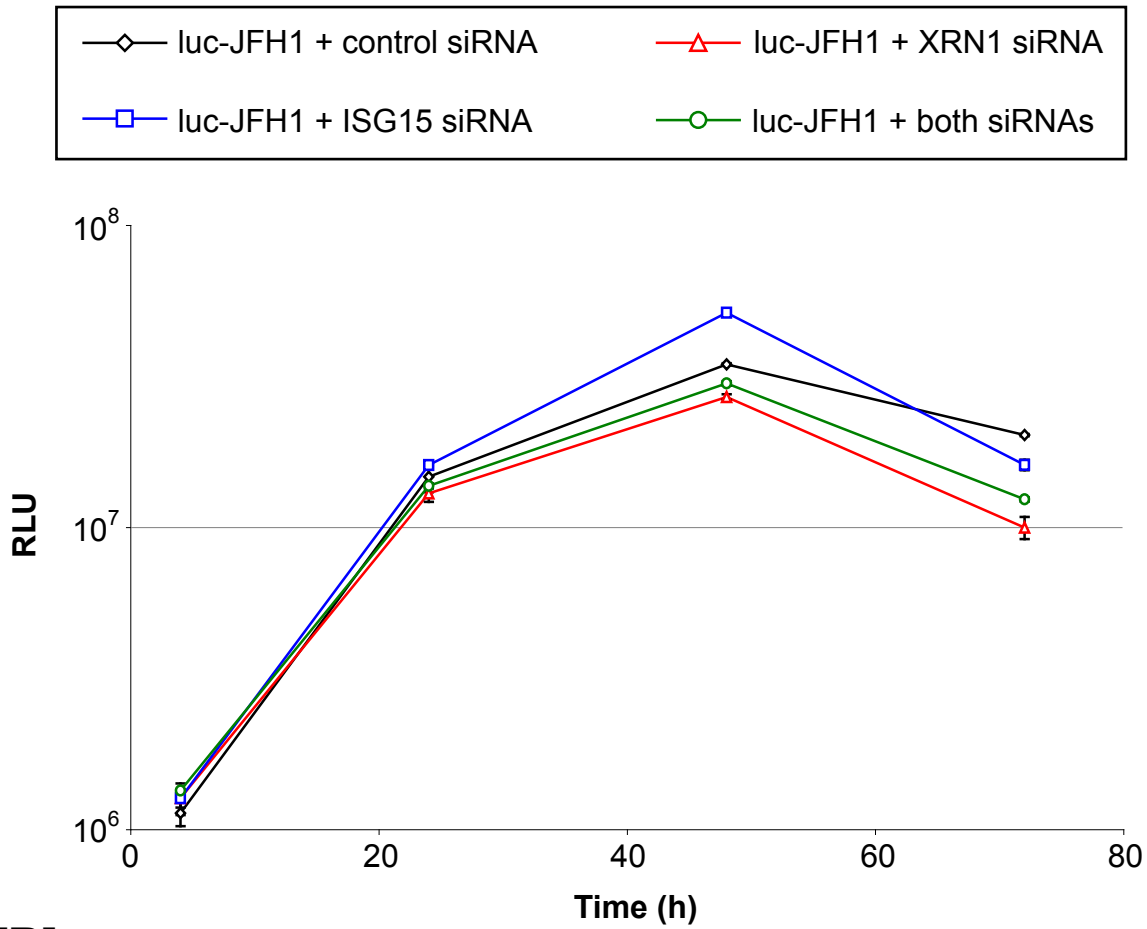
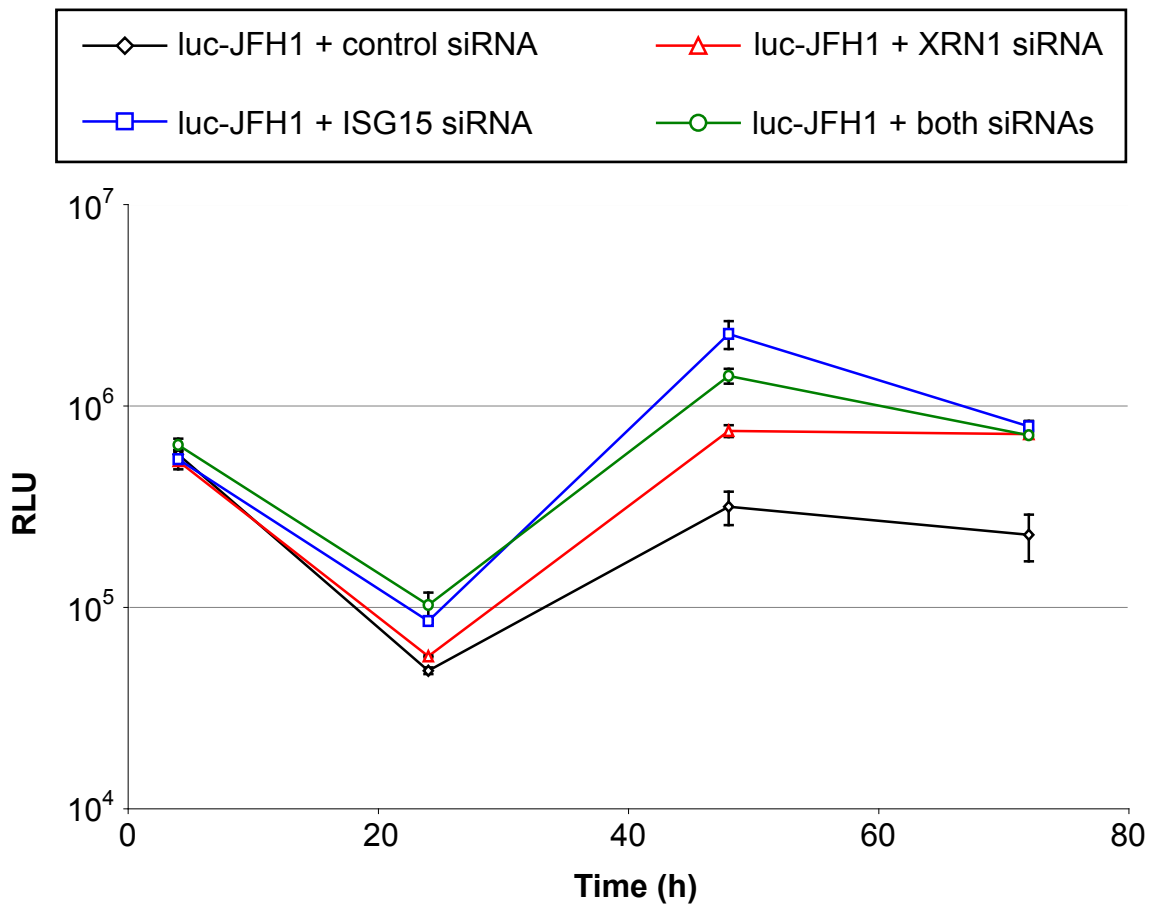
[A]**[B]**

Figure 7.9 Effect of silencing ISG15 and XRN1 on transient HCV RNA replication

RNA encoding luc-JFH1 was electroporated into **[A]** Huh-7 cells and **[B]** U2OS cells and cells were immediately transfected with 50nM of the control siRNA, or 75nM of siRNAs directed against ISG15, XRN1, or both genes (to a final siRNA concentration of 150nM). Cells were lysed at 4, 24, 48 and 72 hours post-electroporation/transfection and extracts were assayed for luciferase activity. All assays were performed in duplicate and average values are shown for each experiment. Error bars represent the range of the values recorded at each time point.

in Tri-Huh-7 cells, albeit to a lesser extent (Tables 5 and 6). To confirm the suppressive effect of these proteins in transient assays, Huh-7 and U2OS cells were electroporated with RNA from luc-JFH1 and then immediately transfected with 75nM of siRNAs targeting either XRN1 or ISG15. Additionally, cells were transfected with a combination of siRNAs against both genes (giving a final siRNA concentration of 150nM) to determine whether any synergistic effect on luciferase activity could be achieved by targeting ISG15 and XRN1 simultaneously. Cells were harvested over 72 hours post-electroporation/transfection and extracts assayed for luciferase activity (Figure 7.9).

In Huh-7 cells, silencing of ISG15 and XRN1, alone or together, did not increase luciferase activity above levels observed with cells transfected with the control siRNA, except at 48 hours where ISG15 siRNA-treated cells gave a 50% increase in luciferase values (Figure 7.9, A). By comparison, luciferase values in U2OS cells were higher in all cells treated with siRNA for 24, 48 and 72 hours (Figure 7.9, B). These data confirm that siRNA treatment is more effective in U2OS cells compared to Huh-7 cells. By 48 hours, ISG15 siRNA-treated cells yielded luciferase values that were over seven-fold greater than cells treated with the scrambled siRNA. The smallest luciferase activity increase in U2OS cells was observed when XRN1 alone was silenced, yet luciferase values were still more than two-fold greater compared to control cells at 48 hours. By 72 hours, luciferase levels in all siRNA-treated cells were approximately three-fold higher than the control U2OS cells (Figure 7.9, B). These results imply that ISG15 and XRN1 are involved in repressing HCV RNA replication in cells and silencing of the genes encoding these proteins allows the genome to replicate with greater efficiency. However, silencing of both genes simultaneously does not provide any synergistic effect.

7.5 Discussion

The aim of this part of the project was to identify cellular nucleotide-binding proteins involved in HCV RNA replication and/or translation. Aside from selecting the genes to target, a suitably robust system in which to screen the library was required. Suitable positive and negative control siRNAs, in addition to two cell lines harbouring tri-cistronic SGRs were created for this purpose.

siHCV is analogous to si313, a siRNA complementary to the 3' end of domain III and 5' end of domain IV of the HCV IRES sequence located in the HCV 5' UTR

(Chevalier et al., 2007). This siRNA was selected as a positive control for two reasons. Firstly, the IRES sequence targeted by siHCV/si313 is highly conserved and therefore unlikely to mutate during the passage of cell lines containing a HCV SGR. This was important, since a siRNA that differs from its target sequence by two or more bases is inefficient at silencing HCV replication (Randall et al., 2003). Secondly, siHCV/si313 has previously been characterised and its capacity to inhibit both HCV RNA replication and virus infection in cell culture has led to exploration of its potential as a therapeutic candidate (Chevalier et al., 2007).

The initial plan was to screen the siRNA library in transient replication assays with the luc-JFH1 SGR. However, the data obtained during optimisation experiments revealed that the process of simultaneously electroporating (luc-JFH1) and transfecting (siHCV/control siRNA) cells simultaneously was cytotoxic and 10-fold reductions in HCV replication were observed even with the scrambled control siRNA (Figure 7.2, A). As an alternative approach, it was decided to create cells containing a tri-cistronic replicon. In this situation, cells would only require transfection with siRNA, thereby avoiding electroporation. Therefore, cell lines were generated using Tri-JFH1, a tri-cistronic JFH1-based SGR containing (i) a neomycin resistance gene for selection of cells (ii) a luciferase gene for quantification of HCV RNA replication and (iii) the NS3-NS5B region required for replication of the SGR (Figure 7.3). Two cell lines, Tri-Huh-7 and Tri-U2OS were created and characterised, which were able to maintain HCV replication under selective pressure. Tri-U2OS cells supported HCV RNA replication far less efficiently compared to Tri-Huh-7 cells (Figure 7.5, B). This reduction in replication was also evident for U2OS cells used in transient replication assays with luc-JFH1 and Tri-JFH1 (Figure 7.4). U2OS cells do support HCV RNA replication, albeit to a lesser extent compared to Huh-7 cells (Targett-Adams & McLauchlan, 2005). Those cellular factors that determine the difference between replication efficiencies in the two cell lines are unknown. Consistently, siRNAs influenced replication and cell viability to a greater degree in Tri-U2OS compared to Tri-Huh-7 cells. This could be due to several reasons. Firstly, parallel experiments in both Huh-7 and U2OS cells revealed that U2OS cells are more efficiently transfected compared to Huh-7 cells. Thus, more siRNA is probably delivered into U2OS cells, giving increased gene silencing. Secondly and as mentioned above, U2OS cells support lower levels of HCV replication compared to Huh-7 cells. Reduced replication may result from limiting quantities of cellular factors or differences in cellular pathways that contribute to viral genome synthesis. Thus, such factors or

pathways may be more readily suppressed by siRNAs in U2OS cells, giving a greater effect on HCV replication levels. U2OS cells may therefore prove to be more suitable than Huh-7 cells for conducting HCV-related siRNA studies.

The contribution of cellular factors to HCV RNA replication was initially assessed by examining the effects of a siRNA targeting CKI- α . The HCV-encoded NS5A protein is a substrate for CKI- α , which is capable of hyperphosphorylating purified NS5A *in vitro* (Quintavalle et al., 2006 and 2007). Furthermore, CKI- α is involved in HCV RNA replication and silencing of this gene by siRNA treatment resulted in reduced genome synthesis (Quintavalle et al., 2006). Our results indicated that knockdown of CKI- α by siRNA treatment led to decreased NS5A hyperphosphorylation in Tri-U2OS cells (Figure 7.8, C), although no apparent effect was observed in Tri-Huh-7 cells (Figure 7.8, A). Additionally, viral RNA synthesis was reduced by seven-fold in CKI- α siRNA-treated Tri-U2OS cells by 72 hours (Figure 7.8, D) but was only decreased by two-fold in Tri-Huh-7 cells transfected in parallel (Figure 7.8, B). Therefore, viral replication was apparently reduced in accordance with decreasing levels of hyperphosphorylated NS5A; this was particularly apparent in the U2OS cell line, whereas a more modest effect was observed in Tri-Huh-7 cells. These results confirmed that CKI- α influences HCV RNA replication, possibly through modulating the phosphorylation status of NS5A. The data also reconfirmed the increased sensitivity of U2OS cells to siRNA treatment compared to Huh-7 cells.

The aim of the siRNA library screen was to identify genes that were required for HCV genome replication and/or translation. However, it became apparent that the system was also useful for identifying genes that suppressed these processes. The largest class of genes implicated in aiding HCV replication encoded subunits of ribosomal proteins, the organelles responsible for cellular protein synthesis (Table 1 and Table 2). Ribosomes consist of a small (40S) and large (60S) subunit, which together are composed of four RNA species and approximately 80 distinct proteins. The 40S subunit mediates interactions between the anticodons of the tRNA and the codons of the mRNA, while the 60S subunit catalyses peptide bond formation in the growing polypeptide chain (Steitz, 2008). Domains II and III of the HCV IRES directly contact and position the 40S ribosomal subunit at the AUG codon for core protein, thus allowing cap-independent translation of the viral polyprotein (Honda et al., 1996a and 1996b). Therefore, it was unsurprising that silencing genes encoding ribosomal subunits resulted in reduced HCV RNA

replication and cellular viability. RPS14 was the only example of a ribosomal subunit that could be silenced without reducing cell viability to less than 80% in both cell lines (Table 2). Knockdown of RPS14 decreased luciferase levels substantially to 6.6% (in Tri-Huh-7 cells) and 12.5% (in Tri-U2OS cells), making this gene worthy of further investigation.

The HCV IRES recruits the 40S ribosomal subunit to the viral RNA sequence in the absence of eukaryotic translation initiation factors (Pestova et al., 1998). However, eIF2 is required for correct placement of the initiator tRNA (Met-tRNA) on the surface of the 40S ribosomal subunit and the resulting eIF2-Met-tRNA complex is stabilised by eIF3 (Ji et al., 2004, Pestova et al., 1998). In support of this model, silencing of EIF3B, EIF3I and EIF3FP2 reduced HCV RNA replication (Table 3). However, cell viability values indicated that any reduction was at least partially due to cell death, likely arising from inhibition of cellular protein synthesis. Interestingly, silencing of two other initiation factors, eIF4A2 and eIF4G2, resulted in enhanced viral replication in both cell lines (Table 3). These proteins, along with others, comprise the eIF4F complex that recognises the modified nucleotide at the 5' end of mRNA in order to initiate cap-dependent translation (Fraser & Doudna, 2007). Since these proteins are involved in the translation of cellular mRNAs, it is possible that their silencing results in an excess of free ribosomes, which are unable to translate cellular mRNA. Therefore, an increased quantity of viral RNA may be able to interact with these free ribosomes, resulting in enhanced HCV replication (Table 3).

Several RNA-binding proteins were identified in the siRNA screen, including RBMS2, hnRNP D and RNPS1. Knockdown of RBMS2 specifically inhibited HCV RNA replication in both cell lines with no effect on cell viability (Table 4). This gene encodes a protein that binds to ssRNA molecules (Kanaoka & Nojima, 1994). Therefore, it is conceivable that RBMS2 is able to bind HCV RNA and facilitate replication. However, a lack of RBMS2 characterisation prevents any further speculation on the implications of such an interaction. In contrast to RBMS2, silencing of RNPS1 resulted in increased viral RNA synthesis. RNPS1 is a component of the cellular post-splicing complex that is involved in both mRNA nuclear export and mRNA surveillance. This system detects mRNAs with truncated ORFs and initiates nonsense-mediated mRNA decay (NMD, Lykke-Andersen, 2001, Lykke-Andersen et al., 2001). It is difficult to speculate why a protein involved in this process would inhibit HCV replication. It is possible that

knockdown of RNPS1 results in decreased export of certain mRNAs that are involved in suppressing HCV RNA synthesis.

Targeting the gene encoding hnRNP D decreased luciferase values in both cell lines (Table 4) and, following completion of the siRNA library screen, a published report has confirmed it contributes to translation of the viral genome (Paek et al., 2008). In that study, hnRNP D functions as an IRES-specific cellular transacting factor (ITAF) that binds to domain II of the HCV IRES (Paek et al., 2008). The authors demonstrated that siRNA-mediated reduction of hnRNP D in cell lines containing mono- and bi-cistronic SGRs and JFH1-infected cells resulted in the repression of viral RNA translation but not replication (Paek et al., 2008). The results from the siRNA library screen are in agreement with the notion that hnRNP D influences the virus life cycle and luciferase levels were reduced to 58.9% (Tri-Huh-7 cells) and 34.3% (Tri-U2OS cells) when hnRNP D was silenced (Table 4). However, our screen does not distinguish between effects on viral replication and those on translation, meaning further investigation would be required to determine whether hnRNP D is involved exclusively in translation of viral RNA, as suggested by Paek et al.

Silencing IFN-stimulated genes ISG15 and ISG20L2 led to increased viral replication, particularly in the case of ISG15 where siRNA treatment enhanced luciferase levels to 354% in the U2OS cell line compared to control cells (Table 5). ISG20L2 is a 3'-5' exoribonuclease that is involved in ribosome biogenesis (Coute et al., 2008), although any further biological function has yet to be determined. In contrast, ISG15 is a relatively well characterised ubiquitin homolog. Like ubiquitin, ISG15 is reversibly conjugated to cellular proteins via a series of steps utilising enzymes that activate, conjugate and finally ligate ISG15 to target proteins (Sadler & Williams, 2008). While protein ubiquitination has been demonstrated to drive a variety of cellular processes, the effect of ISG15 addition (referred to as ISGylation) to proteins is unclear. ISG15 is thought to act as an antiviral protein and various studies have demonstrated that it interferes with the life cycles of several viruses, including human immunodeficiency virus (HIV, Okumura et al., 2006) and Ebola virus (Malakhova & Zhang, 2008, Okumura et al., 2008). An antiviral role for ISG15 is further supported by the fact that some viruses have evolved strategies to target cellular ISGylation, as seen with the NS1 protein of influenza B virus (Yuan & Krug, 2001). Cellular proteins targeted for ISGylation include the protein kinase PKR and the cytoplasmic helicase RIG-I (Zhao et al., 2005), both of which are involved in the innate immune response to HCV infection

(Gale et al., 1997, Saito et al., 2008). Innate immune responses are typically triggered by the recognition of viral motifs known as pathogen-associated molecular patterns (PAMPs) and the RIG-I protein binds the polyuridine tract present within the 3' UTR of HCV RNA (Saito et al., 2008). This leads to the activation of IFN regulatory factor (IRF3), upregulation of IFN- α/β production and further activation of IFN-stimulated genes. In contrast, dsRNA or the cellular protein PACT usually activate PKR, leading to its autophosphorylation and subsequent phosphorylation of the α subunit of eIF2, shutting down cellular translation initiation as a result (Samuel, 1993). These two proteins exhibit different mechanisms of viral suppression and both pathways are targeted and suppressed by HCV-encoded NS5A (Gale et al., 1998, Gale et al., 1997) and NS3/4A (Breiman et al., 2005, Tasaka et al., 2007). It is possible that ISGylation of RIG-I and PKR is a defence against their inactivation by HCV, thereby enhancing their antiviral effect. However, the precise mechanism by which ISG15 mediates inhibition of HCV replication is likely to be complex since at least 160 cellular genes modified by ISG15 have been identified to date (Zhao et al., 2005).

One other gene worthy of note encoded XRN1, a 5'-3' exoribonuclease that degrades RNA molecules (Muhlrad et al., 1994). This process is thought to occur within cytoplasmic processing bodies (Cougot et al., 2004, Ingelfinger et al., 2002) following uncapping of target RNA by the Dcp1:Dcp2 decapping complex. Silencing of XRN1 resulted in HCV replication efficiencies of 154.7% and 350.7% in Tri-Huh-7 and Tri-U2OS cells respectively (Table 6). These results suggest that, like mRNAs, HCV RNA genomes are degraded by XRN1. Viral RNA is uncapped, therefore association with the Dcp1:Dcp2 complex is presumably unnecessary. However, the mechanism allowing XRN1 to negotiate structured RNA elements such as the HCV IRES is unclear. It would be interesting to determine whether the cytoplasmic dots observed by confocal microscopy for dsRNA (Targett-Adams et al., 2008a), believed to represent HCV replication complexes, co-localised with those dots representing processing bodies (Cougot et al., 2004, Ingelfinger et al., 2002). Even if this were not the case, it remains to be determined whether RNA decay is limited to processing bodies, or can occur within other regions of the cell. For example, the exosome, implicated in NMD, does not localise to processing bodies (Sheth & Parker, 2003).

In conclusion, the siRNA library screen revealed a number of cellular proteins that are potentially involved in the HCV life cycle, either through aiding or suppressing

viral RNA replication and/or translation. The role of ISG15 in suppressing HCV is particularly interesting and further work is being conducted on this protein.

8 Conclusions and Further Perspectives

8.1 Summary

During the course of this study, several findings that contribute to the current understanding of HCV biology have emerged. The main findings are summarised below.

(i) GFP can be inserted within the C-terminal coding region of NS5A, in the context of a JFH1-based SGR. RNA transcribed from this construct replicates efficiently in cells and permits live-cell analysis of NS5A.

(ii) When expressed from a NS3-NS5B polyprotein, NS5A exhibits an ER-like distribution and localises to discrete cytoplasmic foci. NS5A displays low mobility in foci but has higher mobility on the ER membrane. This result was confirmed using SGRs containing photoactivatable NS5A (NS5A-PAGFP).

(iii) Removal of NS4B from the polyprotein results in loss of NS5A within foci. In this situation, NS5A displays an ER-like pattern and is more mobile compared to when expressed from polyproteins that include NS4B. Thus, the localisation and mobility of NS5A is influenced by NS4B.

(iv) From mutation studies, residues within the NS4B C-terminus are important for foci formation. As a consequence of blocking foci formation, NS5A no longer localises to these sites and exhibits increased mobility. NS5A hyperphosphorylation seemingly does not occur when foci production is abolished.

(v) Based on analysis of NS4B mutations that prevented replication but did not disrupt foci formation or alter the properties of NS5A, NS4B appears to play a direct role in HCV RNA synthesis.

(vi) At least for some mutations, NS4B can be *trans*-complemented, leading to the rescue of replication for defective SGRs. Replication can be also be reconstituted from two inactive SGRs harbouring lethal mutations within NS4B and NS5A. These SGRs appear to be mutually dependent upon each other for RNA synthesis.

(vii) The C-terminus of NS4B influences virus production via an unknown mechanism. In JFH1, a point mutation resulted in viral titres being increased by up to ~5-fold. However, introduction of the same mutation into the chimeric J6-JFH1 virus resulted in decreased production of infectious progeny. Therefore, the

influence of NS4B appears to be genotype-specific and suggests that the protein interacts with one or more of the core-NS2 components.

(viii) U2OS cells are capable of supporting autonomous HCV RNA replication over extended time periods. Thus, there are alternatives to Huh-7 cells for identification of cell factors that support viral RNA synthesis. In the study presented in this thesis, U2OS cells support higher transfection efficiencies for siRNA screening compared to Huh-7 cells, facilitating the identification of cellular genes important for replication of the HCV genome.

(ix) Several cellular proteins that influence HCV RNA replication have been identified, which are capable of enhancing and repressing genome synthesis. Repression of ISGs, particularly ISG15, resulted in substantially increased viral RNA synthesis.

Some of the ideas and implications generated from the above findings are now explored in greater detail, including potential approaches to further these studies. Particular emphasis is placed on the continued investigation into HCV replication, through developing the techniques employed in this study. In addition, ideas concerning HCV quasispecies and treatment are also discussed.

8.2 Applications of Technology to Examine HCV RNA Replication

8.2.1 GFP and FRAP

The properties of GFP (see Section 1.7.1) make it ideal for investigating the localisation and behaviour of proteins. In this study, GFP was inserted into domain III of NS5A and replicons harbouring the fusion protein were replication competent. Utilising IF and FRAP analysis, the GFP insertion allowed assessment of the interaction of NS5A with RCs. FRAP analysis provides a possible alternative to biochemical assays for measuring the interactions of proteins with other proteins, complexes or organelles. For example, NS5A was relatively immobile when localised to foci/RCs, suggesting that the protein is tightly tethered at these sites. Biochemical assays support this notion, since NS5A expressed alone could be extracted more readily from membranes, compared to protein expressed in a context where RCs would be predicted to form (Brass et al., 2002). While FRAP analysis is useful for defining protein interactions, it can also reveal the binding strength of such associations. For example, studies utilising D2 domains from core

linked to GFP have shown that the domain from HCV strain HC-J6 exhibits lower mobility on LDs compared to the domain from JFH1, indicating that HC-J6 core binds LDs more tightly (Shavinskaya et al., 2007). These changes in mobility can be subtle, and it is doubtful they would be detected by other techniques typically used to analyse protein interactions, such as immunoprecipitation assays or membrane extraction methods. Thus, FRAP is a highly sensitive method and GFP-fusion technology means that it can be readily applied to the study of a wide range of biologically important proteins (Sprague & McNally, 2005).

Improvements in FRAP-based methods could prove useful for determining the nature of association of HCV-encoded replicase proteins with membranes. For example, palmitoylation is a lipid modification of Cys residues that can promote the binding of proteins to cell membranes, as found with H-Ras trafficking (Kenworthy, 2006). The contribution of palmitoylation to membrane association has been determined recently using FRAP laser beam-size analysis. This technique, unlike standard FRAP, uses two lasers to bleach different-sized cellular areas and can distinguish between fluorescence recovery by diffusion (movement of protein on the membrane) and recovery by membrane exchange (movement of protein between membranes and cytoplasmic pools, Henis et al., 2006). Assessing changes in diffusion/membrane exchange rates can reveal the contribution of amino acids to membrane association. For instance, it has been revealed that only one of the two palmitoylated Cys residues within the H-Ras HVR is required to stabilise its membrane interaction (Henis et al., 2006). Interestingly, HCV-encoded NS4B apparently undergoes palmitoylation on two C-terminal Cys residues and this lipid modification is suggested to aid interactions between the viral NS proteins during RC formation (Yu et al., 2006). Unlike H-Ras however, palmitoylation apparently had no effect on NS4B membrane association, although the method by which this conclusion was reached was not described (Yu et al., 2006). It would be interesting to further examine this observation using FRAP laser-beam size analysis. Here, the contribution of each Cys residue to NS4B membrane binding, if any, could be determined. In particular, this may help define the importance of one NS4B Cys residue (Cys257 in Yu et al., 2006) that undergoes palmitoylation, yet was dispensable for RNA replication in assays described in this study (referred to as M15, see Section 4.3.1).

8.2.2 Alternative Fluorescent Technologies

While GFP-fusion proteins permit FRAP analysis as discussed above, the relatively large size of GFP (27kDa) means that tagging or insertion can also lead to a loss of function in the protein of interest. For HCV, the flexibility of NS5A is unique and no other protein within the NS3-NS5B coding region can tolerate GFP insertion without abolishing RNA replication (Moradpour et al., 2004b). Thus, smaller fluorescent tags may provide alternate means of tagging HCV proteins while retaining replicative function.

One alternative approach would be the use of tetracysteine tags, which can be only six amino acids in length (Cys-Cys-Xaa-Xaa-Cys-Cys) and are capable of binding bi-arsenical derivatives (such as FIAsh [green] and ReAsH [red]) to produce fluorescence (Frischknecht et al., 2006). The small size of the motif coupled with live-cell compatibility means that tetracysteine tags provide an alternative for studying proteins that are sensitive to GFP insertion or tagging. For example, HIV budding is inhibited when the viral Gag protein (which constitutes the retroviral capsid), is tagged with GFP and this process can only be rescued by over-expression of unlabelled Gag (Larson et al., 2005). However, insertion of a tetracysteine motif within HIV-encoded Gag allows monitoring of protein localisation, while remaining competent for HIV budding (Rudner et al., 2005). Tetracysteine tags also offer other advantages over GFP fusion. Firstly, combinatorial use of FIAsh/ReAsH labelling is useful for 'pulse chase'-like experiments, where newly synthesised protein populations can be tracked over time, as demonstrated with HIV proteins Gag (Perlman & Resh, 2006, Rudner et al., 2005) and integrase (Arhel et al., 2006). Secondly, labelling can be achieved concurrently with translation, independently of any protein maturation events that may be required to observe GFP (Campbell & Hope, 2008). Finally, FIAsh and ReAsH tags can be used to photoconvert diaminobenzidine (DAB), yielding electron-dense deposits that can be visualised by EM (Frischknecht et al., 2006). This opens up the possibility of examining proteins using light microscopy, and then correlating the analysis with that gained through EM observation of the same sample. For example, the technique has previously been used to show that the same tetracysteine-tagged connexins can be visualised by IF and EM within the same cell (Gaietta et al., 2002).

Future studies on HCV may well utilise tetracysteine-tagged viral proteins. Indeed, such a motif has already been inserted into the core protein of JFH1 and this

construct is capable of producing infectious virus (Lindenbach, B., 15th International Symposium on Hepatitis C and Related Viruses, 2008). It would be interesting to determine whether such a tag could be inserted into the NS4B coding region without abolishing replication. In this study, we have shown that mutations, particularly within Region 2 (see Chapter 4) of the protein, can tolerate substitution without affecting RNA synthesis. Furthermore, the C-terminal end of NS4B Region 2 harbours a Asp-Cys-Pro-Ile-Pro-Cys motif. One possibility would be to mutate this genome segment to encode a Cys-Cys-Pro-Ile-Cys-Cys motif and determine whether RNA replication was affected. If such mutations could be tolerated, this might allow examination of NS4B localisation in live cells that actively replicate HCV RNA. Moreover, FIAsH/ReAsH and DAB labelling may permit visualisation of NS4B localisation sites by EM in the same sample. Such an approach may help define the nature of NS4B-induced RCs more precisely.

Aside from labelling virus components using dyes as described above, exciting implications for virus study have recently emerged from the use of fluorescent semiconductor nanocrystals, typically referred to as quantum dots (QDs). QDs exhibit remarkable photostability and brightness (Michalet et al., 2005), allowing QD-labelled proteins to be tracked over extensive periods with little risk of photobleaching. Recently, conjugation of QDs to viral particles has provided an alternative method for investigating virion localisation. For example, QDs encapsulated within the virion itself (Dixit et al., 2006, Li et al., 2009), or conjugated to virus glycoproteins via antibodies (Agrawal et al., 2005, Bentzen et al., 2005) have been used to examine simian virus 40 (SV40) and respiratory syncytial virus (RSV). More recently, biotinylated acceptor peptides incorporated within the viral membrane of HIV virions could be labelled using streptavidin-coated QDs, allowing virus particle trafficking to be monitored in live cells (Joo et al., 2008). To date, QDs have not been used to label viral proteins involved in intracellular events, such as genome replication. One possibility could involve insertion of a biotinylation motif within the C-terminus of NS5A, which could then be labelled using streptavidin-coated QDs. Insertion of such a motif into NS5A has previously been achieved using a domain of *Propionibacterium shermanii* transcarboxylase (PSTCD), resulting in a tagged NS5A protein that is metabolically biotinylated within cells (McCormick et al., 2006). Labelling of NS5A-PSTCD would then require intracellular delivery of QDs, perhaps through microinjection. If technical challenges could be overcome (e.g. specific

incorporation of QDs), this approach may allow analysis of viral replication in live cells over extended time periods.

8.2.3 siRNA and Alternative Approaches

During this project, a siRNA library was used to identify novel cellular factors that influenced HCV RNA replication. In particular, ISG15 was identified as a protein apparently involved in suppressing viral RNA synthesis in both Huh-7 and U2OS cells. It would be interesting to determine the effect of ISG15 levels on HCV replication over longer time periods. Unfortunately, siRNA molecules are short-lived and therefore offer only transient inhibition of gene expression (Paddison et al., 2002). An alternative approach would be to utilise short hairpin RNAs (shRNAs), synthetic RNA molecules conceptually modelled upon cellular micro RNAs (miRNAs). miRNAs are not translated into protein but are processed to form short RNA duplexes with siRNA-like properties (Bernards et al., 2006). Several groups have produced retroviral, adenoviral or lentiviral vectors that produce shRNAs, and successful integration of the vector into the host genome can mediate persistent gene silencing in mammalian cells (Rubinson et al., 2003) as well as whole animals, including mice (Rubinson et al., 2003, Tiscornia et al., 2003) and rats (Dann et al., 2006). Inducible systems for reversible temporal inactivation have also been developed. Here, a promoter that incorporates a bacterial operator sequence drives shRNA expression. Expression is blocked by the autonomous production of a repressor that binds the operator, thereby blocking transcription from the promoter. However, addition of a small molecule (such as doxycycline [Dox]) that binds the repressor (and therefore prevents binding of the repressor to the operator), results in shRNA expression. In effect, the addition of Dox induces shRNA production and consequently gene silencing and removal of Dox reverses this effect. Such inducible shRNAs have been used in cell culture (van de Wetering et al., 2003) and more recently in mice (Seibler et al., 2007) and rats (Herold et al., 2008).

An inducible shRNA encoding ISG15 would be invaluable for analysing the apparent anti-viral effect of the protein. In this system, HCV replication could be monitored by silencing ISG15 production for varying periods of time. IFN could be administered to Dox-treated and untreated cells, meaning the individual contribution of ISG15 to HCV replication knockdown could then be directly assessed. Furthermore, it has recently become possible to infect mouse cells with

HCVpp and HCVcc (Ploss et al., 2009). With further advances in producing small animal models for HCV infection, the effect of tuneable ISG15 silencing on HCV replication *in vivo* could perhaps be determined. This system could be applied to a variety of ISGs and the importance of each could be established. Such an approach may have important implications for HCV treatment. For example, although the current method of treatment for HCV-infected patients involves IFN- α administration, it is currently unclear how the compound eradicates the virus. Therefore, the studies described above may provide an important step in understanding the anti-viral mechanisms induced by IFN treatment, possibly improving prospects for a more effective HCV therapy. These types of study could be applied to other viral infections, since IFN has also been used to treat HBV and HIV (Chevaliez & Pawlotsky, 2009).

8.3 HCV and *trans*-Complementation

Previous investigation into HCV *trans*-complementation had demonstrated that NS5A was the only replicase component that could be supplied from a separate polyprotein (Appel et al., 2005a, Tong & Malcolm, 2006). In contrast, NS4B could not be *trans*-complemented in these assays. It is probable that this result arose from a combination of the limitations of the system used to analyse complementation (genotype 1 SGRs and selectable cell lines) alongside the particular set of NS4B mutants tested. Hence, the superior replication capacity of JFH1 offers a more robust system for the study of *trans*-complementation and may provide a useful tool for testing the complementation abilities of other NS proteins. Our results suggest NS4B harbouring mutations within its predicted C-terminal α -helices may not *trans*-complement, compared to unstructured regions. This hypothesis could form the basis for the design of other mutations within NS4B that can be complemented *in trans*. If mutations within inaccessible areas of protein (as shown with the TMDs of NS4B) are incapable of complementation (Appel et al., 2005a), producing a map of NS4B regions that can and cannot be rescued by functional protein supplied *in trans* may give further insight into its contribution to HCV RNA replication.

Although the ability to *trans*-complement SGRs containing either non-functional NS5A or NS4B was tested, it would be interesting to determine whether a single SGR harbouring mutations within both proteins could be complemented. Complementation of a series of mutations is possible with KV, where replication of

defective genomes containing mutations in NS1, NS3 and NS5 can be rescued *in trans* (Khromykh et al., 2000). Similarly, more than one of the complementing NS4B mutations (those in M2 and M8) could be combined within a single RNA molecule to determine whether protein function could still be rescued under these conditions. Finally, it would also be intriguing to investigate whether two defective NS4B proteins were able to complement each other. If cells electroporated with RNAs carrying mutations M2 and M8 exhibited replication, it may indicate that distinct regions of the NS4B C-terminus are capable of *trans*-complementing each other, resulting in production of functional protein. This approach could also be tested for other regions of NS4B, such as the N-terminus.

8.3.1 Implications for Quasispecies Maintenance

In the assays described here, non-replicating SGRs containing mutations within either NS4B or NS5A were able to reconstitute replication. The ability to recover active replication from defective genomes has possible implications for the formation of RCs within HCV-infected cells. RNA synthesis from each of the genomes appeared to be mutually dependent, since they were unable to replicate individually in cells. One interpretation of the data is that NS4B complementation occurs within RCs (see model, Figure 5.9) and that both genomes are present within these structures. This possibility raises a question as to how many different RNA species can be incorporated within a single RC during its formation. In HCV-infected patients, the virus circulates as a broad spectrum of heterogeneous genomes termed quasispecies. The results from this study suggest that viral genomes incapable of replicating individually may be able to survive in the infected host, via incorporation into RCs harbouring genomes that could provide functional, complementing proteins. Studies have shown that HCV genomes lacking the structural proteins can be packaged into virions via proteins supplied *in trans* (Ishii et al., 2008, Steinmann et al., 2008). Thus, it is possible that the proteins supplied from other functional quasispecies may maintain HCV RNAs containing both deletions and point mutations in structural and NS genes. It would be interesting to sequence HCV variants isolated from infected individuals, with the purpose of identifying mutations that would render SGRs replication-incompetent in cell culture. Identification of such mutants would imply that functional proteins supplied by replication-competent viruses are important for the survival of defective viral species.

If quasispecies persist through *trans*-complementation, this mechanism could have important implications for HCV therapy. In patients treated with telaprevir monotherapy, a sharp reduction in wt virus is seen, at which point pre-existing telaprevir-resistant variants become prevalent (Kieffer et al., 2007). These resistant mutations typically arise in NS3, the protein targeted by telaprevir (Sarrazin et al., 2007). Similarly, IFN- α and ribavirin combination therapy does not eradicate the virus in ~50-60% of patients infected with genotype 1 HCV strains (Soriano et al., 2009). Thus, viral quasispecies in some HCV-infected individuals may encompass viruses resistant to telaprevir, IFN- α and ribavirin. Indeed, viral breakthrough (HCV re-emergence) has been observed during the off-study period of patients receiving telaprevir, IFN- α and ribavirin triple therapy (Lawitz et al., 2008). Breakthrough could be a consequence of *trans*-complementation between HCV quasispecies. For example, a low level of HCV replication might be maintained within RCs harbouring two populations of viral genomes; those resistant to telaprevir, and those resistant to IFN- α /ribavirin. In this scenario, triple therapy would select for these resistant viruses, which may then exchange between them the proteins responsible for conferring resistance. As with NS4B complementation, such events may be rare or inefficient, possibly accounting for the undetectable levels of HCV RNA during the treatment period (Lawitz et al., 2008). However, this low level of replication could be sufficient to permit HCV breakthrough following cessation of therapy. Thus, assessing the extent to which HCV is able to maintain RNA replication by *trans*-complementation may be important for the future development of HCV therapies.

Appendices

Appendix 1: Primers for NS4B C-terminal Mutagenesis

Mutant		Primer (5'-3')
M1	F	C ATC TGC GCG GCC ATT CTG <u>GCC</u> CGC CAC GTG GGA CCG GG
	R	CC CGG TCC CAC GTG GCG <u>GGC</u> CAG AAT GGC CGC GCA GAT G
M2	F	CTG CGC CGC CAC GTG <u>GCA</u> CCG GGG GAG GGC GCG
	R	CGC GCC CTC CCC CGG <u>TGC</u> CAC GTG GCG GCG CAG
M3	F	GTG GGA CCG GGG GAG <u>GCC</u> GCG GTC CAA TGG ATG
	R	CAT CCA TTG GAC CGC <u>GGC</u> CTC CCC CGG TCC CAC
M4	F	GGC GCG GTC CAA TGG ATG <u>GCC</u> AGG CTT ATT GCC TTT GC
	R	GC AAA GGC AAT AAG CCT <u>GGC</u> CAT CCA TTG GAC CGC GCC
M5	F	G ATG AAC AGG CTT ATT GCC <u>GCT</u> GCT TCC AGA GGA AAC CAC
	R	GTG GTT TCC TCT GGA AGC <u>AGC</u> GGC AAT AAG CCT GTT CAT C
M6	F	GCC TTT GCT TCC AGA GGA <u>GCC</u> CAC GTC GCC CCT ACT CAC
	R	GTG AGT AGG GGC GAC GTG <u>GGC</u> TCC TCT GGA AGC AAA GGC
M7	F	GGA AAC CAC GTC GCC CCT <u>GCT</u> CAC TAC GTG ACG GAG
	R	CTC CGT CAC GTA GTG <u>AGC</u> AGG GGC GAC GTG GTT TCC
M8	F	CT ACT CAC TAC GTG ACG <u>GCG</u> TCG GAT GCG TCG CAG
	R	CTG CGA CGC ATC CGA <u>CGC</u> CGT CAC GTA GTG AGT AG
M9	F	G ACG GAG TCG GAT GCG TCG <u>GCG</u> CGT GTG ACC CAA CTA CTT G
	R	C AAG TAG TTG GGT CAC ACG <u>CGC</u> CGA CGC ATC CGA CTC CGT C

M10	F	G TCG CAG CGT GTG ACC CAA <u>GCA</u> CTT GGC TCT CTT ACT ATA AC
	R	GT TAT AGT AAG AGA GCC AAG <u>TGC</u> TTG GGT CAC ACG CTG CGA C
M11	F	CT GAG TAG GCT GGT TAT <u>AGC</u> AAG AGA GCC AAG TAG TTG
	R	CT GAG TAG GCT GGT TAT <u>AGC</u> AAG AGA GCC AAG TAG TTG
M12	F	CTT ACT ATA ACC AGC CTA <u>GCC</u> AGA AGA CTC CAC AAT TG
	R	CA ATT GTG GAG TCT TCT <u>GGC</u> TAG GCT GGT TAT AGT AAG
M13	F	CTC AGA AGA CTC CAC AAT <u>GCG</u> ATA ACT GAG GAC TGC CC
	R	GG GCA GTC CTC AGT TAT <u>CGC</u> ATT GTG GAG TCT TCT GAG
M14	F	GA CTC CAC AAT TGG ATA <u>GCT</u> GAG GAC TGC CCC ATC
	R	GAT GGG GCA GTC CTC <u>AGC</u> TAT CCA ATT GTG GAG TC
M15	F	C AAT TGG ATA ACT GAG GAC <u>GCC</u> CCC ATC CCA TGC TCC
	R	GGA GCA TGG GAT GGG <u>GGC</u> GTC CTC AGT TAT CCA ATT G

Appendix 2: siRNA Library Screen – Names and Data for all 299 genes

Plate 1

Plate position	Gene	Full name
A1	ADAR	Adenosine deaminase, RNA-specific
A2	CDC6	Cell division cycle 6 homolog
A3	CIRBP	Cold inducible RNA binding protein
A4	EE1A1	Eukaryotic translation elongation factor 1 alpha 1
A5	EE1A2	Eukaryotic translation elongation factor 1 alpha 2
A6	EE1B2	Eukaryotic translation elongation factor 1 beta 2
A7	EEF1D	Eukaryotic translation elongation factor 1 delta

A8	EEF1G	Eukaryotic translation elongation factor 1 gamma
A9	EEF2	Eukaryotic translation elongation factor 2
A10	EIF2S1	Eukaryotic translation initiation factor 2, subunit 1 alpha, 35kDa
A11	EIF2B1	Eukaryotic translation initiation factor 2B, subunit 1 alpha, 26kDa
B1	EIF2S3	Eukaryotic translation initiation factor 2, subunit 3 gamma, 52kDa
B2	EIF4A1	Eukaryotic translation initiation factor 4A, isoform 1
B3	EIF4A2	Eukaryotic translation initiation factor 4A, isoform 2
B4	EIF4B	Eukaryotic translation initiation factor 4B
B5	EIF4E	Eukaryotic translation initiation factor 4E
B6	EIF4EBP1	Eukaryotic translation initiation factor 4E binding protein 1
B7	EIF4EBP2	Eukaryotic translation initiation factor 4E binding protein 2
B8	EIF4G1	Eukaryotic translation initiation factor 4 gamma 1
B9	EIF4G2	Eukaryotic translation initiation factor 4 gamma 2
B10	EIF5	Eukaryotic translation initiation factor 5
B11	EIF5A	Eukaryotic translation initiation factor 5A
C1	FBL	Fibrillarin
C2	ETF1	Eukaryotic translation termination factor 1
C3	GRSF1	G-rich RNA sequence binding factor 1
C4	GSPT1	G1 to S phase transition 1
C5	HCFC1	Host cell factor C1
C6	HNRPD	Heterogeneous nuclear ribonucleoprotein D
C7	AGFG1	ArfGAP with FG repeats 1
C8	AGFG2	ArfGAP with FG repeats 2

C9	SP110	SP110 nuclear body protein
C10	EIF3S6	Eukaryotic translation initiation factor 3, subunit 6 48kDa
C11	ISG20	Interferon stimulated exonuclease gene 20kDa
D1	EIF6	Eukaryotic translation initiation factor 6
D2	MAZ	Myc-associated zinc finger protein
D3	RPL10A	Ribosomal protein L10a
D4	OAS1	2',5'-oligoadenylate synthetase 1, 40/46kDa
D5	OAS2	2',5'-oligoadenylate synthetase 2, 69/71 kDa
D6	OAS3	2',5'-oligoadenylate synthetase 3, 100kDa
D7	PA2G4	Proliferation-associated 2G4, 38kDa
D8	MED1	Mediator complex subunit 1
D9	PTBP1	Polypyrimidine tract binding protein 1
D10	PURA	Purine-rich element binding protein A
D11	PURB	Purine-rich element binding protein B
E1	RBBP6	Retinoblastoma binding protein 6
E2	RBM3	RNA binding motif (RNP1, RRM) protein 3
E3	RBM4	RNA binding motif protein 4
E4	RBMS1	RNA binding motif, single-stranded interacting protein 1
E5	RBMS2	RNA binding motif, single-stranded interacting protein 2
E6	UPF1	UPF1 regulator of nonsense transcripts homolog
E7	RPL5	Ribosomal protein L5
E8	RPL6	Ribosomal protein L6
E9	RPL7	Ribosomal protein L7
E10	RPL7A	Ribosomal protein L7a
E11	RPL8	Ribosomal protein L8

F1	RPL9	Ribosomal protein L9
F2	RPL10	Ribosomal protein L10
F3	RPL11	Ribosomal protein L11
F4	RPL12	Ribosomal protein L12
F5	RPL13	Ribosomal protein L13
F6	RPL15	Ribosomal protein L15
F7	RPL18	Ribosomal protein L18
F8	RPL18A	Ribosomal protein L18a
F9	RPL19	Ribosomal protein L19
F10	RPL21	Ribosomal protein L21
F11	RPL22	Ribosomal protein L22
G1	RPL23A	Ribosomal protein L23a
G2	RPL24	Ribosomal protein L24
G3	RPL26	Ribosomal protein L26
G4	RPL27	Ribosomal protein L27
G5	RPL30	Ribosomal protein L30
G6	RPL27A	Ribosomal protein L27a
G7	RPL28	Ribosomal protein L28
G8	RPL29	Ribosomal protein L29
G9	RPL31	Ribosomal protein L31
G10	RPL32	Ribosomal protein L32
G11	RPL34	Ribosomal protein L34
H1	RPL35A	Ribosomal protein L35a
H2	RPL37	Ribosomal protein L37
H3	RPL37A	Ribosomal protein L37a
H4	RPL38	Ribosomal protein L38
H5	RPL39	Ribosomal protein L39

H6	RPLP2	Ribosomal protein, large P2
H7	RPS2	Ribosomal protein S2
H8	RPS3	Ribosomal protein S3
H9	RPS3A	Ribosomal protein S3a
H10	RPS5	Ribosomal protein S5
H11	RPS7	Ribosomal protein S7

Plate 2

Plate position	Gene	Full name
A1	RPS8	Ribosomal protein S8
A2	RPS9	Ribosomal protein S9
A3	RPS11	Ribosomal protein S11
A4	RPS14	Ribosomal protein S14
A5	RPS15	Ribosomal protein S15
A6	RPS15A	Ribosomal protein S15a
A7	RPS16	Ribosomal protein S16
A8	RPS17	Ribosomal protein S17
A9	RPS18	Ribosomal protein S18
A10	RPS19	Ribosomal protein S19
A11	RPS20	Ribosomal protein S20
B1	RPS21	Ribosomal protein S21
B2	RPS23	Ribosomal protein S23
B3	RPS24	Ribosomal protein S24
B4	RPS26	Ribosomal protein S26
B5	RPS27	Ribosomal protein S27

B6	RPS27A	Ribosomal protein S27a
B7	RPS28	Ribosomal protein S28
B8	SP1	SP1 transcription factor
B9	SP2	SP2 transcription factor
B10	SP3	SP3 transcription factor
B11	SP4	SP4 transcription factor
C1	SP100	Nuclear antigen SP100
C2	SRP14	Signal recognition particle 14kDa
C3	STAU1	Staufen, RNA binding protein, homolog 1
C4	TARBP1	TAR (HIV-1) RNA binding protein 1
C5	TARBP2	TAR (HIV-1) RNA binding protein 2
C6	TFDP1	Transcription factor Dp-1
C7	TFDP2	Transcription factor Dp-2
C8	UBA52	Ubiquitin A-52 residue ribosomal protein fusion product 1
C9	UBB	Ubiquitin B
C10	UBC	Ubiquitin C
C11	EIF4H	Eukaryotic translation initiation factor 4H
D1	CNBP	CCHC-type zinc finger, nucleic acid binding protein
D2	ZNF143	Zinc finger protein 143
D3	ZNF148	Zinc finger protein 148
D4	ZNF161	Zinc finger protein 161
D5	SLBP	Stem-loop binding protein
D6	CDK2AP1	Cyclin-dependent kinase 2 associated protein 1
D7	TAF15	TAF15 RNA polymerase II, TATA box binding protein associated factor, 68kDa
D8	RBM10	RNA binding motif protein 10
D9	UBL4A	Ubiquitin-like 4A

D10	CDC45L	CDC45 cell division cycle 45-like
D11	PRKRA	Protein kinase, interferon-inducible double-stranded RNA dependent activator
E1	OASL	2',5'-oligoadenylate synthetase-like
E2	EIF3B	Eukaryotic translation initiation factor 3, subunit B
E3	EIF3C	Eukaryotic translation initiation factor 3, subunit C
E4	EIF3D	Eukaryotic translation initiation factor 3, subunit D
E5	EIF3F	Eukaryotic translation initiation factor 3, subunit F
E6	EIF3I	Eukaryotic translation initiation factor 3, subunit I
E7	EIF4E	Eukaryotic translation initiation factor 4E
E8	EIF2B4	Eukaryotic translation initiation factor 2B, subunit 4 delta, 67kDa
E9	EIF2B3	Eukaryotic translation initiation factor 2B, subunit 3 gamma, 58kDa
E10	EIF2B2	Eukaryotic translation initiation factor 2B, subunit 2 beta, 39kDa
E11	EIF2B5	Eukaryotic translation initiation factor 2B, subunit 5 epsilon, 82kDa
F1	EIF2S2	Eukaryotic translation initiation factor 2, subunit 2 beta, 38kDa
F2	RPL14	Ribosomal protein L14
F3	LRRFIP1	Leucine rich repeat (in FLII) interacting protein 1
F4	LRRFIP2	Leucine rich repeat (in FLII) interacting protein 2
F5	RPL23	Ribosomal protein L23
F6	QKI	Quaking homolog, KH domain RNA binding
F7	EIF4E2	Eukaryotic translation initiation factor 4E family member 2
F8	EEF1E1	Eukaryotic translation elongation factor 1 epsilon 1
F9	RBM39	RNA binding motif protein 39

F10	ISG15	SG15 ubiquitin-like modifier
F11	EIF5B	Eukaryotic translation initiation factor 5B
G1	BZW1	Basic leucine zipper and W2 domains 1
G2	ACAP1	ArfGAP with coiled-coil, ankyrin repeat and PH domains 1
G3	RBM19	RNA binding motif protein 19
G4	HELZ	Helicase with zinc finger
G5	RBM8A	RNA binding motif protein 8A
G6	RBM12	RNA binding motif protein 12
G7	RBM7	RNA binding motif protein 7
G8	RBM6	RNA binding motif protein 6
G9	RBM5	RNA binding motif protein 5
G10	RBM14	RNA binding motif protein 14
G11	ZNF238	Zinc finger protein 238
H1	SYNCRIP	Synaptotagmin binding, cytoplasmic RNA interacting protein
H2	RNASEH2A	Ribonuclease H2, subunit A
H3	UBD	Ubiquitin D
H4	KHDRBS3	KH domain containing, RNA binding, signal transduction associated 3
H5	KHDRBS1	KH domain containing, RNA binding, signal transduction associated 1
H6	CUGBP1	CUG triplet repeat, RNA binding protein 1
H7	CUGBP2	CUG triplet repeat, RNA binding protein 1
H8	HBS1L	HBS1-like
H9	RNPS1	RNA binding protein S1, serine-rich domain
H10	ASCC3	Activating signal cointegrator 1 complex subunit 3
H11	RBPMS	RNA binding protein with multiple splicing

Plate 3

Plate position	Gene	Full name
A1	ADAP1	ArfGAP with dual PH domains 1
A2	RBM16	RNA binding motif protein 16
A3	PDCD11	Programmed cell death 11
A4	SNRNP200	Small nuclear ribonucleoprotein 200kDa
A5	RBM34	RNA binding motif protein 34
A6	LARP5	La ribonucleoprotein domain family, member 5
A7	KIAA0664	KIAA0664
A8	LARP	La ribonucleoprotein domain family, member 1
A9	PUM2	Pumilio homolog 2
A10	DICER1	Dicer 1, ribonuclease type III
A11	RPL13A	Ribosomal protein L13a
B1	ACAP2	ArfGAP with coiled-coil, ankyrin repeat and PH domains 2
B2	ZNF281	Zinc finger protein 281
B3	RBM9	RNA binding motif protein 9
B4	GSPT2	G1 to S phase transition 2
B5	RPL36	Ribosomal protein L36
B6	ZNF451	Zinc finger protein 451
B7	ZBTB20	Zinc finger and BTB domain containing 20
B8	RSL1D1	Ribosomal L1 domain containing 1
B9	EIF2C1	Eukaryotic translation initiation factor 2C, 1
B10	ZBTB32	Zinc finger and BTB domain containing 32
B11	STAU2	Staufen, RNA binding protein, homolog 2
C1	EIF2C2	Eukaryotic translation initiation factor 2C, 2

C2	PDCD4	Programmed cell death 4
C3	RBMS3	RNA binding motif, single-stranded interacting protein
C4	BZW2	Basic leucine zipper and W2 domains 2
C5	RBM15B	RNA binding motif protein 15B
C6	PURG	Purine-rich element binding protein G
C7	ZNF593	Zinc finger protein 593
C8	TFDP3	Transcription factor Dp family, member 3
C9	ZBTB7	Zinc finger and BTB domain containing 7
C10	TRMT6	tRNA methyltransferase 6 homolog
C11	ZFR	Zinc finger RNA binding protein
D1	RBM11	RNA binding motif protein 11
D2	Custom	XM_291128
D3	XRN1	5'-3' exoribonuclease 1
D4	RBM28	RNA binding motif protein 28
D5	LARP2	La ribonucleoprotein domain family, member 2
D6	RBM23	RNA binding motif protein 23
D7	ZNF692	Zinc finger protein 692
D8	RBM22	RNA binding motif protein 22
D9	ADAP2	ArfGAP with dual PH domains 2
D10	EIF5A2	Eukaryotic translation initiation factor 5A2
D11	BRUNOL4	Bruno-like 4, RNA binding protein
E1	PCBP4	Poly(rC) binding protein 4
E2	REXO1	REX1, RNA exonuclease 1 homolog
E3	ZNF410	Zinc finger protein 410
E4	PTBP2	Polypyrimidine tract binding protein 2
E5	RBM25	RNA binding motif protein 25
E6	GUF1	GUF1 GTPase homolog

E7	BRUNOL6	Bruno-like 6, RNA binding protein
E8	SELB	Eukaryotic elongation factor, selenocysteine-tRNA-specific
E9	BRUNOL5	Bruno-like 5, RNA binding protein
E10	IFIH1	Interferon induced with helicase C domain 1
E11	CPEB1	Cytoplasmic polyadenylation element binding protein 1
F1	AEN	Apoptosis enhancing nuclease
F2	RBM15	RNA binding motif protein 15
F3	YTHDC2	YTH domain containing 2
F4	EFTUD1	Elongation factor Tu GTP binding domain containing 1
F5	LIN28	Lin-28 homolog
F6	ISG20L2	Interferon stimulated exonuclease gene 20kDa-like 2
F7	RBM30	RNA binding motif protein 30
F8	EIF3FP2	Eukaryotic translation initiation factor 3, subunit F pseudogene 2
F9	EIF2A	Eukaryotic translation initiation factor 2A, 65kDa
F10	MGC3207	Translation initiation factor EIF2B subunit alpha/beta/delta-like protein
F11	RNASE7	Ribonuclease, RNase A family, 7
G1	ZNF499	Zinc finger protein 499
G2	LOC91431	Prematurely terminated mRNA decay factor-like
G3	C12orf65	Chromosome 12 open reading frame 65
G4	TDRD12	Tudor domain containing 12
G5	ZNF276	Zinc finger protein 276
G6	LARP4	La ribonucleoprotein domain family, member 4
G7	ZNF653	Zinc finger protein 653

G8	TDRD9	Tudor domain containing 9
G9	RNASE8	Ribonuclease, RNase A family, 8
G10	Custom	XM_498389
G11	RPL10L	Ribosomal protein L10-like
H1	Custom	XM_016093
H2	ZNF362	Zinc finger protein 362
H3	LOC649561	Similar to basic leucine zipper and W2 domains 1
H4	ZNF342	Zinc finger protein 342
H5	HFM1	HFM1, ATP-dependent DNA helicase homolog
H6	DQX1	DEAQ box polypeptide 1 (RNA-dependent ATPase)
H7	ZNF384	Zinc finger protein 384
H8	EIF2C3	Eukaryotic translation initiation factor 2C, 3
H9	EIF2C4	Eukaryotic translation initiation factor 2C, 4
H10	Custom	XM_113971
H11	KHDRBS2	KH domain containing, RNA binding, signal transduction associated 2

Plate 4

Plate position	Gene	Full name
A1	MTIF3	Mitochondrial translational initiation factor 3
A2	RNASEH1	Ribonuclease H1
A3	Custom	XM_171094
A4	ZNF740	Zinc finger protein 740
A5	ZNF575	Zinc finger protein 575
A6	Custom	XM_208320
A7	Custom	XM_497256

A8	Custom	XM_497117
A9	EIF4E3	Eukaryotic translation initiation factor 4E family member 3
A10	Custom	XM_497370
A11	Custom	XM_370684
B1	Custom	XM_370893
B2	Custom	XM_371034
B3	Custom	XM_496717
B4	LIN28B	Lin-28 homolog B
B5	LOC390282	Similar to hCG2040283
B6	LOC390352	Hypothetical LOC390352
B7	Custom	XM_497376
B8	LOC401677	Hypothetical LOC401677
B9	Custom	XM_377231
B10	Custom	XM_497339
B11	Custom	XM_377558
C1	Custom	XM_497758
C2	Custom	XM_498388
C3	Custom	XM_495963
C4	Custom	XM_496086
C5	Custom	XM_496711
C6	hCG_1982709	Transcription factor Dp-1-like pseudogene
C7	Custom	XM_497121
C8	Custom	XM_497923
C9	LOC442227	Hypothetical LOC442227
C10	Custom	XM_498260
C11	Custom	XM_498335

D1	Custom	XM_498390
D2	DDX19A	DEAD (Asp-Glu-Ala-As) box polypeptide 19A

Plate 1 (a)

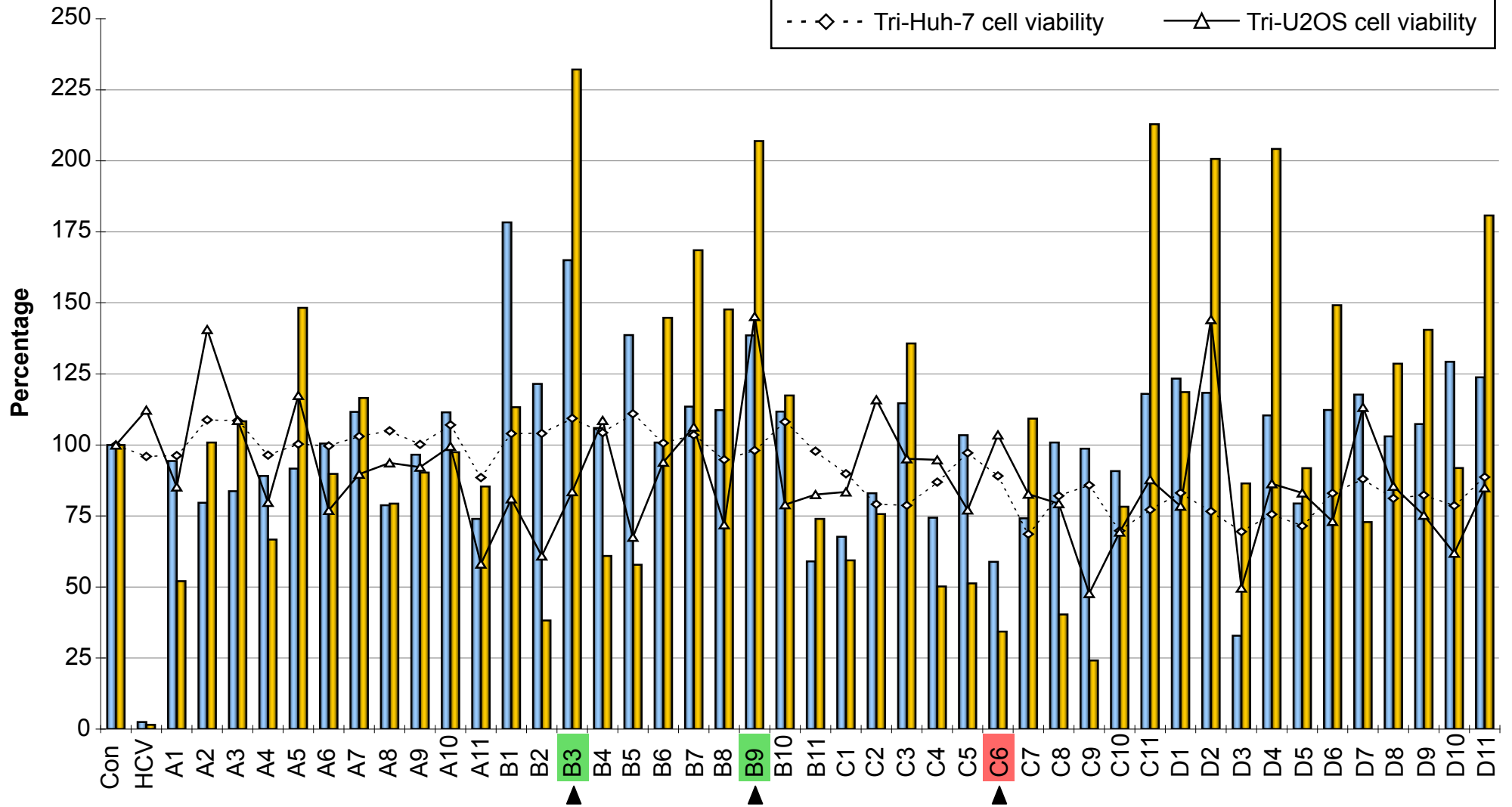
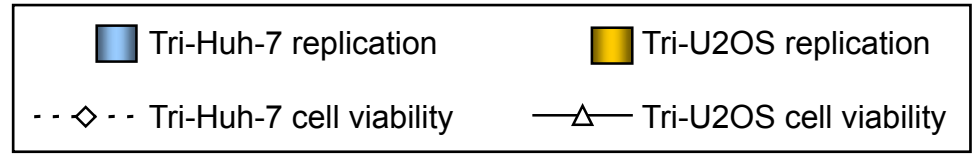


Plate 1 (b)

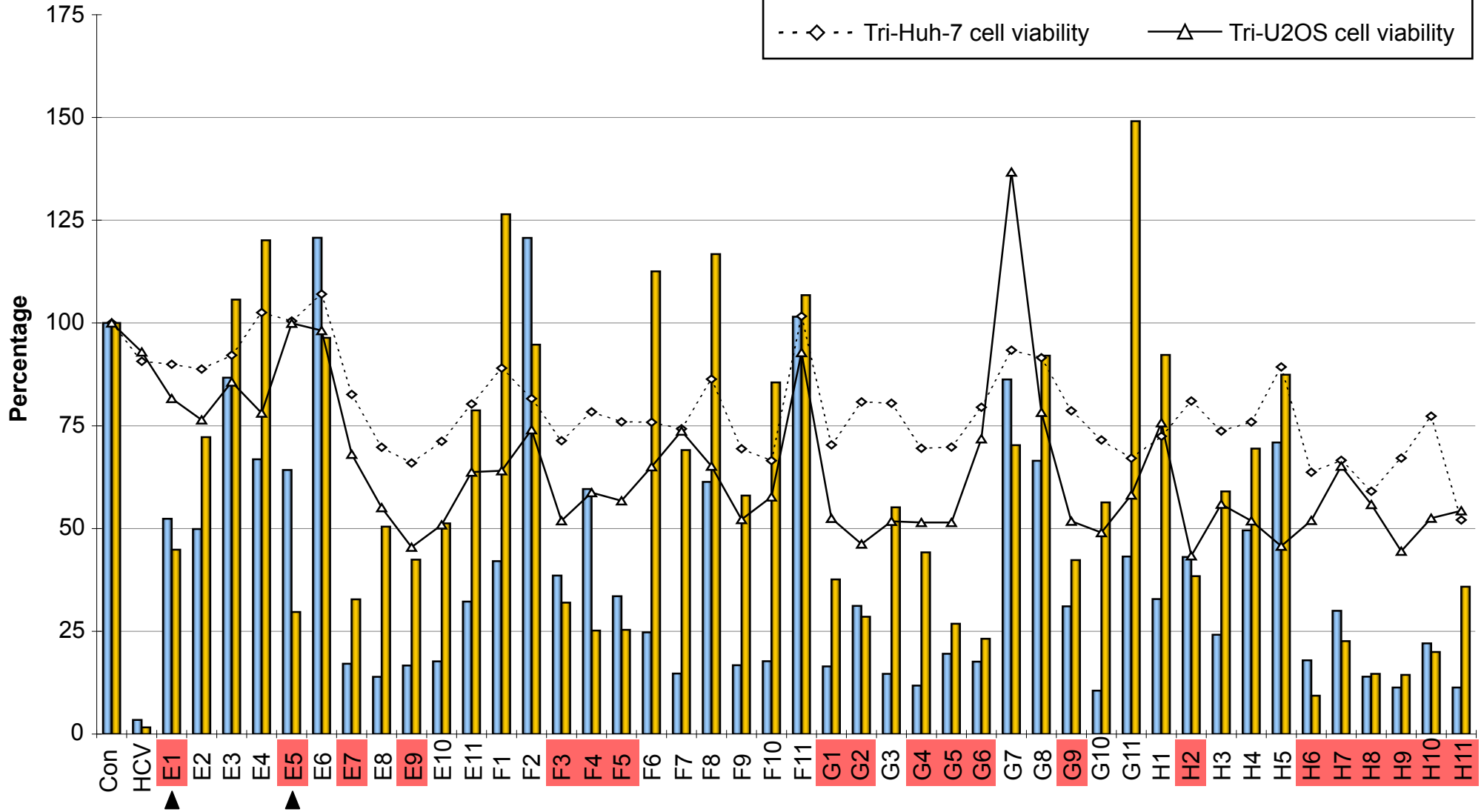
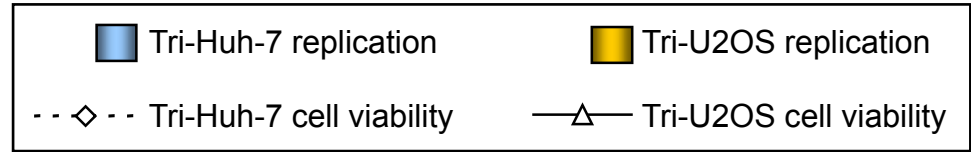


Plate 2 (a)

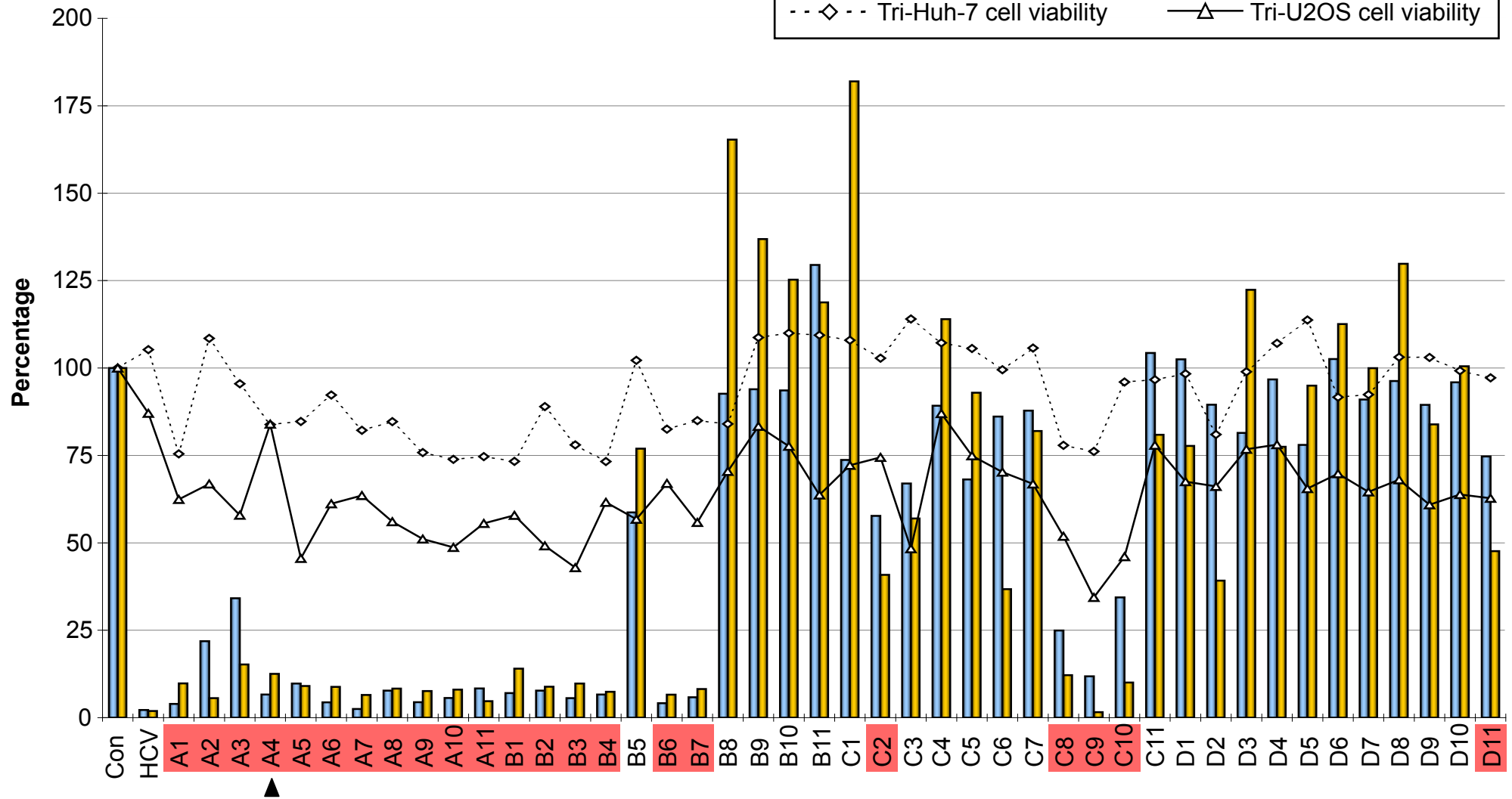
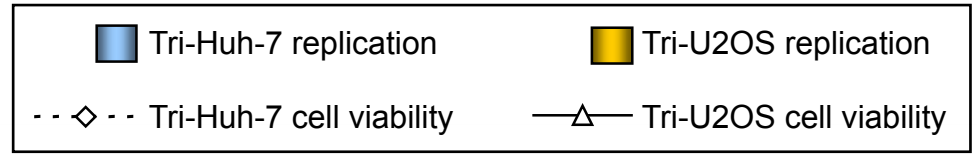


Plate 2 (b)

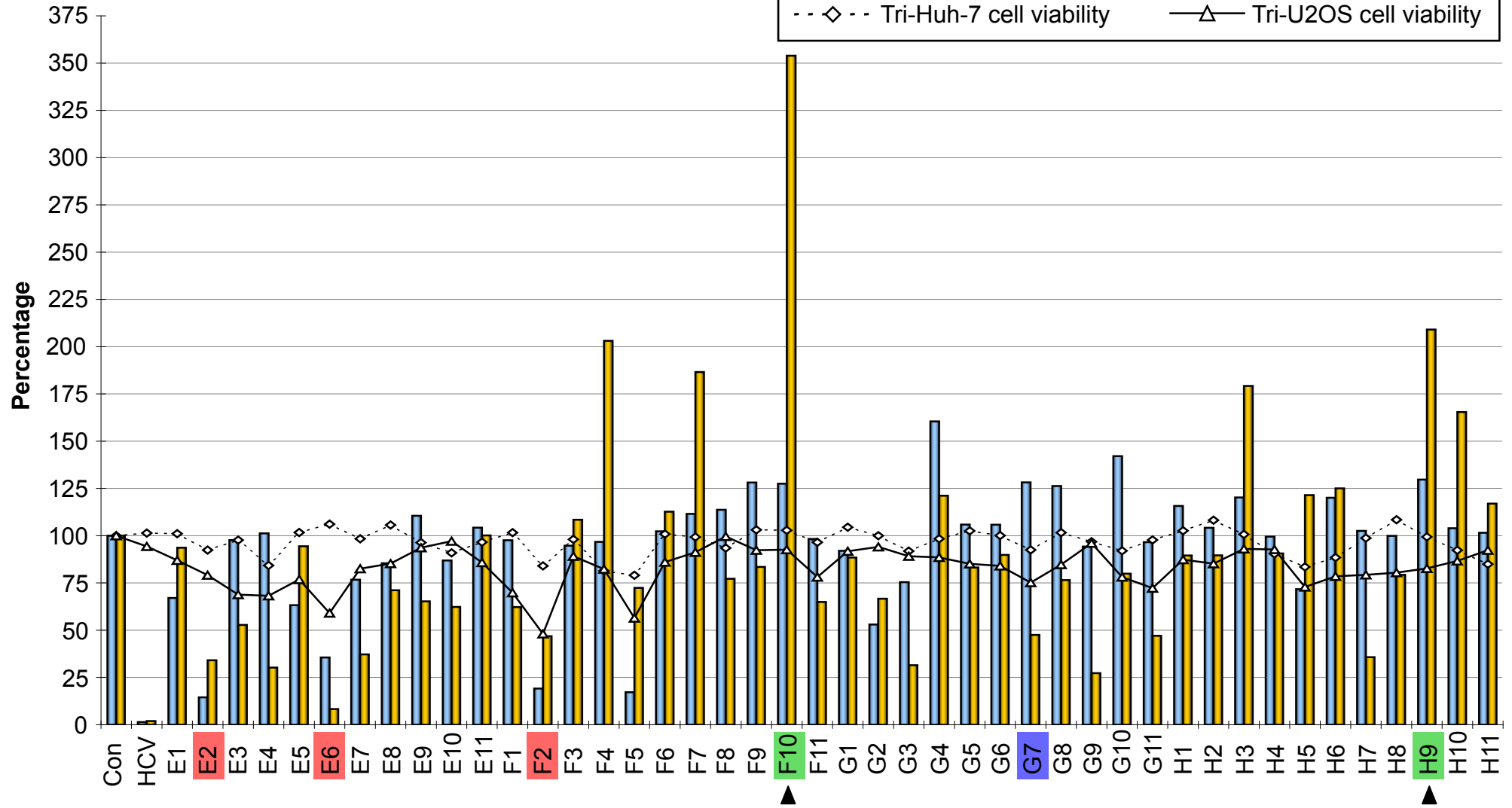
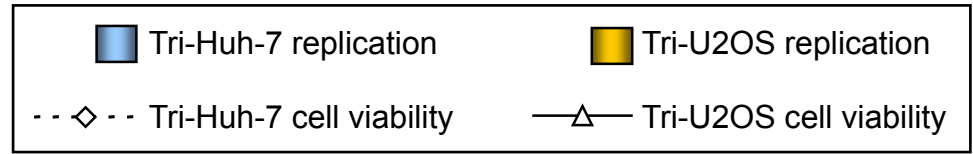


Plate 3 (a)

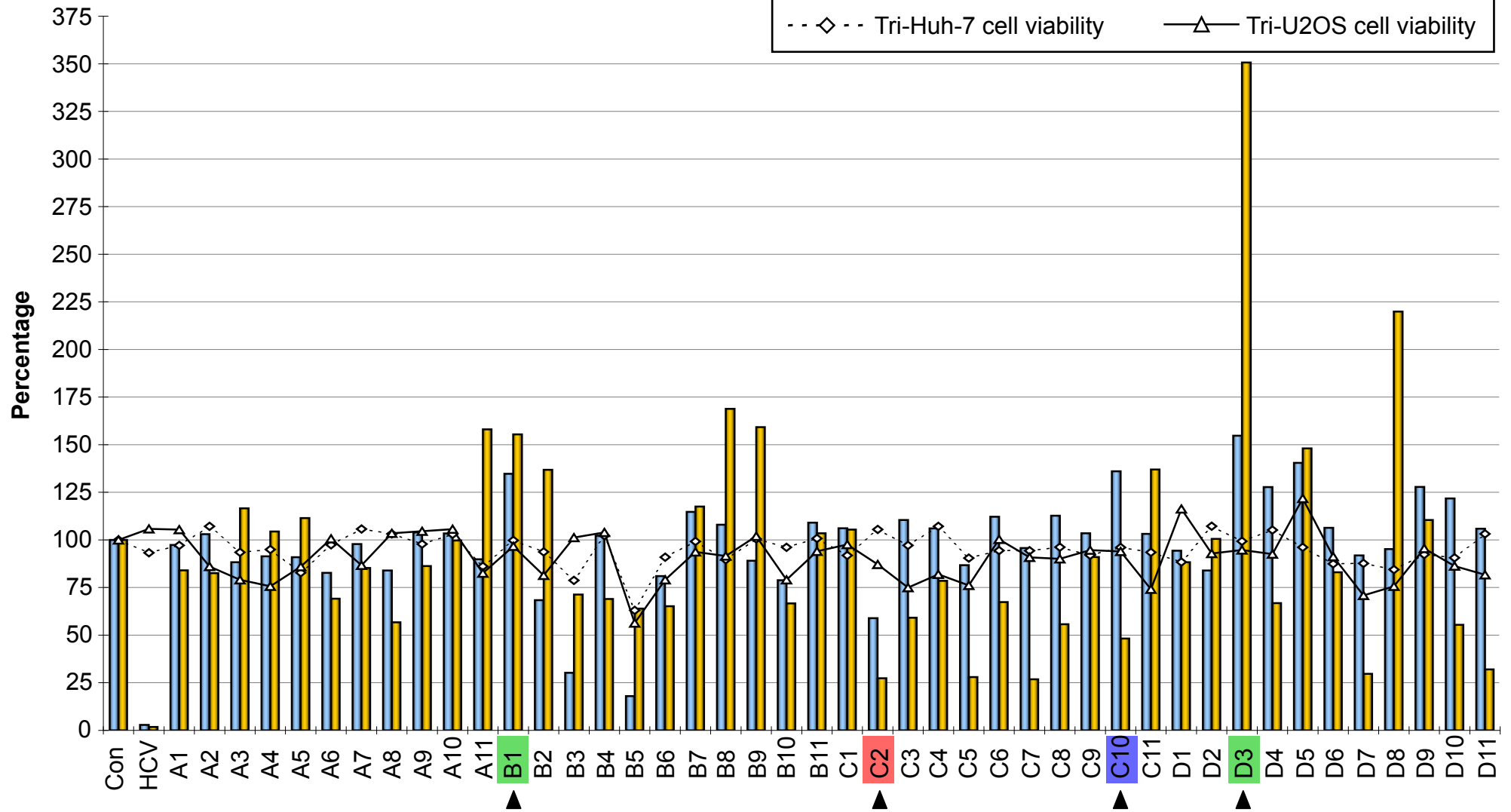
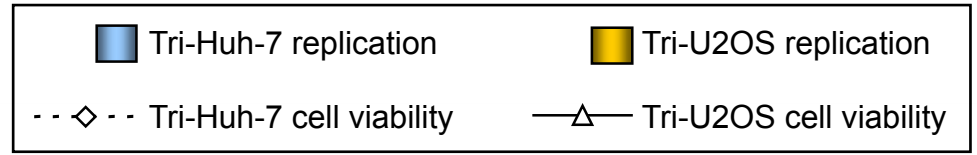


Plate 3 (b)

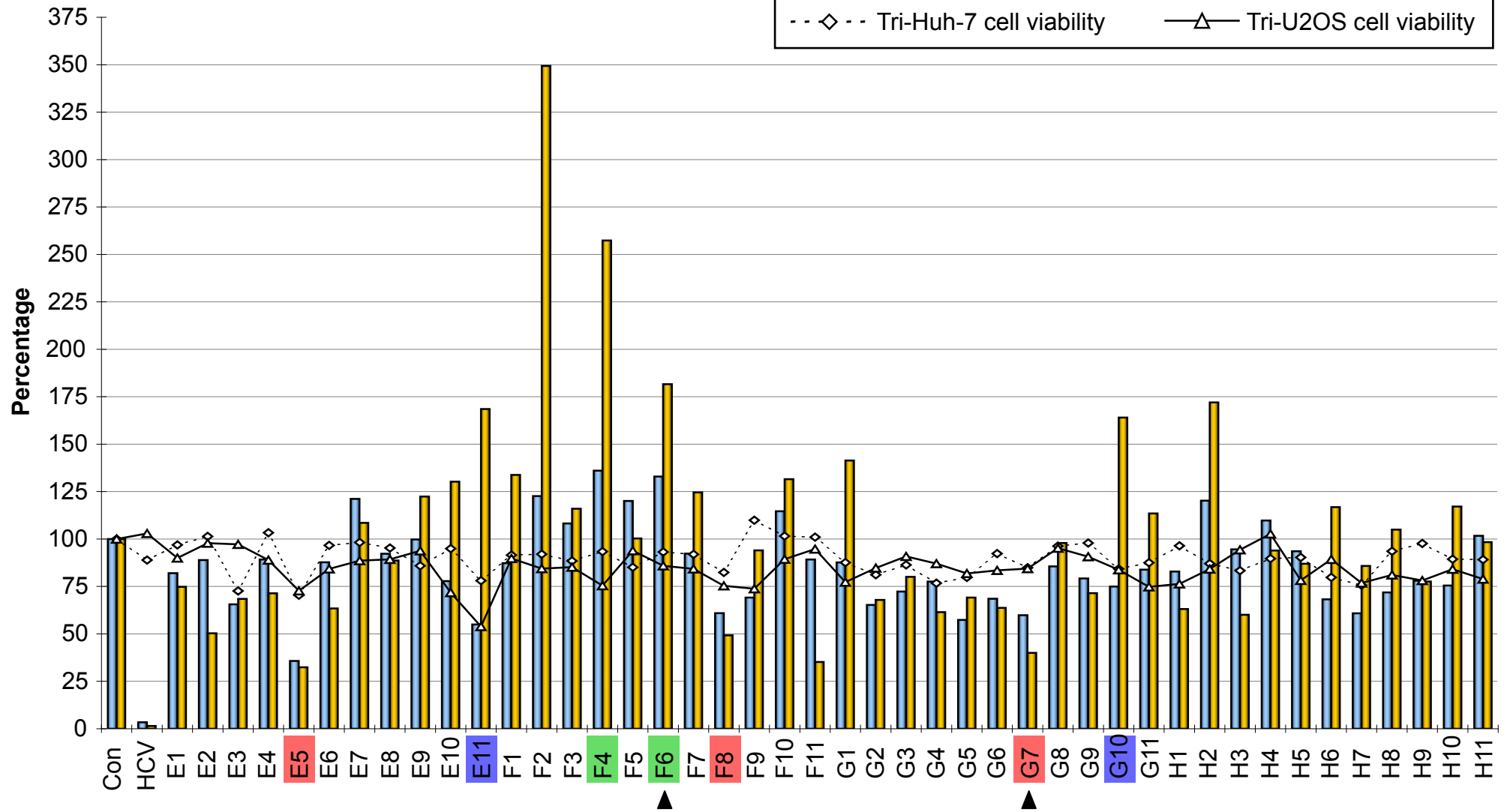
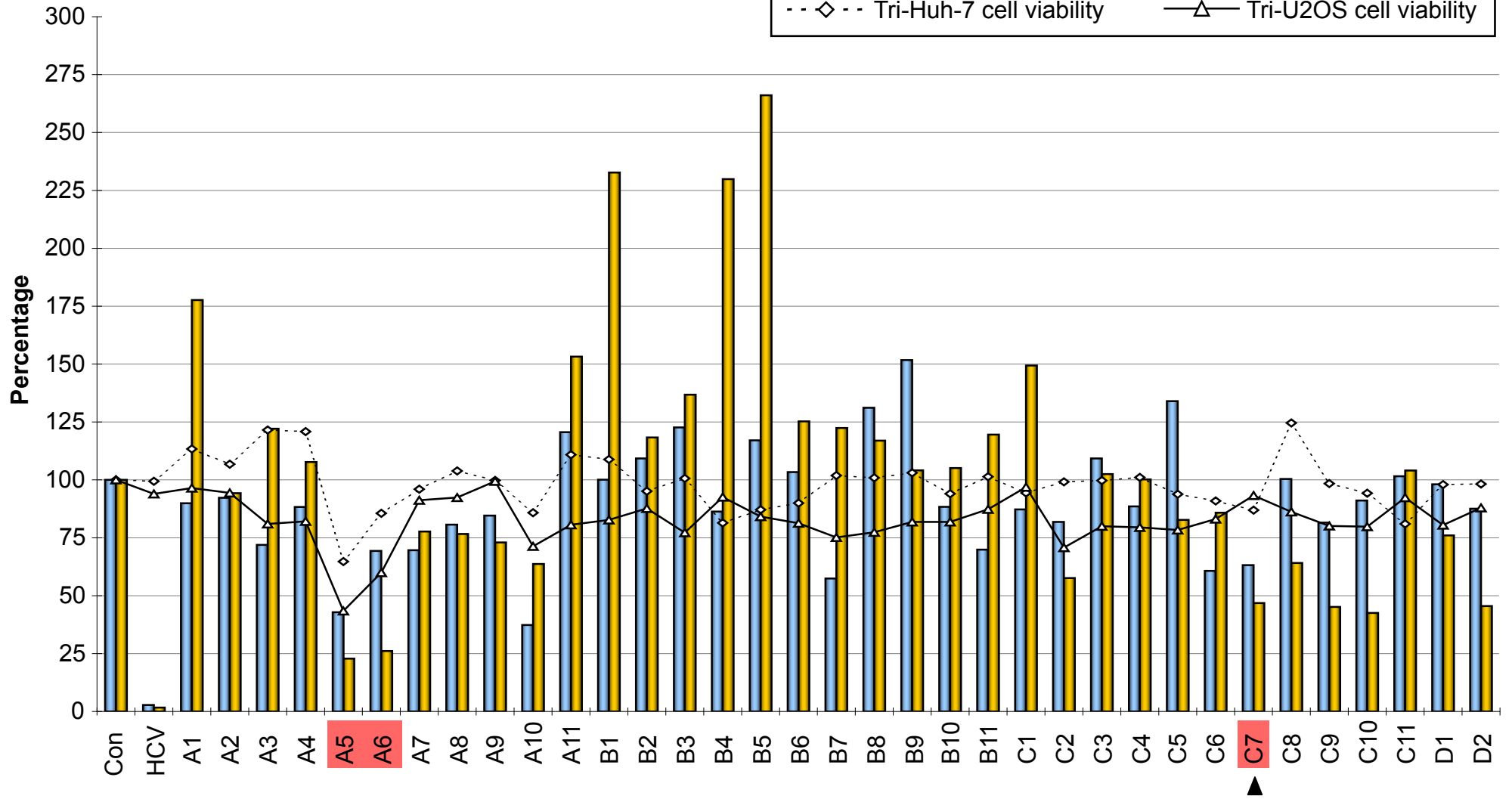
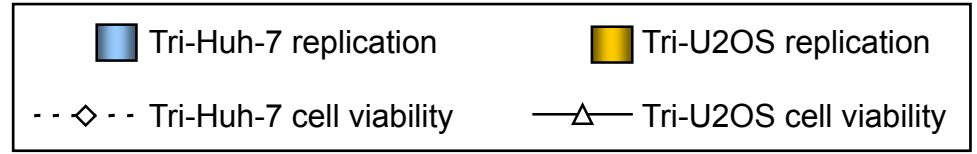


Plate 4



References

- Agnello, V., Abel, G., Elfahal, M., Knight, G. B. & Zhang, Q. X. (1999). Hepatitis C virus and other flaviviridae viruses enter cells via low density lipoprotein receptor. *Proc Natl Acad Sci U S A* **96**, 12766-71.
- Agrawal, A., Tripp, R. A., Anderson, L. J. & Nie, S. (2005). Real-time detection of virus particles and viral protein expression with two-color nanoparticle probes. *J Virol* **79**, 8625-8.
- Aizaki, H., Lee, K. J., Sung, V. M., Ishiko, H. & Lai, M. M. (2004). Characterization of the hepatitis C virus RNA replication complex associated with lipid rafts. *Virology* **324**, 450-61.
- Ali, N. & Siddiqui, A. (1995). Interaction of polypyrimidine tract-binding protein with the 5' noncoding region of the hepatitis C virus RNA genome and its functional requirement in internal initiation of translation. *J Virol* **69**, 6367-75.
- Ali, N. & Siddiqui, A. (1997). The La antigen binds 5' noncoding region of the hepatitis C virus RNA in the context of the initiator AUG codon and stimulates internal ribosome entry site-mediated translation. *Proc Natl Acad Sci U S A* **94**, 2249-54.
- Ali, S., Pellerin, C., Lamarre, D. & Kukolj, G. (2004). Hepatitis C virus subgenomic replicons in the human embryonic kidney 293 cell line. *J Virol* **78**, 491-501.
- Alter, H. J., Purcell, R. H., Holland, P. V. & Popper, H. (1978). Transmissible agent in non-A, non-B hepatitis. *Lancet* **1**, 459-63.
- Andre, P., Komurian-Pradel, F., Deforges, S., Perret, M., Berland, J. L., Sodoyer, M., Pol, S., Brechot, C., Paranhos-Baccala, G. & Lotteau, V. (2002). Characterization of low- and very-low-density hepatitis C virus RNA-containing particles. *J Virol* **76**, 6919-28.
- Appel, N., Herian, U. & Bartenschlager, R. (2005a). Efficient rescue of hepatitis C virus RNA replication by trans-complementation with nonstructural protein 5A. *J Virol* **79**, 896-909.
- Appel, N., Pietschmann, T. & Bartenschlager, R. (2005b). Mutational analysis of hepatitis C virus nonstructural protein 5A: potential role of differential phosphorylation in RNA replication and identification of a genetically flexible domain. *J Virol* **79**, 3187-94.
- Appel, N., Zayas, M., Miller, S., Krijnse-Locker, J., Schaller, T., Friebe, P., Kallis, S., Engel, U. & Bartenschlager, R. (2008). Essential role of domain III of nonstructural protein 5A for hepatitis C virus infectious particle assembly. *PLoS Pathog* **4**, e1000035.
- Arhel, N., Genovesio, A., Kim, K. A., Miko, S., Perret, E., Olivo-Marin, J. C., Shorte, S. & Charneau, P. (2006). Quantitative four-dimensional tracking of cytoplasmic and nuclear HIV-1 complexes. *Nat Methods* **3**, 817-24.
- Ariumi, Y., Kuroki, M., Dansako, H., Abe, K., Ikeda, M., Wakita, T. & Kato, N. (2008). The DNA damage sensors ataxia-telangiectasia mutated kinase and checkpoint kinase 2 are required for hepatitis C virus RNA replication. *J Virol* **82**, 9639-46.
- Armstrong, G. L., Wasley, A., Simard, E. P., McQuillan, G. M., Kuhnert, W. L. & Alter, M. J. (2006). The prevalence of hepatitis C virus infection in the United States, 1999 through 2002. *Ann Intern Med* **144**, 705-14.
- Barba, G., Harper, F., Harada, T., Kohara, M., Goulinet, S., Matsuura, Y., Eder, G., Schaff, Z., Chapman, M. J., Miyamura, T. & Brechot, C. (1997). Hepatitis C virus core protein shows a cytoplasmic localization and associates to cellular lipid storage droplets. *Proc Natl Acad Sci U S A* **94**, 1200-5.

- Bartenschlager, R., Ahlborn-Laake, L., Mous, J. & Jacobsen, H. (1993). Nonstructural protein 3 of the hepatitis C virus encodes a serine-type proteinase required for cleavage at the NS3/4 and NS4/5 junctions. *J Virol* **67**, 3835-44.
- Bartenschlager, R., Ahlborn-Laake, L., Mous, J. & Jacobsen, H. (1994). Kinetic and structural analyses of hepatitis C virus polyprotein processing. *J Virol* **68**, 5045-55.
- Bartenschlager, R., Lohmann, V., Wilkinson, T. & Koch, J. O. (1995). Complex formation between the NS3 serine-type proteinase of the hepatitis C virus and NS4A and its importance for polyprotein maturation. *J Virol* **69**, 7519-28.
- Bartenschlager, R. & Pietschmann, T. (2005). Efficient hepatitis C virus cell culture system: what a difference the host cell makes. *Proc Natl Acad Sci U S A* **102**, 9739-40.
- Barth, H., Schafer, C., Adah, M. I., Zhang, F., Linhardt, R. J., Toyoda, H., Kinoshita-Toyoda, A., Toida, T., Van Kuppevelt, T. H., Depla, E., Von Weizsacker, F., Blum, H. E. & Baumert, T. F. (2003). Cellular binding of hepatitis C virus envelope glycoprotein E2 requires cell surface heparan sulfate. *J Biol Chem* **278**, 41003-12.
- Bartosch, B., Bukh, J., Meunier, J. C., Granier, C., Engle, R. E., Blackwelder, W. C., Emerson, S. U., Cosset, F. L. & Purcell, R. H. (2003a). In vitro assay for neutralizing antibody to hepatitis C virus: evidence for broadly conserved neutralization epitopes. *Proc Natl Acad Sci U S A* **100**, 14199-204.
- Bartosch, B., Dubuisson, J. & Cosset, F. L. (2003b). Infectious hepatitis C virus pseudo-particles containing functional E1-E2 envelope protein complexes. *J Exp Med* **197**, 633-42.
- Bartosch, B., Vitelli, A., Granier, C., Goujon, C., Dubuisson, J., Pascale, S., Scarselli, E., Cortese, R., Nicosia, A. & Cosset, F. L. (2003c). Cell entry of hepatitis C virus requires a set of co-receptors that include the CD81 tetraspanin and the SR-B1 scavenger receptor. *J Biol Chem* **278**, 41624-30.
- Behrens, S. E., Tomei, L. & De Francesco, R. (1996). Identification and properties of the RNA-dependent RNA polymerase of hepatitis C virus. *Embo J* **15**, 12-22.
- Bentzen, E. L., House, F., Utley, T. J., Crowe, J. E., Jr. & Wright, D. W. (2005). Progression of respiratory syncytial virus infection monitored by fluorescent quantum dot probes. *Nano Lett* **5**, 591-5.
- Beran, R. K., Lindenbach, B. D. & Pyle, A. M. (2009). The NS4A protein of hepatitis C virus promotes RNA-coupled ATP hydrolysis by the NS3 helicase. *J Virol* **83**, 3268-75.
- Berenguer, M., Prieto, M., Rayon, J. M., Mora, J., Pastor, M., Ortiz, V., Carrasco, D., San Juan, F., Burgueno, M. D., Mir, J. & Berenguer, J. (2000). Natural history of clinically compensated hepatitis C virus-related graft cirrhosis after liver transplantation. *Hepatology* **32**, 852-8.
- Bernards, R., Brummelkamp, T. R. & Beijersbergen, R. L. (2006). shRNA libraries and their use in cancer genetics. *Nat Methods* **3**, 701-6.
- Binder, M., Quinkert, D., Bochkarova, O., Klein, R., Kezmic, N., Bartenschlager, R. & Lohmann, V. (2007). Identification of determinants involved in initiation of hepatitis C virus RNA synthesis by using intergenotypic replicase chimeras. *J Virol* **81**, 5270-83.
- Blanchard, E., Belouzard, S., Goueslain, L., Wakita, T., Dubuisson, J., Wychowski, C. & Rouille, Y. (2006). Hepatitis C virus entry depends on clathrin-mediated endocytosis. *J Virol* **80**, 6964-72.
- Blanchard, E., Hourieux, C., Brand, D., Ait-Goughoulte, M., Moreau, A., Trassard, S., Sizaret, P. Y., Dubois, F. & Roingeard, P. (2003). Hepatitis C virus-like

- particle budding: role of the core protein and importance of its Asp111. *J Virol* **77**, 10131-8.
- Blight, K. J. (2007). Allelic variation in the hepatitis C virus NS4B protein dramatically influences RNA replication. *J Virol* **81**, 5724-36.
- Blight, K. J., Kolykhalov, A. A. & Rice, C. M. (2000). Efficient initiation of HCV RNA replication in cell culture. *Science* **290**, 1972-4.
- Blight, K. J., McKeating, J. A., Marcotrigiano, J. & Rice, C. M. (2003). Efficient replication of hepatitis C virus genotype 1a RNAs in cell culture. *J Virol* **77**, 3181-90.
- Blight, K. J., McKeating, J. A. & Rice, C. M. (2002). Highly permissive cell lines for subgenomic and genomic hepatitis C virus RNA replication. *J Virol* **76**, 13001-14.
- Blight, K. J. & Rice, C. M. (1997). Secondary structure determination of the conserved 98-base sequence at the 3' terminus of hepatitis C virus genome RNA. *J Virol* **71**, 7345-52.
- Boulant, S., Douglas, M. W., Moody, L., Budkowska, A., Targett-Adams, P. & McLauchlan, J. (2008). Hepatitis C virus core protein induces lipid droplet redistribution in a microtubule- and dynein-dependent manner. *Traffic* **9**, 1268-82.
- Boulant, S., Montserret, R., Hope, R. G., Ratinier, M., Targett-Adams, P., Lavergne, J. P., Penin, F. & McLauchlan, J. (2006). Structural determinants that target the hepatitis C virus core protein to lipid droplets. *J Biol Chem* **281**, 22236-47.
- Boulant, S., Targett-Adams, P. & McLauchlan, J. (2007). Disrupting the association of hepatitis C virus core protein with lipid droplets correlates with a loss in production of infectious virus. *J Gen Virol* **88**, 2204-13.
- Boulant, S., Vanbelle, C., Ebel, C., Penin, F. & Lavergne, J. P. (2005). Hepatitis C virus core protein is a dimeric alpha-helical protein exhibiting membrane protein features. *J Virol* **79**, 11353-65.
- Bowen, D. G. & Walker, C. M. (2005). Adaptive immune responses in acute and chronic hepatitis C virus infection. *Nature* **436**, 946-52.
- Bradley, D. W., McCaustland, K. A., Cook, E. H., Schable, C. A., Ebert, J. W. & Maynard, J. E. (1985). Posttransfusion non-A, non-B hepatitis in chimpanzees. Physicochemical evidence that the tubule-forming agent is a small, enveloped virus. *Gastroenterology* **88**, 773-9.
- Bradrick, S. S., Walters, R. W. & Gromeier, M. (2006). The hepatitis C virus 3'-untranslated region or a poly(A) tract promote efficient translation subsequent to the initiation phase. *Nucleic Acids Res* **34**, 1293-303.
- Brass, V., Bieck, E., Montserret, R., Wolk, B., Hellings, J. A., Blum, H. E., Penin, F. & Moradpour, D. (2002). An amino-terminal amphipathic alpha-helix mediates membrane association of the hepatitis C virus nonstructural protein 5A. *J Biol Chem* **277**, 8130-9.
- Breiman, A., Grandvaux, N., Lin, R., Ottone, C., Akira, S., Yoneyama, M., Fujita, T., Hiscott, J. & Meurs, E. F. (2005). Inhibition of RIG-I-dependent signaling to the interferon pathway during hepatitis C virus expression and restoration of signaling by IKKepsilon. *J Virol* **79**, 3969-78.
- Bukh, J., Pietschmann, T., Lohmann, V., Krieger, N., Faulk, K., Engle, R. E., Govindarajan, S., Shapiro, M., St Claire, M. & Bartenschlager, R. (2002). Mutations that permit efficient replication of hepatitis C virus RNA in Huh-7 cells prevent productive replication in chimpanzees. *Proc Natl Acad Sci U S A* **99**, 14416-21.
- Burckstummer, T., Kriegs, M., Lupberger, J., Pauli, E. K., Schmitt, S. & Hildt, E. (2006). Raf-1 kinase associates with hepatitis C virus NS5A and regulates viral replication. *FEBS Lett*, **580**, 575-80.

- Callens, N., Ciczora, Y., Bartosch, B., Vu-Dac, N., Cosset, F. L., Pawlotsky, J. M., Penin, F. & Dubuisson, J. (2005). Basic residues in hypervariable region 1 of hepatitis C virus envelope glycoprotein e2 contribute to virus entry. *J Virol* **79**, 15331-41.
- Campbell, E. M. & Hope, T. J. (2008). Live cell imaging of the HIV-1 life cycle. *Trends Microbiol* **16**, 580-7.
- Campello, C., Poli, A., Dal, M. G. & Besozzi-Valentini, F. (2002). Seroprevalence, viremia and genotype distribution of hepatitis C virus: a community-based population study in northern Italy. *Infection* **30**, 7-12.
- Carrere-Kremer, S., Montpellier-Pala, C., Cocquerel, L., Wychowski, C., Penin, F. & Dubuisson, J. (2002). Subcellular localization and topology of the p7 polypeptide of hepatitis C virus. *J Virol* **76**, 3720-30.
- Catanese, M. T., Graziani, R., von Hahn, T., Moreau, M., Huby, T., Paonessa, G., Santini, C., Luzzago, A., Rice, C. M., Cortese, R., Vitelli, A. & Nicosia, A. (2007). High-avidity monoclonal antibodies against the human scavenger class B type I receptor efficiently block hepatitis C virus infection in the presence of high-density lipoprotein. *J Virol* **81**, 8063-71.
- Chalfie, M., Tu, Y., Euskirchen, G., Ward, W. W. & Prasher, D. C. (1994). Green fluorescent protein as a marker for gene expression. *Science* **263**, 802-5.
- Chang, K. S., Jiang, J., Cai, Z. & Luo, G. (2007). Human apolipoprotein e is required for infectivity and production of hepatitis C virus in cell culture. *J Virol* **81**, 13783-93.
- Chevalier, C., Saulnier, A., Benureau, Y., Flechet, D., Delgrange, D., Colbere-Garapin, F., Wychowski, C. & Martin, A. (2007). Inhibition of hepatitis C virus infection in cell culture by small interfering RNAs. *Mol Ther* **15**, 1452-62.
- Chevaliez, S. & Pawlotsky, J. M. (2007). Hepatitis C virus: virology, diagnosis and management of antiviral therapy. *World J Gastroenterol* **13**, 2461-6.
- Chevaliez, S. & Pawlotsky, J. M. (2009). Interferons and their use in persistent viral infections. *Handb Exp Pharmacol*, 203-41.
- Choo, Q. L., Kuo, G., Weiner, A. J., Overby, L. R., Bradley, D. W. & Houghton, M. (1989). Isolation of a cDNA clone derived from a blood-borne non-A, non-B viral hepatitis genome. *Science* **244**, 359-62.
- Choo, Q. L., Richman, K. H., Han, J. H., Berger, K., Lee, C., Dong, C., Gallegos, C., Coit, D., Medina-Selby, R., Barr, P. J. & et al. (1991). Genetic organization and diversity of the hepatitis C virus. *Proc Natl Acad Sci U S A* **88**, 2451-5.
- Ciczora, Y., Callens, N., Penin, F., Pecheur, E. I. & Dubuisson, J. (2007). Transmembrane domains of hepatitis C virus envelope glycoproteins: residues involved in E1E2 heterodimerization and involvement of these domains in virus entry. *J Virol* **81**, 2372-81.
- Cocquerel, L., Duvet, S., Meunier, J. C., Pillez, A., Cacan, R., Wychowski, C. & Dubuisson, J. (1999). The transmembrane domain of hepatitis C virus glycoprotein E1 is a signal for static retention in the endoplasmic reticulum. *J Virol* **73**, 2641-9.
- Cocquerel, L., Kuo, C. C., Dubuisson, J. & Levy, S. (2003). CD81-dependent binding of hepatitis C virus E1E2 heterodimers. *J Virol* **77**, 10677-83.
- Cocquerel, L., Meunier, J. C., Pillez, A., Wychowski, C. & Dubuisson, J. (1998). A retention signal necessary and sufficient for endoplasmic reticulum localization maps to the transmembrane domain of hepatitis C virus glycoprotein E2. *J Virol* **72**, 2183-91.
- Cocquerel, L., Wychowski, C., Minner, F., Penin, F. & Dubuisson, J. (2000). Charged residues in the transmembrane domains of hepatitis C virus

- glycoproteins play a major role in the processing, subcellular localization, and assembly of these envelope proteins. *J Virol* **74**, 3623-33.
- Contreras, A. M., Hiasa, Y., He, W., Terella, A., Schmidt, E. V. & Chung, R. T. (2002). Viral RNA mutations are region specific and increased by ribavirin in a full-length hepatitis C virus replication system. *J Virol* **76**, 8505-17.
- Cooper, S., Erickson, A. L., Adams, E. J., Kansopon, J., Weiner, A. J., Chien, D. Y., Houghton, M., Parham, P. & Walker, C. M. (1999). Analysis of a successful immune response against hepatitis C virus. *Immunity* **10**, 439-49.
- Cormier, E. G., Tsamis, F., Kajumo, F., Durso, R. J., Gardner, J. P. & Dragic, T. (2004). CD81 is an entry coreceptor for hepatitis C virus. *Proc Natl Acad Sci U S A* **101**, 7270-4.
- Cougot, N., Babajko, S. & Seraphin, B. (2004). Cytoplasmic foci are sites of mRNA decay in human cells. *J Cell Biol* **165**, 31-40.
- Coute, Y., Kindbeiter, K., Belin, S., Dieckmann, R., Duret, L., Bezin, L., Sanchez, J. C. & Diaz, J. J. (2008). ISG20L2, a novel vertebrate nucleolar exoribonuclease involved in ribosome biogenesis. *Mol Cell Proteomics* **7**, 546-59.
- Crotty, S., Cameron, C. E. & Andino, R. (2001). RNA virus error catastrophe: direct molecular test by using ribavirin. *Proc Natl Acad Sci U S A* **98**, 6895-900.
- Dann, C. T., Alvarado, A. L., Hammer, R. E. & Garbers, D. L. (2006). Heritable and stable gene knockdown in rats. *Proc Natl Acad Sci U S A* **103**, 11246-51.
- Date, T., Kato, T., Miyamoto, M., Zhao, Z., Yasui, K., Mizokami, M. & Wakita, T. (2004). Genotype 2a hepatitis C virus subgenomic replicon can replicate in HepG2 and IMY-N9 cells. *J Biol Chem* **279**, 22371-6.
- De Francesco, R. & Migliaccio, G. (2005). Challenges and successes in developing new therapies for hepatitis C. *Nature* **436**, 953-60.
- De Francesco, R., Urbani, A., Nardi, M. C., Tomei, L., Steinkuhler, C. & Tramontano, A. (1996). A zinc binding site in viral serine proteinases. *Biochemistry* **35**, 13282-7.
- Deleersnyder, V., Pillez, A., Wychowski, C., Blight, K., Xu, J., Hahn, Y. S., Rice, C. M. & Dubuisson, J. (1997). Formation of native hepatitis C virus glycoprotein complexes. *J Virol* **71**, 697-704.
- Di Bisceglie, A. M., Shindo, M., Fong, T. L., Fried, M. W., Swain, M. G., Bergasa, N. V., Axiotis, C. A., Waggoner, J. G., Park, Y. & Hoofnagle, J. H. (1992). A pilot study of ribavirin therapy for chronic hepatitis C. *Hepatology* **16**, 649-54.
- Dimitrova, M., Imbert, I., Kieny, M. P. & Schuster, C. (2003). Protein-protein interactions between hepatitis C virus nonstructural proteins. *J Virol* **77**, 5401-14.
- Dixit, S. K., Goicochea, N. L., Daniel, M. C., Murali, A., Bronstein, L., De, M., Stein, B., Rotello, V. M., Kao, C. C. & Dragnea, B. (2006). Quantum dot encapsulation in viral capsids. *Nano Lett* **6**, 1993-9.
- Dominguez, A., Bruguera, M., Vidal, J., Plans, P. & Salleras, L. (2001). Community-based seroepidemiological survey of HCV infection in Catalonia, Spain. *J Med Virol* **65**, 688-93.
- Domitrovich, A. M., Diebel, K. W., Ali, N., Sarker, S. & Siddiqui, A. (2005). Role of La autoantigen and polypyrimidine tract-binding protein in HCV replication. *Virology* **335**, 72-86.
- Dubuisson, J. (2007). Hepatitis C virus proteins. *World J Gastroenterol* **13**, 2406-15.
- Dubuisson, J., Helle, F. & Cocquerel, L. (2008). Early steps of the hepatitis C virus life cycle. *Cell Microbiol* **10**, 821-7.

- Dubuisson, J., Hsu, H. H., Cheung, R. C., Greenberg, H. B., Russell, D. G. & Rice, C. M. (1994). Formation and intracellular localization of hepatitis C virus envelope glycoprotein complexes expressed by recombinant vaccinia and Sindbis viruses. *J Virol* **68**, 6147-60.
- Dubuisson, J., Penin, F. & Moradpour, D. (2002). Interaction of hepatitis C virus proteins with host cell membranes and lipids. *Trends Cell Biol* **12**, 517-23.
- Dykxhoorn, D. M., Novina, C. D. & Sharp, P. A. (2003). Killing the messenger: short RNAs that silence gene expression. *Nat Rev Mol Cell Biol* **4**, 457-67.
- Egger, D., Wolk, B., Gosert, R., Bianchi, L., Blum, H. E., Moradpour, D. & Bienz, K. (2002). Expression of hepatitis C virus proteins induces distinct membrane alterations including a candidate viral replication complex. *J Virol* **76**, 5974-84.
- Einav, S., Elazar, M., Danieli, T. & Glenn, J. S. (2004). A nucleotide binding motif in hepatitis C virus (HCV) NS4B mediates HCV RNA replication. *J Virol* **78**, 11288-95.
- Einav, S., Gerber, D., Bryson, P. D., Sklan, E. H., Elazar, M., Maerkl, S. J., Glenn, J. S. & Quake, S. R. (2008a). Discovery of a hepatitis C target and its pharmacological inhibitors by microfluidic affinity analysis. *Nat Biotechnol* **26**, 1019-27.
- Einav, S., Sklan, E. H., Moon, H. M., Gehrig, E., Liu, P., Hao, Y., Lowe, A. W. & Glenn, J. S. (2008b). The nucleotide binding motif of hepatitis C virus NS4B can mediate cellular transformation and tumor formation without Ha-ras co-transfection. *Hepatology* **47**, 827-35.
- Elazar, M., Cheong, K. H., Liu, P., Greenberg, H. B., Rice, C. M. & Glenn, J. S. (2003). Amphipathic helix-dependent localization of NS5A mediates hepatitis C virus RNA replication. *J Virol* **77**, 6055-61.
- Elazar, M., Liu, P., Rice, C. M. & Glenn, J. S. (2004). An N-terminal amphipathic helix in hepatitis C virus (HCV) NS4B mediates membrane association, correct localization of replication complex proteins, and HCV RNA replication. *J Virol* **78**, 11393-400.
- Elbashir, S. M., Harborth, J., Lendeckel, W., Yalcin, A., Weber, K. & Tuschl, T. (2001a). Duplexes of 21-nucleotide RNAs mediate RNA interference in cultured mammalian cells. *Nature* **411**, 494-8.
- Elbashir, S. M., Martinez, J., Patkaniowska, A., Lendeckel, W. & Tuschl, T. (2001b). Functional anatomy of siRNAs for mediating efficient RNAi in *Drosophila melanogaster* embryo lysate. *Embo J* **20**, 6877-88.
- El-Hage, N. & Luo, G. (2003). Replication of hepatitis C virus RNA occurs in a membrane-bound replication complex containing nonstructural viral proteins and RNA. *J Gen Virol* **84**, 2761-9.
- Evans, M. J., Rice, C. M. & Goff, S. P. (2004a). Genetic interactions between hepatitis C virus replicons. *J Virol* **78**, 12085-9.
- Evans, M. J., Rice, C. M. & Goff, S. P. (2004b). Phosphorylation of hepatitis C virus nonstructural protein 5A modulates its protein interactions and viral RNA replication. *Proc Natl Acad Sci U S A* **101**, 13038-43.
- Evans, M. J., von Hahn, T., Tscherne, D. M., Syder, A. J., Panis, M., Wolk, B., Hatzioannou, T., McKeating, J. A., Bieniasz, P. D. & Rice, C. M. (2007). Claudin-1 is a hepatitis C virus co-receptor required for a late step in entry. *Nature* **446**, 801-5.
- Failla, C., Tomei, L. & De Francesco, R. (1994). Both NS3 and NS4A are required for proteolytic processing of hepatitis C virus nonstructural proteins. *J Virol* **68**, 3753-60.
- Farci, P., Alter, H. J., Wong, D. C., Miller, R. H., Govindarajan, S., Engle, R., Shapiro, M. & Purcell, R. H. (1994). Prevention of hepatitis C virus infection

- in chimpanzees after antibody-mediated in vitro neutralization. *Proc Natl Acad Sci U S A* **91**, 7792-6.
- Feinstone, S. M., Kapikian, A. Z., Purcell, R. H., Alter, H. J. & Holland, P. V. (1975). Transfusion-associated hepatitis not due to viral hepatitis type A or B. *N Engl J Med* **292**, 767-70.
- Feinstone, S. M., Mihalik, K. B., Kamimura, T., Alter, H. J., London, W. T. & Purcell, R. H. (1983). Inactivation of hepatitis B virus and non-A, non-B hepatitis by chloroform. *Infect Immun* **41**, 816-21.
- Feld, J. J. & Hoofnagle, J. H. (2005). Mechanism of action of interferon and ribavirin in treatment of hepatitis C. *Nature* **436**, 967-72.
- Fire, A., Xu, S., Montgomery, M. K., Kostas, S. A., Driver, S. E. & Mello, C. C. (1998). Potent and specific genetic interference by double-stranded RNA in *Caenorhabditis elegans*. *Nature* **391**, 806-11.
- Fleming, D. M. (2001). Influenza diagnosis and treatment: a view from clinical practice. *Philos Trans R Soc Lond B Biol Sci* **356**, 1933-43.
- Flint, M., Maidens, C., Loomis-Price, L. D., Shotton, C., Dubuisson, J., Monk, P., Higginbottom, A., Levy, S. & McKeating, J. A. (1999). Characterization of hepatitis C virus E2 glycoprotein interaction with a putative cellular receptor, CD81. *J Virol* **73**, 6235-44.
- Forns, X., Purcell, R. H. & Bukh, J. (1999). Quasispecies in viral persistence and pathogenesis of hepatitis C virus. *Trends Microbiol* **7**, 402-10.
- Frank, C., Mohamed, M. K., Strickland, G. T., Lavanchy, D., Arthur, R. R., Magder, L. S., El Khoby, T., Abdel-Wahab, Y., Aly Ohn, E. S., Anwar, W. & Sallam, I. (2000). The role of parenteral antischistosomal therapy in the spread of hepatitis C virus in Egypt. *Lancet* **355**, 887-91.
- Fraser, C. S. & Doudna, J. A. (2007). Structural and mechanistic insights into hepatitis C viral translation initiation. *Nat Rev Microbiol* **5**, 29-38.
- Frick, D. N., Rypma, R. S., Lam, A. M. & Gu, B. (2004). The nonstructural protein 3 protease/helicase requires an intact protease domain to unwind duplex RNA efficiently. *J Biol Chem* **279**, 1269-80.
- Friebe, P. & Bartenschlager, R. (2002). Genetic analysis of sequences in the 3' nontranslated region of hepatitis C virus that are important for RNA replication. *J Virol* **76**, 5326-38.
- Friebe, P., Lohmann, V., Krieger, N. & Bartenschlager, R. (2001). Sequences in the 5' nontranslated region of hepatitis C virus required for RNA replication. *J Virol* **75**, 12047-57.
- Fried, M. W., Shiffman, M. L., Reddy, K. R., Smith, C., Marinos, G., Goncalves, F. L., Jr., Haussinger, D., Diago, M., Carosi, G., Dhumeaux, D., Craxi, A., Lin, A., Hoffman, J. & Yu, J. (2002). Peginterferon alfa-2a plus ribavirin for chronic hepatitis C virus infection. *N Engl J Med* **347**, 975-82.
- Frischknecht, F., Renaud, O. & Shorte, S. L. (2006). Imaging today's infectious animalcules. *Curr Opin Microbiol* **9**, 297-306.
- Fukushi, S., Okada, M., Kageyama, T., Hoshino, F. B., Nagai, K. & Katayama, K. (2001). Interaction of poly(rC)-binding protein 2 with the 5'-terminal stem loop of the hepatitis C-virus genome. *Virus Res* **73**, 67-79.
- Gaietta, G., Deerinck, T. J., Adams, S. R., Bouwer, J., Tour, O., Laird, D. W., Sosinsky, G. E., Tsien, R. Y. & Ellisman, M. H. (2002). Multicolor and electron microscopic imaging of connexin trafficking. *Science* **296**, 503-7.
- Gale, M., Jr., Blakely, C. M., Kwieciszewski, B., Tan, S. L., Dossett, M., Tang, N. M., Korth, M. J., Polyak, S. J., Gretch, D. R. & Katze, M. G. (1998). Control of PKR protein kinase by hepatitis C virus nonstructural 5A protein: molecular mechanisms of kinase regulation. *Mol Cell Biol* **18**, 5208-18.
- Gale, M. J., Jr., Korth, M. J., Tang, N. M., Tan, S. L., Hopkins, D. A., Dever, T. E., Polyak, S. J., Gretch, D. R. & Katze, M. G. (1997). Evidence that hepatitis C

- virus resistance to interferon is mediated through repression of the PKR protein kinase by the nonstructural 5A protein. *Virology* **230**, 217-27.
- Gallinari, P., Brennan, D., Nardi, C., Brunetti, M., Tomei, L., Steinkuhler, C. & De Francesco, R. (1998). Multiple enzymatic activities associated with recombinant NS3 protein of hepatitis C virus. *J Virol* **72**, 6758-69.
- Gao, L., Aizaki, H., He, J. W. & Lai, M. M. (2004). Interactions between viral nonstructural proteins and host protein hVAP-33 mediate the formation of hepatitis C virus RNA replication complex on lipid raft. *J Virol* **78**, 3480-8.
- Gastaminza, P., Cheng, G., Wieland, S., Zhong, J., Liao, W. & Chisari, F. V. (2008). Cellular determinants of hepatitis C virus assembly, maturation, degradation, and secretion. *J Virol* **82**, 2120-9.
- Gastaminza, P., Kapadia, S. B. & Chisari, F. V. (2006). Differential biophysical properties of infectious intracellular and secreted hepatitis C virus particles. *J Virol* **80**, 11074-81.
- Germi, R., Crance, J. M., Garin, D., Guimet, J., Lortat-Jacob, H., Ruigrok, R. W., Zarski, J. P. & Drouet, E. (2002). Cellular glycosaminoglycans and low density lipoprotein receptor are involved in hepatitis C virus adsorption. *J Med Virol* **68**, 206-15.
- Gibbons, G. F., Wiggins, D., Brown, A. M. & Hebbachi, A. M. (2004). Synthesis and function of hepatic very-low-density lipoprotein. *Biochem Soc Trans* **32**, 59-64.
- Goffard, A., Callens, N., Bartosch, B., Wychowski, C., Cosset, F. L., Montpellier, C. & Dubuisson, J. (2005). Role of N-linked glycans in the functions of hepatitis C virus envelope glycoproteins. *J Virol* **79**, 8400-9.
- Goffard, A. & Dubuisson, J. (2003). Glycosylation of hepatitis C virus envelope proteins. *Biochimie* **85**, 295-301.
- Gosert, R., Egger, D., Lohmann, V., Bartenschlager, R., Blum, H. E., Bienz, K. & Moradpour, D. (2003). Identification of the hepatitis C virus RNA replication complex in Huh-7 cells harboring subgenomic replicons. *J Virol* **77**, 5487-92.
- Grakoui, A., McCourt, D. W., Wychowski, C., Feinstone, S. M. & Rice, C. M. (1993a). Characterization of the hepatitis C virus-encoded serine proteinase: determination of proteinase-dependent polyprotein cleavage sites. *J Virol* **67**, 2832-43.
- Grakoui, A., McCourt, D. W., Wychowski, C., Feinstone, S. M. & Rice, C. M. (1993b). A second hepatitis C virus-encoded proteinase. *Proc Natl Acad Sci U S A* **90**, 10583-7.
- Grassmann, C. W., Isken, O., Tautz, N. & Behrens, S. E. (2001). Genetic analysis of the pestivirus nonstructural coding region: defects in the NS5A unit can be complemented in trans. *J Virol* **75**, 7791-802.
- Gretton, S. N., Taylor, A. I. & McLauchlan, J. (2005). Mobility of the hepatitis C virus NS4B protein on the endoplasmic reticulum membrane and membrane-associated foci. *J Gen Virol* **86**, 1415-21.
- Griffin, S., Stgelais, C., Owsianka, A. M., Patel, A. H., Rowlands, D. & Harris, M. (2008). Genotype-dependent sensitivity of hepatitis C virus to inhibitors of the p7 ion channel. *Hepatology* **48**, 1779-90.
- Griffin, S. D., Beales, L. P., Clarke, D. S., Worsfold, O., Evans, S. D., Jaeger, J., Harris, M. P. & Rowlands, D. J. (2003). The p7 protein of hepatitis C virus forms an ion channel that is blocked by the antiviral drug, Amantadine. *FEBS Lett* **535**, 34-8.
- Griffin, S. D., Harvey, R., Clarke, D. S., Barclay, W. S., Harris, M. & Rowlands, D. J. (2004). A conserved basic loop in hepatitis C virus p7 protein is required for amantadine-sensitive ion channel activity in mammalian cells but is dispensable for localization to mitochondria. *J Gen Virol* **85**, 451-61.

- Grove, J., Huby, T., Stamatakis, Z., Vanwolleghem, T., Meuleman, P., Farquhar, M., Schwarz, A., Moreau, M., Owen, J. S., Leroux-Roels, G., Balfe, P. & McKeating, J. A. (2007). Scavenger receptor BI and BII expression levels modulate hepatitis C virus infectivity. *J Virol* **81**, 3162-9.
- Guidotti, L. G. & Chisari, F. V. (2001). Noncytolytic control of viral infections by the innate and adaptive immune response. *Annu Rev Immunol* **19**, 65-91.
- Haigh, S. E., Twig, G., Molina, A. A., Wikstrom, J. D., Deutsch, M. & Shirihai, O. S. (2007). PA-GFP: a window into the subcellular adventures of the individual mitochondrion. *Novartis Found Symp* **287**, 21-36; discussion 36-46.
- Hanoulle, X., Verdegem, D., Badillo, A., Wieruszkeski, J. M., Penin, F. & Lippens, G. (2009). Domain 3 of non-structural protein 5A from hepatitis C virus is natively unfolded. *Biochem Biophys Res Commun* **381**, 634-8.
- Hauri, A. M., Armstrong, G. L. & Hutin, Y. J. (2004). The global burden of disease attributable to contaminated injections given in health care settings. *Int J STD AIDS* **15**, 7-16.
- Heathcote, E. J., Shiffman, M. L., Cooksley, W. G., Dusheiko, G. M., Lee, S. S., Balart, L., Reindollar, R., Reddy, R. K., Wright, T. L., Lin, A., Hoffman, J. & De Pamphilis, J. (2000). Peginterferon alfa-2a in patients with chronic hepatitis C and cirrhosis. *N Engl J Med* **343**, 1673-80.
- Helle, F. & Dubuisson, J. (2008). Hepatitis C virus entry into host cells. *Cell Mol Life Sci* **65**, 100-12.
- Helle, F., Wychowski, C., Vu-Dac, N., Gustafson, K. R., Voisset, C. & Dubuisson, J. (2006). Cyanovirin-N inhibits hepatitis C virus entry by binding to envelope protein glycans. *J Biol Chem* **281**, 25177-83.
- Henis, Y. I., Rotblat, B. & Kloog, Y. (2006). FRAP beam-size analysis to measure palmitoylation-dependent membrane association dynamics and microdomain partitioning of Ras proteins. *Methods* **40**, 183-90.
- Henke, J. I., Goergen, D., Zheng, J., Song, Y., Schuttler, C. G., Fehr, C., Junemann, C. & Niepmann, M. (2008). microRNA-122 stimulates translation of hepatitis C virus RNA. *Embo J* **27**, 3300-10.
- Herold, M. J., van den Brandt, J., Seibler, J. & Reichardt, H. M. (2008). Inducible and reversible gene silencing by stable integration of an shRNA-encoding lentivirus in transgenic rats. *Proc Natl Acad Sci U S A* **105**, 18507-12.
- Hijikata, M., Mizushima, H., Akagi, T., Mori, S., Kakiuchi, N., Kato, N., Tanaka, T., Kimura, K. & Shimotohno, K. (1993). Two distinct proteinase activities required for the processing of a putative nonstructural precursor protein of hepatitis C virus. *J Virol* **67**, 4665-75.
- Hollinger, F. B., Gitnick, G. L., Aach, R. D., Szmunes, W., Mosley, J. W., Stevens, C. E., Peters, R. L., Weiner, J. M., Werch, J. B. & Lander, J. J. (1978). Non-A, non-B hepatitis transmission in chimpanzees: a project of the transfusion-transmitted viruses study group. *Intervirology* **10**, 60-8.
- Honda, M., Beard, M. R., Ping, L. H. & Lemon, S. M. (1999). A phylogenetically conserved stem-loop structure at the 5' border of the internal ribosome entry site of hepatitis C virus is required for cap-independent viral translation. *J Virol* **73**, 1165-74.
- Honda, M., Brown, E. A. & Lemon, S. M. (1996a). Stability of a stem-loop involving the initiator AUG controls the efficiency of internal initiation of translation on hepatitis C virus RNA. *Rna* **2**, 955-68.
- Honda, M., Ping, L. H., Rijnbrand, R. C., Amphlett, E., Clarke, B., Rowlands, D. & Lemon, S. M. (1996b). Structural requirements for initiation of translation by internal ribosome entry within genome-length hepatitis C virus RNA. *Virology* **222**, 31-42.

- Hope, R. G. & McLauchlan, J. (2000). Sequence motifs required for lipid droplet association and protein stability are unique to the hepatitis C virus core protein. *J Gen Virol* **81**, 1913-25.
- Houghton, M. & Abrignani, S. (2005). Prospects for a vaccine against the hepatitis C virus. *Nature* **436**, 961-6.
- Hourioux, C., Ait-Goughoulte, M., Patient, R., Fouquenot, D., Arcanger-Doudet, F., Brand, D., Martin, A. & Roingard, P. (2007). Core protein domains involved in hepatitis C virus-like particle assembly and budding at the endoplasmic reticulum membrane. *Cell Microbiol* **9**, 1014-27.
- Hsu, M., Zhang, J., Flint, M., Logvinoff, C., Cheng-Mayer, C., Rice, C. M. & McKeating, J. A. (2003). Hepatitis C virus glycoproteins mediate pH-dependent cell entry of pseudotyped retroviral particles. *Proc Natl Acad Sci U S A* **100**, 7271-6.
- Huang, H., Sun, F., Owen, D. M., Li, W., Chen, Y., Gale, M., Jr. & Ye, J. (2007a). Hepatitis C virus production by human hepatocytes dependent on assembly and secretion of very low-density lipoproteins. *Proc Natl Acad Sci U S A* **104**, 5848-53.
- Huang, L., Hwang, J., Sharma, S. D., Hargittai, M. R., Chen, Y., Arnold, J. J., Raney, K. D. & Cameron, C. E. (2005). Hepatitis C virus nonstructural protein 5A (NS5A) is an RNA-binding protein. *J Biol Chem* **280**, 36417-28.
- Huang, Y., Staschke, K., De Francesco, R. & Tan, S. L. (2007b). Phosphorylation of hepatitis C virus NS5A nonstructural protein: a new paradigm for phosphorylation-dependent viral RNA replication? *Virology* **364**, 1-9.
- Hugle, T., Fehrmann, F., Bieck, E., Kohara, M., Krausslich, H. G., Rice, C. M., Blum, H. E. & Moradpour, D. (2001). The hepatitis C virus nonstructural protein 4B is an integral endoplasmic reticulum membrane protein. *Virology* **284**, 70-81.
- Hussy, P., Langen, H., Mous, J. & Jacobsen, H. (1996). Hepatitis C virus core protein: carboxy-terminal boundaries of two processed species suggest cleavage by a signal peptide peptidase. *Virology* **224**, 93-104.
- Hutchinson, S. J., Bird, S. M. & Goldberg, D. J. (2005). Modeling the current and future disease burden of hepatitis C among injection drug users in Scotland. *Hepatology* **42**, 711-23.
- Ingelfinger, D., Arndt-Jovin, D. J., Luhrmann, R. & Achsel, T. (2002). The human LSM1-7 proteins colocalize with the mRNA-degrading enzymes Dcp1/2 and Xrn1 in distinct cytoplasmic foci. *Rna* **8**, 1489-501.
- Ishii, K., Murakami, K., Hmwe, S. S., Zhang, B., Li, J., Shirakura, M., Morikawa, K., Suzuki, R., Miyamura, T., Wakita, T. & Suzuki, T. (2008). Trans-encapsidation of hepatitis C virus subgenomic replicon RNA with viral structure proteins. *Biochem Biophys Res Commun* **371**, 446-50.
- Ishii, S. & Koziel, M. J. (2008). Immune responses during acute and chronic infection with hepatitis C virus. *Clin Immunol* **128**, 133-47.
- Ito, T. & Lai, M. M. (1997). Determination of the secondary structure of and cellular protein binding to the 3'-untranslated region of the hepatitis C virus RNA genome. *J Virol* **71**, 8698-706.
- Ivashkina, N., Wolk, B., Lohmann, V., Bartenschlager, R., Blum, H. E., Penin, F. & Moradpour, D. (2002). The hepatitis C virus RNA-dependent RNA polymerase membrane insertion sequence is a transmembrane segment. *J Virol* **76**, 13088-93.
- Ji, H., Fraser, C. S., Yu, Y., Leary, J. & Doudna, J. A. (2004). Coordinated assembly of human translation initiation complexes by the hepatitis C virus internal ribosome entry site RNA. *Proc Natl Acad Sci U S A* **101**, 16990-5.

- Ji, J., Glaser, A., Wernli, M., Berke, J. M., Moradpour, D. & Erb, P. (2008). Suppression of short interfering RNA-mediated gene silencing by the structural proteins of hepatitis C virus. *J Gen Virol* **89**, 2761-6.
- Jirasko, V., Montserret, R., Appel, N., Janvier, A., Eustachi, L., Brohm, C., Steinmann, E., Pietschmann, T., Penin, F. & Bartenschlager, R. (2008). Structural and functional characterization of nonstructural protein 2 for its role in hepatitis C virus assembly. *J Biol Chem* **283**, 28546-62.
- Jones, C. T., Murray, C. L., Eastman, D. K., Tassello, J. & Rice, C. M. (2007). Hepatitis C virus p7 and NS2 proteins are essential for production of infectious virus. *J Virol* **81**, 8374-83.
- Joo, K. I., Lei, Y., Lee, C. L., Lo, J., Xie, J., Hamm-Alvarez, S. F. & Wang, P. (2008). Site-specific labeling of enveloped viruses with quantum dots for single virus tracking. *ACS Nano* **2**, 1553-62.
- Jopling, C. L., Schutz, S. & Sarnow, P. (2008). Position-dependent function for a tandem microRNA miR-122-binding site located in the hepatitis C virus RNA genome. *Cell Host Microbe* **4**, 77-85.
- Jopling, C. L., Yi, M., Lancaster, A. M., Lemon, S. M. & Sarnow, P. (2005). Modulation of hepatitis C virus RNA abundance by a liver-specific MicroRNA. *Science* **309**, 1577-81.
- Kaito, M., Watanabe, S., Tsukiyama-Kohara, K., Yamaguchi, K., Kobayashi, Y., Konishi, M., Yokoi, M., Ishida, S., Suzuki, S. & Kohara, M. (1994). Hepatitis C virus particle detected by immunoelectron microscopic study. *J Gen Virol* **75 (Pt 7)**, 1755-60.
- Kanaoka, Y. & Nojima, H. (1994). SCR: novel human suppressors of cdc2/cdc13 mutants of *Schizosaccharomyces pombe* harbour motifs for RNA binding proteins. *Nucleic Acids Res* **22**, 2687-93.
- Kanda, T., Steele, R., Ray, R. & Ray, R. B. (2007). Small interfering RNA targeted to hepatitis C virus 5' nontranslated region exerts potent antiviral effect. *J Virol* **81**, 669-76.
- Kapadia, S. B., Barth, H., Baumert, T., McKeating, J. A. & Chisari, F. V. (2007). Initiation of hepatitis C virus infection is dependent on cholesterol and cooperativity between CD81 and scavenger receptor B type I. *J Virol* **81**, 374-83.
- Kapadia, S. B., Brideau-Andersen, A. & Chisari, F. V. (2003). Interference of hepatitis C virus RNA replication by short interfering RNAs. *Proc Natl Acad Sci U S A* **100**, 2014-8.
- Kaplan, D. E., Sugimoto, K., Newton, K., Valiga, M. E., Ikeda, F., Aytaman, A., Nunes, F. A., Lucey, M. R., Vance, B. A., Vonderheide, R. H., Reddy, K. R., McKeating, J. A. & Chang, K. M. (2007). Discordant role of CD4 T-cell response relative to neutralizing antibody and CD8 T-cell responses in acute hepatitis C. *Gastroenterology* **132**, 654-66.
- Kato, T., Date, T., Miyamoto, M., Furusaka, A., Tokushige, K., Mizokami, M. & Wakita, T. (2003). Efficient replication of the genotype 2a hepatitis C virus subgenomic replicon. *Gastroenterology* **125**, 1808-17.
- Kato, T., Date, T., Miyamoto, M., Zhao, Z., Mizokami, M. & Wakita, T. (2005). Nonhepatic cell lines HeLa and 293 support efficient replication of the hepatitis C virus genotype 2a subgenomic replicon. *J Virol* **79**, 592-6.
- Kato, T., Furusaka, A., Miyamoto, M., Date, T., Yasui, K., Hiramoto, J., Nagayama, K., Tanaka, T. & Wakita, T. (2001). Sequence analysis of hepatitis C virus isolated from a fulminant hepatitis patient. *J Med Virol* **64**, 334-9.
- Kenworthy, A. K. (2006). Fluorescence-based methods to image palmitoylated proteins. *Methods* **40**, 198-205.
- Khromykh, A. A., Sedlak, P. L., Guyatt, K. J., Hall, R. A. & Westaway, E. G. (1999a). Efficient trans-complementation of the flavivirus kunjin NS5 protein

- but not of the NS1 protein requires its coexpression with other components of the viral replicase. *J Virol* **73**, 10272-80.
- Khromykh, A. A., Sedlak, P. L. & Westaway, E. G. (1999b). trans-Complementation analysis of the flavivirus Kunjin ns5 gene reveals an essential role for translation of its N-terminal half in RNA replication. *J Virol* **73**, 9247-55.
- Khromykh, A. A., Sedlak, P. L. & Westaway, E. G. (2000). cis- and trans-acting elements in flavivirus RNA replication. *J Virol* **74**, 3253-63.
- Kieffer, T. L., Sarrazin, C., Miller, J. S., Welker, M. W., Forestier, N., Reesink, H. W., Kwong, A. D. & Zeuzem, S. (2007). Telaprevir and pegylated interferon-alpha-2a inhibit wild-type and resistant genotype 1 hepatitis C virus replication in patients. *Hepatology* **46**, 631-9.
- Kim, C.S., Seol, S. K., Song, O.K., Park, J.H. & Jang, S.K. (2007). An RNA-binding protein, hnRNP A1, and a scaffold protein, septin 6, facilitate hepatitis C virus replication. *J Virol* **81**, 3852-65.
- Kim, D. H. & Rossi, J. J. (2007). Strategies for silencing human disease using RNA interference. *Nat Rev Genet* **8**, 173-84.
- Kim, J. E., Song, W. K., Chung, K. M., Back, S. H. & Jang, S. K. (1999). Subcellular localization of hepatitis C viral proteins in mammalian cells. *Arch Virol* **144**, 329-43.
- Kim, J. L., Morgenstern, K. A., Griffith, J. P., Dwyer, M. D., Thomson, J. A., Murcko, M. A., Lin, C. & Caron, P. R. (1998). Hepatitis C virus NS3 RNA helicase domain with a bound oligonucleotide: the crystal structure provides insights into the mode of unwinding. *Structure* **6**, 89-100.
- Kim, J. L., Morgenstern, K. A., Lin, C., Fox, T., Dwyer, M. D., Landro, J. A., Chambers, S. P., Markland, W., Lepre, C. A., O'Malley, E. T., Harbeson, S. L., Rice, C. M., Murcko, M. A., Caron, P. R. & Thomson, J. A. (1996). Crystal structure of the hepatitis C virus NS3 protease domain complexed with a synthetic NS4A cofactor peptide. *Cell* **87**, 343-55.
- Kim, S. Y., Park, K. W., Lee, Y. J., Back, S. H., Goo, J. H., Park, O. K., Jang, S. K. & Park, W. J. (2000). In vivo determination of substrate specificity of hepatitis C virus NS3 protease: genetic assay for site-specific proteolysis. *Anal Biochem* **284**, 42-8.
- Kim, Y. K., Kim, C. S., Lee, S. H. & Jang, S. K. (2002). Domains I and II in the 5' nontranslated region of the HCV genome are required for RNA replication. *Biochem Biophys Res Commun* **290**, 105-12.
- Koch, J. O. & Bartenschlager, R. (1999). Modulation of hepatitis C virus NS5A hyperphosphorylation by nonstructural proteins NS3, NS4A, and NS4B. *J Virol* **73**, 7138-46.
- Kolykhalov, A. A., Agapov, E. V., Blight, K. J., Mihalik, K., Feinstone, S. M. & Rice, C. M. (1997). Transmission of hepatitis C by intrahepatic inoculation with transcribed RNA. *Science* **277**, 570-4.
- Koutsoudakis, G., Kaul, A., Steinmann, E., Kallis, S., Lohmann, V., Pietschmann, T. & Bartenschlager, R. (2006). Characterization of the early steps of hepatitis C virus infection by using luciferase reporter viruses. *J Virol* **80**, 5308-20.
- Krieger, N., Lohmann, V. & Bartenschlager, R. (2001). Enhancement of hepatitis C virus RNA replication by cell culture-adaptive mutations. *J Virol* **75**, 4614-24.
- Kronke, J., Kittler, R., Buchholz, F., Windisch, M. P., Pietschmann, T., Bartenschlager, R. & Frese, M. (2004). Alternative approaches for efficient inhibition of hepatitis C virus RNA replication by small interfering RNAs. *J Virol* **78**, 3436-46.

- Lai, C. K., Jeng, K. S., Machida, K. & Lai, M. M. (2008). Association of hepatitis C virus replication complexes with microtubules and actin filaments is dependent on the interaction of NS3 and NS5A. *J Virol* **82**, 8838-48.
- Lai, V. C., Dempsey, S., Lau, J. Y., Hong, Z. & Zhong, W. (2003). In vitro RNA replication directed by replicase complexes isolated from the subgenomic replicon cells of hepatitis C virus. *J Virol* **77**, 2295-300.
- Lam, A. M. & Frick, D. N. (2006). Hepatitis C virus subgenomic replicon requires an active NS3 RNA helicase. *J Virol* **80**, 404-11.
- Larson, D. R., Johnson, M. C., Webb, W. W. & Vogt, V. M. (2005). Visualization of retrovirus budding with correlated light and electron microscopy. *Proc Natl Acad Sci U S A* **102**, 15453-8.
- Lawitz, E., Rodriguez-Torres, M., Muir, A. J., Kieffer, T. L., McNair, L., Khunvichai, A. & McHutchison, J. G. (2008). Antiviral effects and safety of telaprevir, peginterferon alfa-2a, and ribavirin for 28 days in hepatitis C patients. *J Hepatol* **49**, 163-9.
- Lehmann, M., Meyer, M. F., Monazahian, M., Tillmann, H. L., Manns, M. P. & Wedemeyer, H. (2004). High rate of spontaneous clearance of acute hepatitis C virus genotype 3 infection. *J Med Virol* **73**, 387-91.
- Lemon, S., Walker, C. M., Alter, M. J. & Yi, M. (2007). Hepatitis C. In *Fields Virology*, 5th edn, pp. 1253-1304. Philadelphia: Lipincott Williams & Wilkins.
- Li, F., Zhang, Z. P., Peng, J., Cui, Z. Q., Pang, D. W., Li, K., Wei, H. P., Zhou, Y. F., Wen, J. K. & Zhang, X. E. (2009). Imaging viral behavior in Mammalian cells with self-assembled capsid-quantum-dot hybrid particles. *Small* **5**, 718-26.
- Liang, Y., Kang, C. B. & Yoon, H. S. (2006). Molecular and structural characterization of the domain 2 of hepatitis C virus non-structural protein 5A. *Mol Cells* **22**, 13-20.
- Lin, C., Lindenbach, B. D., Pragai, B. M., McCourt, D. W. & Rice, C. M. (1994a). Processing in the hepatitis C virus E2-NS2 region: identification of p7 and two distinct E2-specific products with different C termini. *J Virol* **68**, 5063-73.
- Lin, C., Pragai, B. M., Grakoui, A., Xu, J. & Rice, C. M. (1994b). Hepatitis C virus NS3 serine proteinase: trans-cleavage requirements and processing kinetics. *J Virol* **68**, 8147-57.
- Lin, C., Thomson, J. A. & Rice, C. M. (1995). A central region in the hepatitis C virus NS4A protein allows formation of an active NS3-NS4A serine proteinase complex in vivo and in vitro. *J Virol* **69**, 4373-80.
- Lin, K., Perni, R. B., Kwong, A. D. & Lin, C. (2006). VX-950, a novel hepatitis C virus (HCV) NS3-4A protease inhibitor, exhibits potent antiviral activities in HCV replicon cells. *Antimicrob Agents Chemother* **50**, 1813-22.
- Lindenbach, B. D., Evans, M. J., Syder, A. J., Wolk, B., Tellinghuisen, T. L., Liu, C. C., Maruyama, T., Hynes, R. O., Burton, D. R., McKeating, J. A. & Rice, C. M. (2005). Complete replication of hepatitis C virus in cell culture. *Science* **309**, 623-6.
- Lindenbach, B. D., Meuleman, P., Ploss, A., Vanwolleghem, T., Syder, A. J., McKeating, J. A., Lanford, R. E., Feinstone, S. M., Major, M. E., Leroux-Roels, G. & Rice, C. M. (2006). Cell culture-grown hepatitis C virus is infectious in vivo and can be recultured in vitro. *Proc Natl Acad Sci U S A* **103**, 3805-9.
- Lindenbach, B. D., Pragai, B. M., Montserret, R., Beran, R. K., Pyle, A. M., Penin, F. & Rice, C. M. (2007). The C terminus of hepatitis C virus NS4A encodes an electrostatic switch that regulates NS5A hyperphosphorylation and viral replication. *J Virol* **81**, 8905-18.

- Lindenbach, B. D. & Rice, C. M. (1997). trans-Complementation of yellow fever virus NS1 reveals a role in early RNA replication. *J Virol* **71**, 9608-17.
- Lindstrom, H., Lundin, M., Haggstrom, S. & Persson, M. A. (2006). Mutations of the hepatitis C virus protein NS4B on either side of the ER membrane affect the efficiency of subgenomic replicons. *Virus Res* **121**, 169-78.
- Liu, S., Ansari, I. H., Das, S. C. & Pattnaik, A. K. (2006). Insertion and deletion analyses identify regions of non-structural protein 5A of hepatitis C virus that are dispensable for viral genome replication. *J Gen Virol* **87**, 323-7.
- Liu, S., Yang, W., Shen, L., Turner, J. R., Coyne, C. B. & Wang, T. (2009). Tight junction proteins claudin-1 and occludin control hepatitis C virus entry and are downregulated during infection to prevent superinfection. *J Virol* **83**, 2011-4.
- Lohmann, V., Hoffmann, S., Herian, U., Penin, F. & Bartenschlager, R. (2003). Viral and cellular determinants of hepatitis C virus RNA replication in cell culture. *J Virol* **77**, 3007-19.
- Lohmann, V., Korner, F., Dobierzewska, A. & Bartenschlager, R. (2001). Mutations in hepatitis C virus RNAs conferring cell culture adaptation. *J Virol* **75**, 1437-49.
- Lohmann, V., Korner, F., Herian, U. & Bartenschlager, R. (1997). Biochemical properties of hepatitis C virus NS5B RNA-dependent RNA polymerase and identification of amino acid sequence motifs essential for enzymatic activity. *J Virol* **71**, 8416-28.
- Lohmann, V., Korner, F., Koch, J., Herian, U., Theilmann, L. & Bartenschlager, R. (1999). Replication of subgenomic hepatitis C virus RNAs in a hepatoma cell line. *Science* **285**, 110-3.
- Lopez-Fraga, M., Wright, N. & Jimenez, A. (2008). RNA interference-based therapeutics: new strategies to fight infectious disease. *Infect Disord Drug Targets* **8**, 262-73.
- Lorenz, I. C., Marcotrigiano, J., Dentzer, T. G. & Rice, C. M. (2006). Structure of the catalytic domain of the hepatitis C virus NS2-3 protease. *Nature* **442**, 831-5.
- Love, R. A., Parge, H. E., Wickersham, J. A., Hostomsky, Z., Habuka, N., Moomaw, E. W., Adachi, T. & Hostomska, Z. (1996). The crystal structure of hepatitis C virus NS3 proteinase reveals a trypsin-like fold and a structural zinc binding site. *Cell* **87**, 331-42.
- Lundin, M., Lindstrom, H., Gronwall, C. & Persson, M. A. (2006). Dual topology of the processed hepatitis C virus protein NS4B is influenced by the NS5A protein. *J Gen Virol* **87**, 3263-72.
- Lundin, M., Monne, M., Widell, A., Von Heijne, G. & Persson, M. A. (2003). Topology of the membrane-associated hepatitis C virus protein NS4B. *J Virol* **77**, 5428-38.
- Lykke-Andersen, J. (2001). mRNA quality control: marking the message for life or death. *Curr Biol* **11**, R88-91.
- Lykke-Andersen, J., Shu, M. D. & Steitz, J. A. (2001). Communication of the position of exon-exon junctions to the mRNA surveillance machinery by the protein RNPS1. *Science* **293**, 1836-9.
- Ma, Y., Yates, J., Liang, Y., Lemon, S. M. & Yi, M. (2008). NS3 helicase domains involved in infectious intracellular hepatitis C virus particle assembly. *J Virol* **82**, 7624-39.
- Macdonald, A., Crowder, K., Street, A., McCormick, C., Saksela, K. & Harris, M. (2003). The hepatitis C virus non-structural NS5A protein inhibits activating protein-1 function by perturbing ras-ERK pathway signaling. *J Biol Chem* **278**, 17775-84.

- Macdonald, A. & Harris, M. (2004). Hepatitis C virus NS5A: tales of a promiscuous protein. *J Gen Virol* **85**, 2485-502.
- Macdonald, A., Mazaleyrat, S., McCormick, C., Street, A., Burgoyne, N. J., Jackson, R. M., Cazeaux, V., Shelton, H., Saksela, K. & Harris, M. (2005). Further studies on hepatitis C virus NS5A-SH3 domain interactions: identification of residues critical for binding and implications for viral RNA replication and modulation of cell signalling. *J Gen Virol* **86**, 1035-44.
- Mackenzie, J. (2005). Wrapping things up about virus RNA replication. *Traffic* **6**, 967-77.
- Maillard, P., Huby, T., Andreo, U., Moreau, M., Chapman, J. & Budkowska, A. (2006). The interaction of natural hepatitis C virus with human scavenger receptor SR-BI/Cla1 is mediated by ApoB-containing lipoproteins. *Faseb J* **20**, 735-7.
- Malakhova, O. A. & Zhang, D. E. (2008). ISG15 inhibits Nedd4 ubiquitin E3 activity and enhances the innate antiviral response. *J Biol Chem* **283**, 8783-7.
- Mankouri, J., Griffin, S. & Harris, M. (2008). The hepatitis C virus non-structural protein NS5A alters the trafficking profile of the epidermal growth factor receptor. *Traffic* **9**, 1497-509.
- Martell, M., Esteban, J. I., Quer, J., Genesca, J., Weiner, A., Esteban, R., Guardia, J. & Gomez, J. (1992). Hepatitis C virus (HCV) circulates as a population of different but closely related genomes: quasispecies nature of HCV genome distribution. *J Virol* **66**, 3225-9.
- Masaki, T., Suzuki, R., Murakami, K., Aizaki, H., Ishii, K., Murayama, A., Date, T., Matsuura, Y., Miyamura, T., Wakita, T. & Suzuki, T. (2008). Interaction of hepatitis C virus nonstructural protein 5A with core protein is critical for the production of infectious virus particles. *J Virol* **82**, 7964-76.
- Matranga, C., Tomari, Y., Shin, C., Bartel, D. P. & Zamore, P. D. (2005). Passenger-strand cleavage facilitates assembly of siRNA into Ago2-containing RNAi enzyme complexes. *Cell* **123**, 607-20.
- McCormick, C. J., Maucourant, S., Griffin, S., Rowlands, D. J. & Harris, M. (2006). Tagging of NS5A expressed from a functional hepatitis C virus replicon. *J Gen Virol* **87**, 635-40.
- McLauchlan, J. (2009). Lipid droplets and hepatitis C virus infection. *Biochim Biophys Acta* **1791**, 552-59.
- McLauchlan, J., Lemberg, M. K., Hope, G. & Martoglio, B. (2002). Intramembrane proteolysis promotes trafficking of hepatitis C virus core protein to lipid droplets. *Embo J* **21**, 3980-8.
- Meertens, L., Bertaux, C., Cukierman, L., Cormier, E., Lavillette, D., Cosset, F. L. & Dragic, T. (2008). The tight junction proteins claudin-1, -6, and -9 are entry cofactors for hepatitis C virus. *J Virol* **82**, 3555-60.
- Meertens, L., Bertaux, C. & Dragic, T. (2006). Hepatitis C virus entry requires a critical postinternalization step and delivery to early endosomes via clathrin-coated vesicles. *J Virol* **80**, 11571-8.
- Mensenkamp, A. R., Havekes, L. M., Romijn, J. A. & Kuipers, F. (2001). Hepatic steatosis and very low density lipoprotein secretion: the involvement of apolipoprotein E. *J Hepatol* **35**, 816-22.
- Meunier, J. C., Engle, R. E., Faulk, K., Zhao, M., Bartosch, B., Alter, H., Emerson, S. U., Cosset, F. L., Purcell, R. H. & Bukh, J. (2005). Evidence for cross-genotype neutralization of hepatitis C virus pseudo-particles and enhancement of infectivity by apolipoprotein C1. *Proc Natl Acad Sci U S A* **102**, 4560-5.
- Meunier, J. C., Russell, R. S., Goossens, V., Priem, S., Walter, H., Depla, E., Union, A., Faulk, K. N., Bukh, J., Emerson, S. U. & Purcell, R. H. (2008).

- Isolation and characterization of broadly neutralizing human monoclonal antibodies to the e1 glycoprotein of hepatitis C virus. *J Virol* **82**, 966-73.
- Michalak, J. P., Wychowski, C., Choukhi, A., Meunier, J. C., Ung, S., Rice, C. M. & Dubuisson, J. (1997). Characterization of truncated forms of hepatitis C virus glycoproteins. *J Gen Virol* **78 (Pt 9)**, 2299-306.
- Michalet, X., Pinaud, F. F., Bentolila, L. A., Tsay, J. M., Doose, S., Li, J. J., Sundaresan, G., Wu, A. M., Gambhir, S. S. & Weiss, S. (2005). Quantum dots for live cells, in vivo imaging, and diagnostics. *Science* **307**, 538-44.
- Miller, R. H. & Purcell, R. H. (1990). Hepatitis C virus shares amino acid sequence similarity with pestiviruses and flaviviruses as well as members of two plant virus supergroups. *Proc Natl Acad Sci U S A* **87**, 2057-61.
- Miller, S., Kastner, S., Krijnse-Locker, J., Buhler, S. & Bartenschlager, R. (2007). The non-structural protein 4A of dengue virus is an integral membrane protein inducing membrane alterations in a 2K-regulated manner. *J Biol Chem* **282**, 8873-82.
- Missale, G., Bertoni, R., Lamonaca, V., Valli, A., Massari, M., Mori, C., Rumi, M. G., Houghton, M., Fiaccadori, F. & Ferrari, C. (1996). Different clinical behaviors of acute hepatitis C virus infection are associated with different vigor of the anti-viral cell-mediated immune response. *J Clin Invest* **98**, 706-14.
- Miyinari, Y., Atsuzawa, K., Usuda, N., Watashi, K., Hishiki, T., Zayas, M., Bartenschlager, R., Wakita, T., Hijikata, M. & Shimotohno, K. (2007). The lipid droplet is an important organelle for hepatitis C virus production. *Nat Cell Biol* **9**, 1089-97.
- Molina, S., Castet, V., Fournier-Wirth, C., Pichard-Garcia, L., Avner, R., Harats, D., Roitelman, J., Barbaras, R., Graber, P., Ghersa, P., Smolarsky, M., Funaro, A., Malavasi, F., Larrey, D., Coste, J., Fabre, J. M., Sa-Cunha, A. & Maurel, P. (2007). The low-density lipoprotein receptor plays a role in the infection of primary human hepatocytes by hepatitis C virus. *J Hepatol* **46**, 411-9.
- Moradpour, D., Brass, V., Bieck, E., Friebe, P., Gosert, R., Blum, H. E., Bartenschlager, R., Penin, F. & Lohmann, V. (2004a). Membrane association of the RNA-dependent RNA polymerase is essential for hepatitis C virus RNA replication. *J Virol* **78**, 13278-84.
- Moradpour, D., Englert, C., Wakita, T. & Wands, J. R. (1996). Characterization of cell lines allowing tightly regulated expression of hepatitis C virus core protein. *Virology* **222**, 51-63.
- Moradpour, D., Evans, M. J., Gosert, R., Yuan, Z., Blum, H. E., Goff, S. P., Lindenbach, B. D. & Rice, C. M. (2004b). Insertion of green fluorescent protein into nonstructural protein 5A allows direct visualization of functional hepatitis C virus replication complexes. *J Virol* **78**, 7400-9.
- Moriishi, K. & Matsuura, Y. (2007). Host factors involved in the replication of hepatitis C virus. *Rev Med Virol* **17**, 343-54.
- Moriya, K., Fujie, H., Shintani, Y., Yotsuyanagi, H., Tsutsumi, T., Ishibashi, K., Matsuura, Y., Kimura, S., Miyamura, T. & Koike, K. (1998). The core protein of hepatitis C virus induces hepatocellular carcinoma in transgenic mice. *Nat Med* **4**, 1065-7.
- Mottola, G., Cardinali, G., Ceccacci, A., Trozzi, C., Bartholomew, L., Torrissi, M. R., Pedrazzini, E., Bonatti, S. & Migliaccio, G. (2002). Hepatitis C virus nonstructural proteins are localized in a modified endoplasmic reticulum of cells expressing viral subgenomic replicons. *Virology* **293**, 31-43.
- Muhlrad, D., Decker, C. J. & Parker, R. (1994). Deadenylation of the unstable mRNA encoded by the yeast MFA2 gene leads to decapping followed by 5'->3' digestion of the transcript. *Genes Dev* **8**, 855-66.

- Murray, C. L., Jones, C. T. & Rice, C. M. (2008). Architects of assembly: roles of Flaviviridae non-structural proteins in virion morphogenesis. *Nat Rev Microbiol* **6**, 699-708.
- Murray, C. L., Jones, C. T., Tassello, J. & Rice, C. M. (2007). Alanine scanning of the hepatitis C virus core protein reveals numerous residues essential for production of infectious virus. *J Virol* **81**, 10220-31.
- Murray, E. M., Grobler, J. A., Markel, E. J., Pagnoni, M. F., Paonessa, G., Simon, A. J. & Flores, O. A. (2003). Persistent replication of hepatitis C virus replicons expressing the beta-lactamase reporter in subpopulations of highly permissive Huh7 cells. *J Virol* **77**, 2928-35.
- Neddermann, P., Clementi, A. & De Francesco, R. (1999). Hyperphosphorylation of the hepatitis C virus NS5A protein requires an active NS3 protease, NS4A, NS4B, and NS5A encoded on the same polyprotein. *J Virol* **73**, 9984-91.
- Neddermann, P., Quintavalle, M., Di Pietro, C., Clementi, A., Cerretani, M., Altamura, S., Bartholomew, L. & De Francesco, R. (2004). Reduction of hepatitis C virus NS5A hyperphosphorylation by selective inhibition of cellular kinases activates viral RNA replication in cell culture. *J Virol* **78**, 13306-14.
- Neumann, A. U., Lam, N. P., Dahari, H., Gretch, D. R., Wiley, T. E., Layden, T. J. & Perelson, A. S. (1998). Hepatitis C viral dynamics in vivo and the antiviral efficacy of interferon-alpha therapy. *Science* **282**, 103-7.
- Ng, T. I., Mo, H., Pilot-Matias, T., He, Y., Koev, G., Krishnan, P., Mondal, R., Pithawalla, R., He, W., Dekhtyar, T., Packer, J., Schurdak, M. & Molla, A. (2007). Identification of host genes involved in hepatitis C virus replication by small interfering RNA technology. *Hepatology* **45**, 1413-21.
- Nguyen, M. H. & Keeffe, E. B. (2005). Prevalence and treatment of hepatitis C virus genotypes 4, 5, and 6. *Clin Gastroenterol Hepatol* **3**, S97-S101.
- Nielsen, S. U., Bassendine, M. F., Burt, A. D., Martin, C., Pumeechockchai, W. & Toms, G. L. (2006). Association between hepatitis C virus and very-low-density lipoprotein (VLDL)/LDL analyzed in iodixanol density gradients. *J Virol* **80**, 2418-28.
- O'Connell, K. M. & Tamkun, M. M. (2005). Targeting of voltage-gated potassium channel isoforms to distinct cell surface microdomains. *J Cell Sci* **118**, 2155-66.
- Ogata, N., Alter, H. J., Miller, R. H. & Purcell, R. H. (1991). Nucleotide sequence and mutation rate of the H strain of hepatitis C virus. *Proc Natl Acad Sci U S A* **88**, 3392-6.
- Okamoto, H., Kojima, M., Okada, S., Yoshizawa, H., Iizuka, H., Tanaka, T., Muchmore, E. E., Peterson, D. A., Ito, Y. & Mishiro, S. (1992). Genetic drift of hepatitis C virus during an 8.2-year infection in a chimpanzee: variability and stability. *Virology* **190**, 894-9.
- Okamoto, K., Mori, Y., Komoda, Y., Okamoto, T., Okochi, M., Takeda, M., Suzuki, T., Moriishi, K. & Matsuura, Y. (2008). Intramembrane processing by signal peptide peptidase regulates the membrane localization of hepatitis C virus core protein and viral propagation. *J Virol* **82**, 8349-61.
- Okamoto, T., Nishimura, Y., Ichimura, T., Suzuki, K., Miyamura, T., Suzuki, T., Moriishi, K. & Matsuura, Y. (2006). Hepatitis C virus RNA replication is regulated by FKBP8 and Hsp90. *Embo J* **25**, 5015-25.
- Okuda, M., Li, K., Beard, M. R., Showalter, L. A., Scholle, F., Lemon, S. M. & Weinman, S. A. (2002). Mitochondrial injury, oxidative stress, and antioxidant gene expression are induced by hepatitis C virus core protein. *Gastroenterology* **122**, 366-75.

- Okumura A., Lu, G., Pitha-Rowe, I. & Pitha, P. M. (2006). Innate antiviral response targets HIV-1 release by the induction of ubiquitin-like protein ISG15. *Proc Natl Acad U S A* **103**, 1440-5.
- Okumura, A., Pitha, P. M. & Harty, R. N. (2008). ISG15 inhibits Ebola VP40 VLP budding in an L-domain-dependent manner by blocking Nedd4 ligase activity. *Proc Natl Acad Sci U S A* **105**, 3974-9.
- Olofsson, S. O. & Boren, J. (2005). Apolipoprotein B: a clinically important apolipoprotein which assembles atherogenic lipoproteins and promotes the development of atherosclerosis. *J Intern Med* **258**, 395-410.
- Op De Beeck, A., Montserret, R., Duvet, S., Cocquerel, L., Cacan, R., Barberot, B., Le Maire, M., Penin, F. & Dubuisson, J. (2000). The transmembrane domains of hepatitis C virus envelope glycoproteins E1 and E2 play a major role in heterodimerization. *J Biol Chem* **275**, 31428-37.
- Op De Beeck, A., Voisset, C., Bartosch, B., Ciczora, Y., Cocquerel, L., Keck, Z., Fong, S., Cosset, F. L. & Dubuisson, J. (2004). Characterization of functional hepatitis C virus envelope glycoproteins. *J Virol* **78**, 2994-3002.
- Orland, J. R., Wright, T. L. & Cooper, S. (2001). Acute hepatitis C. *Hepatology* **33**, 321-7.
- Paddison, P. J., Caudy, A. A., Bernstein, E., Hannon, G. J. & Conklin, D. S. (2002). Short hairpin RNAs (shRNAs) induce sequence-specific silencing in mammalian cells. *Genes Dev* **16**, 948-58.
- Paek, K. Y., Kim, C. S., Park, S. M., Kim, J. H. & Jang, S. K. (2008). RNA-binding protein hnRNP D modulates internal ribosome entry site-dependent translation of hepatitis C virus RNA. *J Virol* **82**, 12082-93.
- Pang, P. S., Jankowsky, E., Planet, P. J. & Pyle, A. M. (2002). The hepatitis C viral NS3 protein is a processive DNA helicase with cofactor enhanced RNA unwinding. *Embo J* **21**, 1168-76.
- Paredes, A. M. & Blight, K. J. (2008). A genetic interaction between hepatitis C virus NS4B and NS3 is important for RNA replication. *J Virol* **82**, 10671-83.
- Patargias, G., Zitzmann, N., Dwek, R. & Fischer, W. B. (2006). Protein-protein interactions: modeling the hepatitis C virus ion channel p7. *J Med Chem* **49**, 648-55.
- Patterson, G. H. & Lippincott-Schwartz, J. (2002). A photoactivatable GFP for selective photolabeling of proteins and cells. *Science* **297**, 1873-7.
- Patterson, G. H. & Lippincott-Schwartz, J. (2004). Selective photolabeling of proteins using photoactivatable GFP. *Methods* **32**, 445-50.
- Pawlotsky, J. M. (1999). Diagnostic tests for hepatitis C. *J Hepatol* **31 Suppl 1**, 71-9.
- Pawlotsky, J. M. (2002). Use and interpretation of virological tests for hepatitis C. *Hepatology* **36**, S65-73.
- Penin, F., Combet, C., Germanidis, G., Frainais, P. O., Deleage, G. & Pawlotsky, J. M. (2001). Conservation of the conformation and positive charges of hepatitis C virus E2 envelope glycoprotein hypervariable region 1 points to a role in cell attachment. *J Virol* **75**, 5703-10.
- Penin, F., Dubuisson, J., Rey, F. A., Moradpour, D. & Pawlotsky, J. M. (2004). Structural biology of hepatitis C virus. *Hepatology* **39**, 5-19.
- Perlman, M. & Resh, M. D. (2006). Identification of an intracellular trafficking and assembly pathway for HIV-1 gag. *Traffic* **7**, 731-45.
- Pestova, T. V., Shatsky, I. N., Fletcher, S. P., Jackson, R. J. & Hellen, C. U. (1998). A prokaryotic-like mode of cytoplasmic eukaryotic ribosome binding to the initiation codon during internal translation initiation of hepatitis C and classical swine fever virus RNAs. *Genes Dev* **12**, 67-83.
- Pfeffer, S., Sewer, A., Lagos-Quintana, M., Sheridan, R., Sander, C., Grasser, F. A., van Dyk, L. F., Ho, C. K., Shuman, S., Chien, M., Russo, J. J., Ju, J.,

- Randall, G., Lindenbach, B. D., Rice, C. M., Simon, V., Ho, D. D., Zavolan, M. & Tuschl, T. (2005). Identification of microRNAs of the herpesvirus family. *Nat Methods* **2**, 269-76.
- Piccininni, S., Varaklioti, A., Nardelli, M., Dave, B., Raney, K. D. & McCarthy, J. E. (2002). Modulation of the hepatitis C virus RNA-dependent RNA polymerase activity by the non-structural (NS) 3 helicase and the NS4B membrane protein. *J Biol Chem* **277**, 45670-9.
- Pieroni, L., Santolini, E., Fipaldini, C., Pacini, L., Migliaccio, G. & La Monica, N. (1997). In vitro study of the NS2-3 protease of hepatitis C virus. *J Virol* **71**, 6373-80.
- Pietschmann, T., Kaul, A., Koutsoudakis, G., Shavinskaya, A., Kallis, S., Steinmann, E., Abid, K., Negro, F., Dreux, M., Cosset, F. L. & Bartenschlager, R. (2006). Construction and characterization of infectious intragenotypic and intergenotypic hepatitis C virus chimeras. *Proc Natl Acad Sci U S A* **103**, 7408-13.
- Pietschmann, T., Lohmann, V., Kaul, A., Krieger, N., Rinck, G., Rutter, G., Strand, D. & Bartenschlager, R. (2002). Persistent and transient replication of full-length hepatitis C virus genomes in cell culture. *J Virol* **76**, 4008-21.
- Pileri, P., Uematsu, Y., Campagnoli, S., Galli, G., Falugi, F., Petracca, R., Weiner, A. J., Houghton, M., Rosa, D., Grandi, G. & Abrignani, S. (1998). Binding of hepatitis C virus to CD81. *Science* **282**, 938-41.
- Ploss, A., Evans, M. J., Gaysinskaya, V. A., Panis, M., You, H., de Jong, Y. P. & Rice, C. M. (2009). Human occludin is a hepatitis C virus entry factor required for infection of mouse cells. *Nature* **457**, 882-6.
- Pockros, P., Nelson, D., Godofsky, E., Rodriguez-Torres, M., Everson, G. T., Fried, M. W., Ghalib, R., Harrison, S., Nyberg, L., Shiffman, M. L., Chan, A. & Hill, G. (2008). High relapse rate seen at week 72 for patients treated with R1626 combination therapy. *Hepatology* **48**, 1349-50.
- Post, J. J., Pan, Y., Freeman, A. J., Harvey, C. E., White, P. A., Palladinetti, P., Haber, P. S., Marinou, G., Levy, M. H., Kaldor, J. M., Dolan, K. A., Ffrench, R. A., Lloyd, A. R. & Rawlinson, W. D. (2004). Clearance of hepatitis C viremia associated with cellular immunity in the absence of seroconversion in the hepatitis C incidence and transmission in prisons study cohort. *J Infect Dis* **189**, 1846-55.
- Poynard, T., Leroy, V., Cohard, M., Thevenot, T., Mathurin, P., Opolon, P. & Zarski, J. P. (1996). Meta-analysis of interferon randomized trials in the treatment of viral hepatitis C: effects of dose and duration. *Hepatology* **24**, 778-89.
- Prabhu, R., Vittal, P., Yin, Q., Flemington, E., Garry, R., Robichaux, W. H. & Dash, S. (2005). Small interfering RNA effectively inhibits protein expression and negative strand RNA synthesis from a full-length hepatitis C virus clone. *J Med Virol* **76**, 511-9.
- Prince, A. M., Brotman, B., Grady, G. F., Kuhns, W. J., Hazzi, C., Levine, R. W. & Millian, S. J. (1974). Long-incubation post-transfusion hepatitis without serological evidence of exposure to hepatitis-B virus. *Lancet* **2**, 241-6.
- Quinkert, D., Bartenschlager, R. & Lohmann, V. (2005). Quantitative analysis of the hepatitis C virus replication complex. *J Virol* **79**, 13594-605.
- Quintavalle, M., Sambucini, S., Di Petro, C., De Francesco, R. & Neddermann, P. (2006). The alpha isoform of protein kinase CKI is responsible for hepatitis C virus NS5A hyperphosphorylation. *J Virol* **80**, 11305-12.
- Quintavalle, M., Sambucini, S., Summa, V., Orsatti, L., Talamo, F., De Francesco, R. & Neddermann, P. (2007). Hepatitis C virus NS5A is a direct substrate of casein kinase I-alpha, a cellular kinase identified by inhibitor affinity

- chromatography using specific NS5A hyperphosphorylation inhibitors. *J Biol Chem* **282**, 5536-44.
- Rand, T. A., Petersen, S., Du, F. & Wang, X. (2005). Argonaute2 cleaves the anti-guide strand of siRNA during RISC activation. *Cell* **123**, 621-9.
- Randall, G., Grakoui, A. & Rice, C. M. (2003). Clearance of replicating hepatitis C virus replicon RNAs in cell culture by small interfering RNAs. *Proc Natl Acad Sci U S A* **100**, 235-40.
- Randall, G., Panis, M., Cooper, J. D., Tellinghuisen, T. L., Sukhodolets, K. E., Pfeffer, S., Landthaler, M., Landgraf, P., Kan, S., Lindenbach, B. D., Chien, M., Weir, D. B., Russo, J. J., Ju, J., Brownstein, M. J., Sheridan, R., Sander, C., Zavolan, M., Tuschl, T. & Rice, C. M. (2007). Cellular cofactors affecting hepatitis C virus infection and replication. *Proc Natl Acad Sci U S A* **104**, 12884-9.
- Randall, G. & Rice, C. M. (2004). Interfering with hepatitis C virus RNA replication. *Virus Res* **102**, 19-25.
- Reits, E. A. & Neefjes, J. J. (2001). From fixed to FRAP: measuring protein mobility and activity in living cells. *Nat Cell Biol* **3**, E145-7.
- Roingeard, P., Hourieux, C., Blanchard, E., Brand, D. & Ait-Goughoulte, M. (2004). Hepatitis C virus ultrastructure and morphogenesis. *Biol Cell* **96**, 103-8.
- Roingeard, P., Hourieux, C., Blanchard, E. & Prensier, G. (2008). Hepatitis C virus budding at lipid droplet-associated ER membrane visualized by 3D electron microscopy. *Histochem Cell Biol* **130**, 561-6.
- Rouille, Y., Helle, F., Delgrange, D., Roingeard, P., Voisset, C., Blanchard, E., Belouzard, S., McKeating, J., Patel, A. H., Maertens, G., Wakita, T., Wychowski, C. & Dubuisson, J. (2006). Subcellular localization of hepatitis C virus structural proteins in a cell culture system that efficiently replicates the virus. *J Virol* **80**, 2832-41.
- Rubbia-Brandt, L., Quadri, R., Abid, K., Giostra, E., Male, P. J., Mentha, G., Spahr, L., Zarski, J. P., Borisch, B., Hadengue, A. & Negro, F. (2000). Hepatocyte steatosis is a cytopathic effect of hepatitis C virus genotype 3. *J Hepatol* **33**, 106-15.
- Rubinson, D. A., Dillon, C. P., Kwiatkowski, A. V., Sievers, C., Yang, L., Kopinja, J., Rooney, D. L., Zhang, M., Ihrig, M. M., McManus, M. T., Gertler, F. B., Scott, M. L. & Van Parijs, L. (2003). A lentivirus-based system to functionally silence genes in primary mammalian cells, stem cells and transgenic mice by RNA interference. *Nat Genet* **33**, 401-6.
- Rudner, L., Nydegger, S., Coren, L. V., Nagashima, K., Thali, M. & Ott, D. E. (2005). Dynamic fluorescent imaging of human immunodeficiency virus type 1 gag in live cells by biarsenical labeling. *J Virol* **79**, 4055-65.
- Russell, R. S., Meunier, J. C., Takikawa, S., Faulk, K., Engle, R. E., Bukh, J., Purcell, R. H. & Emerson, S. U. (2008). Advantages of a single-cycle production assay to study cell culture-adaptive mutations of hepatitis C virus. *Proc Natl Acad Sci U S A* **105**, 4370-5.
- Sadler, A. J. & Williams, B. R. (2008). Interferon-inducible antiviral effectors. *Nat Rev Immunol* **8**, 559-68.
- Saito, T., Owen, D. M., Jiang, F., Marcotrigiano, J. & Gale, M., Jr. (2008). Innate immunity induced by composition-dependent RIG-I recognition of hepatitis C virus RNA. *Nature* **454**, 523-7.
- Sakai, A., Claire, M. S., Faulk, K., Govindarajan, S., Emerson, S. U., Purcell, R. H. & Bukh, J. (2003). The p7 polypeptide of hepatitis C virus is critical for infectivity and contains functionally important genotype-specific sequences. *Proc Natl Acad Sci U S A* **100**, 11646-51.
- Salonen, A., Ahola, T. & Kaariainen, L. (2005). Viral RNA replication in association with cellular membranes. *Curr Top Microbiol Immunol* **285**, 139-73.

- Samuel, C. E. (1993). The eIF-2 alpha protein kinases, regulators of translation in eukaryotes from yeasts to humans. *J Biol Chem* **268**, 7603-6.
- Santolini, E., Migliaccio, G. & La Monica, N. (1994). Biosynthesis and biochemical properties of the hepatitis C virus core protein. *J Virol* **68**, 3631-41.
- Santolini, E., Pacini, L., Fipaldini, C., Migliaccio, G. & Monica, N. (1995). The NS2 protein of hepatitis C virus is a transmembrane polypeptide. *J Virol* **69**, 7461-71.
- Sarrazin, C., Kieffer, T. L., Bartels, D., Hanzelka, B., Muh, U., Welker, M., Wincheringer, D., Zhou, Y., Chu, H. M., Lin, C., Weegink, C., Reesink, H., Zeuzem, S. & Kwong, A. D. (2007). Dynamic hepatitis C virus genotypic and phenotypic changes in patients treated with the protease inhibitor telaprevir. *Gastroenterology* **132**, 1767-77.
- Scarselli, E., Ansuini, H., Cerino, R., Roccasecca, R. M., Acali, S., Filocamo, G., Traboni, C., Nicosia, A., Cortese, R. & Vitelli, A. (2002). The human scavenger receptor class B type I is a novel candidate receptor for the hepatitis C virus. *Embo J* **21**, 5017-25.
- Schaller, T., Appel, N., Koutsoudakis, G., Kallis, S., Lohmann, V., Pietschmann, T. & Bartenschlager, R. (2007). Analysis of hepatitis C virus superinfection exclusion by using novel fluorochrome gene-tagged viral genomes. *J Virol* **81**, 4591-603.
- Schmidt-Mende, J., Bieck, E., Hugle, T., Penin, F., Rice, C. M., Blum, H. E. & Moradpour, D. (2001). Determinants for membrane association of the hepatitis C virus RNA-dependent RNA polymerase. *J Biol Chem* **276**, 44052-63.
- Seibler, J., Kleinridders, A., Kuter-Luks, B., Niehaves, S., Bruning, J. C. & Schwenk, F. (2007). Reversible gene knockdown in mice using a tight, inducible shRNA expression system. *Nucleic Acids Res* **35**, e54.
- Sen, G. C. (2001). Viruses and interferons. *Annu Rev Microbiol* **55**, 255-81.
- Seo, M. Y., Abrignani, S., Houghton, M. & Han, J. H. (2003). Small interfering RNA-mediated inhibition of hepatitis C virus replication in the human hepatoma cell line Huh-7. *J Virol* **77**, 810-2.
- Serebrov, V. & Pyle, A. M. (2004). Periodic cycles of RNA unwinding and pausing by hepatitis C virus NS3 helicase. *Nature* **430**, 476-80.
- Sharma, P. & Lok, A. (2006). Viral hepatitis and liver transplantation. *Semin Liver Dis* **26**, 285-97.
- Shavinskaya, A., Boulant, S., Penin, F., McLauchlan, J. & Bartenschlager, R. (2007). The lipid droplet binding domain of hepatitis C virus core protein is a major determinant for efficient virus assembly. *J Biol Chem* **282**, 37158-37169.
- Shepard, C. W., Finelli, L. & Alter, M. J. (2005). Global epidemiology of hepatitis C virus infection. *Lancet Infect Dis* **5**, 558-67.
- Sheth, U. & Parker, R. (2003). Decapping and decay of messenger RNA occur in cytoplasmic processing bodies. *Science* **300**, 805-8.
- Shimakami, T., Hijikata, M., Luo, H., Ma, Y. Y., Kaneko, S., Shimotohno, K. & Murakami, S. (2004). Effect of interaction between hepatitis C virus NS5A and NS5B on hepatitis C virus RNA replication with the hepatitis C virus replicon. *J Virol* **78**, 2738-48.
- Shimakami, T., Honda, M., Kusakawa, T., Murata, T., Shimotohno, K., Kaneko, S. & Murakami, S. (2006). Effect of hepatitis C virus (HCV) NS5B-nucleolin interaction on HCV replication with HCV subgenomic replicon. *J Virol* **80**, 3332-40.
- Shimizu, Y. K., Feinstone, S. M., Kohara, M., Purcell, R. H. & Yoshikura, H. (1996). Hepatitis C virus: detection of intracellular virus particles by electron microscopy. *Hepatology* **23**, 205-9.

- Shimomura, O., Johnson, F. H. & Saiga, Y. (1962). Extraction, purification and properties of aequorin, a bioluminescent protein from the luminous hydromedusan, *Aequorea*. *J Cell Comp Physiol* **59**, 223-39.
- Shirota, Y., Luo, H., Qin, W., Kaneko, S., Yamashita, T., Kobayashi, K. & Murakami, S. (2002). Hepatitis C virus (HCV) NS5A binds RNA-dependent RNA polymerase (RdRP) NS5B and modulates RNA-dependent RNA polymerase activity. *J Biol Chem* **277**, 11149-55.
- Simmonds, P. (2004). Genetic diversity and evolution of hepatitis C virus--15 years on. *J Gen Virol* **85**, 3173-88.
- Simmonds, P., Bukh, J., Combet, C., Deleage, G., Enomoto, N., Feinstone, S., Halfon, P., Inchauspe, G., Kuiken, C., Maertens, G., Mizokami, M., Murphy, D. G., Okamoto, H., Pawlotsky, J. M., Penin, F., Sablon, E., Shin, I. T., Stuyver, L. J., Thiel, H. J., Viazov, S., Weiner, A. J. & Widell, A. (2005). Consensus proposals for a unified system of nomenclature of hepatitis C virus genotypes. *Hepatology* **42**, 962-73.
- Sklan, E. H., Serrano, R. L., Einav, S., Pfeffer, S. R., Lambright, D. G. & Glenn, J. S. (2007). TBC1D20 is a Rab1 GTPase-activating protein that mediates hepatitis C virus replication.
- Song, Y., Friebe, P., Tzima, E., Junemann, C., Bartenschlager, R. & Niepmann, M. (2006). The hepatitis C virus RNA 3'-untranslated region strongly enhances translation directed by the internal ribosome entry site. *J Virol* **80**, 11579-88.
- Soriano, V., Peters, M. G. & Zeuzem, S. (2009). New therapies for hepatitis C virus infection. *Clin Infect Dis* **48**, 313-20.
- Spangberg, K., Goobar-Larsson, L., Wahren-Herlenius, M. & Schwartz, S. (1999). The La protein from human liver cells interacts specifically with the U-rich region in the hepatitis C virus 3' untranslated region. *J Hum Virol* **2**, 296-307.
- Sprague, B. L. & McNally, J. G. (2005). FRAP analysis of binding: proper and fitting. *Trends Cell Biol* **15**, 84-91.
- Steinmann, E., Brohm, C., Kallis, S., Bartenschlager, R. & Pietschmann, T. (2008). Efficient trans-encapsidation of hepatitis C virus RNAs into infectious virus-like particles. *J Virol* **82**, 7034-46.
- Steinmann, E., Penin, F., Kallis, S., Patel, A. H., Bartenschlager, R. & Pietschmann, T. (2007). Hepatitis C virus p7 protein is crucial for assembly and release of infectious virions. *PLoS Pathog* **3**, e103.
- Steitz, T. A. (2008). A structural understanding of the dynamic ribosome machine. *Nat Rev Mol Cell Biol* **9**, 242-53.
- StGelais, C., Tuthill, T. J., Clarke, D. S., Rowlands, D. J., Harris, M. & Griffin, S. (2007). Inhibition of hepatitis C virus p7 membrane channels in a liposome-based assay system. *Antiviral Res* **76**, 48-58.
- Stone, M., Jia, S., Heo, W. D., Meyer, T. & Konan, K. V. (2007). Participation of rab5, an early endosome protein, in hepatitis C virus RNA replication machinery. *J Virol* **81**, 4551-63.
- Supekova, L., Supek, F., Lee, J., Chen, S., Gray, N., Pezacki, J. P., Schlapbach, A. & Schultz, P. G. (2008). Identification of human kinases involved in hepatitis C virus replication by small interference RNA library screening. *J Biol Chem* **283**, 29-36.
- Tai, C. L., Chi, W. K., Chen, D. S. & Hwang, L. H. (1996). The helicase activity associated with hepatitis C virus nonstructural protein 3 (NS3). *J Virol* **70**, 8477-84.
- Taguwa, S., Okamoto, T., Abe, T., Mori, Y., Suzuki, T., Moriishi, K. & Matsuura, Y. (2008). Human butyrate-induced transcript 1 interacts with hepatitis C virus NS5A and regulates viral replication. *J Virol*, **82**, 2631-41.

- Takehara, T., Hayashi, N., Mita, E., Hagiwara, H., Ueda, K., Katayama, K., Kasahara, A., Fusamoto, H. & Kamada, T. (1992). Detection of the minus strand of hepatitis C virus RNA by reverse transcription and polymerase chain reaction: implications for hepatitis C virus replication in infected tissue. *Hepatology* **15**, 387-90.
- Tanabe, Y., Sakamoto, N., Enomoto, N., Kurosaki, M., Ueda, E., Maekawa, S., Yamashiro, T., Nakagawa, M., Chen, C. H., Kanazawa, N., Kakinuma, S. & Watanabe, M. (2004). Synergistic inhibition of intracellular hepatitis C virus replication by combination of ribavirin and interferon- alpha. *J Infect Dis* **189**, 1129-39.
- Tanaka, T., Kato, N., Cho, M. J., Sugiyama, K. & Shimotohno, K. (1996). Structure of the 3' terminus of the hepatitis C virus genome. *J Virol* **70**, 3307-12.
- Tanji, Y., Kaneko, T., Satoh, S. & Shimotohno, K. (1995). Phosphorylation of hepatitis C virus-encoded nonstructural protein NS5A. *J Virol* **69**, 3980-6.
- Targett-Adams, P., Boulant, S. & McLauchlan, J. (2008a). Visualization of double-stranded RNA in cells supporting hepatitis C virus RNA replication. *J Virol* **82**, 2182-95.
- Targett-Adams, P., Hope, G., Boulant, S. & McLauchlan, J. (2008b). Maturation of hepatitis C virus core protein by signal Peptide peptidase is required for virus production. *J Biol Chem* **283**, 16850-9.
- Targett-Adams, P. & McLauchlan, J. (2005). Development and characterization of a transient-replication assay for the genotype 2a hepatitis C virus subgenomic replicon. *J Gen Virol* **86**, 3075-80.
- Tasaka, M., Sakamoto, N., Itakura, Y., Nakagawa, M., Itsui, Y., Sekine-Osajima, Y., Nishimura-Sakurai, Y., Chen, C. H., Yoneyama, M., Fujita, T., Wakita, T., Maekawa, S., Enomoto, N. & Watanabe, M. (2007). Hepatitis C virus non-structural proteins responsible for suppression of the RIG-I/Cardif-induced interferon response. *J Gen Virol* **88**, 3323-33.
- Tellinghuisen, T. L., Foss, K. L. & Treadaway, J. (2008a). Regulation of hepatitis C virion production via phosphorylation of the NS5A protein. *PLoS Pathog* **4**, e1000032.
- Tellinghuisen, T. L., Foss, K. L., Treadaway, J. C. & Rice, C. M. (2008b). Identification of residues required for RNA replication in domains II and III of the hepatitis C virus NS5A protein. *J Virol* **82**, 1073-83.
- Tellinghuisen, T. L., Marcotrigiano, J., Gorbalenya, A. E. & Rice, C. M. (2004). The NS5A protein of hepatitis C virus is a zinc metalloprotein. *J Biol Chem* **279**, 48576-87.
- Tellinghuisen, T. L., Marcotrigiano, J. & Rice, C. M. (2005). Structure of the zinc-binding domain of an essential component of the hepatitis C virus replicase. *Nature* **435**, 374-9.
- Terrault, N. A. & Berenguer, M. (2006). Treating hepatitis C infection in liver transplant recipients. *Liver Transpl* **12**, 1192-204.
- Thimme, R., Oldach, D., Chang, K. M., Steiger, C., Ray, S. C. & Chisari, F. V. (2001). Determinants of viral clearance and persistence during acute hepatitis C virus infection. *J Exp Med* **194**, 1395-406.
- Thompson, A. A., Zou, A., Yan, J., Duggal, R., Hao, W., Molina, D., Cronin, C. N. & Wells, P. A. (2009). Biochemical characterization of recombinant hepatitis C virus nonstructural protein 4B: evidence for ATP/GTP hydrolysis and adenylate kinase activity. *Biochemistry* **48**, 906-16.
- Thomson, B. J. (2009). Hepatitis C virus: the growing challenge. *Br Med Bull* **89**, 153-67.
- Thomson, B. J. & Finch, R. G. (2005). Hepatitis C virus infection. *Clin Microbiol Infect* **11**, 86-94.

- Tiscornia, G., Singer, O., Ikawa, M. & Verma, I. M. (2003). A general method for gene knockdown in mice by using lentiviral vectors expressing small interfering RNA. *Proc Natl Acad Sci U S A* **100**, 1844-8.
- Tong, X. & Malcolm, B. A. (2006). Trans-complementation of HCV replication by non-structural protein 5A. *Virus Res* **115**, 122-30.
- Towner, J. S., Mazanet, M. M. & Semler, B. L. (1998). Rescue of defective poliovirus RNA replication by 3AB-containing precursor polyproteins. *J Virol* **72**, 7191-200.
- Tsien, R. Y. (1998). The green fluorescent protein. *Annu Rev Biochem* **67**, 509-44.
- van de Wetering, M., Oving, I., Muncan, V., Pon Fong, M. T., Brantjes, H., van Leenen, D., Holstege, F. C., Brummelkamp, T. R., Agami, R. & Clevers, H. (2003). Specific inhibition of gene expression using a stably integrated, inducible small-interfering-RNA vector. *EMBO Rep* **4**, 609-15.
- Voisset, C., Callens, N., Blanchard, E., Op De Beeck, A., Dubuisson, J. & Vu-Dac, N. (2005). High density lipoproteins facilitate hepatitis C virus entry through the scavenger receptor class B type I. *J Biol Chem* **280**, 7793-9.
- Wachter, R. M. (2006). The family of GFP-like proteins: structure, function, photophysics and biosensor applications. Introduction and perspective. *Photochem Photobiol* **82**, 339-44.
- Wakita, T., Pietschmann, T., Kato, T., Date, T., Miyamoto, M., Zhao, Z., Murthy, K., Habermann, A., Krausslich, H. G., Mizokami, M., Bartenschlager, R. & Liang, T. J. (2005). Production of infectious hepatitis C virus in tissue culture from a cloned viral genome. *Nat Med* **11**, 791-6.
- Wang C., Gale, M., Jr., Keller, B. C., Huang, H., Brown, M. S., Goldstein, J. L. & Ye, J. (2005). Identification of FBL2 as a geranylgeranylated cellular protein required for hepatitis C virus RNA replication. *Mol Cell* **18**, 425-34.
- Wang, Y., Kato, N., Jazag, A., Dharel, N., Otsuka, M., Taniguchi, H., Kawabe, T. & Omata, M. (2006). Hepatitis C virus core protein is a potent inhibitor of RNA silencing-based antiviral response. *Gastroenterology* **130**, 883-92.
- Waris, G., Sarker, S. & Siddiqui, A. (2004). Two-step affinity purification of the hepatitis C virus ribonucleoprotein complex. *Rna* **10**, 321-9.
- Wasley, A. & Alter, M. J. (2000). Epidemiology of hepatitis C: geographic differences and temporal trends. *Semin Liver Dis* **20**, 1-16.
- Watashi, K., Hijikata, M., Hosaka, M., Yamaji, M. & Shimotohno, K. (2003). Cyclosporin A suppresses replication of hepatitis C virus genome in cultured hepatocytes. *Hepatology* **38**, 1282-8.
- Watashi, K., Ishii, N., Hijikata, M., Inoue, D., Murata, T., Miyanari, Y. & Shimotohno, K. (2005). Cyclophilin B is a functional regulator of hepatitis C virus RNA polymerase. *Mol Cell* **19**, 111-22.
- Weber, F., Wagner, V., Rasmussen, S. B., Hartmann, R. & Paludan, S. R. (2006). Double-stranded RNA is produced by positive-strand RNA viruses and DNA viruses but not in detectable amounts by negative-strand RNA viruses. *J Virol* **80**, 5059-64.
- Weiner, A. J., Brauer, M. J., Rosenblatt, J., Richman, K. H., Tung, J., Crawford, K., Bonino, F., Saracco, G., Choo, Q. L., Houghton, M. & et al. (1991). Variable and hypervariable domains are found in the regions of HCV corresponding to the flavivirus envelope and NS1 proteins and the pestivirus envelope glycoproteins. *Virology* **180**, 842-8.
- Welsch, C., Albrecht, M., Maydt, J., Herrmann, E., Welker, M. W., Sarrazin, C., Scheidig, A., Lengauer, T. & Zeuzem, S. (2007). Structural and functional comparison of the non-structural protein 4B in flaviviridae. *J Mol Graph Model* **26**, 546-57.
- Westaway, E. G., Mackenzie, J. M., Kenney, M. T., Jones, M. K. & Khromykh, A. A. (1997). Ultrastructure of Kunjin virus-infected cells: colocalization of NS1

- and NS3 with double-stranded RNA, and of NS2B with NS3, in virus-induced membrane structures. *J Virol* **71**, 6650-61.
- Wolk, B., Buchele, B., Moradpour, D. & Rice, C. M. (2008). A dynamic view of hepatitis C virus replication complexes. *J Virol* **82**, 10519-31.
- Wolk, B., Sansonno, D., Krausslich, H. G., Dammacco, F., Rice, C. M., Blum, H. E. & Moradpour, D. (2000). Subcellular localization, stability, and trans-cleavage competence of the hepatitis C virus NS3-NS4A complex expressed in tetracycline-regulated cell lines. *J Virol* **74**, 2293-304.
- Xue, Q., Ding, H., Liu, M., Zhao, P., Gao, J., Ren, H., Liu, Y. & Qi, Z. T. (2007). Inhibition of hepatitis C virus replication and expression by small interfering RNA targeting host cellular genes. *Arch Virol* **152**, 955-62.
- Yamada, N., Tanihara, K., Takada, A., Yorihuri, T., Tsutsumi, M., Shimomura, H., Tsuji, T. & Date, T. (1996). Genetic organization and diversity of the 3' noncoding region of the hepatitis C virus genome. *Virology* **223**, 255-61.
- Yamaga, A. K. & Ou, J. H. (2002). Membrane topology of the hepatitis C virus NS2 protein. *J Biol Chem* **277**, 33228-34.
- Yanagi, M., St Claire, M., Emerson, S. U., Purcell, R. H. & Bukh, J. (1999). In vivo analysis of the 3' untranslated region of the hepatitis C virus after in vitro mutagenesis of an infectious cDNA clone. *Proc Natl Acad Sci U S A* **96**, 2291-5.
- Yang, F., Moss, L. G. & Phillips, G. N., Jr. (1996). The molecular structure of green fluorescent protein. *Nat Biotechnol* **14**, 1246-51.
- Yang, G., Pevear, D. C., Collett, M. S., Chunduru, S., Young, D. C., Benetatos, C. & Jordan, R. (2004). Newly synthesized hepatitis C virus replicon RNA is protected from nuclease activity by a protease-sensitive factor(s). *J Virol* **78**, 10202-5.
- Yao, N., Hesson, T., Cable, M., Hong, Z., Kwong, A. D., Le, H. V. & Weber, P. C. (1997). Structure of the hepatitis C virus RNA helicase domain. *Nat Struct Biol* **4**, 463-7.
- Yi, M. & Lemon, S. M. (2003). Structure-function analysis of the 3' stem-loop of hepatitis C virus genomic RNA and its role in viral RNA replication. *Rna* **9**, 331-45.
- Yi, M. & Lemon, S. M. (2004). Adaptive mutations producing efficient replication of genotype 1a hepatitis C virus RNA in normal Huh7 cells. *J Virol* **78**, 7904-15.
- Yi, M., Villanueva, R. A., Thomas, D. L., Wakita, T. & Lemon, S. M. (2006). Production of infectious genotype 1a hepatitis C virus (Hutchinson strain) in cultured human hepatoma cells. *Proc Natl Acad Sci U S A* **103**, 2310-5.
- Yi, M., Ma, Y., Yates, J. & Lemon, S. M. (2007). Compensatory mutations in E1, p7, NS2, and NS3 enhance yields of cell culture-infectious intergenotypic chimeric hepatitis C virus. *J Virol* **81**, 629-38.
- Yokota, T., Sakamoto, N., Enomoto, N., Tanabe, Y., Miyagishi, M., Maekawa, S., Yi, L., Kurosaki, M., Taira, K., Watanabe, M. & Mizusawa, H. (2003). Inhibition of intracellular hepatitis C virus replication by synthetic and vector-derived small interfering RNAs. *EMBO Rep* **4**, 602-8.
- Yu, G. Y., Lee, K. J., Gao, L. & Lai, M. M. (2006). Palmitoylation and polymerization of hepatitis C virus NS4B protein. *J Virol* **80**, 6013-23.
- Yuan, W. & Krug, R. M. (2001). Influenza B virus NS1 protein inhibits conjugation of the interferon (IFN)-induced ubiquitin-like ISG15 protein. *Embo J* **20**, 362-71.
- Zein, N. N. (2000). Clinical significance of hepatitis C virus genotypes. *Clin Microbiol Rev* **13**, 223-35.
- Zeuzem, S., Feinman, S. V., Rasenack, J., Heathcote, E. J., Lai, M. Y., Gane, E., O'Grady, J., Reichen, J., Diago, M., Lin, A., Hoffman, J. & Brunda, M. J.

- (2000). Peginterferon alfa-2a in patients with chronic hepatitis C. *N Engl J Med* **343**, 1666-72.
- Zhang, J., Randall, G., Higginbottom, A., Monk, P., Rice, C. M. & McKeating, J. A. (2004a). CD81 is required for hepatitis C virus glycoprotein-mediated viral infection. *J Virol* **78**, 1448-55.
- Zhang, J., Yamada, O., Sakamoto, T., Yoshida, H., Iwai, T., Matsushita, Y., Shimamura, H., Araki, H. & Shimotohno, K. (2004b). Down-regulation of viral replication by adenoviral-mediated expression of siRNA against cellular cofactors for hepatitis C virus. *Virology* **320**, 135-43.
- Zhang, M., Sun, X. D., Mark, S. D., Chen, W., Wong, L., Dawsey, S. M., Qiao, Y. L., Fraumeni, J. F., Jr., Taylor, P. R. & O'Brien, T. R. (2005). Hepatitis C virus infection, Linxian, China. *Emerg Infect Dis* **11**, 17-21.
- Zhang, R., Durkin, J., Windsor, W. T., McNemar, C., Ramanathan, L. & Le, H. V. (1997). Probing the substrate specificity of hepatitis C virus NS3 serine protease by using synthetic peptides. *J Virol* **71**, 6208-13.
- Zhang, Z., Harris D. & Pandey, V. N. (2008). The FUSE binding protein is a cellular factor required for efficient replication of hepatitis C virus. *J Virol* **82**, 5761-73.
- Zhao, C., Denison, C., Huijbregtse, J. M., Gygi, S. & Krug, R. M. (2005). Human ISG15 conjugation targets both IFN-induced and constitutively expressed proteins functioning in diverse cellular pathways. *Proc Natl Acad Sci U S A* **102**, 10200-5.
- Zheng, A., Yuan, F., Li, Y., Zhu, F., Hou, P., Li, J., Song, X., Ding, M. & Deng, H. (2007). Claudin-6 and claudin-9 function as additional coreceptors for hepatitis C virus. *J Virol* **81**, 12465-71.
- Zhong, J., Gastaminza, P., Cheng, G., Kapadia, S., Kato, T., Burton, D. R., Wieland, S. F., Uprichard, S. L., Wakita, T. & Chisari, F. V. (2005). Robust hepatitis C virus infection in vitro. *Proc Natl Acad Sci U S A* **102**, 9294-9.
- Zhu, Q., Guo, J. T. & Seeger, C. (2003). Replication of hepatitis C virus subgenomes in nonhepatic epithelial and mouse hepatoma cells. *J Virol* **77**, 9204-10.
- Zimmer, M. (2002). Green fluorescent protein (GFP): applications, structure, and related photophysical behavior. *Chem Rev* **102**, 759-81.